DynLAB

Course on Dynamics of Multidisplicinary Systems

Part I

January 19, 2011

Herman Mann

Czech Technical University in Prague

herman.j.mann@gmail.com

Contents

About this course

All aspects of modern technology are underlined by the subject of system dynamics, which plays the determining role in the market competition of engineering products. Its importance increases with the ever-growing demands on operational speed, energetic efficiency, safety, reliability, and environment protection. At the same time, the engineering products become more and more complex with regards both to the number of their components as well as to the variety of phenomena affecting the product dynamics, either in a useful or undesirable way.

To understand and predict dynamic behavior of existing systems as well as to design new systems, engineers resort to computer-assisted modeling, simulation and analysis of the systems. Modeling is in this context a procedure for forming a simplified representation of those features of real dynamic systems that are relevant to their dynamic behavior. The simplification is based on an abstraction of the relevant system features and on their idealization. The resulting model representation can take the form of equations, diagrams, or tables of data, for example. Simulation is a procedure imitating dynamic behavior of the modelled real systems. Analysis is a procedure investigating changes of the system behavior if the system or its surroundings are changing so it gives more thorough information about the system dynamics than simulation.

Such techniques can replace to a certain degree expensive and time consuming design verification based on construction of system prototypes and their experimental investigation using measuring instruments. At the same time, these techniques allow engineers considering a larger variety of system design alternatives and their more thorough verification. Design verification by simulation is the only option in cases where the experimentation with real systems would be too expensive or too dangerous. Analysis can also simplify the system operation and maintenance by detecting an impending system failure as well as by helping to locate a fault in the system and to diagnose its cause. As these computation techniques allow for faster introduction of a new product into the market as well as for attaining and maintaining the product higher quality, they help in acquiring higher profits.

This Web-based course on dynamics of multidisciplinary controlled systems has been developed for

- regular students wishing to complement the traditional face-to-face courses

- distance-education students at different levels of vocational study and training

- practising engineers in the context of continuing education or lifelong learning

- teachers intending to innovate the courses they teach

- industrial enterprisers interested in enhancing the qualification and efficiency of their personnel

- providers of regular, continuing and life-long-learning courses

The subject of dynamics and control underlies all aspects of modern technology and plays the determining role in the world-market competition of engineering products. Its importance increases with the ever-growing demands on operational speed, efficiency, safety, reliability, or environment protection. Nevertheless, entrepreneurs report lack of professionals sufficiently qualified in this field and vocational schools complain about the overall decline of interest in engineering study among young people. Professional associations call for radical changes in the engineering curriculum and for innovative approaches to vocational training.

The existing courses on dynamics and control are criticized for discouraging young people from engineering study by overemphasizing theory and mathematics at the expense of practical engineering issues. Dynamics is usually covered in several courses separated along the borders between the traditional engineering disciplines despite the fact that most of the contemporary engineering products are of

multidisciplinary nature. Control courses are criticized for presenting 'textbook' problems engineered to fit the theory without undertaking a realistic modeling of the controlled systems. Computers are often used to carry out old exercises without radical modification of the curriculum to fully incorporate current computer capabilities.

The contents, emphasis and style of this course differs from most of the existing courses by a number of factors. The first part of the course exposes learners in a systematic and unified way to realistic modelling and simulation of multidisciplinary systems. This approach is supported by a free online access to the simulation software DYNAST. It allows for submitting dynamic models directly in a graphical form isomorphic to the geometric configuration of the modelled real systems. The underlying equations are not only solved, but also automatically formulated.

Using this tool, learners can be introduced to dynamics through modeling and simulation of simple yet practical examples. This stimulates their interest before they are exposed to more abstract subjects like equation formulation, block-diagram construction, Laplace transformation, etc. In addition, learners are given in the course a better 'feel' for system dynamics by graphical visualization, 3D animation and interactive virtual experiments. Computers are thus integrated into the course curriculum from the very start as learning tools without distracting learners from dynamics by issues not related directly to it. In the same way, learners are given the hands-on opportunity to acquire the skills necessary for efficient solving real-life problems in their engineering profession.

Different target groups can select individual paths through the course, paths tailor-made to their previous experience and respecting their learning needs. Depending on their background, learners can choose to start from the module on dynamics of either mechanical, electrical or fluid systems. More advanced learners can go directly to the dynamics of multidisciplinary systems, or even to control. The course material as well as the learning environment suit both to self-study and remote tutoring. They both strongly support investigative and collaborative modes of learning.

Learners are given the opportunity to benefit from 'organizational learning', i.e. from utilizing knowledge recorded during previous problem solving both in academia and industry. This knowledge is available to learners in the form of a large collection of online re-solvable examples and submodels of systems components and physical phenomena.

References

Multidisciplinary systems

R. H. Cannon: Dynamics of Physical Systems. McGraw-Hill, New York 1967

H. E. Koenig, Y. Tokad, H. K. Kesavan: Analysis of Discrete Physical Systems. McGraw-Hill, New York 1967

S. H. Crandall, D. C. Karnopp, E. F. Kurtz, D. C. Pridmore-Brown: Dynamics of Mechanical and Electromechanical Systems. McGraw-Hill, New York 1968

J. L. Shearer, A. T. Murphy, H. H. Richardson: Introduction to System Dynamics. Addison Wesley, Reading 1971

F. E. Cellier: Continuous System Modeling. Springer-Verlag, New York 1991

D.C. Karnopp, D.L. Margolis, R.C. Rosenberg: System Dynamics: A Unified Approach. John Wiley, New York 1990 (2nd ed.)

M.M. Tiller: Introduction to Physical Modeling with Modelica. Kluwer Academic Publishers 2001

P. Gawthrop, L. Smith: Metamodelling: Bong graphs and dynamic systems. Prentice Hall 1996.

R. Bjrke: Manufacturing Theory. Tapir 1995.

R. Isermann: Mechatronische Systeme. Grundlagen. Springer 1999.

F.T. Forbes: Modeling and Analysis of Engineering Systems, a Unified Graph-Centered Approach, Marcel Dekker 2001.

R.A. Layton: Principles of Analytical System Dynamics. Springer 1998.

D.K. Miu: Mechatronics. Electromechanics and Contromechanics. Springer 1993.

D. Rowell, D.N. Wormley: System Dynamics: An Introduction. Prentice Hall, 1997.

J.L. Shearer, B.T. Kulakowski, J.F. Gardner: Dynamic Modeling and Control of Engineering Systems. Prentice Hall, 1997.

R.L. Woods, K.L. Lawrence: Modeling and Simulation of Dynamic Systems. Prentice Hall, 1997.

I. Cochin, W. Caldwallender: Analysis and Design of Dynamic Systems. Addison-Wesley, 1997 (3rd. ed.)

W.J. Palm III: Modeling, Analysis, and Control of Dynamic Systems. John Wiley & Sons, 1999.

Electrical, magnetic and electronic systems

D.H. Sheingold: Nonlinear Circuits Handbook. Designing with Analog Function Modules and ICs. Analog Devices, Norwood MA 1974

Fano, R.M., Chu, L.J.: Fields, Energy, and Forces. Wiley, New York 1959.

M.H. Rashid: SPICE for Circuits and Electronics Using PSpice. Prentice-Hall Int. Editions, Engl. Ciffs 1990.

Slemon G.R.: Magnetoelectric Devices. Transducers, transformers, and machines. John Wiley, New York 1966.

R. Kielkowski: Inside SPICE. Overcoming the Obstacles of Circuit Simulation. McGraw-Hill, New York 1994.

J.A. Connelly, P. Choi: Macromodeling with SPICE. Prentice Hall, Engl. Cliffs 1992.

K.H. Muller: A Spice Cookbook. Intusoft 1991.

M.H. Rashid: Power Electronics. Circuits, Devices, and Applications. Prentice-Hall Int. Editions, Engl. Ciffs 1988.

C.A. Desoer, E.S. Kuh: Basic Circuit Theory. McGraw-Hill 1969

J. Vlach, K. Singhal: Computer Methods for Circuit Analysis and Design. Van Nostrand Reinhold 1994 (2nd ed.).

N. Mohan, T.M. Undeland, W.P. Robbins: Power electronics. Converters, Applications, and Design. Wiley 1995 (2nd ed.).

G. Schweitzer, H. Bleuler, A. Traxler: Active Magnetic Bearings. VDF 1994.

Mechanical systems

P.E. Nikravesh: Computer-Aided Analysis of Mechanical Systems. Prentice-Hall 1988

E.J. Haug: Computer Aided Kinematics and Dynamics of Mechanical Systems. Allyn and Bacon 1989.

R.D. Klafter, T.A. Chmielewski, M. Negin: Robotic Engineering. Prentice-Hall 1989.

J.L. Meriam, L.G. Kraige: Engineering Mechanics. Statics. Dynamics. Wiley 1998 (4th ed.).

R.L. Norton: Design of Machinery. McGraw-Hill 1999.

F.S. Tse, I.E. Morse, R.T. Hinkle: Mechanical Vibrations. Theory and Applications. Prentice-Hall 1978.

SimMechanics, The MathWorks, Natick MA, 2002.

C.A. Rubin: Working Model. Addison-Wesley 1995.

J.J. Craig: Introduction to Robotics. Mechanics and Control. Addison-Wesley 1989 (2nd ed.).

DUBBEL Handbook of Mechanical Engineering. Springer 1994.

H. Mayr: Virtual Automation Environments. Design, Modeling, Visualization, Simulation. Marcel Dekker 2002.

Electro-mechanical systems

A. Lenk, G. Pfeifer, R. Wertschtzky: Elektromechanische Systeme. Mechanische und akustische Netzwerke, deren Wechselwirkungen und Anwendungen. Springer 2001.

W. Leonhard: Control of Electrical Drives. Springer 1985.

P. Krause, D. Wasynczuk, S. D. Sudhoff: Analysis of Electric Machinery. IEEE Press 1995.

H. Gross: Electrical Feed Drives for Machine Tools. Wiley 1983.

P.C. Krause: Analysis of Electric Machinery. McGraw-Hill 1987.

H.H. Woodson, J.R. Melcher: Electromechanical Dynamics. Part I: Discrete Systems. Part II: Continuum Electromechanics. Part III: Elastic and Fluid Media. Wiley 1968 [repub. by Krieger 1990].

J. Meisel: Principles of Electromechanical-Energy Conversion. McGraw-Hill 1966.

D.C. White, H.H. Woodson: Electromechanical Energy Conversion. Wiley 1959.

T. Kenjo: Stepping motors and their microprocessor controls. Clarendon Press 1992.

R.T. Smith: Analysis of Electrical Machines. Pergamon Press 1982.

S.A. Nasar, L.E. Unnewehr: Electromechanics and Electric Machines. Wiley 1979.

J.R. Melcher: Continuum Electromechanics. MIT Press 1981

Fluid and thermal systems

T. J. Viersma: Analysis, Synthesis and Design of Hydraulic Servosystems and Pipelines. Elsevier, Amsterdam 1980

J.H. Lienhard: A Heat Transfer Handbook. Prentice-Hall, Inc., Englewood Cliffs, N.J., 1981.

Y.A. Çengel: Thermodynamics. An Engineering Approach. McGraw-Hill, New York 1994 (2nd ed.).

H.E. Meritt: Hydraulic Control Systems. Wiley 1967.

J. Watton: Fluid Power Systems. Modelling, simulation, analog and microcomputer control. Prentice Hall 1989.

Module 1

Introduction to dynamics

Module units

Module overview. *Welcome to the course part focused on system dynamics. It is well recognized that computer-assisted modeling and simulation are indispensable for understanding dynamics of existing systems as well as for designing new systems. This module attempts to explain why is it so.*

1.1   Modeling and simulation

The behavior of real physical systems which engineers must design, analyze, and understand is controlled by the flow, storage, and interchange of various forms of energy. In almost all cases, real systems are extremely complex and may involve several interacting energy phenomena, such as electromagnetic fields, heat and fluid flow, or nuclear reaction.

Simulation or analysis of a dynamic system always involves forming a model made up of basic building-blocks that are idealizations of the essential physical phenomena occurring in real systems. An adequate model of a particular physical device or system will behave approximately like the real system. The best system model is the simplest one which yields the information necessary for engineering action or decision.

It is important that the learners appreciate the advantages of simplified ideal models without over-simplifying their picture of the real physical world. An approximate answer to an engineering problem is often the best answer if the degree of approximation is known and a more precise answer is not really needed. The cost of precision is often exceedingly high, since the model complexity of the conceptual models needed to represent systems usually increases very rapidly with increased requirements for accuracy. Hence efforts to attain high precision should be made only when the cost in time, money, and effort can be justified.

Of the many fundamental building blocks which the engineer must use in forming models of particular dynamic systems, we shall concentrate in this part of the course on simple physical elements which store, dissipate, and transform energy. By proper use of these idealized elements, we will be able to model any physical system, linear or nonlinear. The extent to which the behavior of the model represents the actual behavior of the real physical system depends on the sophistication and completeness of the model and on the degree of insight and judgment with which the model is formulated. When the engineers are confronted with a dynamic system problem, they must first recognize that the problem is one to which they can apply the principles developed in this course.

We shall see that there are many striking similarities between mechanical, electrical, magnetic, fluid, acoustic, and thermal systems, which will permit a unified study of the system behavior. A uniform terminology and symbolism applicable to all of the physical systems considered will be developed. The integration of subject matter in this course is designed to allow the learners to recognize that a large class of problems can be considered in a similar and systematic fashion.

In the next step, the engineers must define the system to be considered (should the ambient-temperature variation be considered an input? is the inertia of a connecting shaft important in this situation? etc.). They then may describe the system by means of the various physical elements or more complex submodels which we will consider. After this, they must investigate the energetic interactions between these system parts.

The next job is to establish a mathematical model of the system to be analyzed. This involves the identification and idealization of individual system components as well as identification and idealization of their interconnection. The mathematical statement of the governing relationships between system variables is called the formulation problem. Interconnection of the elements imposes constraints on the variation of system variables, and the convenient way of specifying these constraints is by a mathematical statement of the way in which the various variables are related.

To investigate the dynamic behavior of the system, this set of equations must be solved. The initial state of the system must also be specified by a set of initial conditions. The system equations must be solved for the desired response under the specified input signal and initial conditions. There are numerous approaches to the solution of the system equation, and the choice of a method or software will depend on the problem at hand.

After obtaining a solution for the response, the engineers have another major job. The tasks of initial modeling and final analyzing or designing are functions which clearly distinguish the engineer from the mathematician. The engineers must check their solution (is it correct dimensionally? does it correspond to physical reality? does it check for simplified situations which can be easily analyzed? etc.). Their interest in the whole matter of dynamic systems is to eventually analyze to determine whether a certain performance is obtained and is satisfactory, or more generally, he must design the system so that it will meet certain performance specifications.

In summary, our approach to a dynamic system problem can be enumerated as follows:

1. define the system and its components,

2. formulate the mathematical model,

3. determine the system equations,

4. solve for the desired output,

5. check the solution,

6. analyze or design.

1.2 Role of simulation in engineering

1.2.1 Design problem

Fig. 1.1 illustrates the life-cycle of an engineering system. The life cycle begins from *design* of the system, the starting point of which is *system specification* based on marketing as well as technical, economic, environmental and other requirements. The specification defines the *correct system* in terms of all critical system properties within the assumed range of operating conditions throughout the system complete life cycle up to the system disposal.

The most rudimentary design activity, the *nominal design*, aims at achieving the requirements on the correct system under the nominal manufacturing and operating conditions. In reality, however, these conditions are never exactly nominal due to manufacturing inaccuracies, variations of the system environment, aging of the system, etc. Thus the design process consists of a variety of additional design activities with different but complementary objectives.

An important role is played in the design process by *tolerance design* which takes into consideration the fact that parameters of components the systems are made of as well as parameters of the environment in which the systems operate deviate from their nominal values but still stay within the admissible
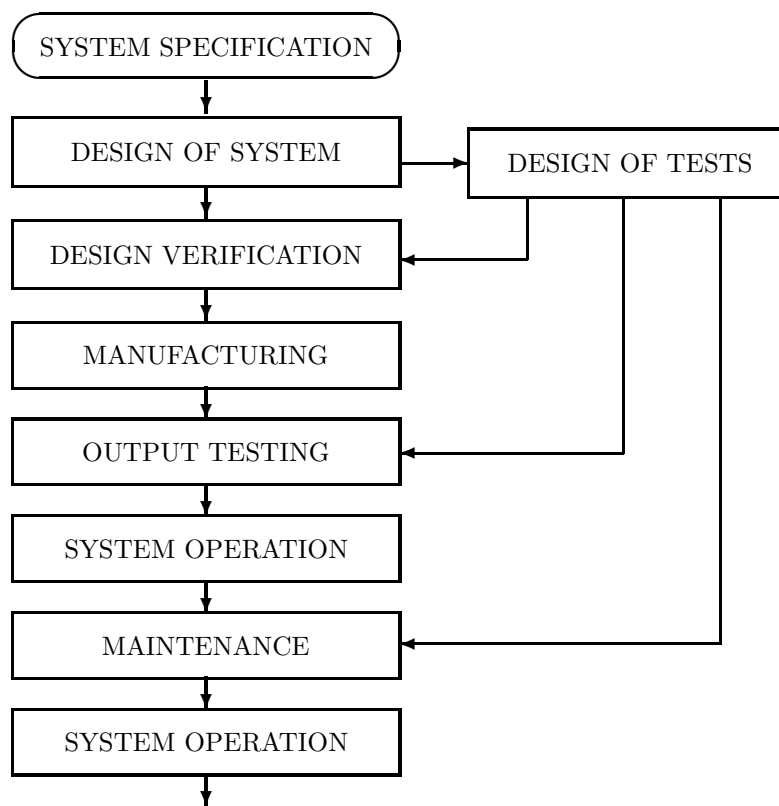
Figure 1.1: Life-cycle of an engineering system.

tolerances. There are two basic approaches to the problem: worst-case and statistical tolerance design. *Worst-case design* aims at preventing system failure even in the case of the most adverse combinations of the parameter deviations. Very few systems, however, are designed for 100% *production yield*, i.e., that all 100% 'copies' of the system are correct at the output of the production process. The reasons are economic one: it is cheaper to dump or repair a part of the production than to utilize components with tolerances more narrow. The aim of *statistical tolerance design* is to achieve the required system production yield with components of given statistical distribution of their tolerances.

Of course, a system may fail also if one or more of the system components fail, i.e. if the properties of these components get outside their admissible tolerances. The probability that the system would not fail in this way during certain time period and under certain operating conditions is called *system reliability*. The objective of *reliability design* is to meet the requirements on the system reliability taking into consideration the limited reliability of the system components.

Design for testing aims at designing systems in such a way that they could be tested easily, some systems are even designed to be self-testing. The design for testing is complemented by *design of tests*. As Fig. 1.1 suggests, different tests are needed for *design verification*, for testing at the output of the production, or for testing of systems during their in-service operation and maintenance. Such experimental testing is increasingly carried out using computer-controlled instruments.

The objectives of system testing can be of different levels of depth:

- *fault detection* recognizes only the system failure occurrence

- *fault localization* reveals in which of the system components the failure occurred

- *fault diagnosis* indicates the reason for the failure

There are also other design activities, like design for producibility, for maintainability, for reproducibility, for built-in obsolescence, for self-destruction, etc.

In all these activities computer-assisted modeling, simulation and analysis makes an indispensable tool today. Used to explore and predict dynamic behavior of dynamic systems, it plays a key role in enhancing their quality and reliability. Simulation also decreases the need for costly and time consuming

DESIGN DESCRIPTIONS:

behavioral   topological   geometrical

DESIGN LEVELS:

conceptual

functional   DESIGN SPACE
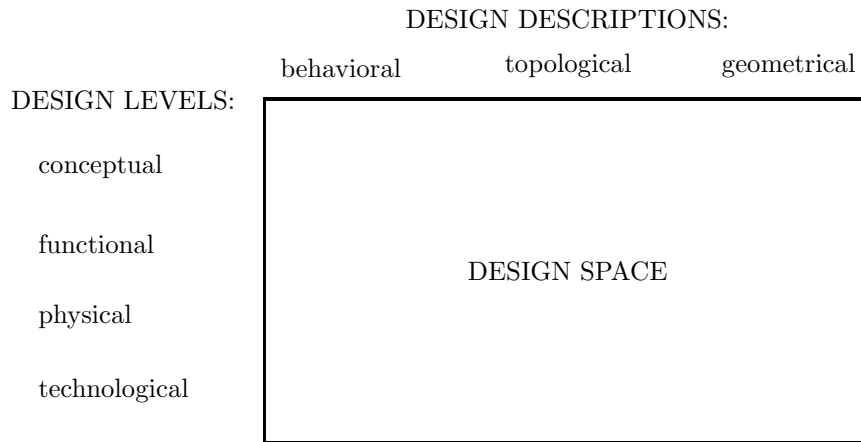
physical

technological

Figure 1.2: Design space

production of real prototypes and for their experimental testing. Many of these activities cannot be performed experimentally at all, like the tolerance or reliability design, for example. Last but not least, by speeding up the design process, simulation allows for acquiring higher profits by introducing new products into the market faster.

1.2.2   Design process

The process of designing is usually an iterative analysis. The results of one analysis point toward a change in the system which may improve the performance; another analysis is done on the new system to determine performance, etc. The design aspects distinguish the engineer from the scientist. The engineer is ultimately interested in building a system which will perform a useful function for the benefit of mankind.

   To manage the designing of an engineering system, the process is usually carried through several *design levels* starting from the conceptual up to the technological design level. At the same time, several different *design descriptions* of the system are used in different phases of the process. In addition to it, if the system is complex, it is imagined as decomposed into numerous *design modules* which can be designed to a certain degree autonomously. Also each module can be considered as decomposed into several submodules, and such a decomposition can proceed through several levels of module complexity.

   Thus the process of designing an engineering system can be imagined as carried through a three-dimensional *design space* the typical settings of which are given in Fig. 1.2. The fundamental design levels are shown along the vertical border of the design space whereas the basic design descriptions are indicated along its horizontal border. The module complexity scale is not shown in the figure – it is assumed to be associated with the axis perpendicular to the plane of the figure.

   The decomposition of a system into *design modules* or *subsystems* is a matter of engineering judgment. The modules may represent both separable parts from which the system is actually assembled (like various mechanical members, actuators, electronic circuits, hydraulic elements, etc.) as well as just some effects which are not separable from the parts (like friction or flexibility, for example).

   To illustrate the process, let us take the example of a copying lathe given in Fig. 1.3*a*. In Fig. 1.3*b*, the lathe is shown disintegrated into several modules: the lathe bed with the slide, the hydraulic cylinder, the spool valve, the stylus following a master, the tool manufacturing the workpiece and, as a separate part, the surfaces of the cylinder container and of the slide between which a friction effect takes place. Fig. 1.3*a* gives an example of a geometric description of the copying lathe in the form of its cutaway view.

1.2.3   Design descriptions

Each of the design descriptions represents a system or module model of certain degree of abstraction and idealization. The *geometric description* of a system or module expresses its geometrical shape, dimensions and position. In the past, the geometric description used to be recorded in the form of a blue print whereas today it is usually stored in an electronic form which may represent not only the traditional engineering drawings of the module, but also its wireframe, solid, surface or some other geometric model.
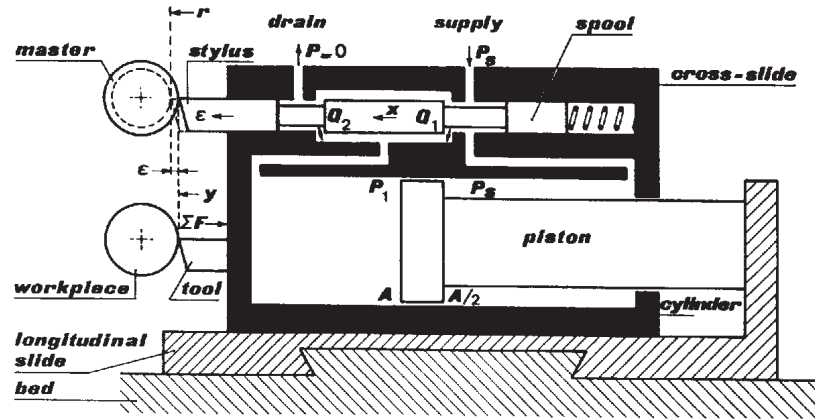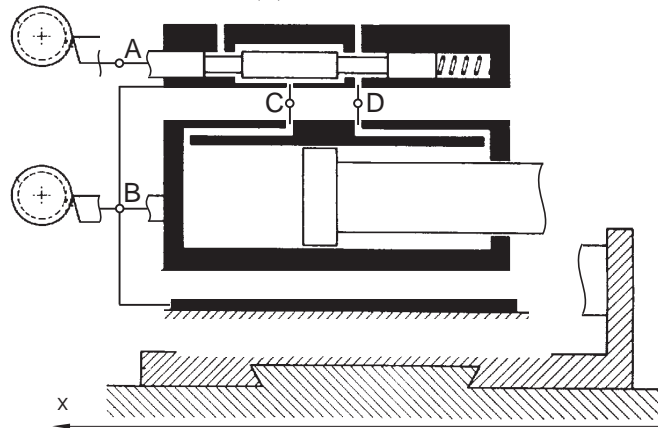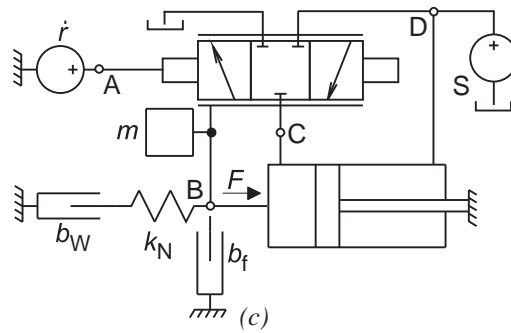
Figure 1.3: (a) Copying lathe, (b) lathe decomposition, (c) multipole model.

The *behavioral description* characterizes external dynamic interactions of a module in terms of the relationship between the interactions ignoring completely the module internal structure, e.g., it characterizes the module just as a 'black-box'. The model, which the behavioral description of a module represents, may be static or dynamic, linear or nonlinear, time-variable or time invariant, lumped-parameter or distributed-parameter, etc. The description may be in the form of various characteristics obtained by experimenting with the real module or in the form equations, transfer functions, state-transition tables, etc., based on a hypothesis about the physical effects taking place within the module. The experimental and hypothetical approaches are usually combined.

On the other hand, to represent mutual interactions between modules in a system, or between submodules in a module, is the aim of the *topological description*. Any module geometrical shapes, dimensions and positions are meaningless in this description, only the coincidences of the module interactions are relevant. The topological descriptions are usually portrayed graphically in the form of diagrams in which modules or their functions are represented by some symbols and the module interactions by line segments interconnecting the symbols.

Fig. 1.3*c* gives an example of a topological description of the copying lathe. Besides the standardized symbols for a spool valve and a hydraulic cylinder, we can see there a damper b_f modeling the friction between the cylinder and the slide, the combination of damper b_W and spring k_N modeling the dynamics of the manufacturing process, the actuator of velocity $\dot{r}$ enforced to the stylus by the rotating master, the square symbol representing inertial mass m of the movable parts, and the symbol S representing there for the oil pressure supply. The interactions between the modules are denoted in Fig. 1.3*c* by small circles. Thus the letters A and B denote interactions carried out by mechanical interlinking of the modules whereas C and D denote interactions between the module fluid inlets.

1.2.4   Design levels

The uppermost design level is committed to the *conceptual design* of the system. It results in an overall architecture and fundamental functions of the designed system. Also decisions of which the functions will be implemented in hardware, either analog or digital, and which of them will be implemented in software. The behavioral description at this level corresponds directly to the introductory specification of the system. The topological description, usually in the form of a *block diagram*, indicates at this level the fundamental 'causes-and-effects' within the system. An example of such a block diagram for the copying lathe is shown in Fig. 1.4*a*. The geometrical description displays the system 'floor-plan', i.e. its overall shape and dimensions.

At the *functional design level*, the system architecture and functions are refined into more detail. The modules at this level are assumed to interact in the form of physically dimensionless continuous-time continuous-level signals, or signals discretized in time or in level or both. The module interactions are governed by algebraic rules. The topological description used at this design level is mostly in the form of block diagrams with blocks characterized by equations, transfer functions, tables, etc. Typically, the design of control strategy and control architecture, either analog or digital, is a matter of functional-level design.

An example of a block diagram showing control of the copying lathe is given in Fig. 1.4*b*. Two inputs affecting the control are considered in the diagram: stylus displacement r, and external forces caused by load and friction F. Output y is the machine-tool displacement, ε stands for control error and s is the Laplace operator. Velocity gain K and load stiffness c are parameters of the lathe. Note that the structure of this block diagram has nothing in common with the geometric structure of the real lathe shown in Fig. 1.3*a*. To set up this diagram, equations based on the physical laws governing the lathe operation must be formulated first, then simplified for the control synthesis purposes, and only after these two steps converted into the diagram.

The *physical design level* is concerned about hardware implementation of the system architecture and functions. Also 'parasitical' physical effects (like unwanted vibrations or heat generated during system operation) are considered there. Design modules take the form of real system components or physical effects and their mutual energetic interactions are expressed in terms of physical quantities. The topological description at the physical level takes on the form of a *multipole diagram*. An example of such a multipole diagram for the copying lathe is shown in Fig. 1.3*c*.

Note the fundamental differences between block and multipole diagrams:

- Each of the line segments interconnecting blocks in a block diagram represents an unidirectional transfer of one mathematical variable. The line segments interconnecting multipoles in a multipole
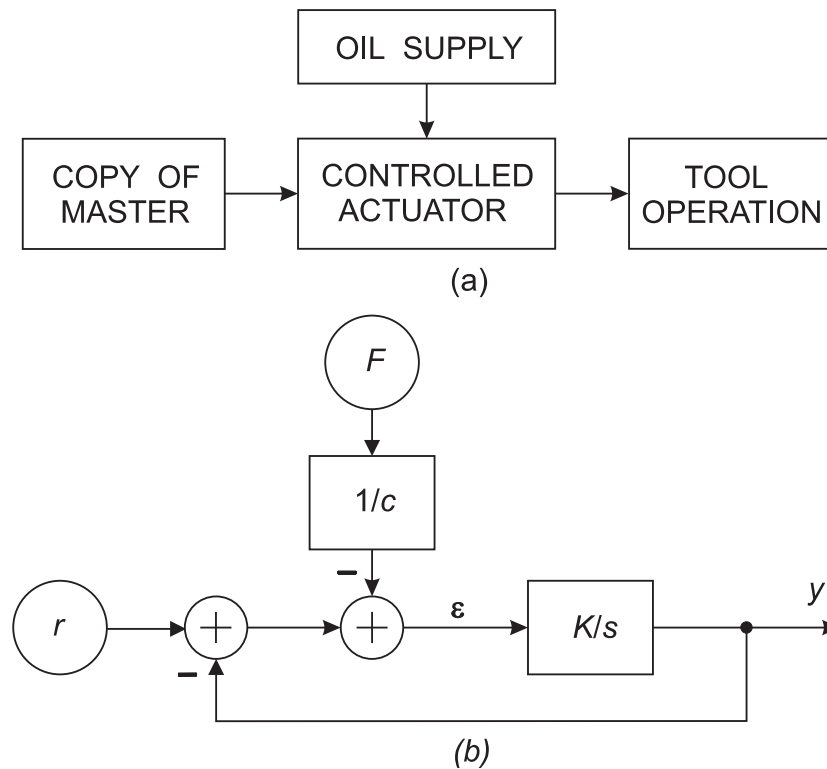
Figure 1.4: Copying lathe block diagrams at (*a*) the conceptual and (*b*) functional design level.

    diagram represent bilateral transfer of energy between system modules via electrical wires, fluid lines, shafts or other mechanical links, etc. Each of the line segments is associated with two physical quantities the product of which is a physical dimension corresponding to power.

- The mutual interactions of blocks follow algebraic rules whereas the multipole interactions are governed by physical laws of energetic balance and geometric compatibility.

- The block diagram is just a graphical representation of equations. To set up this diagram these equations must be formulated first and then converted into the diagram. The structure of this diagram has nothing in common with the structure of the real system which the equations characterize. The topological structure of the multipole diagram corresponds directly to the geometrical structure of the real system. Thus setting up of this diagram can be based simply on inspection of the real system.

    At the *technological design level* the assembly or another manufacturing process for the system and for its components is designed.

1.2.5 Design methodologies

Obviously, the aim of the design process is to proceed through the design space from its upper-left corner, representing the system specification, up to its lower-right corner, corresponding to the detailed technological documentation. The actual route through the design space corresponds to the chosen *design methodology*.

    There are two extremes in design methodologies: bottom-up and top-down. The *bottom-up methodology*, consisting of consecutively building the system from available components based on a sequence of design decisions, does not guarantee achieving an optimal system design. In fact, it does not guarantee that the system specification will be met at all. The *top-down methodology* is the most preferable, as it leads to optimal results. The down-going design routes, however, are subjected to constraints imposed by the lower design levels. Thus the actual design routes consist inevitably of many horizontal as well as vertical loops corresponding to the individual design iterations.

Module 2

Rectilinear mechanical systems

2.1   Rectilinear systems and their surroundings

To define the rectilinear system of our interest, we usually begin the investigation of the system dynamic behavior with drawing a sketch of the **system geometric configuration** showing dimensions and positions of the system bodies. To determine directions of the body motions and of the related forces, we associate the system sketch with a coordinate axes.

Fig. 2.1 shows, for example, a sketch of two cars in the rectilinear motion along a straight horizontal road. A car is towing another car using a towing rod connected between the car hooks A and B. The assumed positive direction of the car motions is in agreement with the direction of the x axis.
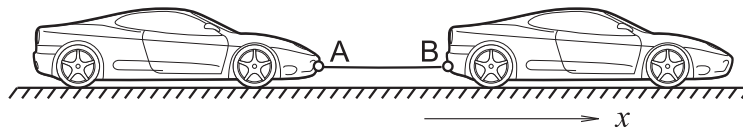

Figure 2.1: Car towing.

Bodies of the cars constitute together with the body of the rod a mechanical rectilinear system. Behavior of the system is influenced by the system surroundings formed by the wind blowing opposite to the car motions as well as by the friction between the car tyres and the road surface.
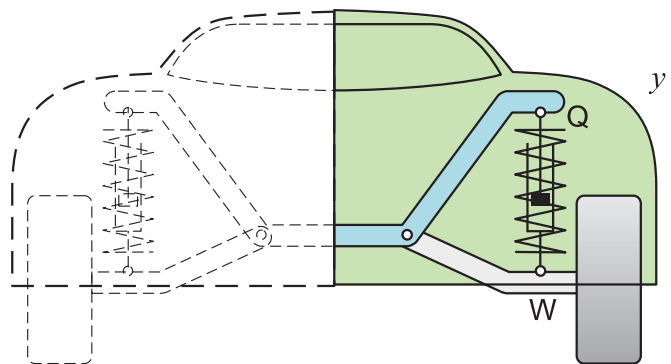

Figure 2.2: Wheel suspension system.

Fig. 2.2 was sketched for the purpose of the dynamic analysis focused on the behavior of a car-wheel suspension. When the car travels along a road, the wheel tyre copies potholes in the road surface. The wheel is thus driven up or down in the vertical direction along the axis y. In this case, the rectilinear system under consideration consists of four bodies: the spring, the shock absorber, the wheel and the quarter of the car body. The system excitation by the road surface and the gravitational attraction of the wheel and the quarter-car body forms the system surroundings in this case.

2.2   Rectilinear interactions

2.2.1   Rectilinear translation

Rectilinear motion of a point is defined as the motion of that point along a straight line. **Translational motion** of a body can be either rectilinear or curvilinear as shown in Fig. 2.3. All points of a body in **rectilinear translation** move in parallel straight lines. This is in contrast to **curvilinear translation** of bodies the points of which move on congruent curves.
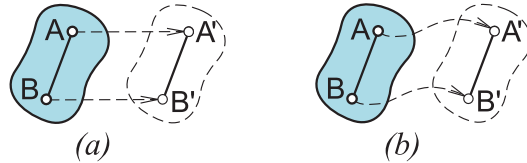
Figure 2.3: Body in (a) rectilinear and (b) curvilinear translation.

If a body can be considered rigid its rectilinear motion is completely specified by the motion of any one point in the body, since all points have the same motion. A **rigid body** is a body whose changes in shape are negligible compared with the overall dimensions of the body or with the changes in position of the body as a whole. If each of the cars shown in Fig. 2.1 is considered as a rigid body, motions of the cars can be represented, for example, by the points A and B denoting the cars' rod hooks.

Absolute rectilinear motion of a given point is defined as the motion of that point relative to a fixed point in space considered as a **reference frame** for the motion. Because of the difficulty of providing a real fixed point in space from which to make measurements, the concept of absolute motion is strictly hypothetical, but nevertheless very useful.

A reference frame fixed to the earth is often a reasonable approximation. However, when dealing with the motion of long-range missiles, for example, the earth cannot be considered to be a nonaccelerating reference and velocities are then measured with respect to the 'fixed' stars instead.

Fig. 2.4 shows a geometric configuration of points A and B representing the car hooks in Fig. 2.1. Motion of the points is constrained to the rectilinear translation along the x-axis 'painted' on the reference frame. The **position** $x_A(t)$ of point A is defined as the distance of this point from the origin 0 chosen on the axis x. In the figure, $x_A(t)$ is shown negative whereas the position $x_B(t)$ of point B is positive. Positions are measured in meters [m].
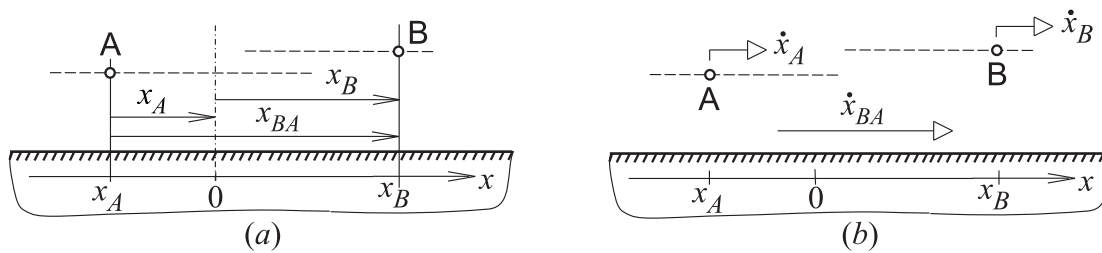
Figure 2.4: (a) Positions and (b) velocities of points in rectilinear motion.

The **absolute velocity** $\dot{x}_A(t)$ [m/s] and the **absolute acceleration** $\ddot{x}_A(t)$ [m/s²] of point A is by definition

$$\dot{x}_A(t) = \frac{d}{dt}x_A \quad \text{and} \quad \ddot{x}_A(t) = \frac{d\dot{x}_A}{dt} = \frac{d^2 x_A}{dt^2}$$

We shall depict the absolute velocities in drawings of geometric configurations by empty-head arrows as shown in Fig. 2.4. Displacements, velocities and accelerations are taken as positive if they correspond to a motion in the chosen positive direction of the related coordinate axis.

We shall often be concerned with the **relative motion** of two points. The relative displacement x_{BA}, relative velocity $\dot{x}_{BA}$ and relative acceleration $\ddot{x}_{BA}$ of point B with respect to point A is at any instant

$$x_{BA} = x_B - x_A, \quad \dot{x}_{BA} = \dot{x}_B - \dot{x}_A, \quad \text{and} \quad \ddot{x}_{BA} = \ddot{x}_B - \ddot{x}_A \tag{2.1}$$

Position, velocity or acceleration of a point with respect to another point can be measured by a device applied to the two points "across" the system without braking into it. Velocity can be thus considered as

an **across variable**, position as an integrated across variable, and acceleration as a differentiated across variable.

2.2.2 Forces

Force is the action on a body characterized by its magnitude, by the direction of its action, and by its point of application. Forces are measured in physical units called newton [N]. A force tends to move a body in the direction of its action.

Forces acting on a body are classified as either contact forces or body forces. **Contact forces** are generated through direct physical contact between two bodies or between a body and a fluid. **Body forces** are those applied by remote action, such as gravitational, electrostatic or electromagnetic forces. Actually both contact and body forces are **distributed forces** as the contact forces are in fact distributed over the cross-section area of the contact. In the system shown in Fig. 2.1, the forces of the wind acting on the cars are distributed over the car surfaces, while the forces in the towing rod are distributed over the rod cross-section area. If a rigid body is constrained to rectilinear translation all the forces acting on the body can be considered as **concentrated forces** acting at a point.

To take a complete account of all forces acting on a body, it is essential to construct the **free-body diagram** by isolating the body completely from the rest of the system and its surroundings. This diagram consists of a closed outline of the external boundary of the body. The diagram shows all the external contact and body forces applied to the body.
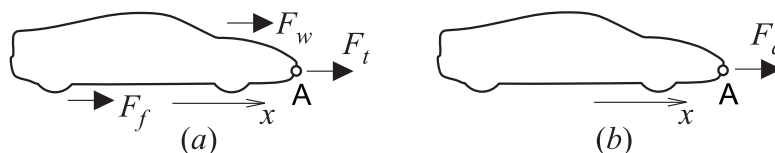

Figure 2.5: (*a*) Free-body diagram, (*b*) concentrated applied force.

Fig. 2.5*a* shows the free-body diagram of a towed car, a part of the rectilinear system introduced in Fig. 2.1. F_t is the force exerted on the car by the towing rod, F_w represents the distributed force of wind acting on the car surface, and F_f is the friction force acting on the car wheels due to the roughness of the road.

As it is indicated by full-head arrows, we have chosen the following convention for the orientation of forces applied to a body. The assumed positive direction of all applied forces is in agreement with the direction of the reference axis. Values of those applied forces that tend to accelerate the body in this direction are positive, if an applied force tends to decelerate the body its value is negative.

When we are dealing with an external action of a force on a rigid body in rectilinear motion, the force may be applied at any point of the body without changing its effect on the body as a whole. Thus, if the car shown in Fig. 2.5*a* is considered as a rigid body, all three forces applied on it can be replaced by one concentrated force F_a acting for example at point A as shown in Fig. 2.5*b*. Obviously,

$$F_a = F_t + F_w + F_f \tag{2.2}$$

A force F can be viewed as the time rate of the **linear momentum** μ [N.s] (called also impulse) acting in the same direction, i.e.

$$F(t) = \frac{d}{dt}\mu = \dot{\mu} \tag{2.3}$$

or

$$\mu = \int_0^t F(t)\, dt + \mu_0 \tag{2.4}$$

where μ_0 is the momentum at $t = 0$.

Forces can be measured directly by means of a calibrated spring, for example. To measure the force at a point directly, we must sever the system at that point and insert the measuring device between the two resultant system sections. Therefore, forces are thought of as being applied "through" the measuring device and hence can be considered as belonging to the family of **through variables**.

2.2.3   Power, energy and work

The **mechanical power** $\mathcal{P}$ delivered to a moving point by the force F which acts at that point in the direction of the positive velocity v is the product of the velocity and the component of force which lies in the direction of the velocity. If the force F and the velocity v are collinear,

$$\mathcal{P}(t) = v(t)\, F(t) \tag{2.5}$$

Power $\mathcal{P}$ is defined as the rate of flow of energy $\mathcal{E}$ or work $\mathcal{W}$ so that

$$\mathcal{P}(t) = \frac{d}{dt}\mathcal{E} = \frac{d}{dt}\mathcal{W} \tag{2.6}$$

In agreement with our convention for the orientation of applied forces, we will assume that energy is consumed in the body if the signs of the body absolute velocity and applied force are the same (both signs are positive or both are negative).

The **mechanical work** $\mathcal{W}$ done by one body on another through a point of connection is the time integral of the power:

$$\mathcal{W}_{ab} = \int_{t_a}^{t_b} v\, F\, dt \tag{2.7}$$

where t_a and t_b are the beginning and end of the time interval over which we desire to compute the work done.

The **mechanical energy** $\mathcal{E}$ supplied to a body is the sum of the work done on the body by all forces acting on it

$$\mathcal{E} = \sum_{k=1}^{n} (\mathcal{W}_{ab})_k \tag{2.8}$$

2.3   Composition of rectilinear interactions

2.3.1   Composition of rectilinear motions

Let us consider again Fig. 2.4 showing a geometric configuration of points A and B constrained to the rectilinear translation along the x-axis. According to (2.1), the relative displacement x_{BA}, relative velocity $\dot{x}_{BA}$ and relative acceleration $\ddot{x}_{BA}$ of point B with respect to point A is at any instant

$$x_{BA} = x_B - x_A, \quad \dot{x}_{BA} = \dot{x}_B - \dot{x}_A, \quad \text{and} \quad \ddot{x}_{BA} = \ddot{x}_B - \ddot{x}_A \tag{2.9}$$

These relations represent **geometric constraints** which are placed on the collinear rectilinear motions of points due to geometric continuity of space. This is just a demonstration of the **postulate of compatibility** in rectilinear translation.

The first relation in (2.9) can be rewritten as

$$x_A + x_{BA} + x_{0B} = 0 \tag{2.10}$$

where $x_{0B} = -x_B$. The left-hand-side of (2.10) expresses the final position of a point that has followed a closed path along the x-axis starting from its origin 0 and continuing through the points A, B and back again to 0. It is not surprising, of course, that the sum of the three path increments equals zero. Note, however, that differentiating (2.10) shows that also the sum of velocity increments as well the sum acceleration increments along the close route equals zero.

Computed examples

Composition of motions

2.3.2   Composition of forces

Fig. 2.6a gives an example in which point A constrained to rectilinear motion along the x-axis is acted on by forces $F_1(t)$ and $F_2(t)$ collinear with x. The assumed positive direction of the forces is indicated

by the full-head arrows. According to **Newton's third law** of action and reaction, the forces acting on a point are in equilibrium, i.e., their resulting effect is zero. Thus,

$$F_1(t) + F_2(t) = 0, \quad \text{or} \quad F_1(t) = -F_2(t) \tag{2.11}$$

This shows that the forces $F_1(t)$ and $F_2(t)$ are of the same magnitude but of the opposite direction at any instant. If F_1 is considered as an action force, F_2 then forms the reaction to F_1, and vice versa.
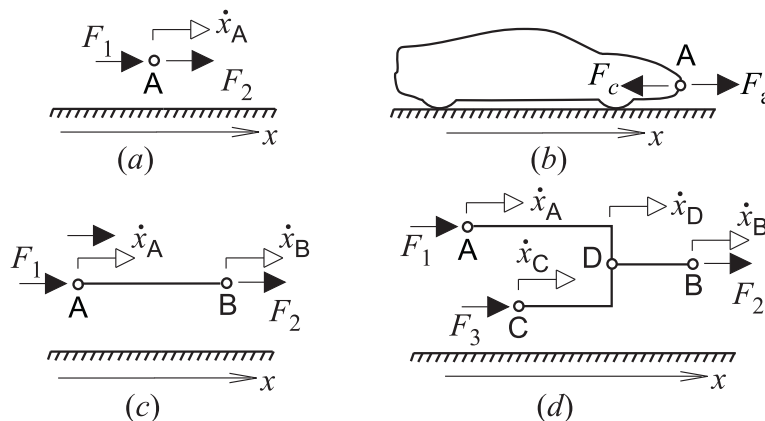

Figure 2.6: Balance of forces acting on (a) a point, (b) a body, (c) an ideal rectilinear link, (d) a configuration of ideal links.

The action of a force on a body can be separated into two effects, external and internal. Forces external to a body are of two kinds, applied forces and reactive forces. The effects of applied forces internal to the body are the resulting internal stresses and strains distributed throughout the material of the body. The relation between internal forces and internal strains involves the material properties of the body and is studied in strength of materials, elasticity, and plasticity. In mechanics of rigid bodies, concern is given only to the net external effects of forces. Fig. 2.6b shows the external force F_a applied on a car and the corresponding reaction force of the car $F_c = F_a$.

The **principle of transmissibility** states that an external force applied at a point of a rigid body constrained to rectilinear motion may be considered to be transmitted or to flow unchanged through the body to any other point of the body.

Fig. 2.6c shows points A and B moving along the x-axis. The points, which are interconnected by an ideal rectilinear link, are acted on in the x-direction by forces F_1 and F_2 external to the link. The **ideal rectilinear link** is by definition absolutely rigid and has no mass. The link is characterized by the relations

$$F_1(t) + F_2(t) = 0 \tag{2.12}$$
$$\dot{x}_A(t) = \dot{x}_B(t) \tag{2.13}$$

The relation (2.13) is identical with (2.11). This indicates that due to the principle of transmissibility the force equilibrium holds also if the forces $F_1(t)$ and $F_2(t)$ applied to the endpoints of an ideal rectilinear link. The second relation (2.13) follows from the assumption that there are no link deformations due to forces acting on the link. As the link is massless it is not subjected to any inertial forces and it neither accumulates, nor dissipates any energy.

This example may be generalized for any number of points interconnected by ideal rectilinear links. Fig. 2.6c shows three points A, B and C acted on by forces F_1, F_2 and F_3, respectively. The points are linked to point D. All the points are in rectilinear translation along the x-axis. The three forces are in equilibrium and the point velocities are identical, i.e.,

$$F_1(t) + F_2(t) + F_3(t) = 0 \tag{2.14}$$
$$\dot{x}_A(t) = \dot{x}_B(t) = \dot{x}_C(t) = \dot{x}_D(t) \tag{2.15}$$

Fig. 2.7a shows two cars interconnected by a towing rod. The cars are considered as rigid bodies and the rod as an ideal rectilinear link. The assume positive orientation of the car reaction forces F_{c1} and
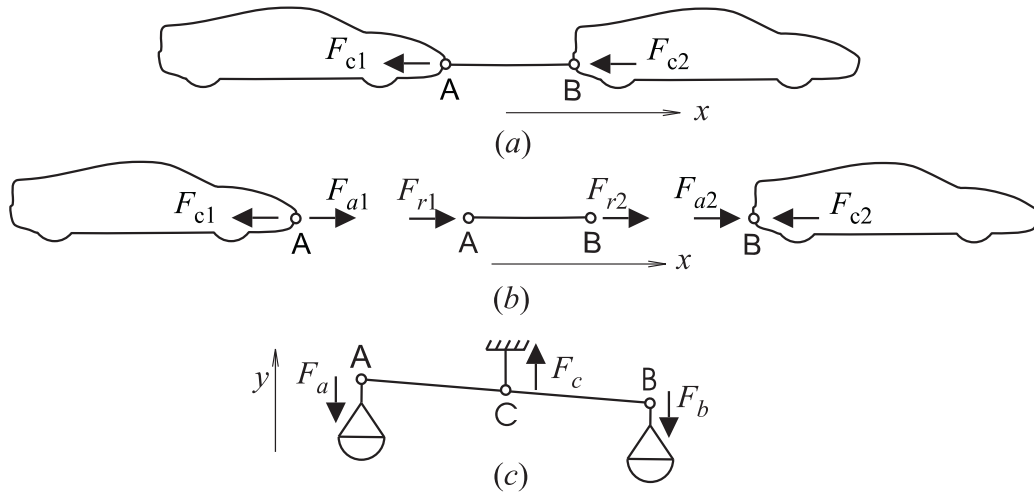
Figure 2.7: (a) Applied and reaction forces. (b) Reaction forces flowing through the system. (c) Reaction forces in the pair of scales.

F_{c2} shown within the car outlines opposes the x-direction. The car reaction forces can be imagined as flowing through the two-car assembly, and they are in balance, i.e.

$$F_{c1} + F_{c2} = 0 \tag{2.16}$$

To prove (2.16), let us consider Fig. 2.7b showing free-body diagrams of the cars and towing rod. The forces denoted outside the cars and the rod are applied forces the assumed positive direction of which is the x-direction. Let us assume that

$$F_{a1} = F_{r1} + F_{o1} \quad \text{and} \quad F_{a1} = F_{r2} + F_{o2}$$

where F_{r1} and F_{r2} are forces applied on the cars by the towing rod, and F_{o1} and F_{o2} are the other external forces applied on the cars. When submitting these relations into (2.16) after taking into consideration that $F_{c1} = F_{a1}$ and $F_{c2} = F_{a2}$ we obtain

$$F_{r1} + F_{o2} + F_{r2} + F_{o2} = 0$$

The forces F_{r1} and F_{r2} acting on the rod are in balance, and the other external forces F_{o1} and F_{o2} applied to the system of rigid bodies must be in balance too.

The reaction forces in the vertical links of the pair of scales shown in Fig. 2.7c must be balanced, i.e.

$$F_a + F_b + F_c = 0$$

This conclusion can be viewed as a demonstration of the **postulate of continuity** in rectilinear translation.

Computed examples

Static equilibrium of forces

2.4   Rectilinear inertia of mass

2.4.1   Pure inertor

Components of mechanical systems having mass resist changes of their velocity due to **inertia forces** acting on the mass. Let us consider a body of a constant mass m [kg] in a rectilinear motion of absolute acceleration a [m/s^2]. According to **Newton's second law**, the inertia force F [N] acting on the mass in the opposite direction to the mass acceleration is

$$F(t) = m\, a(t) = m\, \frac{d}{dt} v(t) \tag{2.17}$$

where v [m/s] is the absolute velocity of the mass with respect to a nonaccelerating reference frame.

Using the definition of force (2.3), Newton's second law (2.17) can be expressed also as

$$\mu(t) = m\,v(t) \tag{2.18}$$

where μ is the linear momentum acting on the mass. By definition, $\mu = 0$ when $v = 0$. Thus

$$m\,v = \int_{t_0}^{t} F(t)\,dt + \mu(t_0) \tag{2.19}$$

The inertia effects encountered in rectilinear translation of bodies can be modelled by the idealized physical element called **pure inertor**. The inertor ignores, however, damping, spring or any other energy effects in bodies. Our symbol for the inertor is shown in Fig. 2.8a. The symbol consists of a square representing the mass and of a short line segment called a **pin**. The pin denotes the **pole** of the inertor which represents the inertor energy interactions with the rest of the system.
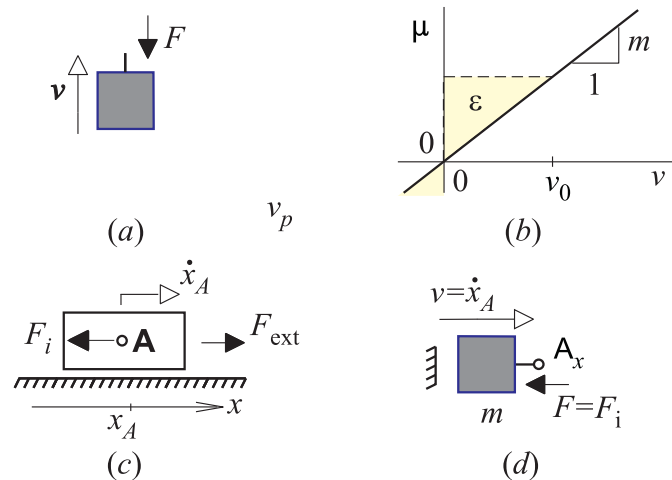

Figure 2.8: (a) Symbol of inertor. (b) Momentum vs. velocity characteristic of ideal inertor. (c) Sliding body, (d) its model.

The pure inertor is associated with two variables: the **inertor force** F representing the inertia force of the modelled mass, and the **inertor velocity** v representing the absolute velocity of the mass. The assumed positive orientation of F and v with respect to the inertor symbol is indicated in Fig. 2.8a by the full-head and empty-head arrow, respectively.

Dynamic behavior of the pure inertor is completely described by the constitutive relation

$$\mu = f(v) \tag{2.20}$$

where $f(\cdot)$ is a function. A pure inertor characterized by the linear constitutive relation (2.18) or (2.17), where the mass m is constant, is called the **ideal inertor**. The relationship (2.18) is plotted in Fig. 2.8b.

From the theory of relativity we know that mass of a given body increases with the body velocity approaching the velocity of light. As the present considerations are limited to velocity levels small compared with the velocity of light, Newton's second law can be applied. No other nonlinear inertia effects are known. In some engineering problems, however, the mass of a body changes with time.

Fig. 2.8c shows the free-body diagram of a rigid body sliding with a negligible friction along a horizontal surface in the x-direction. Let us assume that point A was chosen to represent the body rectilinear motion as well as the site of application of all the external forces F_{ext} acting on the body. Such a point can be considered as the body **mass point**, i.e. a point of the body associated with the lumped body mass constrained to the rectilinear motion.

Fig. 2.8d gives the dynamic model of the sliding body in the form of a multipole diagram. Point A of the real body moving in the x-direction as shown in Fig. 2.8c is represented in the diagram by the node A_x. Diagram **nodes** represent sites of energy interaction between bodies.

This is in agreement with our convention about the orientation arrows for reactions to external forces applied to bodies. The empty-head arrow, which denotes the assumed positive orientation of the inertor velocity v, is directed towards the inertor pole away from the reference frame.

As we assume that the body is not subjected to any other effects except its own inertia, there is only one physical element in the diagram – the inertor – which is attached to node A_x. If no external force F_{ext} is acting on the body in this example, the inertia force F_i is zero and the body velocity $\dot{x}_A$ is also zero or constant.

The inertor is in fact a two-pole physical element. But its second pole, with respect to which the inertor velocity should be 'measured', must be always attached to the reference frame. For this reason, the second pole need not be shown in the inertor symbol just to simplify the diagrams.

2.4.2   Inertia energy

From (2.17) it is obvious that the power entering an ideal inertor at a given instant is

$$\mathcal{P}(t) = v(t)\, F(t) = m\, v(t)\, \dot{v}(t) \tag{2.21}$$

If $\mathcal{P} > 0$, energy is being stored in the inertor, and if $\mathcal{P} < 0$, the stored energy is being retrieved from it. Which of these two states is occurring depends both on the relative velocity and acceleration at the moment.

Integration of (2.21) gives the expression for the energy accumulated in the ideal inertor

$$\mathcal{E} = \frac{1}{2} m\, v^2$$

which is called **rectilinear kinetic energy**. The energy is represented by the area in Fig. 2.8b between the μ axis and the μ-v characteristic.

We can see that this energy depends directly on the velocity acquired by the inertor, but not on its force. Hence the inertor stores energy by virtue of its velocity. The inertor energy is always positive and does not depend on the sign of either its velocity or acceleration.

2.5   Prescribed rectilinear interactions

2.5.1   Prescribed velocities

If a body is driven by a prescribed velocity $v(t)$ [m/s], the actuator driving the body can be modelled by the **pure source of velocity**. This idealized physical element is characterized by the constitutive relation

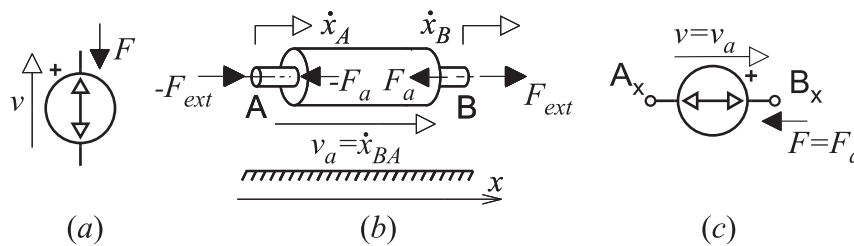$$v(t) = f(t) \tag{2.22}$$

where $f(t)$ is a known function of time.

Figure 2.9: (a) Symbol of pure source of velocity. (b) Actuator of prescribed relative velocity and (c) its multipole model.

Fig. 2.9a gives our graphical symbol for the pure source of velocity. The two pins sticking out of the circle denote the source poles representing the energy interaction of the source with the rest of the system. Besides the prescribed velocity $v(t)$, the source is associated with its force $F(t)$. This force counterbalances the forces imposed on the source by the system in which the source operates. The source polarity denotes the + sign by one of its poles. The assumed positive orientation of $v(t)$ and $F(t)$ in relation to the symbol polarity is indicated in Fig. 2.9a by the empty-head and full-head arrow, respectively.

Fig. 2.9b shows a real rectilinear actuator of negligible mass acting between the interaction sites A and B so that $\dot{x}_{BA}(t) = v_a(t)$ where $v_a(t)$ is the actuator velocity. Let us assume that $v_a(t)$ is sufficiently

independent from the external forces F_{ext} and $-F_{ext}$ exerted on the actuator by the system. Then the actuator can be modelled by a pure source of velocity as shown in Fig. 2.9c. The rectilinear motion of the interaction sites A and B in the x-direction is represented in the model by nodes A_x and B_x.

F_a and $-F_a$ are the internal actuator forces counterbalancing the external forces. Let us assume that the source symbol modeling the actuator is placed in the diagram in such a way that the orientation of its velocity v is in agreement with the velocity v_a of the actuator. Then the source force F represents the internal actuator force F_a acting at the site of interaction represented by the node to which the $+$ pole of the source is attached.

The power consumed by the source of velocity is

$$\mathcal{P}(t) = v(t) \cdot F(t) \tag{2.23}$$

If the velocity v and force F of the source are either both positive or both negative the modelled actuator consumes energy supplied by the remaining system. In the former case, the system forces the actuator to extend its length whereas in the latter case the actuator length is shortened by the system. If, however, the signs of the source velocity v and force F are different the modelled actuator delivers energy into the system. If both signs are positive the actuator pushes the system sites apart, if both signs are negative the sites pulled closer to each other.
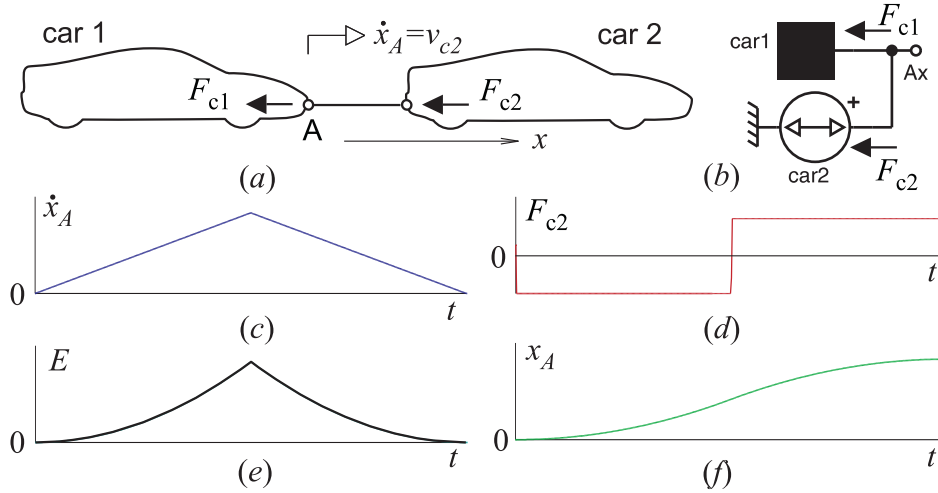
Example:

Figure 2.10: (a) Car towing, (b) its model. (c) Towing velocity profile, (d) corresponding force exerted by towing car, (e) energy accumulated in towed car, (f) position of both cars.

The most trivial dynamic model of the two-car system shown in Fig. 2.10a is given in Fig. 2.10b. As it is assumed that all the system bodies are rigid and the towing rod is massless a single point – the point A – is sufficient for representing the system rectilinear motion along x. Only inertia is considered in the towed car dynamics and the towing car is modelled by a source of velocity.

Let us consider the case when the velocity profile of the towing car velocity v_{c2} is triangular (Fig. 2.10c). The source force F_{c2} response (Fig. 2.10d) is then negative constant when the velocity increases, and positive constant when the velocity decreases. Therefore, the towing car supplies energy into the system in the former case whereas it consumes energy in the latter case. In both cases, the energy accumulated in the towed car is positive (Fig. 2.10e).

The forces F_{c1} and F_{c2} are in balance, i.e.

$$F_{c1}(t) + F_{c2}(t) = 0 \tag{2.24}$$

In conformity with our conventions, the arrows indicating orientation of the forces F_{c1} and F_{c2} oppose the x-direction in the system geometric representation, while they are directed away from the non-reference node A_x in the model of the system.

2.5.2   Indicators of position and acceleration

Unlike velocities or forces, positions and accelerations are not primary variables representing rectilinear motion in multipole diagrams. Nevertheless, they can be indicated very easily using blocks: integrators for positions and differentiators for accelerations.
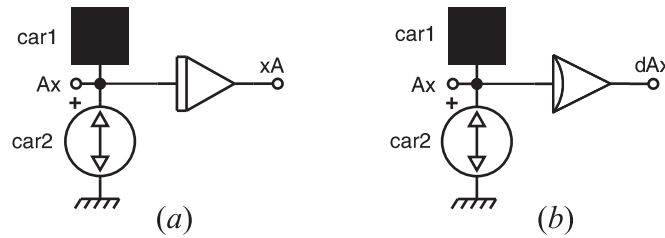

Figure 2.11: Indication of (a) position and (b) acceleration.

To demonstrate this, Fig. 2.11a shows indication of the car position x_A in the car-towing model given in Fig. 2.10b. The input of an integrator is attached to the node A_x. Thus the velocity $\dot{x}_A(t)$ associated with this node is integrated to obtain at the integrator output the position $x_A(t)$ of the point A representing the car motion:

$$x_A(t) = \int_{t_0}^{t} v(\tau)d\tau + x_A(t_0)$$

The initial condition of the integration $x_A(t_0)$ corresponds to the initial position of point A at $t = t_0$. The car position is for the triangular velocity profile shown in Fig. 2.10f.

In a similar way, a differentiating block can be used to indicate the car acceleration. This illustrates Fig. 2.11b in which the differentiator is attached to the node A_x. The indicated acceleration

$$\ddot{x}_A = \frac{d}{dt}\dot{x}_A$$

is denoted at the differentiating block output as dAx.

Note that attaching a block input to a node does not disturb the force balance at the node as no force enters any block.

2.5.3   Prescribed forces

To model actuators of prescribed forces we need to introduce a **pure source of force**. In general, such a source exhibits a force $F(t)$ characterized by the constitutive relation

$$F = f(t) \tag{2.25}$$

where $f(t)$ is a known function of time.

Our graphical symbol for the source of force is given in Fig. 2.12a. The full-head and empty-head arrows indicate the assumed positive orientation of the force $F(t)$ and velocity $v(t)$ associated with the source. The variable orientation is related to polarity of the source symbol denoted by the $+$ sign. The relative velocity $v(t)$ of the source represents the velocity imposed on the force source by the rest of the system in which the source operates.
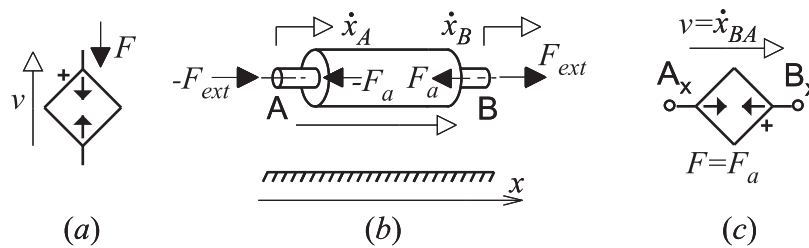

Figure 2.12: (a) Symbol of pure source of force. (b) Actuator of prescribed force and (c) its multipole model.

Fig. 2.12b shows a real rectilinear actuator of a prescribed force F_a acting along the x-axis between the interaction sites A and B of a system. The actuator force F_a is counterbalancing the external force F_{ext} to the actuator. The effect of the real actuator is modelled in Fig. 2.12c using the pure source of force. The motion of the interaction sites A and B in the x-direction is represented in the model by the nodes A$_x$ and B$_x$.

Polarity of the full-head arrow for the force F_a indicates that if $F_a > 0$ the actuator pulls the sites A and B closer. If $F_a < 0$ the actuator pushes the sites A and B apart.

The source symbol should be oriented between the nodes in agreement with the orientation of the x axis associated with the real actuator. Therefore, the $+$ pin of the symbol should be attached to the node B$_x$ representing the actuator site of interaction B that is assumed to move 'faster' then its site A. If the source is oriented properly its force F represents the prescribed force F_p acting at the site B related to the $+$ pole of the source.

If the source symbol modeling the actuator is placed in the diagram in such a way that the orientation of its velocity v is in agreement with the velocity v_a of the actuator, the source force F represents the actuator force F_a at the actuator end which is related to the $+$ pole of the source.

If the source velocity v and force F are either both positive or both negative the modelled actuator consumes energy supplied by the remaining system. In the former case, the system forces the actuator to extend its length whereas in the latter case the actuator length is shortened by the system. If, however, the signs of the source velocity v and force F are different the modelled actuator delivers energy into the system. If both signs are positive the actuator pushes the system sites apart, if both signs are negative the sites pulled closer to each other.
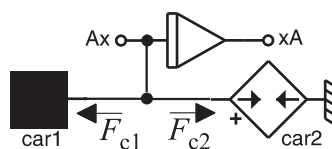
Examples:

Figure 2.13: Car towing.

The free vertical fall of a ball shown in Fig. 2.14a is modelled in Fig. 2.14b using a source of force F_g to model the gravitational force $F_g = 9.81m$ acting on the body. The ball air resistance is neglected in the model.
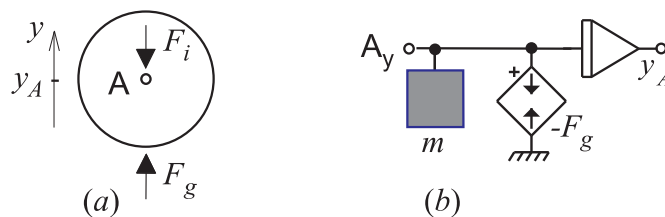

Figure 2.14: (a) Free fall of ball, (b) its model.

2.5.4   Indicators of velocities and forces

Pure sources of *zero* force can be used as physical elements modeling ideal **indicators of velocity**, i.e. instruments measuring relative velocity of distinct sites of interaction. Our graphical symbol for such an indicator is given in Fig. 2.15a. Direction of the arrow showing the assumed positive polarity of the indicated velocity is fixed to the polarity of the symbol.

Fig. 2.15b shows this symbol utilized to indicate the relative velocity of a force actuator modelled by the pure source of force placed between nodes A$_x$ and B$_x$.

Pure sources of *zero* velocity can be utilized as physical elements modeling ideal measuring instruments or **indicators of force**. Our graphical symbol for such an indicator is given in Fig. 2.16a. Direction of the arrow showing the assumed positive polarity of the indicated force is fixed to the polarity of the
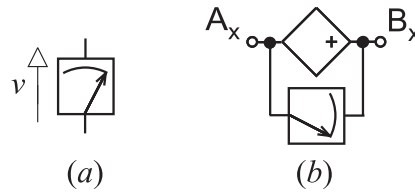
(a)   (b)

Figure 2.15: (a) Symbol of ideal indicator of velocity. (b) Indication of a source-of-force velocity.

symbol. Fig. 2.16b shows this symbol utilized to indicate the force of a source of velocity representing the force exerted on a velocity actuator by the system in which it operates.

Note the difference between measuring velocity and force. The direct measurement of forces requires disconnecting the system and connecting it back by a force indicator. Velocities (as well as positions or accelerations) are measured by indicators applied to systems without any need to disconnect them. This is the reason why velocities represent **rectilinear across variables** while forces are **rectilinear through variables**.

(a)   (b)
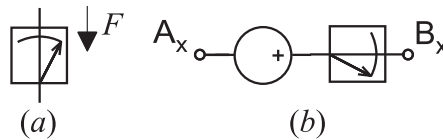
Figure 2.16: (a) Symbol of ideal indicator of force. (b) Indication of a source-of-velocity force.

Solved problems
    Composition of motions
Solved problems Static equilibrium of forces
Solved problems
    Body driven by given force
    Body driven by given velocity
    Vertical throw of a ball
    Body driven by a frequency-variable force

2.6   Rectilinear damping

Almost every mechanical motion is associated with some inherent degree of friction which resists the motion. Sometimes friction is unwanted but must be tolerated and accounted for, as, for example, in bearings or in the aerodynamic drag on a moving body. In other cases friction is desired and is designed into equipment, as in brakes, clutches, belt drives, and wedges. Wheeled vehicles depend on friction for both starting and stopping, and ordinary walking depends on friction between the shoe and the ground. Friction is utilized in vibration dampers and shock absorbers such as dashpots used in car suspension systems to damp car oscillations caused by riding over bumps in the road.
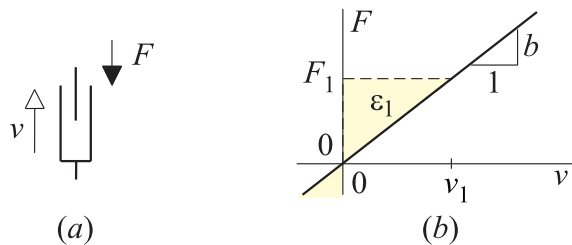

(a)   (b)

Figure 2.17: (a) Symbol of pure damper, (b) $F - v$ characteristic of the ideal damper.

Fig. 2.17a gives our graphical symbol for pure rectilinear dampers. A **pure rectilinear damper** exerts a resistive force F that is a function of the relative velocity v of its motion, but exhibits no mass

or spring effects. Thus,

$$F = f(v) \tag{2.26}$$

where $f(\cdot)$ is a function such that $F = 0$ when $v = 0$. In the case of an **ideal rectilinear damper** this constitutive relation is linear, i.e.,

$$F(t) = b \cdot \dot{x}(t) \tag{2.27}$$

where b [N.s/m] is the **damping constant** of the ideal damper. The ideal damper characteristic is shown in Fig. 2.17b.

Characteristics close to those of an ideal damper demonstrate, for example, the sliding surfaces shown in Fig. 2.18a if they are separated by a thin layer of a fluid lubricant, or the dashpot in Fig. 2.18c if it does not move too fast. In such cases the friction forces result from the viscous drag of a fluid under laminar flow conditions.

Fig. 2.18a shows sliding surfaces in contact pushed towards each other by some forces F_n normal to the motion. The frictional forces F_r resisting a relative motion of the surfaces must be compensated for by external forces F_{ext}.
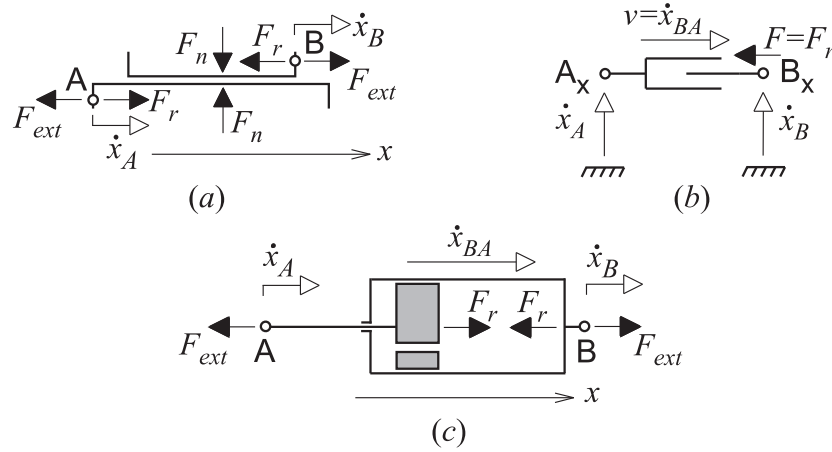
Figure 2.18: (a) Sliding surfaces in contact, (b) corresponding model. (c) Oil-filled shock absorber.

In Fig. 2.18b, the friction effect between sliding surfaces is modelled by an ideal damper. Nodes A_x and B_x in the model represent x-motions of points A and B of the real surfaces in the x-direction. If the surfaces are well lubricated by a fluid, the damping constant

$$b = \frac{A\nu}{d} \tag{2.28}$$

where A is the common area and d is the thickness of the lubrication film between the surfaces, ν is the viscosity coefficient of the lubricant.

Note the way in which the polarities of the damper relative velocity v and resistive force F are associated with the damper symbol shown in Fig. 2.17a. As the symbol is asymmetric, no $+$ sign is necessary to denote the symbol polarity (as it was the case of pure sources). If the damper symbol is placed in a multipole diagram in such a way that its velocity v represents polarity of the relative velocity $\dot{x}_{BA}$, then the damper force F represents the resistive force F_r at the 'faster' site of interaction. The damper force F thus corresponds in Fig. 2.18b to the resistive force counterbalancing the net external force F_{ext} acting on point B in the real bodies.

Since no mass is associated with the surfaces, the external forces F_{ext} applied to the interaction sites A and B are balanced, and the same must be true about the reaction forces F_r at these sites. Thus an external force applied to point B is assumed to flow through the damper to point A without any change.

The shock absorber shown in Fig. 2.18c consists of a piston inside an oil-filled cylinder in which fluid is forced through a narrow orifice in the piston by relative motion, thus producing resisting force. In this case, the damping constant can be approximated as

$$b = 8\pi\nu\ell \left[\left(\frac{D}{d}\right)^2 - 1 \right]^2 \tag{2.29}$$

where D is the cylinder diameter, d is the diameter of the orifice, and ℓ is the length of the orifice.

The mechanical power dissipated in the pure damper as heat is

$$\mathcal{P} = \dot{x} \cdot F$$

Note that it is always positive regardless of the direction of the damper relative motion.

Solved problems

Viscous friction experiment

Car suspension system

2.7   Rectilinear compliance

2.7.1   Rectilinear deformations

Materials undergo a deformation when they are compressed or stretched. If a mechanical component experiences a steady deformation when acted on by steady forces, it is exhibiting **compliance**. The component compliance can be modelled by **pure springs**. As these physical elements ignore any inertial and dissipative effects, their deformation is a function only of the applied forces. Fig. 2.19a gives our symbol of pure springs. The symbol resembles a wire coil spring shown in Fig. 2.19b, the most familiar mechanical device design to exhibit compliance.
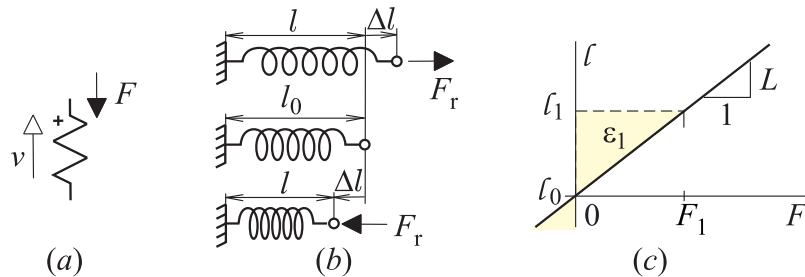
Figure 2.19: (a) Symbol of pure spring. (b) Coil spring stretched and compressed. (c) Ideal-spring deformation characteristic.

The spring deformations due to compliance are often approximated to be proportional to the applied force. A linear pure spring, which is called an **ideal spring**, has a proportional relation between deformation and force,

$$\Delta\ell = L \cdot F \tag{2.30}$$

where $\Delta\ell$ [m] is the spring deformation, F [N] is the spring restoring force, and the constant parameter L [m.N^{-1}] is the **compliance factor** of the spring. The reciprocal value of the compliance factor, $K = 1/L$ [N.m^{-1}], is the spring **stiffness** termed also the **spring constant**.

For example, the compliance factor of a coil spring can be derived using the methods of applied mechanics to be approximately

$$L = \frac{8D^3 n}{G d^4}$$

where D [m] is the spring pitch diameter (mean coil diameter), d [m] is the diameter of the wire, n [–] is the number of coil turns, and G [N.m^{-2}] is the shear modulus of the coil material.

The compliance factor of a cylindrical bar made of homogenous ideally elastic material is according to **Hook's law**

$$L = \frac{\ell_0}{E \cdot A} \tag{2.31}$$

where ℓ_0 [m] is the force-free length of the rod, A [m^2] is the rod cross-sectional area, and E [N.m^{-2}] is the Young's modulus of elasticity of the rod material.

Fig. 2.19b shows a stretched, force-free and compressed spring. The spring deformation $\Delta\ell = \ell - \ell_0$ where ℓ is the spring actual length $\ell = x_B - x_A$ and ℓ_0 is the free length of the spring. If $\Delta\ell > 0$ the spring is stretched, if $\Delta\ell < 0$ the spring is compressed. Fig. 2.19c shows the $\ell - F$ characteristic of the ideal spring.

By differentiating (2.30), we can arrive at the constitutive relation of an ideal rectilinear springs

$$v = L \cdot \frac{d}{dt} F \qquad (2.32)$$

where $v = d\ell/dt$ is the spring relative velocity. Alternatively, the relation (2.32) can be expressed in the integral form

$$F = K \int_{t_0}^{t} v \, d\tau + F(t_0) \qquad (2.33)$$

Fig. 2.20a shows a coil spring placed between the interaction sites A and B in the x-motion. If the spring mass is negligible in comparison with masses of the interacting components it can assumed that the external forces F_{ext} applied to the spring end-points are balanced. This implies that also the restoring forces F_r, opposing the external forces, are balanced at the spring end-points.
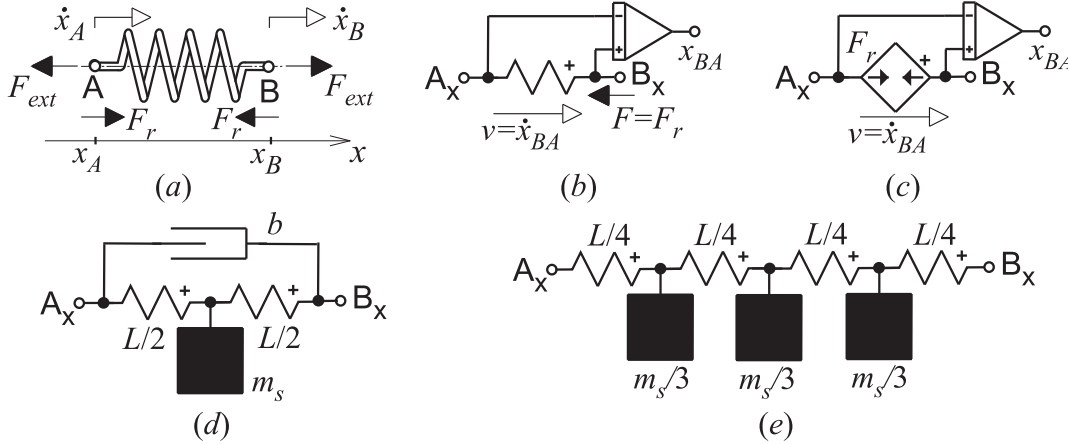
Figure 2.20: (a) Coil spring, (b) force-controlled and (c) elongation-controlled model. (d) Model respecting spring mass and damping. (e) Distributed-parameter model.

Note that one of the pins of the pure-spring symbol given in Fig. 2.19b is denoted by the $+$ sign. This allows for an unambiguous association of the polarities of the spring velocity v and the spring force F with the polarity of the symbol. In Fig. 2.20b, the pure-spring symbol is oriented in conformity with the chosen orientation of the modelled real spring shown in Fig. 2.20a. Then the pure-spring force F represents the real-spring restoring force F_r at the assumed 'faster' end of the real spring.

To express the total length of the modelled spring, the pure spring is combined with an integrator in Fig. 2.20b. For a chosen pre-loading force $F(t_0)$ of the spring, the initial relative distance between the spring end-points at $t = t_0$ should be specified as

$$x_{BA}(t_0) = \ell_0 + L \cdot F(t_0) \qquad (2.34)$$

where $\ell(t_0)$ is the initial length of the spring.

Fig. 2.20c gives an alternative elongation-controlled model to the ideal rectilinear spring shown in Fig. 2.20b. The ideal spring is replaced there by a source of the restoring force

$$F_r = k\left[x_{BA}(t) - \ell_0\right] \qquad (2.35)$$

The source is controlled by the relative distance of the spring end points x_{BA}. The initial value of this distance for a chosen initial length of the spring $\ell(t_0)$ is

$$x_{BA}(t_0) = \ell(t_0) \qquad (2.36)$$

Examples:
Fig. 2.21c shows a dynamic model of the ball suspended on a spring given in Fig. 2.21a. Node A_y represents the y-motion of point A of the ball. The spring symbol is placed between the node A_y and the reference node in such a way that the polarity of its velocity v is in agreement with the polarity of the relative velocity of the real spring along the y axis. As a result, the pure spring force F represents,
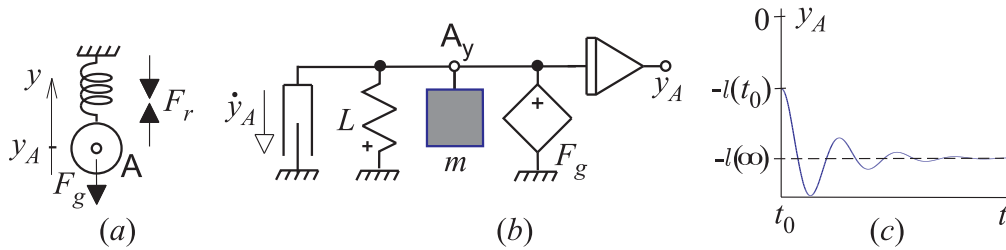
Figure 2.21: (a) Suspended ball, (b) its dynamic model, (c) ball position.
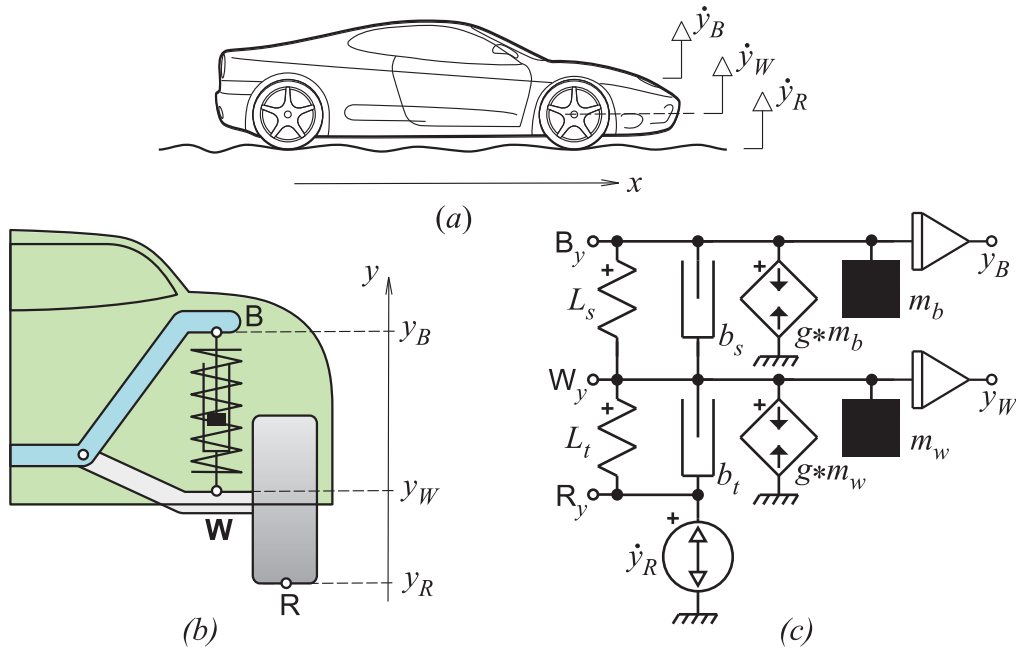

Figure 2.22: (a) Car following bumpy road, (b) car-wheel suspension, (c) quarter-car model.

both by its magnitude and polarity, the actual restoring force counterbalancing the gravitational force F_g acting on point A in the real bodies. The effect of the gravitational force $F_g = 9.81m$ is modelled using a source of force.

Fig. 2.22a shows a car following a bumpy road while Fig. 2.22b shows just a detail of the car, the suspension of one of its wheels. In Fig. 2.22c point R_y represents the y-motion of the contact point between the car tyre and the road surface R when the car moves in the x-direction. Points W_y and B_y represent the y-motion of the wheel axis W and the body-suspension interaction point B, respectively. L_t and b_t is the compliance and damping and mass of the wheel tyre, respectively. Similarly, L_s and b_s is the compliance and damping of the wheel tyre, m_w is the mass of the complete wheel and m_b is the quarter of the mass of the car body. The model is excited by the source of the velocity $\dot{y}_R$ resulting from the tyre copying the road bumps.

2.7.2   Spring potential energy

From (2.30) and (2.31) we can see that the energy flow into an ideal rectilinear spring at a given instant is

$$\mathcal{P} = \dot{x} \cdot F = L \cdot F \cdot \dot{F} \tag{2.37}$$

If $\mathcal{P} > 0$, energy is being stored in the spring, and if $\mathcal{P} < 0$, the stored energy is being retrieved from the spring. Which of these two states is occurring depends both on the spring deflection and relative velocity at the moment.

Integration of (2.37) gives an expression for the energy accumulated in the ideal rectilinear spring

$$\mathcal{E} = \frac{1}{2} L \cdot F^2$$

which is called **rectilinear potential energy**.

We note that this energy depends directly on the force transmitted through the spring, but not on the velocity difference. Hence the spring stores energy by virtue of its force. This energy is always positive and does not depend on the sign of either the force or the spring deflection.

2.8 Summary

To set up a dynamic model of a real rectilinear system and to simulate its behavior using DYNAST, you should proceed through the following steps.

1. Sketch the geometric configuration of your system, i.e.:

    - clearly separate the system of your concern from the system surroundings and determine a reference frame for the system
    - associate the rectilinear motions with a coordinate axis
    - for each body denote the geometric point representing its rectilinear motion and give it a name
    - assume the positive velocity of each such point in the direction of the chosen coordinate axis

2. Set up a multipole diagram representing the dynamic model of your system and its surroundings (you may use directly the DYNAST schematic editor):

    - for each body place a node into the diagram corresponding to the geometric point representing the body velocity
    - give each node a name identical with the name of the point (using a label in the DYNAST schematic editor)
    - associate each of the nodes with the symbol for inertors
    - place into the diagram one or more symbols for reference nodes representing the reference frame
    - place symbols for elements representing couplings between the nodes (if necessary, interconnect the element pins with the nodes by links)
    - add symbols for elements representing the system surroundings
    - invert the element symbols if their velocity is oriented in the opposite direction with respect to the chosen coordinate axis
    - give names to the inertors and the other elements and specify values of their parameters

3. Specify analysis of your system model:

    - select the Numerical Nonlinear Analysis
    - specify the required Time Interval of the analysis and set the values of Initial Conditions
    - select Desired Variables like node and element velocities, element forces, and block outputs
    - To invoke the analysis, select Run Analysis & Plot in menu Run

4. Interpret the analyzed results:

    - Set the desired variables in menu Plot
    - in menu Axes choose the way you want to plot the variables
    - the assumed positive polarity of velocities are oriented in the direction of the chosen coordinate axes whereas the assumed positive polarity of forces of the elements is opposite to this direction

Module 3

Rotational mechanical systems

3.1 Rotational interactions

3.1.1 Rotational motion

In rotation about a fixed or nonaccelerating axis all points of the site other than those on the axis move in concentric circles about the fixed axis.
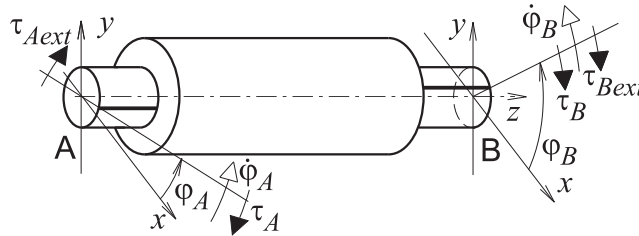

Figure 3.1: Subsystems in rotational motion.

Fig. 3.1 shows a subsystem with two concentric shafts rotating about the z-axis fixed to the reference frame. The subsystem might be a torsional spring, a rotational damper, or a gearbox, for example. The ends of the shafts A and B are in contact with shafts of some other subsystems. The power intake of the subsystem due to the rotational motion of its energy entries A and B about the z axis is

$$\mathcal{P}(t) = \dot{\varphi}_A(t) \cdot \tau_A(t) + \dot{\varphi}_B(t) \cdot \tau_B(t)$$

where $\dot{\varphi}_A(t)$ and $\dot{\varphi}_B(t)$ are absolute angular velocities of the entries A and B about the z axis. $\tau_A(t)$ and $\tau_B(t)$ internal torques counterbalancing external torques $\tau_A ext(t)$ and $\tau_B ext(t)$ applied to the entries.

Absolute angular motion about the axis z is described in Fig. 3.1 by the **angular displacement** φ, i.e., by the angle subtended between a line drawn on the rotating entry which lies in the x-y-plane perpendicular to the axis of rotation z and the coordinate axis x fixed to the reference frame. In this text, the counterclockwise direction will be considered as the positive orientation of rotation in a plane perpendicular to the axis of rotation.

Absolute angular velocity $\dot{\varphi}(t)$ [rad/s] and **absolute angular acceleration** $\ddot{\varphi}(t)$ [rad/s2] of an entry is by definition

$$\dot{\varphi}(t) = \frac{d\varphi}{dt} \quad \text{and} \quad \ddot{\varphi}(t) = \frac{d\dot{\varphi}}{dt} = \frac{d2\varphi}{dt2}$$

where $\varphi(t)$ is the angular displacement of the entry. The **relative angular displacement**, **relative angular velocity** and **relative angular acceleration** of the entry B with respect to the entry A is

$$\varphi_{BA} = \varphi_B - \varphi_A \quad \dot{\varphi}_{BA} = \dot{\varphi}_B - \dot{\varphi}_A \quad \ddot{\varphi}_{BA} = \ddot{\varphi}_B - \ddot{\varphi}_A$$

3-1

3.1.2   Torque

A **moment of force** or **torque** τ [N.m] can be viewed as the time rate of the **angular momentum** $\rho(t)$ acting in the same direction, i.e.

$$\tau = \frac{d\rho}{dt}$$

The complete specification of a moment of force $\tau(t)$ must include its magnitude and the axis of rotation. To have the energy flow through an entry into a subsystem positive, the torques acting on the entry must be oriented in the opposite way with respect to the direction of the entry angular velocity.

3.2   Ideal rotational inertors

An *ideal rotational inertor* models the rotational motion of a rigid body about an axis fixed to the reference frame. The constituency relation of this physical element corresponds to Newton's second law which can be written as

$$\rho(t) = J\dot{\varphi}(t) \tag{3.1}$$

or as

$$\tau(t) = J\frac{d}{dt}\dot{\varphi} \tag{3.2}$$

where $\rho(t)$ is the element rotational momentum, $\tau(t)$ is the element moment of force, $\dot{\varphi}(t)$ is the element angular velocity, and J [kg.m^2/rad] is the moment of inertia of the element.

(a) (b) (c)
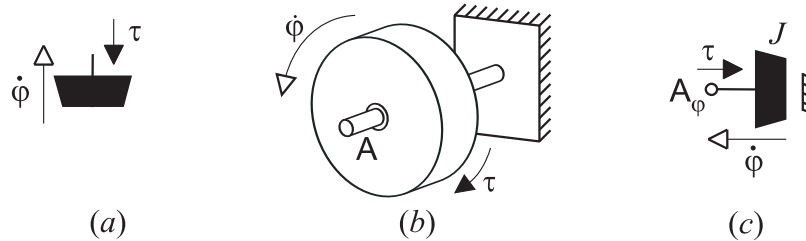
Figure 3.2: (a) Symbol of rotational inertor. (b) Flywheel, and (c) its model.

Rotational inertors model inertial effect in rotational motion of bodies exclusively, they ignore any damping or spring effects as shown in Fig. 3.2. The angular velocity $\dot{\varphi}(t)$ of a rotational inertor represents the absolute angular velocity of a body measured in relation to a nonaccelerating reference frame. Thus the $-$pole of rotational inertors must be always coalesced with a node corresponding to the reference. This is the reason why only the $+$pole is shown in the element symbol.

If the moment of inertia J_T of a body about a fixed axis passing through the mass center T is known, the moment of inertia J of the body about another fixed axis parallel to the former one can be determined as

$$J = J_T + mr^2 \tag{3.3}$$

where m is the mass of the body, and d is the separation of the axes. This formula, known as the **parallel-axis** or **Steiner's theorem**, is illustrated by Fig. 3.3. The diameter of the ball of the mathematical pendulum of Fig. 3.3a is so small that its moment of inertia is negligible. If also the mass of the pendulum string is neglected, the pendulum moment of inertia with respect to the axis of rotation A is $J = mr^2$. Fig. 3.3b shows a compound pendulum. If only the moment of inertia J_T with respect to mass center of the compound pendulum body is known, the pendulum moment of inertia with respect to the axis of rotation A must be determined using (3.3). The mass center of each of the pendulums is acted on by the moment of the gravitational force $F_g = mg$, the moment arm of length $r\sin\varphi$ varies with the pendulum deflection φ. In the dynamic model for both pendulums shown in Fig. 3.3c, the ideal rotational damper of factor B respects damping of the pendulums.

3.3   Ideal rotational dampers

The constituency relation of an *ideal rotational damper* with the symbol of Fig. 3.4a is

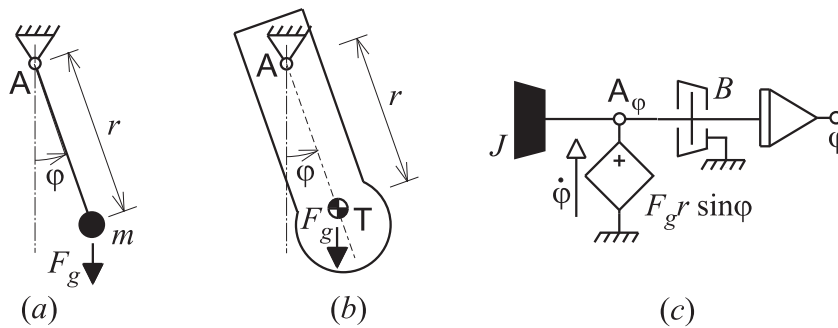$$\tau(t) = b_r \cdot \varphi(t) \tag{3.4}$$

Figure 3.3: (*a*) Mathematical and (*b*) compound pendulum, (*c*) pendulum dynamic model.

where $\tau(t)$ is the moment of force, $\dot{\varphi}(t)$ is the relative angular velocity, and b_r [N.m.s/rad] is the *rotational damping constant* of the damper.
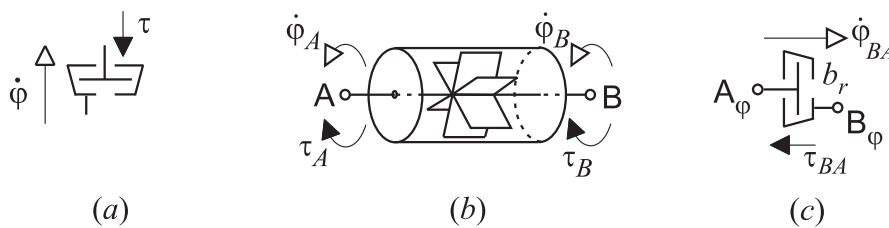

Figure 3.4: (*a*) Symbol of pure rotational damper. (*b*) Oil-filled rotational damper, and (*c*) its model.

An ideal rotational damper is a twopole model that ignores any mass or spring effects and assumes that a moment of force is proportional to the relative angular velocity of its poles. An example of a real device with the τ-$\dot{\varphi}$ characteristic close to that of the ideal damper, is the viscous rotational damper shown in Fig. 3.4*b*. It is a propeller rotating in oil inside a cylinder and producing the resisting moment of force.

The poles represent φ-motions of the energy entries B and A of a real damping subsystem. τ represents the internal moment of force at the entry associated with the +pole, i.e. at the entry B, counterbalancing an external moment of force applied to this entry. The positive direction of τ is opposite to that for the damper angular velocity $\dot{\varphi}$ corresponding to the relative velocity of the entries $\dot{\varphi}_{BA} = \dot{\varphi}_B - \dot{\varphi}_A$.

Since an ideal rotational damper has no moment of inertia, the moments of force acting on it must be balanced. Thus, an external moment of force applied to B_x in the φ-direction flows through the damper and out through A_x without a change and, at the same time, the internal moment of force at the damper $-$pole denoted by A_x must be $-\tau$. Note that the power flow into the ideal damper $\mathcal{P} = \dot{\varphi}\tau$ is always positive regardless of the direction of its relative motion.

Fig. 3.5*a* shows the symbol of the ideal rotational damper used to model a shaft passing through a well lubricated journal bearing fixed to the reference frame. In Fig. 3.5*b*, the same model is utilized for an oil-polluted clutch the discs of which are slipping with respect to each other so that they rotate with different angular velocity and there is a viscous friction effect between them.
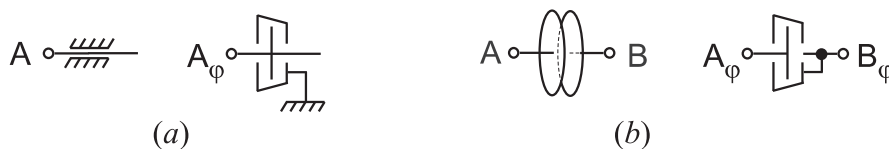

Figure 3.5: Ideal model of (*a*) a shaft in journal bearing, and (*b*) a slipping clutch.

3.4 Ideal rotational springs

For an *ideal rotational* or *torsional spring*, the constituency relation is

$$\varphi(t) = L_r \tau(t) \tag{3.5}$$

or

$$\dot{\varphi}(t) = L_r \frac{d}{dt} \tau(t) \tag{3.6}$$

where $\varphi(t)$ is the ideal spring angular displacement, $\dot{\varphi}(t)$ is the ideal spring angular velocity, $\tau(t)$ is the ideal spring moment of force, and L_r [rad.N^{-1}.m^{-1}] is the *torsional compliance* of the spring. The reciprocal value of L_r is the spring *torsional stiffness* or *torsional spring constant*.
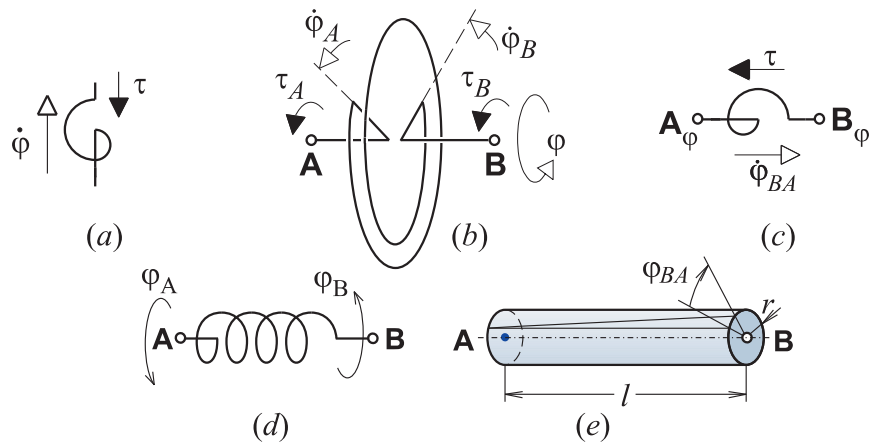
Figure 3.6: (*a*) Symbol of pure torsional spring. (*b*) Spiral torsional spring, and (*c*) its model. (*d*) Helical-coil spring. (*e*) Twisted rod.

The pure spring has no inertia by definition and hence transmits torque undiminished. One of the most common mechanical components which exhibit the characteristics of a rotational spring is the torsional spiral spring shown in Fig. 3.6*b*. Fig. 3.6*c* shows a helical-coil torsional spring, and Fig. 3.6*d* a twisted rod. φ_{BA} corresponds to the relative angular deformation of the real spring, while τ represents the spring internal moment of the force counterbalancing the external moment of a force applied to the spring.
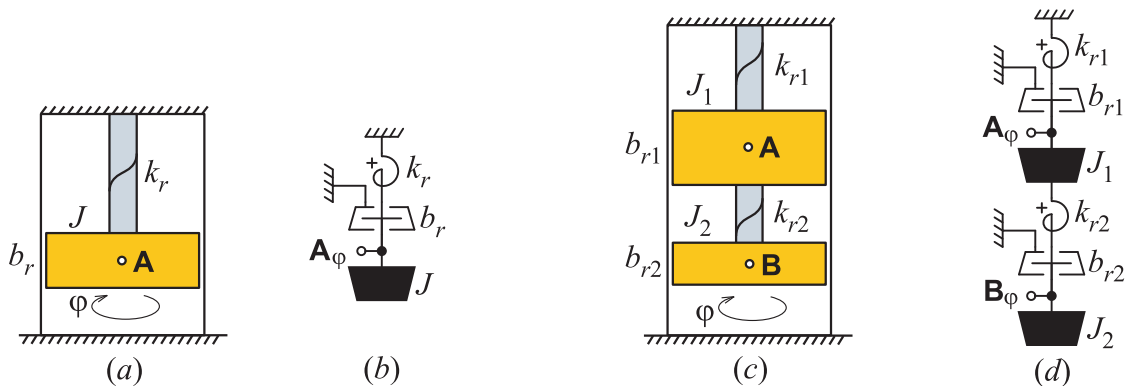
Figure 3.7: (*a*), (*b*) torsional pendulum. (*c*), (*d*) double torsional pendulum.

Module 4

Coupled mechanical systems

4.1 Translatory-to-translatory couplings

4.1.1 Translational transformer

Translatory-to-translatory coupling is the coupling between the translational motion of one point and the translational motion of another point along the same or different axis. Such couplings can be easily modelled by the **pure translational transformer**. It is an idealized mechanical device which neither dissipates nor stores any energy and determines ratios of velocities and forces associated with the two coupled motions. Fig. 4.1 shows our symbol for pure transformers. The variables associated in Fig. 4.1 with this symbol correspond to the special case when the symbol is applied to a translational transformer.
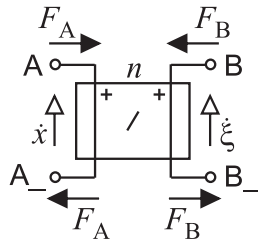
Figure 4.1: Pure translational transformer.

Motion of point A with respect to point A_ along the x axis is represented by poles A_x and A_{-x}, respectively. Similarly, motion of point B with respect to point B_ along the ξ axis is represented by poles A_ξ and $A_{-\xi}$. F_x is the force exerted by the transformer to move points A and A_ apart while counterbalancing external forces applied to these points. F_ξ is the force counterbalancing external forces applied to points B and B_.

The relation between velocities associated with the translational transformer is defined as

$$\dot{x}/\dot{\xi} = n \tag{4.1}$$

where $\dot{x}$ is the relative velocity of point A with respect to point A_, and $\dot{\xi}$ is the relative velocity of point B with respect to point B_, n is the **transformer ratio**. An ideal transformer has this ratio constant.

Forces associated with the translational transformer are related by definition as

$$F_\xi/F_x = -n \tag{4.2}$$

The power put into the translational transformer is

$$\mathcal{P} = F_x\dot{x} + F_\xi\dot{\xi} \tag{4.3}$$

After submitting (4.1) and (4.2), (4.3) becomes $\mathcal{P} = 0$. A pure translational transformer thus transforms a translational motion into another translational motion and vice versa. It performs this function with no energy loss or storage, so that the net power flow into a pure transformer is zero.

Table 4.1 shows examples of pure models of some translatory-to-translatory transducers. They include levers, pulleys and a rigid link of a fixed length the endpoints of which are constrained to a linear or circular path.

4.1.2   Levers

A translatory-to-translatory coupling is typified by a lever which has no mass, is infinitely stiff, and is free from frictional effects. Such a lever is shown in Fig. 4.2a.
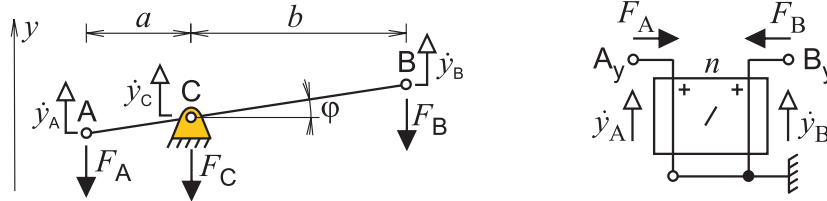

Figure 4.2: (a) Lever, (b) its dynamic model.

The relationship between the velocities of endpoints A and B of the lever with respect to the pivot C is

$$\dot{y}_A/\dot{y}_B = -a/b = n \tag{4.4}$$

where n is the **lever ratio**. Note that a and b change as φ varies, but that a/b remains constant. Often φ will be limited to a small angle, so that a and b are essentially constant.

The full-head arrows denote forces F_A, F_B and F_C exerted by the lever at its end points A and B and at the pivot C, respectively, to counterbalance external forces applied to these points. Since the massless lever has no momentum, then by definition the sum of the forces in any direction and the moments of the forces about the pivot must be zero:

$$F_A + F_B + F_C \;\; = \;\; 0 \tag{4.5}$$
$$F_A a + F_B b \;\; = \;\; 0 \tag{4.6}$$

Therefore,

$$F_B/F_A = a/b = -1/n \tag{4.7}$$

Note, that the relationships between velocities (4.4) and between forces (4.7) are the same as in the translational transformer used in Fig. 4.2b to model the lever.

4.2   Rotary-to-rotary couplings

4.2.1   Rotational transformer

Rotary-to-rotary coupling is the coupling between the rotational motion about a fixed axis and another rotational motion about the same or different axis. Such couplings can be easily modelled by the **pure rotational transformer**. It is an idealized mechanical device which determines ratios of angular velocities and torques associated with the coupled motions. Fig. 4.3 shows our symbol for pure transformers. The variables associated with this symbol in Fig. 4.3 correspond to the special case when the symbol is applied to a rotational transformer.
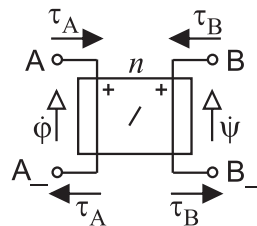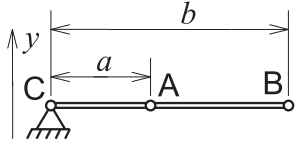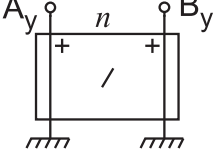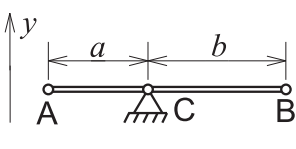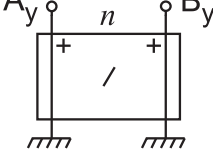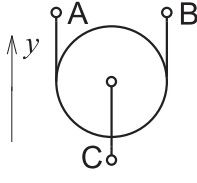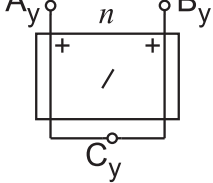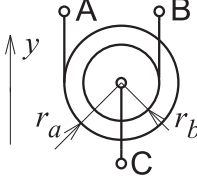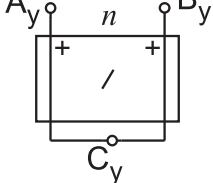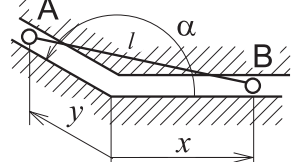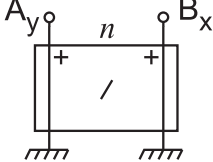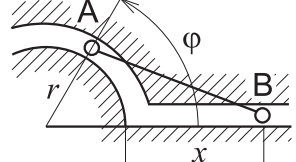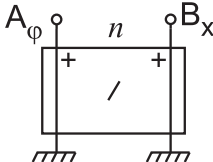

Figure 4.3: Pure rotational transformer.

Table 4.1: Examples of translatory-to-translatory motion converters.

Converter	Pure model	Coupling ratio n
		$\dfrac{a}{b}$
		$-\dfrac{a}{b}$
		-1
		$-\dfrac{r_a}{r_b}$
		$-\dfrac{x + y\cos\varphi}{y + x\cos\varphi}$
		$-\dfrac{x + r(1 - \cos\varphi)}{r(r + x)\sin\varphi}$

Rotational motion of point A with respect to point A_ rotating about the same axis with angular velocity $\dot{\varphi}$ is represented by poles A$_\varphi$ and A$_{-\varphi}$, respectively. Similarly, the rotational motion of point B with respect to rotating point B_ with the velocity $\dot{\psi}$ is represented by poles A$_\psi$ and A$_{-\psi}$. τ_φ is the torque exerted by the transformer to move points A and A_ apart while counterbalancing external torques applied to these points. τ_ψ is the force counterbalancing external torques applied to points B and B_.

Relation between angular velocities associated with the rotational transformer is

$$\dot{\varphi}/\dot{\psi} = n \tag{4.8}$$

where $\dot{\varphi}$ is the relative angular velocity of point A with respect to point A_, and $\dot{\psi}$ is the relative angular velocity of point B with respect to point B_. n is the **transformer ratio**. An ideal transformer has this ratio constant.

Torques associated with the rotational transformer are related as

$$\tau_\psi/\tau_\varphi = -n \tag{4.9}$$

The power put into the rotational transformer is

$$\mathcal{P} = \tau_\varphi\dot{\varphi} + \tau_\psi\dot{\psi} \tag{4.10}$$

After submitting (4.8) and (4.9), (4.10) becomes $\mathcal{P} = 0$.

A pure rotational transformer is thus an idealized mechanical device which transforms a rotational motion into another rotational motion and vice versa. A pure transformer performs this function with no energy loss or storage, so that the net power flow into a pure transformer is zero.

4.2.2   Gear trains

The simplest and most familiar example of a rotary-to-rotary coupling is the elementary gear train shown in Fig. 4.4a. Two mating gears of different sizes are attached to two parallel shafts which in turn are free to rotate supported in a housing. Gear-tooth profiles machined into the periphery of the gear disks cause the gears to behave like circular cylinders of radii r_a and r_b, which roll on each other without slipping, provided that the gears are rigid and the gear teeth are geometrically perfect. The radii r_a and r_b are called the *pitch radii* of the gears, and their magnitudes are proportional to the numbers of teeth N_a and N_b. The **gear ratio** is defined as
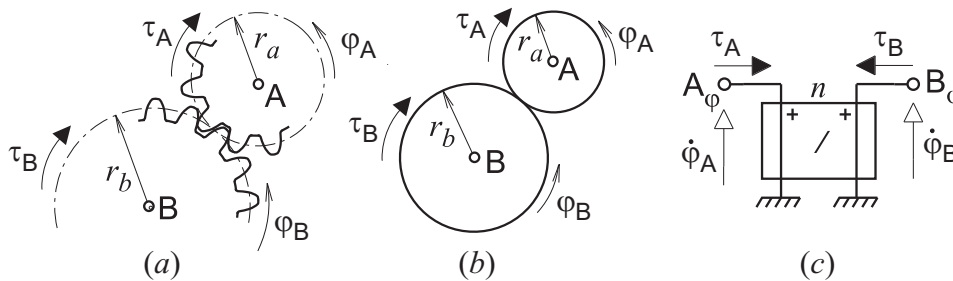
$$r_a/r_b = N_a/N_b$$

Figure 4.4: (*a*) Gear train, (*b*) its free-body diagram, (*c*) transformer model.

Since the gears are assumed to roll without slipping, the arc distance $r_a\dot{\varphi}_A\Delta t$ turned off on gear a must equal minus the arc distance $r_b\dot{\varphi}_B\Delta t$ turned off on gear b. Hence

$$\frac{\dot{\varphi}_A}{\dot{\varphi}_B} = -\frac{r_b}{r_a} = -\frac{N_b}{N_a} = n \tag{4.11}$$

where the negative sign indicates that the direction of $\dot{\varphi}_B$ is opposite to that of $\dot{\varphi}_A$.

To determine the relationship between the torques τ_A and τ_B, let us isolate the two gears from each other and from the frame, thus forming their free-body diagrams of Fig. 4.4b. Only torques and torque-producing forces are shown on these free bodies, and friction between the gear-tooth surfaces is assumed

Table 4.2: Rotary-to-rotary motion converters

Gear train	Configuration	Coupling ratio n
External spur gears		$-\dfrac{r_b}{r_a}$
Internal spur gears		$\dfrac{r_b}{r_a}$
Bevel gear pair		$\dfrac{r_b}{r_a}$
Planet gear		$\dfrac{r_b}{r_a}$
Skew gear pair		$\dfrac{r_b}{r_a}$

to be zero. If we further assume that the gears have zero inertia or constant speed, the net torque on each gear is zero. If we also assume the bearing torques to be negligible,

$$\tau_A = F_t r_a \quad \text{and} \quad \tau_B = F_t r_b$$

Employing now the definition of n in (4.11), we obtain

$$\frac{\tau_A}{\tau_B} = \frac{r_a}{r_b} = \frac{N_a}{N_b} = -1/n \tag{4.12}$$

Thus the speed is changed as n while the torque is changed as $1/n$. The net power into the gear train for $\dot{\varphi}_A = 0$ is therefore zero:

$$\mathcal{P} = \tau_A \dot{\varphi}_A + \tau_B \dot{\varphi}_B = \tau_A \dot{\varphi}_A + (\tau_A/n)(-\tau_A n) = 0$$

Since the gear system is assumed to have constant angular momentum, the torque τ_C shown acting on the container Fig. 4.4a must be equal to minus the sum of τ_A and τ_B, or

$$\tau_A + \tau_B + \tau_C = 0 \tag{4.13}$$

Since $\dot{\varphi}_C = 0$ in the preceding discussion, τ_C does no work on the system.

Table 4.2 shows various setups of gear trains that can be modeled by a single pure rotational transformer. The table gives the corresponding gear ratios.

4.2.3 Gear backlash

Fig. 4.5 indicates the way in which a pure model of a pair of spur gears can be augmented to take into the consideration backlash between the gears. Fig. 4.5b shows a simple characteristic approximating the

torque τ exerted by the gears on each other in relation to the angle φ_{AB} between the gears. The finite slope of the nonzero branches of the characteristic corresponds to the torsional stiffness of the gear teeth. The backlash effect is implemented in the model by adding the source of torque τ controlled by the angle φ_{AB} in accordance with the characteristic shown in Fig. 4.5b to the energy-transfer transformer modeling the backslashes motion conversion. Also slippage in rotary-to-rotary motion converter due to friction can be modelled in a similar way.
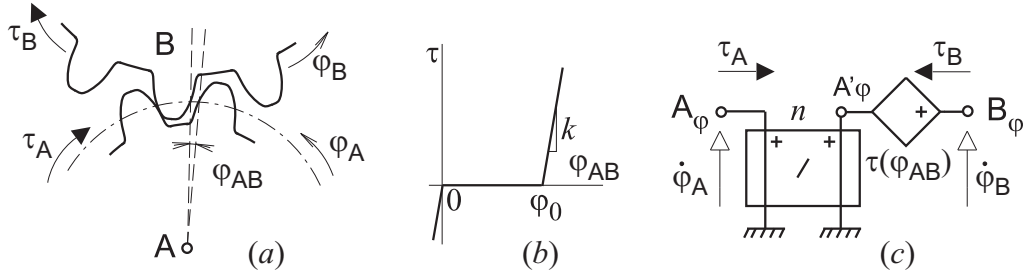
Figure 4.5: (a) Gear train with backslash, (b) backslash characteristic, (c) multipole model.
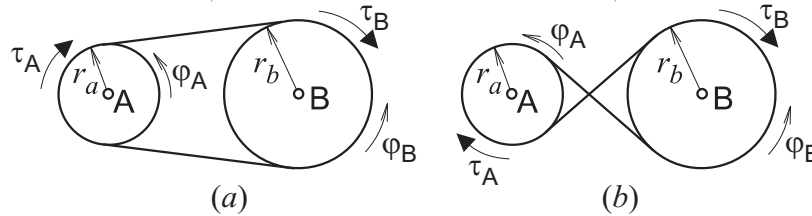
4.2.4　Belt and chain systems

Figure 4.6: Belt-and-pulley and chain-and-sprocket assemblies.

Fig. 4.6 shows pure belt-and-pulley and chain-and-sprocket systems that perform essentially the same function as gear trains. As opposed to a belt and pulley, the latter system does not allow slippage between the belt and sprocket due to the sprocket teeth. Note that the sign of n is positive in the case of the system in Fig. 4.6a as the pulleys rotate in the same direction, whereas in the case of the system in Fig. 4.6b the sign is negative.

4.2.5　Belt friction

Fig. 4.7a shows a flat belt passing over a fixed cylindrical drum. To model belt slipping let us consider interactions between segments of the belt and drum surface which are in contact. This can be taken as a one-dimensional translational problem if the belt segment as well as the adhering drum surface is straighten up as shown in Fig. 4.7b. The variables can be then related to the coordinate axis x.

The *Eytelwein's formula* gives the relation between the forces F_A and F_B acting at the belt-segment endpoints A and B. For the case when the belt is just about to slip if pulled to the right, i.e. if $F_A > F_B > 0$, the formula is:

$$\frac{F_A}{F_B} = e^{\mu\gamma} \tag{4.14}$$

where μ [–] is the coefficient of friction, and γ [rad] is the angle of the belt contact. This formula is derived under the assumption that the belt segment is massless and rigid, and the friction between the belt and the drum is governed by the 'law of dry friction'.

A multipole diagram of the belt friction constructed under the above assumptions is given in Fig. 4.7c. The contact areas of the belt and drum segments are represented there by poles A and C, respectively. Friction is modelled by a source of friction force F_f acting between these two poles. The rigid belt segment is modelled by the source of zero velocity $\dot{x}_{AB}$ placed between the poles A and B representing the belt-segment end points. At the same time, this source is employed in the model as a sensor of the tension in the belt segment. This tension force F_t is used to control the friction-force source F_f.
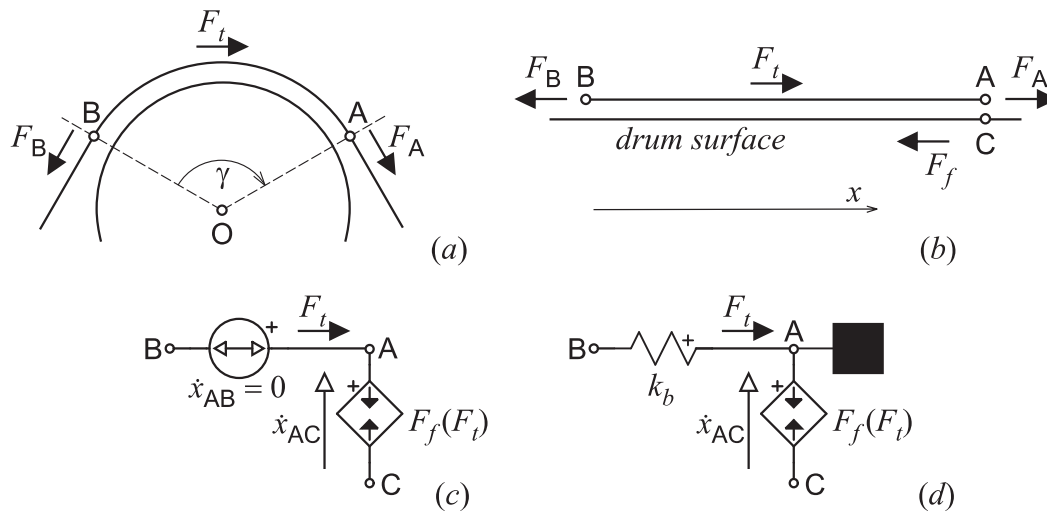
Figure 4.7: Belt friction.

Taking into consideration the balance relations for forces at the poles

$$F_A = F_t - F_f \qquad \text{and} \qquad F_B = -F_t \tag{4.15}$$

and substituting them into the formula we shall obtain the constitutive relation of the friction-force source

$$F_f = F_t \left(1 + e^{\mu\gamma \cdot \text{sgn}(F_t)}\right) \tag{4.16}$$

The function $\text{sgn}(F_t)$ was included into the formula to make it valid also for the case when the belt is pulled to the left, i.e. for $F_B > F_A > 0$. (You are encouraged to check its correctness.)

Equation (4.16) can be used both for static friction of impending slipping as well as for the slipping kinetic friction after substituting there either the coefficient of static friction μ_s or the coefficient of kinetic friction μ_k for μ. Fig. 4.8 shows an example of the F_f-$\dot{x}$ characteristic of combined static and kinetic friction governed by (4.16) for the tension $F_t = \pm 1$. Note that the characteristic is asymmetric with respect to the origin.
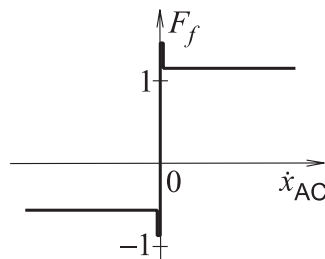

Figure 4.8: Belt friction characteristic.

As shown in Fig. 4.7d, the belt friction model from Fig. 4.7c can be completed to respect the belt segment flexibility k_b, and mass m_b. The belt friction model we have derived for moving belt and fixed drum applies equally well to problems involving fixed belt and rotating drum, like band brakes, and to problems involving both belt and drum rotating, like belt drives. It can be also used to systems with the belt replaced by a rope or a string.

In case of V-shaped belts (4.16) should be replaced by

$$F_f = F_t \left(1 + e^{\mu\gamma \cdot \text{sgn}(F_t)/\sin(\delta/2)}\right) \tag{4.17}$$

where δ is the angle of the 'V' of the belt cross section.

Fig. 4.9a shows an example of a hoisting machine lifting a load by means of a cable passing over an undriven sheave and wrapped around a driven drum. The rotary motion of the drum drive is transformed

into the translational motion of the cable by means of an ideal transformer with the ratio $1 : r_1$, where r_1 is the drum radius. The c_1 and c_2 parts of the cable are modelled by elements characterizing the cable flexibility and damping. The element parameters of the cable part c_2 depend on the cable length ℓ of c_2. The friction between the cable and the sheave is represented by the belt-friction model given above. The sheave dynamics, converted from rotary to translational motion along the cable, is represented by the elements of reduced parameters

$$m_r = J_s/r^2, \qquad b_r = b_s/r_2^2 \tag{4.18}$$

where J_s is the moment of inertia of the sheave, r_2 is its radius and b_s is the damping of the sheave bearing.
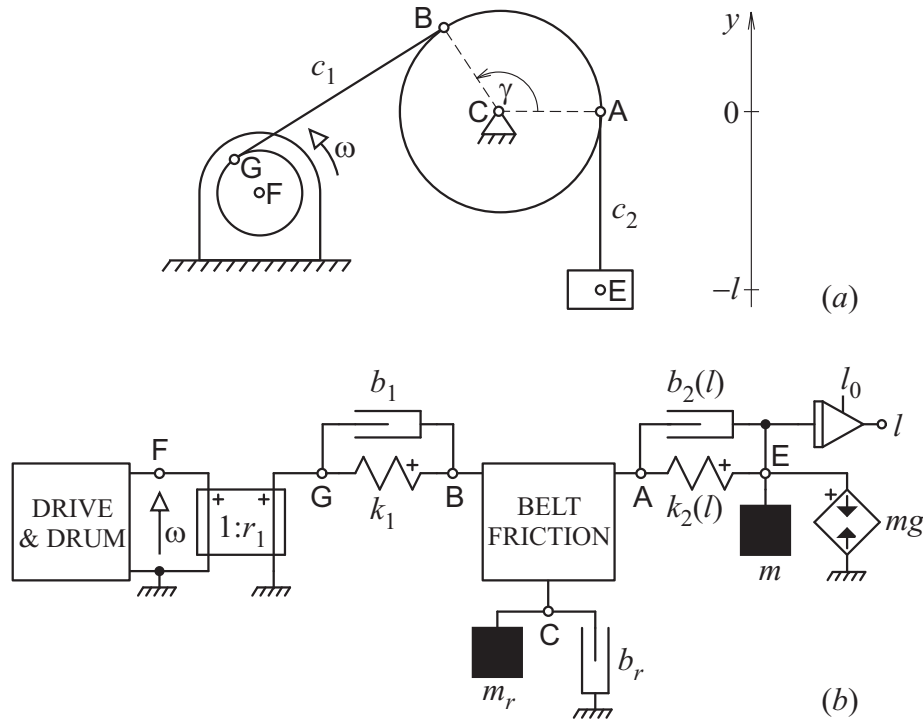

Figure 4.9: Hoisting machine.

4.3   Translatory-to-rotary couplings

4.3.1   Translatory-rotational transformer

Translatory-to-rotary coupling is a coupling between the translational motion and a rotational motion about a fixed axis. Such couplings can be easily modeled by the **pure translatory-rotational transformer**. It is an idealized mechanical device which determines ratio of the velocities as well as the ratio of the force and torque associated with the two coupled motions. Fig. 4.10 shows our symbol for pure transformers. The variables associated with this symbol in Fig. 4.10 correspond to the special case when the symbol is applied to a rotational transformer.

Rotational motion of point A with respect to point A_ along the x axis is represented by poles A_x and A_{-x}, respectively. Rotational motion of point B with respect to point B_ rotating about the same axis with the velocity $\dot{\varphi}$ is represented by poles A_φ and $A_{-\varphi}$. F is the force exerted by the transformer to move points A and A_ apart while counterbalancing external forces applied to these points. τ is the torque counterbalancing external torques applied to points B and B_.

Relation between angular velocities associated with the rotational transformer is
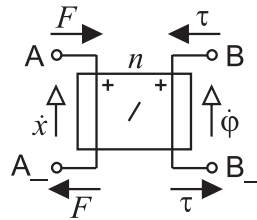
$$\dot{x}/\dot{\varphi} = n \tag{4.19}$$

Figure 4.10: Pure translatory-rotational transformer.

where $\dot{x}$ is the relative velocity of point A with respect to point A_, and $\dot{\varphi}$ is the relative angular velocity of point B with respect to point B_. n is the **transformer ratio**. An ideal transformer has this ratio constant.

The force and torque associated with the translatory-rotary transformer are related as

$$F/\tau = -n \tag{4.20}$$

The power put into the rotational transformer is

$$\mathcal{P} = F\dot{x} + \tau\dot{\varphi} \tag{4.21}$$

After submitting (4.19) and (4.20), (4.21) becomes $\mathcal{P} = 0$. A pure translatory-rotary transformer is thus an idealized mechanical device which transforms a translational motion into a rotational motion and vice versa. A pure transformer performs this function with no energy loss or storage, so that the net power flow into a pure transformer is zero.

4.3.2 Rack-and-pinion

In motion control problems it is often necessary to convert rotational motion into a translational one and vice versa. For instance, a load may be controlled to move along a straight line through a rotary motor and rack-and-pinion assembly, such as that shown in Fig. 4.11a. The pinion is a small gear, and the rack is a linear member with the gear on one side. The describing relation of this system is defined as
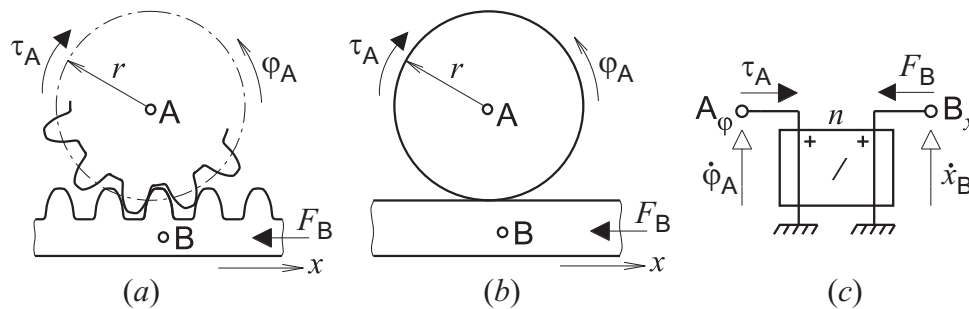
$$x = r\varphi \tag{4.22}$$

Figure 4.11: (a) Rack-and-pinion gear train, (b) equivalent system, (c) pure model.

Thus the constitutive relation of pure rotary-linear motion converters is

$$\begin{bmatrix} \dot{\varphi}(t) \\ F(t) \end{bmatrix} = \begin{bmatrix} 0 & n \\ -n & 0 \end{bmatrix} \cdot \begin{bmatrix} \tau(t) \\ \dot{x}(t) \end{bmatrix}$$

where the coupling ratio

$$n = \frac{\dot{\varphi}}{\dot{x}} = -\frac{F}{\tau} = \frac{1}{r}$$

To apply this result to the rack-and-pinion assembly movable along the x-axis as that shown in Fig. 4.12a, the variable x should be replaced by x_{AB}.
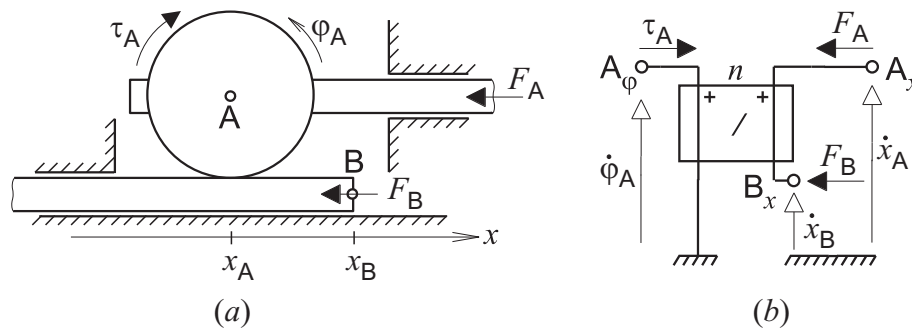
Figure 4.12: Movable rack-and-pinion assembly.

4.3.3   Pulley or sprocket assembly

Another approach to rotary-translatory motion conversion is to utilize the rotary motion of a pulley combined with the linear motion of a belt. The same effect is achieved by combining a sprocket with a chain, a drum with a rope or cable wound around it, etc. This concept is outlined in Fig. 4.13a.

A common assembly of two pulleys and a belt used for the control of a mass through one of the pulleys by a rotary prime mover is shown in Fig. 4.13b. Both the drive and idle pulley have the same radius r.
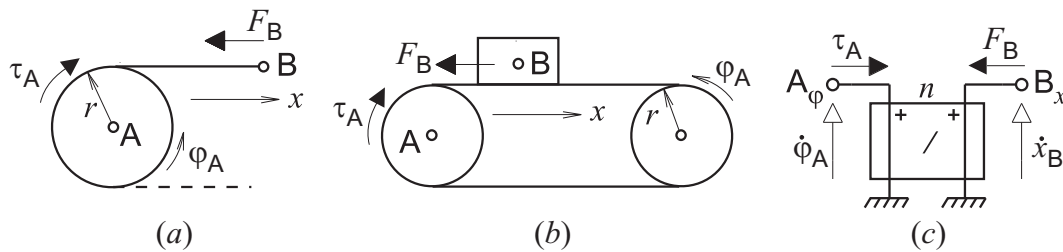

Figure 4.13: (a) Pulley or sprocket. (b) Belt and pulley rotary-translatory assembly.

4.3.4   Lead screws

Fig. 4.14 shows a similar situation in which a lead screw is used as the rotary-to-translatory mechanical linkage. The lead screw is used there to drive a payload along the z-axis. The screw is fixed free to rotate and as it is turned, the nut moves along the screw with the payload attached. In this case, the describing relation is defined as the screw rotation φ per unit of linear motion x. This is also referred to as the pitch P of the screw (the reciprocal of the pitch is called the lead). Therefore, the describing relation is

$$\varphi = \pm Px$$

and the coupling ratio of the lead screw is simply

$$n = \pm P$$

The sign is related to the mutual orientation of the rotational and translational motions.
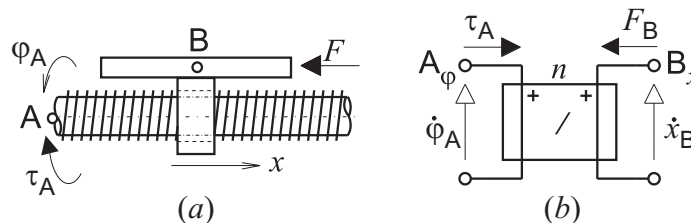

Figure 4.14: Lead screw assembly.

4.3.5 Slider cranks

Also various mechanical linkages are used as rotary-translatory converters. As an example of this approach, Fig. 4.15 shows a configuration of a crank driving a linear stage. The crank of length r rotates about its center A and has a rod of fixed length l mounted to its rotating end. The other end of the connecting rod B is attached to a linear stage which is constrained to move in only along the x-axis. As the describing relation is

$$x_{BA} = r \cos \varphi_A + \sqrt{l^2 - (r \sin \varphi_A + y_0)^2}$$

the reciprocal of the coupling ratio is

$$\frac{1}{n} = \frac{\dot{x}_{BA}}{\dot{\varphi}_A} = -r \sin \varphi_A - \frac{r \cos \varphi_A (r \sin \varphi_A + y_0)}{\sqrt{l^2 - (r \sin \varphi_A + y_0)^2}}$$
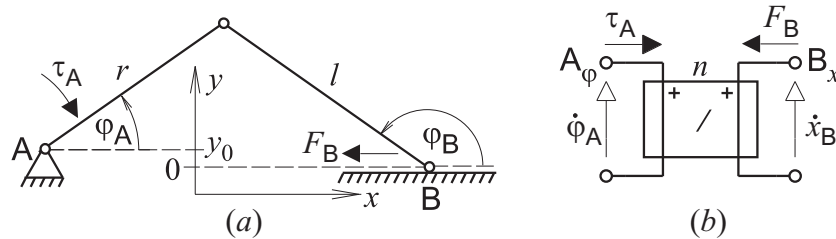

Figure 4.15: Slider crank.

As the crank rotates by 360°, the linear stage moves in both directions along x. There are two distinct angular positions of the crank that correspond to full extension and retraction of the stage called dead-center positions. If this module is used to convert linear to rotary motion the direction of rotation may go in either way in these positions (this problem is usually overcome by combining the crank with a flywheel).
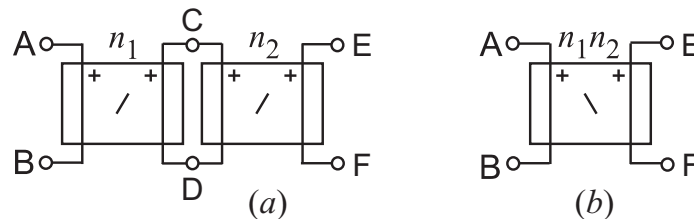
4.4 Load conversions

Figure 4.16: (a) Cascade interconnection of energy-transfer transformers, (b) one-transformer equivalent.

Fig. 4.16a shows a 'cascade' interconnection of energy-transfer transformers of coupling ratios n_1 and n_2. A simple analysis of the total transformation of across and through variables in the interconnection indicates that the cascade can be replaced by only one transformer with the coupling ratio $n_1 n_2$ shown in Fig. 4.16b.

Fig. 4.17 indicates the way in which series or parallel combinations of physical elements connected to a pole-pair of an energy-transfer transformer are 'seen through' the transformer, or referred to at the other transformer pole-pair. Z resp. Y is an impedance resp. admittance of the generic element, E resp. J is an independent source of an across resp. through variable. This is the principle behind utilizing various transducers and couplings to convert the amount of an actuator load at the price of changed related across and through variables.
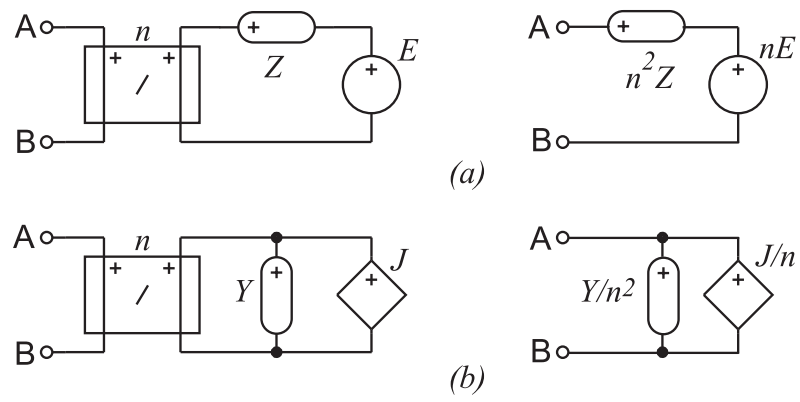
Figure 4.17: Load 'seen through' an energy-transfer transformer.

Module 5

Planar mechanical systems

5.1 Planar motion of particles

5.1.1 Planar curvilinear motion

Recollect that a particle is a body whose physical dimensions are so small compared with the radius of curvature of its path that the motion of the particle can be approximated as that of a point. A particle is in a planar motion if its path lies in a single plane. Consider the example of a planar curvilinear path of a particle shown in Fig. 5.1a where point A represents the particle position at time t.
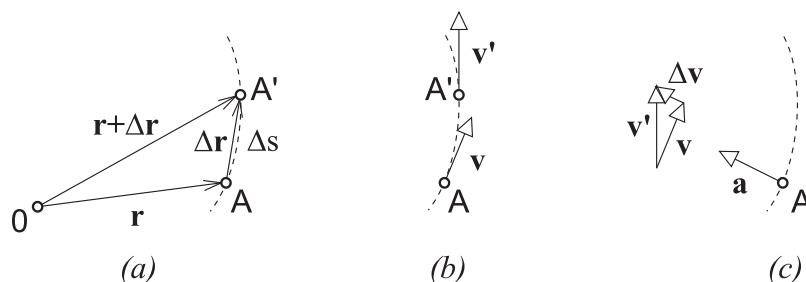

Figure 5.1: (a) Particle position, (b) velocity, and (c) acceleration vectors.

The particle position can be completely specified by the *position vector* **r** measured from a fixed origin O. At time $t + \Delta t$, the particle is at point A', the position of which is specified by the vector **r** + Δ**r**. The particle *displacement* during time Δt is indicated by the vector Δ**r** representing the vector change of position. If an origin O' is chosen at some location different from O, the position vector **r** changes, but Δ**r** remains unchanged. The *distance* traveled by the particle as it moves along the path from A to A' is the scalar length Δs measured along the curved path. Thus, the vector displacement Δ**r** is distinguished from the scalar distance Δs.

The *instantaneous velocity* **v** of the particle is defined as the limiting value of the particle average velocity between the points A and A' as the points become closer together and the time interval Δt approaches zero. Thus,

$$\mathbf{v} = \lim_{\Delta t \to 0} \frac{\Delta \mathbf{r}}{\Delta t}$$

The direction of Δ**r** approaches that of the tangent to the path as Δt approaches zero and, hence, the velocity **v** is always a vector tangent to the path as shown in Fig. 5.1b.

The definition of the derivative of a scalar quantity can be extended to include a vector quantity so that

$$\mathbf{v} = \frac{d\mathbf{r}}{dt} = \dot{\mathbf{r}}$$

Thus the derivative of a vector is itself a vector having both a magnitude and a direction. The magnitude of **v** is called the *speed* and is the scalar

$$v = |\dot{\mathbf{r}}| = \frac{ds}{dt} = \dot{s}$$

In Fig. 5.1*b*, the velocity of the particle at A is denoted by the tangent vector **v** and the velocity at A' by the tangent vector **v'**. There is thus a vector change in the velocity during the time Δt. The velocity **v** at A plus the change Δ**v** must equal the velocity at A'. So we may write **v'** − **v** = Δ**v**. Inspection of the vector diagram in Fig. 5.1*c* shows that Δ**v** depends both on the change in magnitude of **v** and on the change in direction of **v**.

The *instantaneous acceleration* **a** of the particle is defined as the limiting value of the average acceleration between A and A' as Δt approaches zero, or

$$\mathbf{a} = \lim_{\Delta t \to 0} \frac{\Delta \mathbf{v}}{\Delta t}$$

By definition of the derivative we write

$$\mathbf{a} = \frac{d\mathbf{v}}{dt} = \dot{\mathbf{v}} = \ddot{\mathbf{r}}$$

As the interval Δt approaches zero, the direction of the change Δ**v** approaches that of the differential change *d***v** and, hence, **a**. It is apparent from Fig. 5.1*c* that the acceleration **a** reflects change in magnitude of **v** as well as the change of direction of **v**. In general, the direction of the acceleration of a particle in curvilinear motion is neither tangent nor normal to the particle path.

5.1.2 Planar motion in rectangular coordinates

Absolute planar motion

Fig. 5.2*a* shows the curvilinear path of a particle represented by point A along with the rectangular coordinate axes x and y. Such a coordinated system, drawn on the plane of the particle motion, is often called *Cartesian*. The particle motion can be described at any time t by specifying its position x_A and y_A measured from the origin of the x- and y-axes O. If the coordinate system is fixed to the absolute frame the rectangular components indicate the *absolute motion* of the particle.
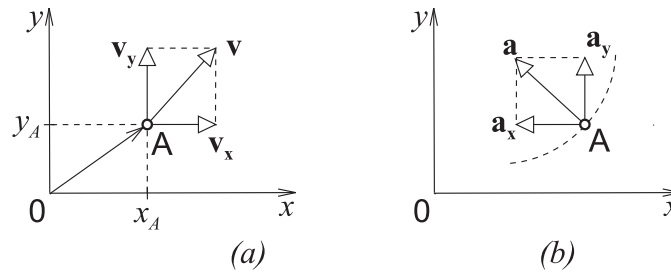

Figure 5.2: Rectangular components of (*a*) of position, velocity, and (*b*) acceleration.

The position vector $\mathbf{r}_A$, the velocity $\mathbf{v}_A$, and the acceleration $\mathbf{a}_A$ of the particle are represented in Fig. 5.2 together with their x- and y-components. Using the unit vectors **i** and **j**, we may write the vectors $\mathbf{r}_A$, $\mathbf{v}_A$, and $\mathbf{a}_A$ as

$$\begin{aligned} \mathbf{r}_A &= & x_A\mathbf{i} + y_A\mathbf{j} \\ \mathbf{v}_A &= \dot{\mathbf{r}}_A = & v_{Ax}\mathbf{i} + v_{Ay}\mathbf{j} \\ \mathbf{a}_A &= \dot{\mathbf{v}}_A = \ddot{\mathbf{r}}_A = & a_{Ax}\mathbf{i} + a_{Ay}\mathbf{j} \end{aligned} \tag{5.1}$$

The unit vectors have no time derivatives since their magnitudes and directions remain constant. Thus the scalar values of the components of $\mathbf{v}_A$ and $\mathbf{a}_A$ are just $v_{Ax} = \dot{x}_A$, $v_{Ay} = \dot{y}_A$ and $a_{Ax} = \dot{v}_{Ax} = \ddot{x}_A$, $a_{Ay} = \dot{v}_{Ay} = \ddot{y}_A$.

It is obvious from Fig. 5.2 that the absolute values $v_A = |\mathbf{v}_A|$ and $a = |\mathbf{a}_A|$ are related to the x- and y-components as

$$v_A = \sqrt{v_{Ax}^2 + v_{Ay}^2} \qquad a_A = \sqrt{a_{Ax}^2 + a_{Ay}^2}$$

Relations (5.1) prove that the planar motion of a particle can be decomposed into motions in two different directions (mutually perpendicular in this case). Practical experience indicates that the opposite procedure – vector composition of planar motions – is also possible. Such *principle of motion composition* is considered as an axiom, it cannot be proven.

Thus, if the coordinates x and y of a particle are known as functions of time, $x = f_x(t)$ and $y = f_y(t)$, then for any value of the time we may combine them to obtain **r**. Similarly, we combine their first

derivatives $\dot{x}$ and $\dot{y}$ to obtain $\mathbf{v}$ and their second derivatives $\ddot{x}$ and $\ddot{y}$ to obtain $\mathbf{a}$. Or, if the acceleration components a_x and a_y are given as functions of the time, we may integrate each one separately with respect to time, once to obtain v_x v_y and again to obtain $x = f_x(t)$ and $y = f_y(t)$. Elimination of the time t between these last two parametric equations gives the equation of the curved path $y = f(x)$.

Relative planar motion

Consider now two particles positioned at points A and B having separate curvilinear motions in a given plane with the x-y axes, Fig. 5.3a. The *absolute positions* of the particles are determined by the vectors $\mathbf{r}_A$ and $\mathbf{r}_B$ measured from the origin O. The *relative position* of A measured with respect to the position of B is represented by the vector

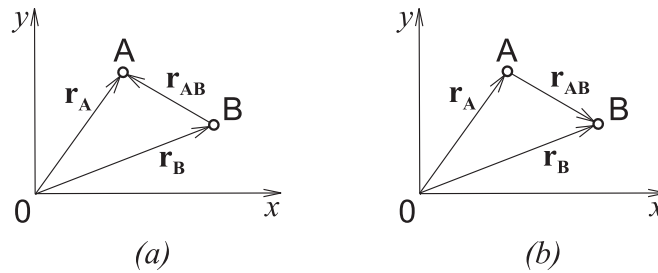$$\mathbf{r}_{AB} = \mathbf{r}_A - \mathbf{r}_B \qquad (5.2)$$

Figure 5.3: Relative motion (a) of A with respect to B, and (b) of B with respect to A.

Using the unit vectors $\mathbf{i}$ and $\mathbf{j}$ along the x- and y-axes we can write

$$\mathbf{r}_{AB} = x_{AB}\mathbf{i} + y_{AB}\mathbf{j} \qquad (5.3)$$

where $x_{AB} = x_A - x_B$ and $y_{AB} = y_A - y_B$ are the x- and y-components of the relative position of A with respect to B.

If we now differentiate (5.2) and (5.3) with respect to time we obtain the relative velocity of A as observed from B

$$\mathbf{v}_{AB} = \dot{\mathbf{r}}_{AB} = \dot{\mathbf{r}}_A - \dot{\mathbf{r}}_B$$

where $v_{ABx} = v_{Ax} - v_{Bx}$ and $v_{ABy} = v_{Ay} - v_{By}$ are the x- and y-components of the relative velocity of A with respect to that of B. These can be expressed in terms of the rectangular components of the absolute velocities v_{Ax}, v_{Bx}, v_{Ax}, v_{By} of points A and B.

If we differentiate (5.2) and (5.3) with respect to time twice we will get the relative acceleration of A with respect to B as

$$\mathbf{a}_{AB} = \dot{\mathbf{a}}_{AB} = \dot{\mathbf{r}}_A - \dot{\mathbf{a}}_B = a_{ABx}\mathbf{i} + a_{ABy}\mathbf{j}$$

where the x- and y-components $a_{ABx} = a_{Ax} - a_{Bx}$ and $a_{ABy} = a_{Ay} - a_{By}$.

Let us now exchange the role of the two points to observe the motion of B as seen from A. Fig. 5.3b indicates that the corresponding expressions for the relative position, velocity, and acceleration become

$$
\begin{aligned}
\mathbf{r}_{BA} &= \mathbf{r}_B - \mathbf{r}_A = -\mathbf{r}_{AB} \\
\mathbf{v}_{BA} &= \mathbf{v}_B - \mathbf{v}_A = -\mathbf{v}_{AB} \\
\mathbf{a}_{BA} &= \mathbf{a}_B - \mathbf{a}_A = -\mathbf{a}_{AB}
\end{aligned}
$$

Postulate of compatibility of planar motions

Due to geometric continuity of space the *postulate of compatibility of motions* holds also for planar motions. Let us consider curvilinear motions of points A, B, and C shown in Fig. 5.4. The vectors $\mathbf{r}_{AB}$, $\mathbf{r}_{BC}$, and $\mathbf{r}_{CA}$ indicate the mutual relative motions of the points.

Note that if the vectors are oriented in the same direction along the loop that they form

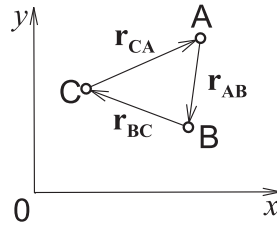$$\mathbf{r}_{AB} + \mathbf{r}_{BC} + \mathbf{r}_{CA} = \mathbf{0}$$

Figure 5.4: Composition of relative positions in a plane.

or
$$(x_{AB} + x_{BC} + x_{CA})\mathbf{i} + (y_{AB} + y_{BC} + y_{CA})\mathbf{j} = \mathbf{0}$$

when the vectors are decomposed into their x- and y-components. Thus postulate of motion compatibility applies independently also to the x- and y-components

$$x_{AB} + x_{BC} + x_{CA} = 0 \quad \text{and} \quad y_{AB} + y_{BC} + y_{CA} = 0$$

The postulate of motion compatibility holds for velocities and accelerations of the three points:

$$\mathbf{v}_{AB} + \mathbf{v}_{BC} + \mathbf{v}_{CA} = \mathbf{0}$$
$$\mathbf{a}_{AB} + \mathbf{a}_{BC} + \mathbf{a}_{CA} = \mathbf{0}$$

In general, the postulate of motion compatibility holds for any motions along a closed loop passing through the sequence of an arbitrary number of points. This trivial-looking statement plays an important role in the formulation of equations describing the behavior of mechanical systems.

5.1.3 Planar forces in rectangular coordinates

Composition of planar forces

A force has been defined as the action of one body on another. We find that force is a vector quantity, since its effect depends on the direction as well as on the magnitude of the action and since forces may be combined according to the parallelogram law of vector combination. Two forces $\mathbf{F}_1$ and $\mathbf{F}_2$ that are concurrent may be added by the parallelogram law in their common plane to obtain their sum or resultant $\mathbf{R}$ as shown in Fig. 5.5.
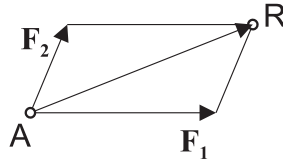

Figure 5.5: Composition of planar forces.

In addition to the need for combining forces to obtain their resultant, we often have occasion to replace a force by its vector components which act in specified directions. By definition, the two or more vector components of a given vector must vectorially add to yield the given vector. Thus, the force $\mathbf{R}$ in Fig. 5.5 may be replaced by or resolved into two vector components $\mathbf{F}_1$ and $\mathbf{F}_2$ with the specified directions merely by completing the parallelogram as shown to obtain the magnitudes of $\mathbf{F}_1$ and $\mathbf{F}_2$.

Let us now consider a particle subjected to the action of concurrent forces $\mathbf{F}_1$, $\mathbf{F}_2$, $\mathbf{F}_3$, ... assuming that the lines of action of all the forces are situated in the same plane as the trajectory of the particle. The vector sum of the applied forces becomes

$$\mathbf{F}_a = \sum_i \mathbf{F}_i \tag{5.4}$$

The sum must include all the external forces applied to the particle in question. The reliable way to account accurately and consistently for every force is to form the *free-body diagram* of the particle under

consideration isolating it from all contacting and influencing bodies and replacing the bodies removed by the forces they exert on the particle isolated.

Fig. 5.6a gives an example of three forces applied to a particle represented by point A while Fig. 5.6b shows the resultant $\mathbf{F}_a$ of the applied forces.
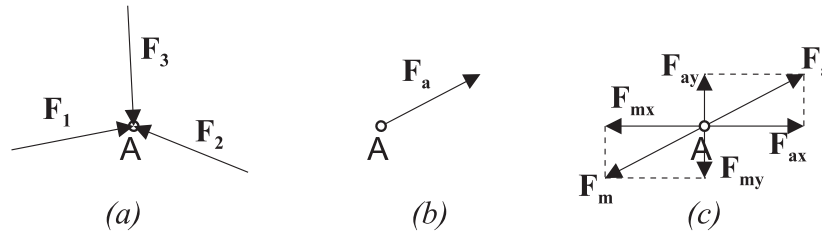

Figure 5.6: (a) Forces applied to a particle, (b) vector and (c) orthogonal components of the resultant external force.

The vector of the total applied force $\mathbf{F}_a$ is shown again in Fig. 5.6c where it is decomposed along the x and y coordinate axes. With the aid of the unit vectors $\mathbf{i}$ and $\mathbf{j}$, we may rewrite (5.4) in terms of the x- and y-components of the individual applied forces as

$$\mathbf{F}_a = F_{ax}\mathbf{i} + F_{ay}\mathbf{j}$$

where

$$F_{ax} = \sum_i F_{xi} \quad \text{and} \quad F_{ay} = \sum_i F_{yi}$$

are the x- and y-components of the resultant force applied to the particle.

The absolute value $F_a = |\mathbf{F}_a|$ is

$$F_a = \sqrt{\left(\sum_i F_{xi}\right)^2 + \left(\sum_i F_{yi}\right)^2}$$

Equilibrium of planar forces

If a particle of mass m is isolated in the inertial system and is subjected to the action of a sum of applied forces $\mathbf{F}_a$ then Newton's second law of motion may be described by the vector relation

$$\mathbf{F}_a = m\mathbf{a} \tag{5.5}$$

where the acceleration $\mathbf{a}$ of the particle is always in the direction of the applied force $\mathbf{F}_a$. This is shown in Fig. 5.7a where the particle is represented by point A. This effect is the *inertia* of the particle mass which is its resistance to rate of change of velocity. Equation (5.5) is usually referred to as the *equation of motion* in the vector form.
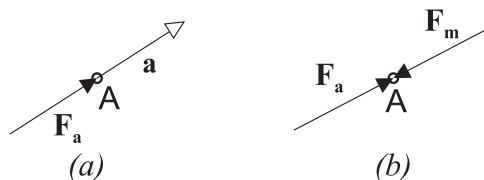

Figure 5.7: (a) Particle acceleration due to applied force, (b) force dynamic equilibrium.

Fig. 5.7b suggests that the inertial effect of the particle mass can be replaced by the hypothetical *inertial force* $\mathbf{F}_m = -m\mathbf{a}$ acting on the massless point representing the particle. Then (5.5) can be written in the alternative form

$$\mathbf{F}_a + \mathbf{F}_m = \mathbf{0} \tag{5.6}$$

interpreted as the *dynamic equilibrium of forces* acting at on the particle.

Relation (5.6), known as *d'Alembert's principle*, has far-reaching implications in dynamic analysis. It allows us to treat the particle inertial force $\mathbf{F}_m$ in the same way as the external forces applied to the particle.

If a particle is subjected to the action of a sum of applied forces $\mathbf{F}_a$ and its velocity with respect to the inertial system is zero or constant

$$\mathbf{F}_a = \mathbf{0}$$

This expresses the *static equilibrium of forces* acting at on the particle.

5.1.4 Dynamic model of particles in planar motion

From the foregoing discussion it should be recognized that the rectangular-coordinate representation of curvilinear motion is merely the superposition of the components of two simultaneous rectilinear motions in the x- and y-directions. Therefore, everything covered so far on rectilinear motion may be applied to the x-motion and to the y-motion.
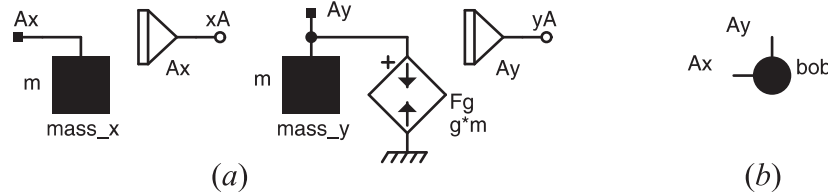

Figure 5.8: (a) Submodel for particle motion in the vertical plane, (b) submodel symbol.

Fig. 5.8b gives the three-pole dynamic model of a particle pursuing a curvilinear motion in the vertical x-y plane which is shown in Fig. 5.8a. The particle position in the x-y plane denotes point Ax. Poles Ax and Ay represent point velocities in the horizontal and vertical directions. The inertia effects of the particle mass m in the x- and y-directions are modelled by inertors. A source of force represents the gravitational force $F_g = g\,m$ acting on the particle in the vertical direction, g is the gravitational acceleration.

The third pole corresponds to the absolute frame representing the velocity reference. Fig. 5.8c shows the symbol of the submodel with pins corresponding to the poles Ax and Ay. The third pole associated with the velocity reference and respected in the submodel does not need to be shown explicitly in the symbol.

Obviously, also a multipole model of a particle in a curvilinear motion can be decomposed into two rectilinear models, one for dynamic interactions in the x direction, and the other one in the y direction. In most practical cases these two models will be coupled, however.

Example: Cannon ball

Let us investigate the trajectory of a cannon ball launched from the coordinate system origin at $t = 0$ with the initial speed $v(0)$ at the angle $\alpha = 45°$. Fig. 5.9a shows the expected parabolic trajectory in the vertical plane if the cannon ball represented by point B.
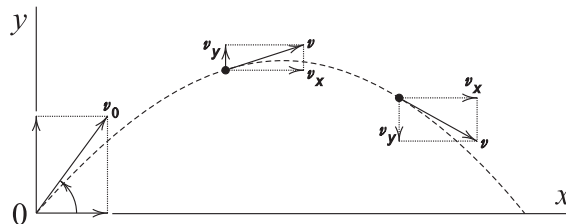

Figure 5.9: (a) Trajectory of a cannon ball, (b) ball dynamic model.

To model the ball dynamics, we apply the submodel shown in Fig. 5.8 augmented by blocks for computing the ball x_B and x_B position by integrating the ball velocities B_x and B_y. The x- and y-components of the ball initial speed $v(0)$ are obviously $v_x(0) = v(0)/\sqrt{2}$ and $v_y(0) = v(0)/\sqrt{2}$.

We can see that the ball x- and y-motions are mutually independent under the simplifying consideration. If we had introduced, for example, aerodynamic drag force exerted on the ball which depends on the speed squared, then the x- and y-parts of the ball model would be coupled. As a result, the ball x- and y-motions would be interdependent, and the trajectory would not be parabolic any more.

5.2 Planar systems with massless rods

5.2.1 Rod with revolute joints

Model in rectangular coordinates

Motion of particles A and B in the x-y plane is constrained by a rigid rod of negligible mass as shown in Fig. 5.10a. The rod configuration can be characterized by the relation

$$x_{AB}^2 + y_{AB}^2 = \ell^2 \tag{5.7}$$

where ℓ is the rod length whereas $x_{AB} = x_A - x_B$ and $y_{AB} = y_A - y_B$ are projections of the rod onto the x and y axes. After differentiating (5.7) with respect to time we get the geometric constraint imposed by the rod on the particle motion

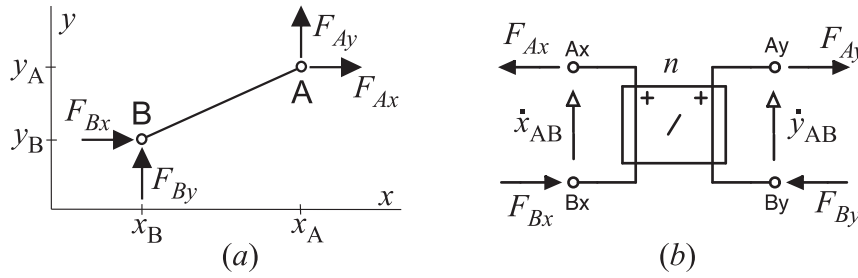$$x_{AB}\dot{x}_{AB} + y_{AB}\dot{y}_{AB} = 0 \tag{5.8}$$

Figure 5.10: (a) Particles interconnected by massless rod, (b) transformer model.

The rod must be in equilibrium, i.e. all forces and moments applied to it must be in balance. The free-body diagram of the rod in Fig. 5.10a indicates that the balance of forces can be written in the form

$$F_{Ax} + F_{Bx} = 0 \qquad F_{Ay} + F_{By} = 0 \tag{5.9}$$

end the balance of moments acting on the rod can be expressed as

$$(F_{Ay} - F_{By})\,x_{AB} - (F_{Ax} - F_{Bx})\,y_{AB} = 0$$

After substituting for F_{Ax} and F_{Ay} from (5.9), the previous relation becomes

$$F_{Ay}x_{AB} - F_{Ax}y_{AB} = 0 \quad \text{or} \quad F_{By}x_{AB} - F_{Bx}y_{AB} = 0 \tag{5.10}$$

Let us now arrange (5.8) and (5.10) in a common matrix form

$$\begin{bmatrix} \dot{x}_{AB} \\ F_{By} \end{bmatrix} = \begin{bmatrix} 0 & n \\ -n & 0 \end{bmatrix} \cdot \begin{bmatrix} F_{Bx} \\ \dot{y}_{AB} \end{bmatrix} \tag{5.11}$$

where $n = -y_{AB}/x_{AB}$.

This result leads us to the conclusion that the constraint provided by the massless rod can be modeled by the pure transformer with the variable ratio n as shown in Fig. 5.10b.

An alternative but dynamically equivalent model characterized by the symbol shown in Fig. 5.11a is given in Fig. 5.10b. Values of variables are interrelated in the model by equations (5.9) and (5.10).

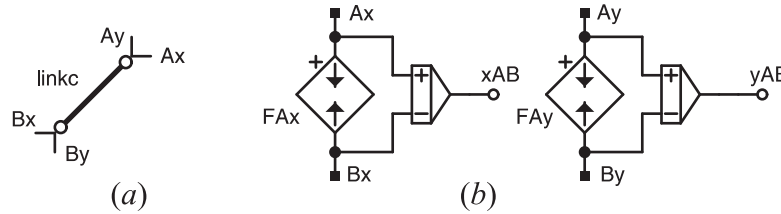**Example: Mathematical pendulum**

$$n = \frac{y_{AB}}{x_{AB}}$$

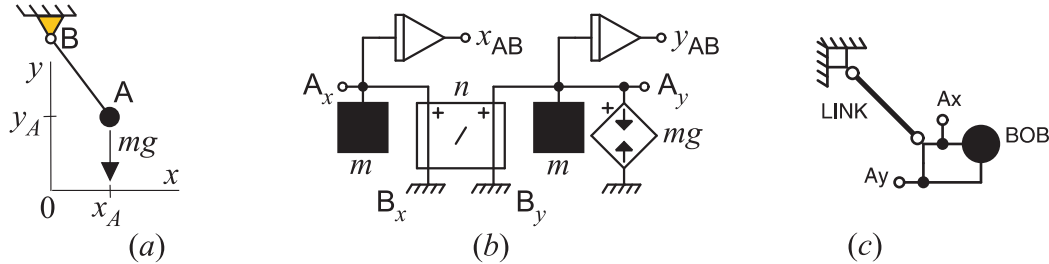Figure 5.11: (a) Massless rod, (b) its model.

Figure 5.12: (a) Mathematical pendulum, (b) its dynamic model.

Example: Double mathematical pendulum

$$n_1 = \frac{y_B}{x_B} \qquad n_2 = \frac{y_C - y_B}{x_C - x_B}$$

Example: Carriage with pendulum

$$n = \frac{y_{AB}}{x_{AB}}$$

Example: Sliding rod

$$n = -\frac{y_{AB}}{x_{AB}}$$

Model in polar coordinates

There are system models in which we need to observe or control the angle or torque of a rod. If this is the case we can apply to the rod one of the models shown in Fig. 5.16 or Fig. 5.17. The models are related to the rod geometric configuration shown in Fig. 5.16a.

Positions of the rod end-points A and B are constrained as

$$x_{AB} = \ell \cos \varphi \qquad y_{AB} = \ell \sin \varphi \tag{5.12}$$

where ℓ is the rod length. Differentiation with respect to time gives the velocity constrains

$$\dot{x}_{AB} = -\ell \sin \varphi \cdot \dot{\varphi} \qquad \dot{y}_{AB} = \ell \cos \varphi \cdot \dot{\varphi} \tag{5.13}$$

Balance of forces can be written in the form

$$F_{Ax} + F_{Bx} = 0 \qquad F_{Ay} + F_{By} = 0 \tag{5.14}$$

Balance of moments related to the rotation of A about B

$$M - F_{Ax}y_{AB} + F_{Ay}x_{AB} = 0 \tag{5.15}$$

where M is an external moment of force applied to the rod.

After substituting for x_{AB} and y_{AB} from (5.12) and setting $M = M_x + M_y$ where

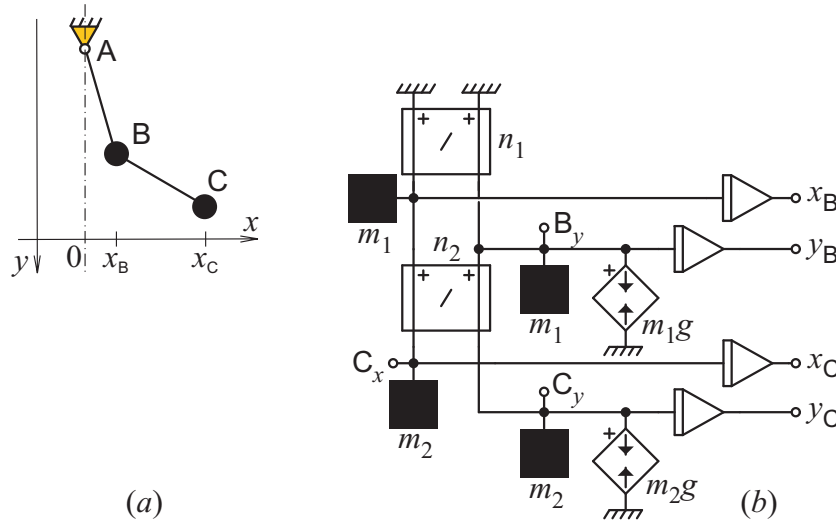$$M_x = -F_{Bx}\,\ell \sin \varphi \qquad M_y = F_{By}\,\ell \cos \varphi$$

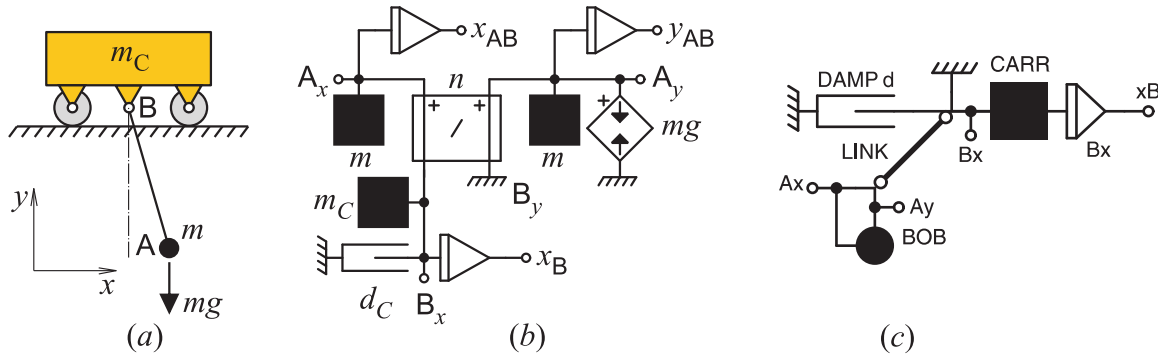Figure 5.13: (a) Mathematical double pendulum, (b) its dynamic model.

Figure 5.14: (a) Carriage with pendulum, (b) its dynamic model.

Combining now these relations with (5.13) we can write

$$\left[\begin{array}{c} \dot{x}_{AB} \\ M_x \end{array}\right] = \left[\begin{array}{cc} 0 & n_x \\ -n_x & 0 \end{array}\right] \cdot \left[\begin{array}{c} F_{Bx} \\ \dot{\varphi} \end{array}\right] \qquad \left[\begin{array}{c} \dot{y}_{AB} \\ M_y \end{array}\right] = \left[\begin{array}{cc} 0 & n_y \\ -n_y & 0 \end{array}\right] \cdot \left[\begin{array}{c} F_{By} \\ \dot{\varphi} \end{array}\right] \qquad (5.16)$$

where

$$n_x = -\ell \sin\varphi \qquad n_y = \ell \cos\varphi$$

Obviously, the resulting model of the rod can be composed from two pure transformers as shown in Fig. 5.16b.

An alternative model combining symbols and equations is in Fig. 5.17. The sources of force and torque are interrelated by equations (5.12), (5.13)(5.14), and (5.28).

Example: Slide-crank mechanism

5.2.2   Rod with revolute and translational joints

Model in rectangular coordinates

Motion of particles A and B in the x-y plane is constrained by a rigid rod of negligible mass as shown in Fig. 5.19a. The rod configuration can be characterized by the relation

$$x_{AB}^2 + y_{AB}^2 = \rho_{AB}^2 \qquad (5.17)$$

where ρ_{AB} is distance of point A measured from point B along the rod. Differentiation of (5.17) with respect to time gives the geometric constraint

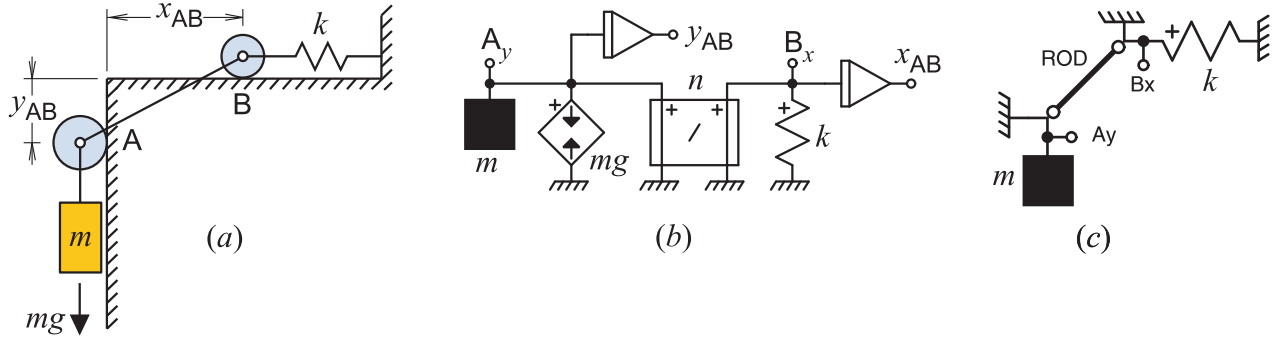$$x_{AB}\,\dot{x}_{AB} + y_{AB}\,\dot{y}_{AB} = \rho_{AB}\,\dot{\rho}_{AB} \qquad (5.18)$$

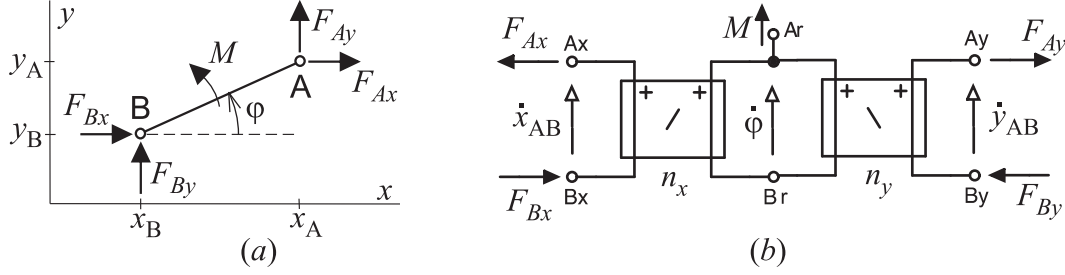Figure 5.15: (a) Sliding rod, (b) its dynamic model.

Figure 5.16: Massless rod in polar coordinates.

Let us rewrite this as

$$\dot{\rho}_{AB} = \dot{\rho}_x + \dot{\rho}_y \tag{5.19}$$

where

$$\dot{\rho}_x = \frac{x_{AB}}{\rho_{AB}}\dot{x}_{AB} \qquad \dot{\rho}_y = \frac{y_{AB}}{\rho_{AB}}\dot{y}_{AB} \tag{5.20}$$

The free-body diagram of the rod in Fig. 5.19a indicates that the balance of forces can be written in the form

$$F_{Ax} + F_{Bx} = 0 \qquad F_{Ay} + F_{By} = 0 \tag{5.21}$$

and the balance of moments as

$$F_{Ax}\rho_{AB} + F_\rho x_{AB} = 0 \qquad F_{Ay}\rho_{AB} + F_\rho y_{AB} = 0 \tag{5.22}$$

Combining now these relations with (5.18) we can write

$$\begin{bmatrix} \dot{\rho}_x \\ F_x \end{bmatrix} = \begin{bmatrix} 0 & n_x \\ -n_x & 0 \end{bmatrix} \cdot \begin{bmatrix} F_\rho \\ \dot{x}_{AB} \end{bmatrix} \qquad \begin{bmatrix} \dot{\rho}_y \\ F_y \end{bmatrix} = \begin{bmatrix} 0 & n_y \\ -n_y & 0 \end{bmatrix} \cdot \begin{bmatrix} F_\rho \\ \dot{y}_{AB} \end{bmatrix} \tag{5.23}$$

where

$$n_x = x_{AB}/\rho_{AB} \qquad n_y = y_{AB}/\rho_{AB}$$

Obviously, the resulting model can be composed from two pure transformers as shown in Fig. 5.19b.

Model in polar coordinates

As shown in Fig. 5.20a, positions of points A and B are constrained as

$$x_{AB} = \rho\cos\varphi \qquad y_{AB} = \rho\sin\varphi \tag{5.24}$$

where ρ is the distance of A from B. Differentiation with respect to time gives the velocity constrains

$$\dot{x}_{AB} = \dot{\rho}\cos\varphi - \rho\dot{\varphi}\sin\varphi \qquad \dot{y}_{AB} = \dot{\rho}\sin\varphi + \rho\dot{\varphi}\cos\varphi \tag{5.25}$$

Balance of forces can be written in the form

$$F_{Ax} + F_{Bx} = 0 \qquad F_{Ay} + F_{By} = 0 \tag{5.26}$$

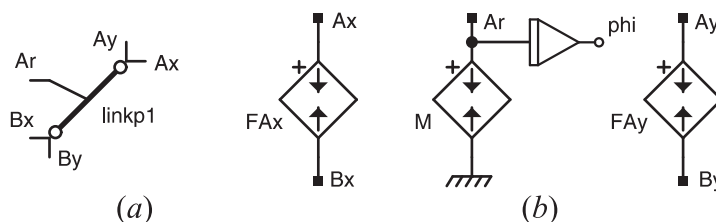(a) (b)

Figure 5.17: Massless rod in polar coordinates: (a) graphical symbol, (b) model diagram.
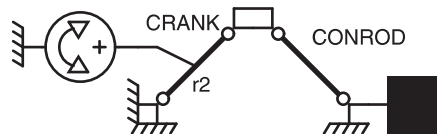

Figure 5.18: (a) Slide crank mechanism, (b) model diagram.

and

$$F_{Ax} \cos \varphi + F_{Ay} \sin \varphi = 0 \tag{5.27}$$

Balance of moments is

$$\tau - F_{Ax} y_{AB} + F_{Ay} x_{AB} = 0 \tag{5.28}$$

where τ is an external moment of force applied to the rod.

In this case, the resulting model can be composed from four pure transformers as shown in Fig. 5.20b where

$$n_{x\varphi} = -\rho \sin \varphi \quad n_{y\varphi} = \rho \cos \varphi \quad n_{x\rho} = \cos \varphi \quad n_{y\rho} = \sin \varphi$$

5.2.3   Transformations

An example of the magnitude of the error introduced by neglect of the motion of the earth may be cited for the case of a particle that is allowed to fall from rest (relative to the earth) at a height h above the ground. We can show that the rotation of the earth gives rise to an eastward acceleration (Coriolis acceleration) relative to the earth and, neglecting air resistance, that the particle falls to the ground a distance

$$x = \frac{2}{3} \omega \sqrt{\frac{2h^3}{g}} \cos \gamma$$

east of the point on the ground directly under that from which it was dropped. The angular velocity of the earth is $\omega = 0.729(10^{-4})$ rad/s, and the latitude, north or south, is γ. At a latitude of 45○ and from a height of 200 m, this eastward deflection would be $x = 43.9$ mm.

These corrections are negligible for most engineering problems which involve the motions of structures and machines on the surface of the earth. In such cases, the accelerations measured with respect to reference axes attached to the surface of the earth may be treated as "absolute," and Eq. 3/2 may be applied with negligible error to experimental measurements made on the surface of the earth.* If the ideal experiment described were performed on the surface of the earth and all measurements were made relative to a reference system attached to the earth, the measured results would show a slight discrepancy upon substitution into Eq. 3/2. This discrepancy would be due to the fact that the measured acceleration would not be the correct absolute acceleration. The disc The discrepancy would disappear when we introduced the corrections due to the acceleration components of the earth.

5.2.4   Planar motion in polar coordinates

$$x = r \cos \varphi \qquad y = r \sin \varphi \tag{5.29}$$

where r is the length of vector $\mathbf{r}$ and φ is the angle between this vector and the axis x.

By differentiating these relation with respect to time we will obtain velocities of point A in the coordinate system x, y expressed in terms of velocities in the coordinate system ρ, φ

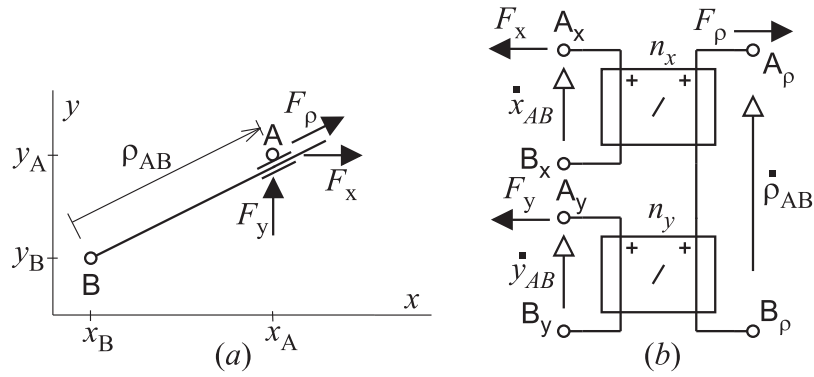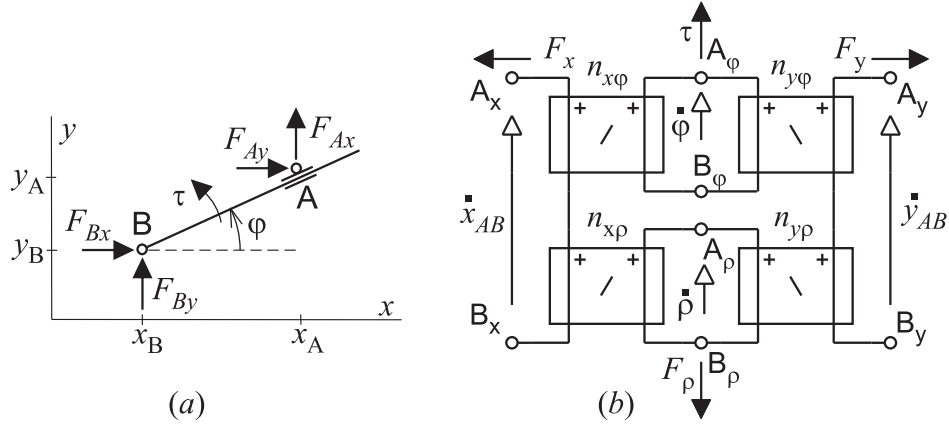Figure 5.19: (a) Rod in rectangular coordinates, (b) model.

Figure 5.20: (a) Rod in polar coordinates, (b) model.

$$v_x = v_\rho \cos\varphi - v_\varphi \sin\varphi \qquad (5.30)$$
$$v_y = v_\rho \sin\varphi + v_\varphi \cos\varphi \qquad (5.31)$$

$$F_\rho = -F_x \cos\varphi - F_y \sin\varphi \qquad (5.32)$$
$$F_\varphi = +F_x \sin\varphi - F_y \cos\varphi \qquad (5.33)$$

$$\begin{bmatrix} \mathbf{v}_{xy} \\ \mathbf{F}_{\rho\varphi} \end{bmatrix} = \begin{bmatrix} \mathbf{0} & \mathbf{N} \\ -\mathbf{N}^t & \mathbf{0} \end{bmatrix} \cdot \begin{bmatrix} \mathbf{F}_{xy} \\ \mathbf{v}_{\rho\varphi} \end{bmatrix} \qquad (5.34)$$

where

$$\mathbf{v}_{xy} = \begin{bmatrix} v_x \\ v_y \end{bmatrix} \qquad \mathbf{v}_{\rho\varphi} = \begin{bmatrix} v_\rho \\ v_\varphi \end{bmatrix} \qquad \mathbf{F}_{xy} = \begin{bmatrix} F_x \\ F_y \end{bmatrix} \qquad \mathbf{F}_{\rho\varphi} = \begin{bmatrix} F_\rho \\ F_\varphi \end{bmatrix} \qquad (5.35)$$

and

$$\mathbf{N} = \begin{bmatrix} \cos\varphi & -\sin\varphi \\ \sin\varphi & \cos\varphi \end{bmatrix} \qquad (5.36)$$

5.2.5   Planar motion of particles in path coordinates

The motion of A may also be described by measurements along the tangent t and normal n to the curve. The direction of n lies in the local plane of the curve. These last measurements are known as path variables.

Module 6

Electrical systems

6.1 Electrical interactions

6.1.1 Electrical voltage and current

The **electrical voltage** [V] (or potential difference) v_{BA} between two points such as B and A is defined as the work which would be done (or the energy required) in carrying a unit positive charge from one point to the other. For the concept of voltage to be applicable, it is necessary that the work determined in this way be independent of the path along which the charge is moved. This requirement implies that the rate of change of the magnetic field in the region of the path must be either zero or negligible.

This requirement fits into the framework of the quasi-static field theory which implies that the rate of change of magnetic field normal to the region of the path on the subsystem energy boundary must be negligible.

If it is necessary to do work on a positive charge (i.e., to apply a force in the direction of motion) as it moves from point A to point B, then point B is said to be at a higher potential than point A and the voltage v_{BA} is considered positive.

Since it is often not known a priori which of two points will be at the higher potential or voltage, it is necessary to establish an algebraic reference convention for voltage. In this course, the assumed positive orientation of voltage is denoted by an empty-head arrow pointing in the direction of the from the point of a lower to the point of a higher potential.

Electrical current i [A] is defined as the rate of flow of charge across a given area, often the cross-sectional area of a wire. As the current may be changing with time, it is

$$i(t) = \frac{dq}{dt} \tag{6.1}$$

where $q = q_+ - q_-$ is the net charge of the particles crossing the entry, q_+ and q_- are charges of the particles charged positively and negatively, respectively. The physical unit of electrical charge – coulomb [C] – is equal in magnitude but opposite in sign to the charge of $6.22 \cdot 10^{18}$ electrons.

Current has a direction as well as a magnitude. The direction convention commonly chosen is that direction in which a net flow of positive charge has occurred. To establish in a reference for the direction of a current we will use full-head arrows indicating the direction of the assumed positive current.

6.1.2 Electrical power, energy and work

From the definition of voltage, the amount of work $d\mathcal{W}_{BA}$ done when an infinitesimal charge dq is moved from A to B is $d\mathcal{W}_{BA} = v_{BA}dq$, or

$$v_{BA} = \frac{d\mathcal{W}_{BA}}{dq} \tag{6.2}$$

One joule [J] is equivalent to one watt-second [W.s].

The **electrical power** $\mathcal{P}$ delivered to a two-terminal electrical element can be computed from the definitions of voltage and current, (6.2) and (6.1). For the element

$$\mathcal{P} = \frac{d\mathcal{W}_{BA}}{dt} = \frac{dq}{dt}\frac{d\mathcal{W}_{BA}}{dq} = i\,v_{BA} \tag{6.3}$$

where i is the current flowing through the element and v_{BA} is the voltage difference across it. In the MKS system of units, power is measured in watts. One watt is equal to one joule/sec or one N.m/sec.

The **electrical energy** $\mathcal{E}$ supplied to an element is the time integral of the power

$$\mathcal{E} = \int_{t_a}^{t_b} i\, v_{BA} d\tau \tag{6.4}$$

where t_a and t_b are the beginning and end of the time interval during which power flows. If energy is delivered to an electrical system through more than one pair of terminals, the total energy supplied is the sum of the energies supplied at all the terminals.

The **law of conservation of energy**, or the first law of thermodynamics, states that the energy (of all forms) which is delivered to a system must either be stored in the system or transferred out of the system.

6.2   Prescribed electrical interactions

6.2.1   Prescribed electrical voltages

If an electric circuit is driven by a prescribed voltage $v(t)$ [m/s], the actuator driving the body can be represented in the circuit model by a **pure source of electrical voltage**. This two-pole physical element is characterized by the constitutive relation

$$v(t) = f(t) \tag{6.5}$$
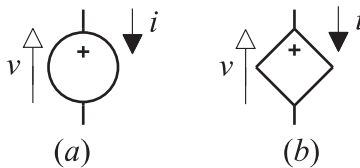
where $i(t)$ is the known single-value function of time.

$$(a) \qquad\qquad (b)$$

Figure 6.1: Symbols of pure source of electrical (a) voltage and (b) current.

Fig. 6.1a gives our graphical symbol representing a pure source of electrical voltage $v(t)$ in multipole diagrams. The two short line segments sticking out of the symbol are called **pins**. They denote **poles** of the source representing terminals of the modelled real source of electrical energy. The **symbol polarity** is indicated by the + sign. Besides the prescribed electrical voltage $v(t)$, the pure source of voltage is also associated with its current $i(t)$. This current is imposed on the source by the system in which the source operates. The assumed positive orientation of $v(t)$ and $i(t)$ in relation to the symbol polarity is shown in Fig. 6.1a by the empty-head and full-head arrow, respectively.

The chosen orientation of source variables is such that the power of the source corresponds to the flow of energy *into* the source. Sources are usually used to model supplies of energy into systems. Despite of this, we shall always use the same "consumer" variable-orientation convention for all the physical elements regardless if they consume or deliver energy. Such a unified approach is for the benefit of modeling and analysis simplicity. Note, that if the source symbol is oriented properly in a multipole diagram there is no need to denote in it the variable orientation by arrows.

6.2.2   Prescribed electrical currents

To model energy sources of prescribed electrical currents we need to introduce **pure sources of electrical current**. In general, such a source exhibits current $i(t)$ characterized by the constitutive relation

$$i = f(t) \tag{6.6}$$

where $i(t)$ is a known single-value function of time.

Our graphical symbol for the source of electrical current is given in Fig. 6.1b. The full-head and empty-head arrows indicate the assumed positive orientation of the electrical current $i(t)$ and electrical voltage $v(t)$ associated with the source. The variable orientation is related to polarity of the source symbol denoted by the + sign. The relative electrical voltage $v(t)$ of the source represents the electrical voltage of the real electrical energy source determined by the system comprising it.

6.2.3 Indicators of electrical voltages and electrical currents

Pure sources of *zero* electrical current can be used as physical elements modeling ideal **indicators of electrical voltage**, i.e. instruments measuring relative electrical voltage between distinct sites of interaction. Our graphical symbol for such an indicator is given in Fig. 6.2*a*. Direction of the arrow showing the assumed positive polarity of the indicated electrical voltage is fixed to the polarity of the symbol.

Figure 6.2: Symbol of ideal indicator of electrical (*a*) voltage and (*b*) current.

Pure sources of *zero* electrical voltage can be utilized as physical elements modeling ideal measuring instruments or **indicators of electrical current**. Our graphical symbol for such an indicator is given in Fig. 6.2*b*. Direction of the arrow showing the assumed positive polarity of the indicated electrical current is fixed to the polarity of the symbol.

Note the difference between measuring electrical voltage and electrical current. The direct measurement of electrical currents requires disconnecting the system and connecting it back by a electrical current indicator. Electrical voltages are measured by indicators applied to systems without any need to disconnect them. This is the reason why electrical voltages represent **electrical across variables** while electrical currents are **electrical through variables**.

6.3 Pure electrical resistors and conductors

All ordinary materials exhibit some resistance to the flow of electric charge. Resistors are encountered in many shapes and forms, often designed to provide a needed resistance effect in an electric system, but sometimes as an unwanted (parasitic) effect. Fig. 6.3*a* shows a real electrical component called resistor formed as a coil of resistive wire wound around a ceramic material.

A *pure electrical resistor* is defined by a single-valued functional relationship between voltage difference across the resistor v and its current i, such that $v = 0$ when $i = 0$, and the signs of v and i are the same. An *ideal electrical resistor* is characterized by the linear relation, known as the *Ohm's law*,

$$v(t) = R_e \cdot i(t) \tag{6.7}$$

where the constituency parameter R_e [Ω] is called *electrical resistance*.

In some models it is useful to use an *pure* or **ideal electrical conductor** instead of a pure resp. ideal resistor. Ideal conductors are characterized by *electrical conductance* G_e reciprocal to R_e, i.e. $G_e = 1/R_e$ [S].
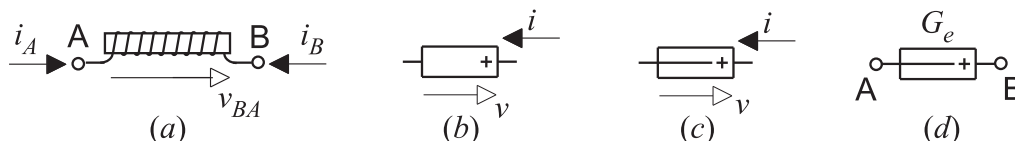

Figure 6.3: (*a*) Real electrical resistor. Pure electrical (*b*) resistor and (*c*) conductor. (*d*) Model of real resistor.

Fig. 6.3*b* gives our symbol for pure electrical resistors while in Fig. 6.3*c* is our symbol for pure conductors. Polarity of both symbols is denoted by the + sign, and the assumed positive orientation of the element voltage v and current i are associated with the symbol polarities. In Fig. 6.3*d*, the pure conductor is used to model the real resistor shown in Fig. 6.3*a*. Note that we do not need to show in the model the orientation of variables by arrows thanks to the unambiguous relation between the symbol polarity and the variables.

Electric and magnetic field effects are assumed to be zero in pure resistors and conductors. These elements can store neither electric-field nor magnetic-field energy. Characteristics of real components

called conductors or resistors utilized in electrical and electronic systems, however, comply often quite well with (6.7) in a fairly wide range of voltages and currents.

For example, if a voltage changing slowly enough is applied across a straight piece of a wire, the electrical current passing through the wire can be approximated by (6.7), and the electrical conductance of the wire

$$G_e = \gamma \frac{A}{\ell} \tag{6.8}$$

where γ [S.m^{-1}] is the specific conductivity of the material from which the wire is made, A is the cross-section area of the wire, and ℓ is the wire length.

Electrical power is delivered to a resistance whenever current flows through it. For an ideal resistance

$$\mathcal{P} = R_e i^2 = v^2/G_e \tag{6.9}$$

Power always flows into the resistor regardless of the signs of i and v. The power transferred to a resistance cannot be retrieved and is said to be dissipated. Usually the power is transformed into thermal internal energy in the resistance and the temperature rise which accompanies the increase in internal energy results in flow of heat to the environment.

6.4   Electrical capacitance

In a dielectric material an electric field can be established without allowing a significant flow of charge through it. If two pieces of conducting material are separated by a dielectric material, an electric field is established between the conductors when charge flows into one conductor and out of the other. This electric field results in a potential difference between the two conductors which depends on the amount of charge placed on the conductors. Physical devices which exhibit this type of relation between charge and voltage are said to have capacitance.
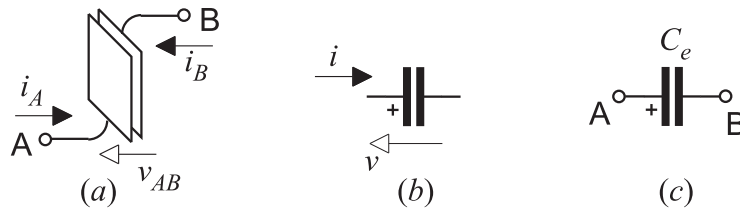

Figure 6.4: (a) Parallel-plate capacitor. (b) Pure electrical capacitor. (c) Model of real capacitor.

Most electrical components exhibit the property of capacitance to some extent. A device designed to behave primarily like a capacitance is called an electrical condenser or capacitor. As an example, Fig. 6.4a shows a real capacitor consisting of two parallel flat plates separated by a dielectric.

To permit this capacitive effect to be separated from other electrical phenomena, we shall define a pure capacitor. It is a two-terminal electrical element in which charge q is a function of the voltage difference across the element:

$$q = f(v)$$

In a pure capacitor, the conductors offer zero resistance to flow of charge, the dielectric separating the conductors has infinite resistance to the flow of charge, and magnetic field effects are absent.

Fig. 6.4b shows the symbol to be used for a pure capacitor. The assumed positive direction of current flow i and voltage drop v is indicated by an arrows drawn beside the symbol. This sign convention is related to the polarity of the symbol indicated by the $+$ sign. In Fig. 6.4c, the pure capacitor is used to model the real capacitor. Note the relation between the orientation of the symbol and the variables in the model.

The constitutive relationship for an ideal capacitor has charge proportional to voltage difference

$$q = C \cdot v$$

where C is the capacitance of the element, having units of farads [F] ($F = A.s/V$). The elemental equation for an ideal capacitor of constant C is therefore

$$i(t) = C \frac{dv}{dt} \tag{6.10}$$

or

$$v(t) = \frac{1}{C} \int_{t_0}^{t} i(\tau) \, d\tau + v(t_0) \tag{6.11}$$

where $v(t_0)$ is the voltage across the capacitance when $t = 0$.

For example, it may be recalled from physics that the capacitance of the closely spaced parallel-plate capacitor shown in Fig. 6.4a is

$$C = \epsilon A / d$$

where C [F] is the capacitance, ϵ [F/m] is the permittivity (a property) of the medium between the plates in farads/meter, A [m^2] is the plate area, and d [m] is the plate spacing. For air, for example, $\epsilon = 8.85 \times 10^{-12}$ [F/m].

The capacitance of various real structures depends only on the geometry and the material properties. In general, the calculation of capacitance for particular structures requires advanced methods of electric-field theory. Of course the capacitance of an existing element can always be determined experimentally.

When charge is caused to flow into a capacitance, electrical energy $\mathcal{E}_e$ is transferred to the element. From the power equation $\mathcal{P}_e = i.v$, the definition of current $i = dq/dt$, and the defining equation for a pure capacitor (6.11), the energy stored in an ideal capacitance is obtained from (2-79) with q = Cv21:

$$\mathcal{E}_e = C \int_0^v v, dv = \frac{1}{2} C v^2 = \frac{1}{2} \frac{q^2}{C}$$

The process of energy storage is reversible, and all the electrical energy stored in an ideal capacitor is retrievable. Note that the energy stored depends neither on the sign of the voltage nor on the instantaneous value of the current:

$$\mathcal{E}_e \geq 0.$$

6.5   Pure electrical inductor

When current flows through a conductor, a magnetic field is established in the space or the material around the conductor. If this current is changed as a function of time, the intensity of the magnetic field will also vary with time. According to Lenz's law, this changing field will induce voltage differences in the conductor which will tend to oppose the changing current.
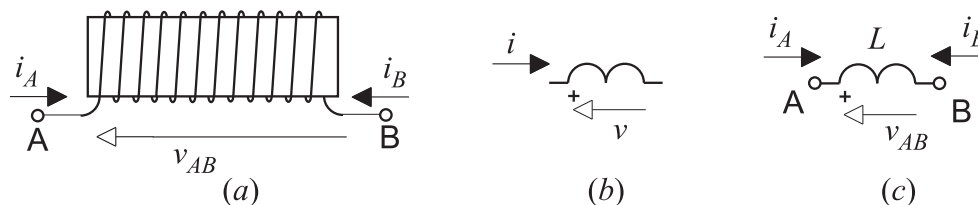

Figure 6.5: (a) Electrical coil. (b) Pure electrical inductor. (c) Coil model.

An electrical element is said to be a **pure electrical inductor** provided that the magnetic flux Φ is a function of the current i in the element generating the flux,

$$\Phi = \Phi(i) \tag{6.12}$$

The function $\Phi(i)$ depends on the magnetic properties of the medium in the vicinity of the current flow.

By winding a wire in a geometry such as the helical coil of Fig. 6.5a, it is possible to reinforce the flux inside the coil and to have the same flux link several turns of the coil. If a flux Φ links N turns, the **flux linkage** λ is

$$\lambda = N \, \Phi = f(i) \tag{6.13}$$

The unit of flux linkage is weber [W] (1 W = 1 V.s).

As shown in Fig. 6.6, the flux linkage λ can be proportional to i, or it can be highly nonlinear depending if the medium surrounding the inductor is, or is not, nonmagnetic.

The relationship of the magnetic flux linkage to terminal voltage of an inductor is given by Faraday's law

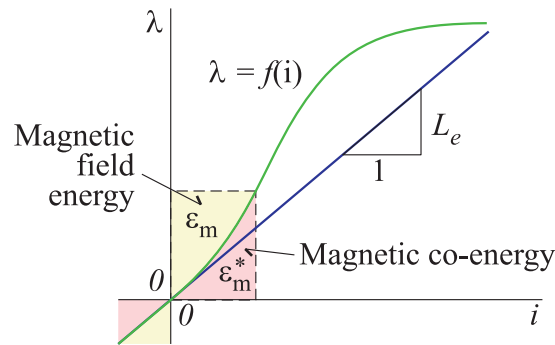$$v(t) = \frac{d\lambda(t)}{dt} \tag{6.14}$$

Figure 6.6: Constitutive characteristics of pure inductors.

A voltage is 'induced' in the inductor which is equal to the rate of change of the flux linkages in the inductor. Substituting (6.13) into (6.14), the terminal voltage can be written

$$v(t) = \frac{d\lambda}{di} \cdot \frac{di}{dt} \tag{6.15}$$

A linear pure electrical inductor, called an **ideal electrical inductor**, has flux linkage proportional to its current:

$$\lambda(t) = L_e \cdot i(t) \tag{6.16}$$

The **electrical inductance** L_e of the ideal inductor is measured in henries [H] (1 H = 1 V.s/A), and λ is defined to be zero when $i = 0$. As with capacitance, the computation of the inductance for a given structure will usually require the use of field theory. It is noted that inductance is determined purely by geometry and material properties.

For example, the inductance of a closely wound, long helical coil as that shown in Fig. 6.5a can be estimated as

$$L_e = \frac{\pi N^2 \mu d^2}{4l}$$

where l is the coil length, d is its diameter, N is the number of its turns, and μ is the permeability of the material in the vicinity of the coil. For a vacuum (or very nearly for air) $\mu = \mu_0 = 4 \times 10^{-7}$ H/m.

The inductance of a coil in air will be nearly linear, but the magnitude of the inductance is very small. This magnitude may be increased by factors up to 10^6 by the use of ferromagnetic material such as iron, cobalt, and nickel. However, inductors which use ferromagnetic materials are nonlinear and give responses somewhat like the nonlinear curve shown in Fig. 6.6. The flattening of this curve as i is increased is called **saturation**.

Inductance of a toroidal coil made of a conducting wire wound around a toroid made of a nonmetallic material such as wood is approximately

$$L_e = \mu_0 \frac{N^2 A}{l} \quad [\text{H}] \tag{6.17}$$

where N is the number of turns, A is the cross-sectional area, and l is the midcircumference along the toroid.

The elemental equation for an ideal inductor of constant L_e follows from (6.14) and (6.16):

$$v(t) = L_e \frac{d}{dt} i \tag{6.18}$$

or

$$i(t) = \frac{1}{L_e} \int_{t_0}^{t} v(\tau) \, d\tau + i(t_0) \tag{6.19}$$

where $i(t_0)$ is the inductor current when $t = t_0$.

Fig. 6.5b gives our symbol of pure electrical inductors. In Fig. 6.5c, the pure inductor is used to model the helical coil.

An inductor stores energy in the magnetic field associated with the current. The electrical energy stored in a pure inductor is called the magnetic-field energy

$$\mathcal{E}_m = \int_{t_a}^{t_b} v\, i d\tau = \int_{\lambda_a}^{\lambda_b} i d\lambda \tag{6.20}$$

The energy $\mathcal{E}_m$ is represented by the shaded area in Fig. 6.6.
If the inductor is ideal, equations (6.16) and (6.20) give

$$\mathcal{E}_m = \frac{1}{2} L_e\, i^2 = \frac{1}{2} \frac{\lambda^2}{L_e} \tag{6.21}$$

This energy is stored by virtue of the current and does not directly depend on the voltage difference. The energy is always positive,

$$\mathcal{E}_m \geq 0$$

and any energy stored by increasing the current from i_a to i_b is recovered completely when the current is decreased to i_a.

6.6   Coupled inductors

In this unit we shall pay a special attention to electrical inductors mutually coupled by a common magnetic field. The coupled inductors are of crucial importance as models in many practical applications, like in electrical transformers, motors and generators. In most cases, such devices are modelled 'from the electrical point of view' without the necessity (or possibility) of modeling detailed structure of the magnetic field inside the device.

Fig. 6.7*a* shows a pair of coils placed close to one another so that there is an interaction between their magnetic fields. The magnetic flux in one coil depends on the currents passing through both coils. Let us assume that the magnetic flux ϕ_1 of the first coil, and the magnetic flux ϕ_2 of the second coil, can be expressed as

$$\begin{aligned} \phi_1(i_1, i_2) &= \phi_{11}(i_1) + \phi_{12}(i_2) \\ \phi_2(i_1, i_2) &= \phi_{21}(i_1) + \phi_{22}(i_2) \end{aligned} \tag{6.22}$$
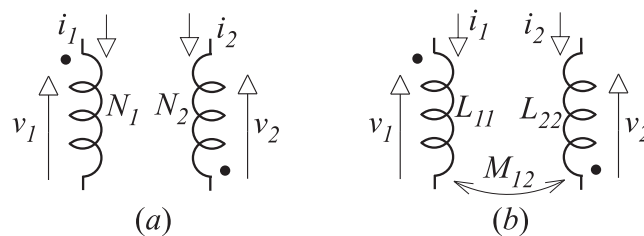

Figure 6.7: (*a*) Pair of interacting coils, (*b*) coupled electrical inductors.

For the following discussions, it will be more convenient to consider magnetic linkages of the coils instead of their fluxes. Recall, that if all the N_1 turns of the first coil are linked by the flux ϕ_1, the flux linkage of the first coil is $\lambda_1 = N_1\phi_1$. Similarly, if all the N_2 turns of the second coil are linked by the flux ϕ_2, than $\lambda_2 = N_2\phi_2$.

Assuming further, that the magnetic fluxes are linear functions of the coil currents, we can express the magnetic linkages of the two coils as

$$\begin{aligned} \lambda_1(t) &= L_{11}\, i_1(t) + L_{12}\, i_2(t) \\ \lambda_2(t) &= L_{21}\, i_1(t) + L_{22}\, i_2(t) \end{aligned} \tag{6.23}$$

where L_{11} and L_{22}, is the *self-inductance* of the first and second inductor, respectively. $L_{12} = L_{21}$ are the *mutual inductances* of the inductors. Thus the two coils can be modelled by a pair of coupled linear electrical inductors shown in Fig. 6.7*b*. Their constitutive relation (6.23) rewritten in matrix form is

$$\begin{bmatrix} \lambda_1(t) \\ \lambda_2(t) \end{bmatrix} = \mathbf{L} \cdot \begin{bmatrix} i_1(t) \\ i_2(t) \end{bmatrix} \quad \text{where} \quad \mathbf{L} = \begin{bmatrix} L_{11} & L_{12} \\ L_{21} & L_{22} \end{bmatrix} \tag{6.24}$$

is the *inductance matrix.*

According to Faraday's law, voltages across the inductors

$$v_1(t) = \frac{d\lambda_1}{dt} + R_1 i_1 \qquad \text{and} \qquad v_2(t) = \frac{d\lambda_2}{dt} + R_2 i_2 \tag{6.25}$$

Hence, by differentiating (6.24), we can arrive at a constitutive relation of the coupled inductors in the form of two differential equations

$$\begin{bmatrix} v_1(t) \\ v_2(t) \end{bmatrix} = \mathbf{L} \cdot \frac{d}{dt} \begin{bmatrix} i_1(t) \\ i_2(t) \end{bmatrix} + \mathbf{R} \begin{bmatrix} i_1(t) \\ i_2(t) \end{bmatrix} \tag{6.26}$$

where

$$\mathbf{R} = \begin{bmatrix} R_1 & 0 \\ 0 & R_2 \end{bmatrix} \tag{6.27}$$

By energy considerations it is established that in general

$$L_{21} = L_{12} = \pm M \tag{6.28}$$

where $M \geq 0$ is the *coupling factor.* Hence, $\mathbf{L}$ is a symmetric matrix. Instead of the coupling factor M, mutual inductance is often expressed in terms of Also the *coefficient of coupling*

$$k = \frac{M}{\sqrt{L_{11} L_{22}}}$$

is often used to express mutual inductance. Note, that $k \leq 1$. For $k = 1$, when $M^2 = L_{11} L_{22}$, the *coupling* is termed *ideal.*

The sign of a mutual inductance depends on the orientation of the coil windings, and can be determined by the *dot-reference convention* used also in Fig. 6.7. The dots denote either the 'beginnings' or the 'ends' of all the coil windings taking into consideration a unique orientation of the coil turns. The mutual inductance of any two of coupled inductors is positive, if the variable reference of each of the two engaged inductors is directed either towards, or from, its dot. If it is not so, the sign of the mutual inductance is negative. In the particular example of the dot reference specification given in Fig. 6.7b, $L_{21} = L_{12} \leq 0$.

6.7 More coupled inductors

If we have more than two linear time-invariant inductors coupled, (6.24) can be easily extended. For example, if there are three coupled inductors like in Fig. 6.8, we have

$$\begin{bmatrix} v_1(t) \\ v_2(t) \\ v_3(t) \end{bmatrix} = \mathbf{L} \cdot \frac{d}{dt} \begin{bmatrix} i_1(t) \\ i_2(t) \\ i_3(t) \end{bmatrix} \qquad \text{where} \qquad \mathbf{L} = \begin{bmatrix} L_{11} & L_{12} & L_{13} \\ L_{21} & L_{22} & L_{23} \\ L_{31} & L_{32} & L_{33} \end{bmatrix} \tag{6.29}$$

In this case, L_{11}, L_{22}, L_{33} are the self-inductances, and

$$L_{jk} = L_{kj} = \pm M_{jk}, \qquad k, j = 1, 2, 3, \qquad k \neq j$$

are the mutual inductances of the three coupled inductors. Taking into consideration the dot references given in Fig. 6.8, $L_{12} = L_{21} = -M_{12}$, $L_{23} = L_{32} = M_{23}$ and $L_{13} = L_{31} = -M_{13}$ in this particular example.

Regardless of the number of coupled inductors, (6.26) can be expressed as

$$\mathbf{v}(t) = \mathbf{L} \cdot \frac{d}{dt} \mathbf{i}(t) \tag{6.30}$$

or, in the integral form as

$$\mathbf{i}(t) = \mathbf{L}^{-1} \int_0^t \mathbf{v}(\tau) \, d\tau + \mathbf{i}(0+) \tag{6.31}$$

where $\mathbf{i}(0+)$ is the vector of initial currents of the coils just right after $t = 0$.

Note that if the coupling between any of the involved inductors is ideal, the *inverse inductance matrix* $\mathbf{L}^{-1}$ does not exist, because $\mathbf{L}$ is singular. This property follows from the fact, that conductances of any two ideally coupled inductors – let us say between L_j and L_k – are interrelated, as $M^2 = L_{jk} L_{kj} = L_{jj} L_{kk}$. Thus the corresponding 2×2 submatrix in $\mathbf{L}$ is singular.
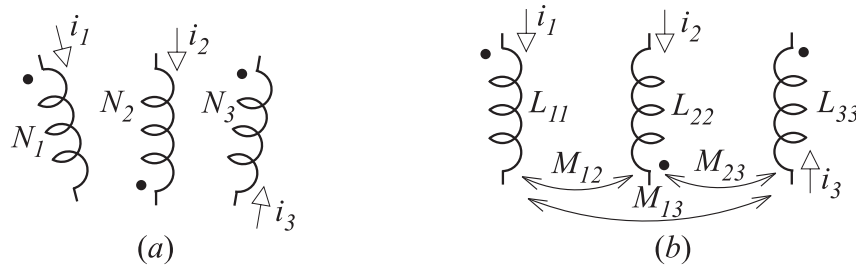
Figure 6.8: (*a*) Three interacting coils, (*b*) coupled electrical inductors.

6.8 Coupled inductors and ideal transformer

Fig. 6.9 shows two models equivalent to the two coupled inductors in Fig. 6.7*b*. Both models are based on ideal transformers. In the case of the model shown in Fig. 6.9*a*, where $n = 1$, the only purpose of the unit-ratio transformer is to 'isolate' the ports corresponding to the inductors from each other.
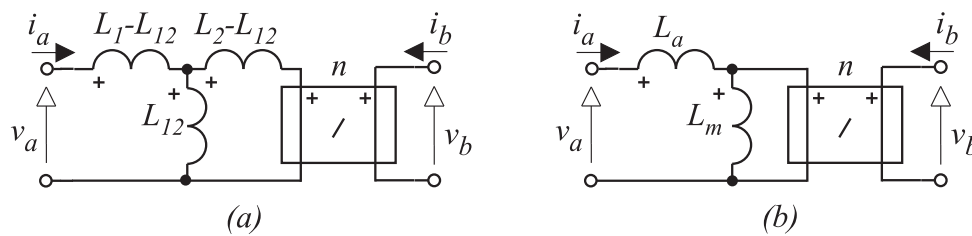

Figure 6.9: Models equivalent to coupled electrical inductors employing an ideal transformer.

In the model given in Fig. 6.9*b*, the ideal-transformer ratio and the inductances are

$$n = \frac{L_{12}}{L_{22}} \qquad L_m = \frac{M^2}{L_{22}} \qquad L_a = L_{11} - \frac{M^2}{L_{22}} \tag{6.32}$$

L_m is called the *magnetizing inductance* as it models the effect of the magnetic flux common to both coils. L_a is the *leakage inductance* modeling the effect of the leakage fluxes seen at the first port. The equivalence of both models to a pair of coupled inductors can be easily verified by their analysis.

It is interesting to investigate the model in Fig. 6.9*b* for the limit case when $L_{11} \to \infty$, $L_{22} \to \infty$, and $k \to 1$. From (6.32) we can see that under these assumptions $L_a \to 0$ and $L_m \to \infty$. Hence, in the limit case, the inductance L_a becomes a closed circuit while the inductance L_m becomes an open circuit. Also, in the limit case, $n = \pm N_2/N_1$ assuming that N_1 and N_2 are the coil turns fully linked by their fluxes. The sign of n can be determined in the same way as the sign of the mutual inductance.

Module 7

Magnetic systems

7.1   Magnetic interactions

Magnetic field can be represented by lines of magnetic flux. Where these flux lines bypass the required path through the circuit, they are termed **flux leakage**. Magnetic **flux fringing** is somewhat similar to leakage and is a term used to describe the spreading of flux lines in an air gap of a magnetic circuit thus increasing its effective area. The toroidal coil in Fig. 7.1a with windings of evenly distributed turns forms a completely closed homogenous magnetic circuit without any leakage flux. This is true even if the core is made from a nonmagnetic material. If the core of such a coil is made from a material with large permeability, there will be no considerable leakage fluxes even if the coil winding is concentrated into one place on the toroid, as indicated by the dashed line in Fig. 7.1a.

$$(a) \qquad\qquad (b) \qquad\qquad (c)$$
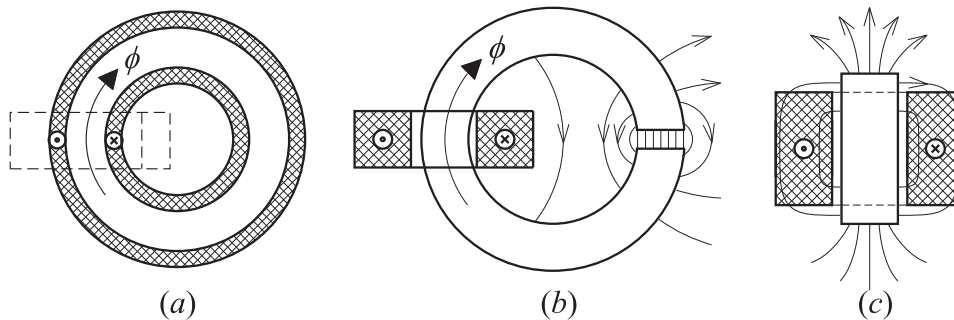
Figure 7.1: Magnetic field of different coils.

If the core is disrupted by an air gap, as in Fig. 7.1b, the flux lines indicate that large leakage and fringing fluxes result and the flux within the core varies with the distance from the coil. Still, such a coil can be modeled as a magnetic circuit if the largest part of the flux lines is concentrated into the core which determines their geometric shape. In the contrary, the short cylindrical coil shown in Fig. 7.1c cannot be modeled as a magnetic circuit. Except for the short part of the flux lines within the core, most of their length is situated in the air.

Magnetic voltage (called also magnetomotive force) $w(t)$ [A] plays the role of the across variable in magnetic interactions. The concept of magnetic voltage is applicable in quasi-magnetic fields when the rate of change of electric field normal to the subsystem energy boundary is negligible.

Magnetic flux rate $\dot{\psi}(t)$ [Wb/s] into a subsystem through an energy entry is defined as

$$\dot{\phi}(t) = \frac{d\phi}{dt}$$

where $\phi(t)$ is the total of magnetic flux B [Wb/m^2] over the entry area passing through it in the perpendicular direction to it.

Magnetic interactions are also governed by laws similar to those of Kirchhoff. The continuity postulate applies to the rate of magnetic flux into the entries of a subsystem assuming the magnetic flux leakage through the subsystem boundary is negligible. If it is not so, the boundary must be enlarged to include also the leakage flux lines.
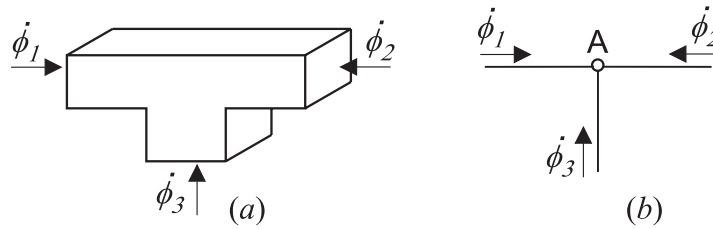
Figure 7.2: Postulate of continuity for magnetic circuits.

Fig. 7.2a shows branching of the magnetic flux in a ferromagnetic material. The dynamic diagram representation of the branching is in Fig. 7.2b. The interconnection portrayed there by node A with three line segments representing ideal magnetic conductors.

Obviously, the magnetic flux in magnetic systems obeys the *continuity postulate* based on the law of conservation of magnetic field. In general, if there are n magnetic conductors interconnected at a point, and if ϕ_k is a magnetic flux of the k-th conductor, then

$$\sum_{k=1}^{n} \phi_k = 0 \tag{7.1}$$

where the fluxes oriented *towards* the interconnection are considered as positive.

According to *Ampere's law* the integral around any closed path ℓ in the magnetic field of intensity **H** equals the sum of electrical current I passing through the path ℓ, i.e.

$$\oint_{\ell} \mathbf{H} \cdot d\ell = I \tag{7.2}$$

Positive current is defined here as flowing in the direction of the advance of a right-handed screw turned in the direction in which the closed path is traversed by **H**.

Assuming that the closed path ℓ is divided into n segments $\ell_k, k = 1, 2, \ldots, n$, then

$$\oint_{\ell} \mathbf{H} \cdot d\ell = \sum_{k=1}^{n} \int_{\ell_k} \mathbf{H}_\ell d\ell \tag{7.3}$$

where

$$\int_{\ell_k} \mathbf{H}_\ell d\ell = w_k \tag{7.4}$$

represents the magnetic voltage across the k-th segment of ℓ.

Hence, the integral (7.2) can be replaced by the sum

$$\sum_{k=1}^{n} w_k + w_m = 0 \tag{7.5}$$

where $w_m = -I$ represents the total *magneto-motoric voltage* of ℓ. We may thus reformulate Ampere's law as stating that "the sum of magnetic voltage drops around any closed path is equal to zero," which represents the *compatibility postulate* for magnetic systems.

7.2   Pure magnetic capacitor

A *pure magnetic capacitor* can be described by the constitutive relation

$$f(\phi, w, t) = 0 \tag{7.6}$$

For an *ideal magnetic capacitor* (7.6) becomes

$$\phi(t) = C_m \cdot w(t) \tag{7.7}$$

where C_m, the *magnetic capacitance*, is known as the *permeance*, and is measured in henrys. Its reciprocal value $D_m = 1/C_m$ is called the *reluctance*.

The energy stored in the magnetic capacitor is

$$W = \int \dot{\phi} w \, dt = C_m \int w \, dw = \frac{1}{2} C_m w^2 = \frac{1}{2} \phi w = \frac{1}{2C_m^2} \phi^2 \tag{7.8}$$

Magnetic flux ϕ through a part of a surface of an area S [m^2] is defined by the integral

$$\phi = \int_S \mathbf{B}_n dS \tag{7.9}$$

where $\mathbf{B}_n$ is the magnetic flux density vector which is normal to the surface. Within a material, $\mathbf{B}$ and $\mathbf{H}$ are related by the *permeability* μ of the material:

$$\mathbf{B} = \mu\mathbf{H} \qquad \mu = \mu_0\mu_r \tag{7.10}$$

where $\mu_0 = 4\pi \times 10^{-7}$ [H.m^{-1}] is the *permeability of free space*, and μ_r [$-$] is the *relative permeability* of the material. Permeability can be qualified as a scalar only in regions of homogenous and isotropic materials. In case of nonmagnetic materials μ_r can be considered as equal to 1.0 for most of the practical purposes. Properties of most of magnetic materials are strongly nonlinear, the expression (7.10) can then be applied to small variations of $\mathbf{H}$ in the vicinity of a certain fixed operating point.
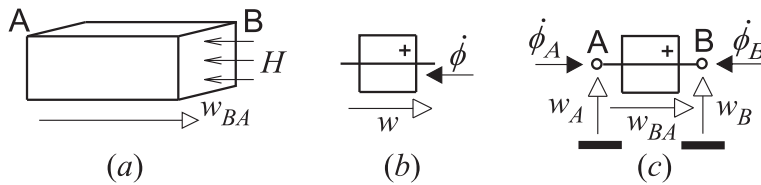
Figure 7.3: (*a*) Ferromagnetic core. (*b*) Symbol of pure magnetic capacitor. (*c*) Dynamic model.

Fig. 7.3*a* shows a piece of a core made of ferromagnetic material of a cross section area A and of length ℓ. If we assume that the magnetic field intensity H is nonvarying along the length ℓ, and that the flux density B is uniform over the area A, the permeance of the component becomes

$$C_m = \frac{\phi(t)}{w(t)} = \frac{BA}{H\ell} = \frac{\mu A}{\ell} \tag{7.11}$$

which is similar to the expression for electrical capacitance in a region with similarly uniform electrical properties.
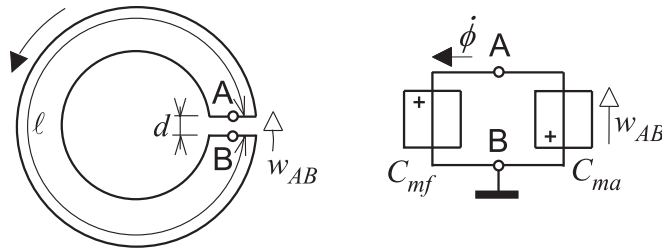
Figure 7.4: (*a*) Ferromagnetic torus. (*b*) Dynamic model.

Fig. 7.4*a* shows a torus made of highly permeable material with a winding of N turns. The magnetic voltage around the magnetic path is $w = N\,i$. This magnetic voltage establishes a magnetic field intensity H, which in turn produces a magnetic flux density $B = \mu H$ in the material. The narrow air gap interrupting the closed magnetic circuit makes an example of a magnetic system components that can be modeled as an ideal magnetic capacitor as shown in Fig. 7.4*b*.

Magnetic circuit with leakage fluxes forms a distributed-parameter system. As in the case of other similar systems, it can be approximated by decomposing it into sections each of which is represented by a lumped parameter model. The larger is the number of the sections, the more accurate is the approximation. For example, the magnetic circuit in Fig. 7.5*a* is divided into a number of parts and assumed fluxes both in the core and in the air are indicated. Fig. 7.5*b* shows the corresponding lumped-parameter model in which the permeances are related to the core segments, to the leakages and to the gap.
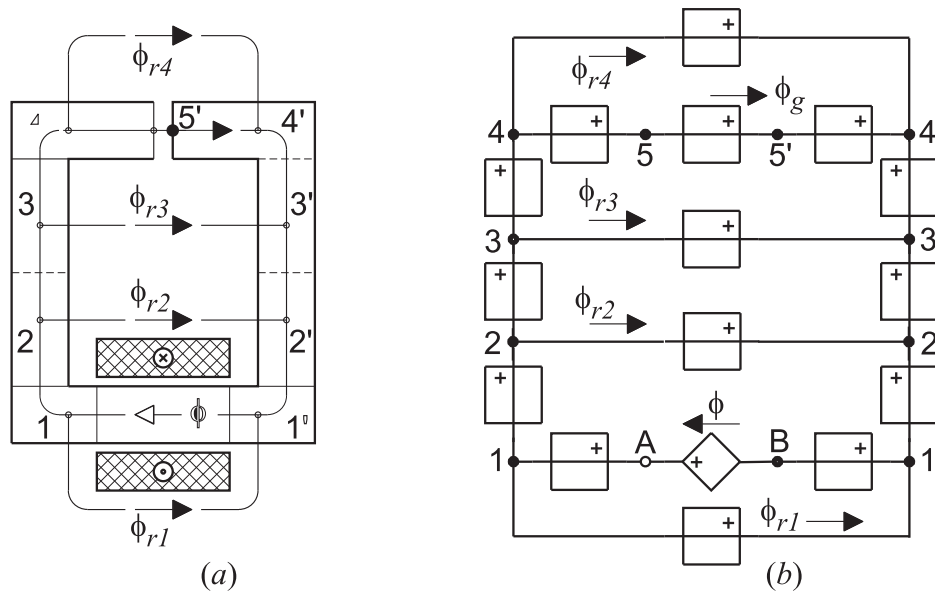
Figure 7.5: Magnetic circuit with distributed parameters and its models.

7.3   Pure magnetic conductor

The constitutive relation of a *pure magnetic conductor* or *resistor* is

$$f(\dot{\phi}, w, t) = 0 \tag{7.12}$$

In case of an *ideal magnetic conductor* (7.12) becomes

$$\dot{\phi}(t) = G_m \cdot w(t) \tag{7.13}$$

where G_m, measured in ohms, is the *magnetic conductance* of the conductor. The *ideal magnetic resistor* is an element characterized by the inverse relation

$$w(t) = R_m \cdot \dot{\phi}(t) \tag{7.14}$$

where R_m is the *magnetic resistance* measured in siemens. Such elements can be used for modeling eddy current losses in magnetic systems, for example. Ideal magnetic conductors or resistors can be used to model energy dissipation losses associated with small variations of magnetic field in some materials.

   Note, that for the sake of consistency in the unified approach to modeling of dynamic effects in different energy domains, we do not adopt the traditional definitions of magnetic conductance and resistance. That is, we do not consider magnetic conductance to be equivalent to permeance, and magnetic resistance to reluctance as it is common on most of the other sources.

7.4   Ideal magnetic inductors

There is no known magnetic phenomenon at ordinary temperatures which acts as a magnetic inductor.

7.5   Magneto-electric conversion

Let us consider Fig. 7.6a with a coil consisting of N turns of wire wrapped around a ferromagnetic core with an air gap. The coil winding is supplied by the electrical current i making an electrical voltage drop v across the winding. The magnetic flux ϕ invoked in the core by the magnetic voltage Ni is divided by the two symmetrical core branches into two equal parts. The directions of the electrical current and magnetic flux comply with the right-handed screw rule.

   A magnetic model of the coil is given in Fig. 7.6b. The magnetic capacitor with the reluctance D_g represent there the magnetic field energy accumulation in the air gap. Similarly, the capacitors of
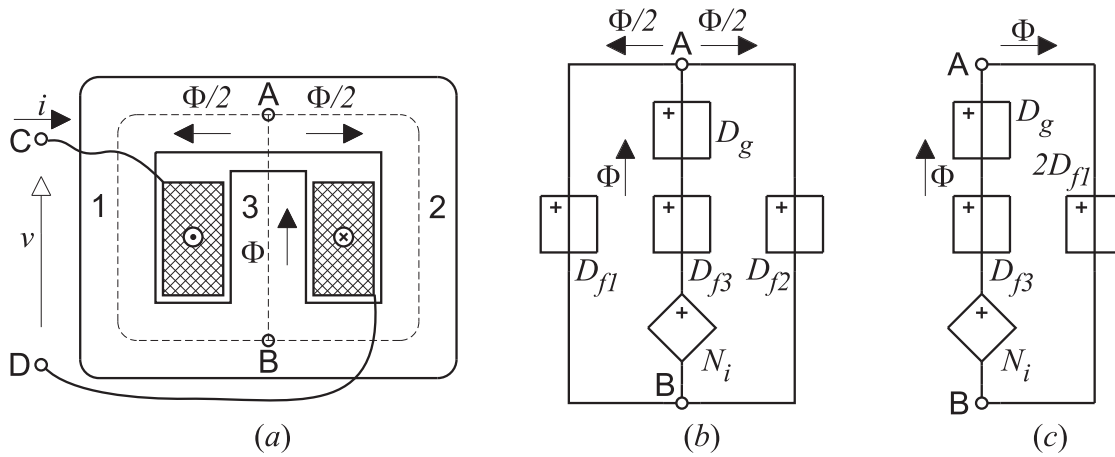
Figure 7.6: (a) Electromagnetic coil, (b) magnetic model, (c) simplified magnetic model.

reluctances D_{f1}, D_{f2} and D_{f3} represent this accumulation in the individual branches of the ferromagnetic core. In Fig. 7.6c, the same model is simplified taking advantage of the core symmetry.

Analyzing the model in Fig. 7.6c we shall obtain

$$\phi = \frac{Ni}{D_m} \tag{7.15}$$

where $D_m = D_g + D_{f1}/2 + D_{f3}$ is the coil reluctance.

So far we were discussing multipole models of the coil from the point of view of the magnetic field only. To be able to interconnect the coil model with a model of an electrical circuit interacting with the coil, we have to add a model of the electromagnetic conversion. In Fig. 7.7a, this conversion is represented by the gyrator of the gyrating ratio equal to the number of the coil turns N. The gyrator model consists of two controlled sources, both with the transfer ratio equal to N. One of them is an electrical voltage source controlled by the magnetic flux rate, the second is a magnetic voltage source controlled by the electrical current.
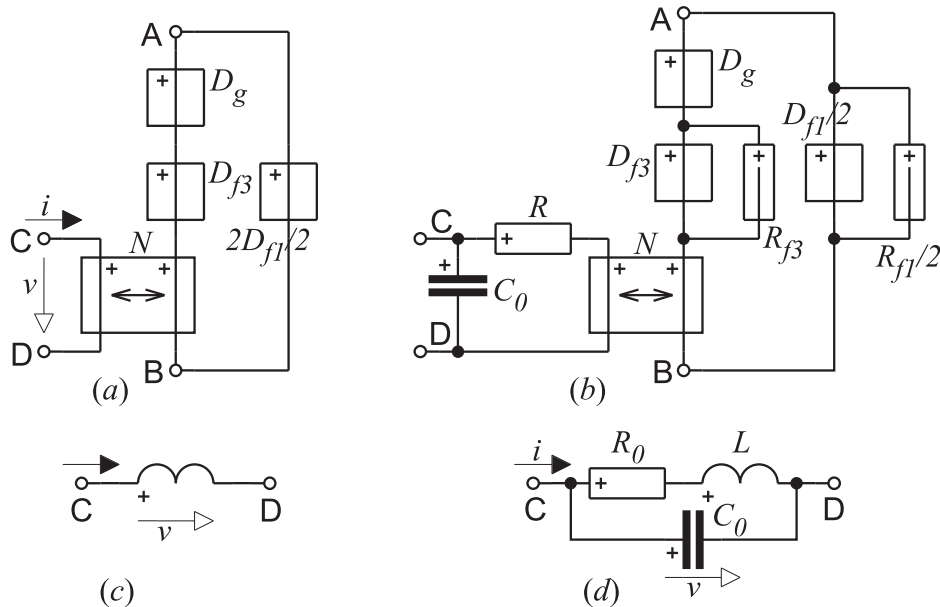
Figure 7.7: (a), (b) Coil electromagnetic models, (c), (d) coil electrical models.

Fig. 7.7b differs from Fig. 7.7a by elements modeling some parasitic effects in the coil. The electrical resistor R corresponds to the electrical resistance of the coil winding, the magnetic resistors R_{f1} and

R_{f2} stand for the energy losses in the segments of the ferromagnetic core, and the electrical capacitor C_0 represents accumulation of electric energy within the coil winding.

Note, that the model in Fig. 7.7b cannot be described just by a set of algebraic equations as it was in the case of the other coil models discussed so far – here we need a set of differential equations.

Analyzing the model shown in Fig. 7.7c we can arrive at the coil electrical model given in Fig. 7.7c, i.e. in a pure inductor. According to the static definition of the coil *inductance*

$$L = \frac{\lambda}{i} \tag{7.16}$$

where $\lambda = N\phi$ is the *flux linkage* measured in webers. Taking into consideration (7.15), the coil inductance can be expressed as

$$L = \frac{N^2}{D_m} \tag{7.17}$$

Similarly, analyzing the model from Fig. 7.7b we can obtain parameters of the coil electrical model with parasitic effect elements in Fig. 7.7d.

7.6   Magnetic nonlinearities

In ferromagnetic materials, the material is divided up into small regions or domains in each of which all dipole moments are spontaneously aligned. When the material is completely demagnetized, these domains have random orientation resulting in zero net flux density in any finite sample. As an external magnetizing force H is applied to the material, those domains that happen to be in line with the direction of H tend to grow, increasing B. The resulting *B-H magnetization characteristic*, known also as the *B-H virgin curve*, is shown in Fig. 7.8.

As H is further increased, this process continues until all domains are aligned with H. This results in magnetic saturation and the flux density within the material cannot increase beyond the *saturation density B_s*.
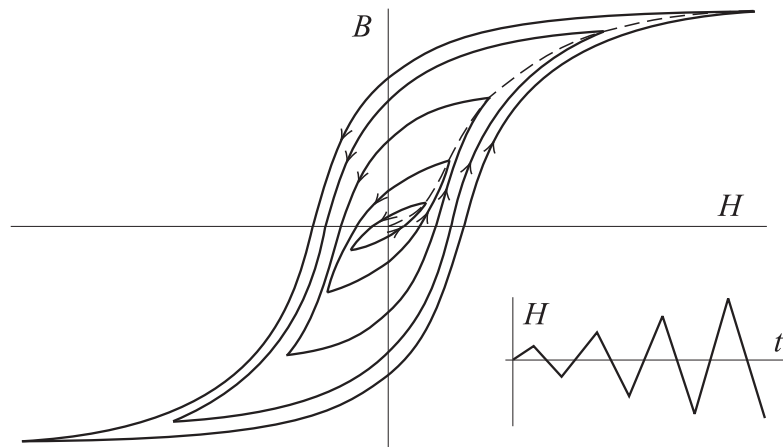
Figure 7.8: Magnetization characteristic.

The small increase that occurs beyond this condition is due to the increase of the flux density in the vicinity of the space occupied by the material. It is often convenient to subtract out this component of 'free space' flux density and observe only the flux density variation within the material. Such a curve is known as the *intrinsic magnetization characteristic* and is of use in the design of permanent magnet devices.

A symmetrical *hysteresis loop* is obtained after a magnetic field intensity reversal between plus and minus H_s. The area within the hysteresis loop corresponds to the *hysteresis losses*, i.e. to the energy dissipated in the material during one reversal cycle. This area varies with temperature of the material and with the frequency of the reversal.

Eddy current losses are caused by electrical currents induced in the core, called eddies, since they tend to flow in closed path within the magnetic material itself. The eddy current loss in a sinusoidally

excited material, neglecting saturation, can be expressed by the relationship

$$P_e = k_e f^2 B_m^2 \quad [\text{W}] \tag{7.18}$$

where B_m is the maximum value of flux density, f the frequency, and k_e is a proportionality constant depending upon the type of material and the lamination thickness.

To reduce eddy current loss, the magnetic material is laminated, that is, divided up into thin sheets with a very thin layer of electrical insulation between each sheet. The sheets must be oriented in a direction parallel with the flow of magnetic flux. It should be recognized that laminating a magnetic material generally increases its volume. The ratio of the volume actually occupied by magnetic material to total volume of a magnetic part is known as the *stacking factor*. This factor is important in accurately calculating flux densities in magnetic parts.

Therefore, instead of Eq. (7.10), for larger variations of magnetic field intensity H the relation

$$B = f(H) \tag{7.19}$$

expressing the flux density B as a function of H has to be considered.

7.7 Permanent magnet excited systems

The second type of excitation source that is commonly used for supplying energy to magnetic circuits used in rotating machines and other types of electromechanical devices is the permanent magnet. The excitation can be described with the aid of the second quadrant B-H curve, often called the *demagnetization curve*.

Theoretically, it is possible to have infinite permeance in the external magnetic circuit that would correspond to $\alpha = 90°$ and the magnet operating point would be at $B = B_r, H = 0$. This situation is approximated by a permanent magnet having an external circuit consisting of no air gap and a high permeability member often called a 'keeper'. In practice, however, there is always a small equivalent air gap and a small reluctance drop in the keeper, and the operating point is to the left of B_r.

For a finite air gap, the operating point will be at some point A on the B-H curve, and the permanent magnet will develop the magnetic field intensity H_A to overcome the reluctance drop of the air gap and other portions of the external magnetic circuit. If the air gap is increased, P_{ge} decreases and the magnet must develop a larger magnetic field intensity H_d. If the air gap is subsequently returned to its original value, the operating point will not return to A but, rather to C.

The slope of the loop is known as *recoil permeability*. Since it is a slope on the B-H plane, it is also sometimes called incremental permeability. Recoil permeability is an important parameter of a permanent magnet for applications with varying air gaps. In general, a permanent magnet is used most efficiently when operated at conditions of B and H that result in the maximum energy product.

Module 8

Electromechanical systems

8.1 Conductor moving in magnetic field

The principle of a variety of electromechanical transducers is shown in Fig. 8.1a. A conductor of length ℓ is placed there in parallel with the y-axis in a homogenous magnetic field with flux density B oriented in the x-direction. If current i flows through the conductor in the y-direction, a z-directional external force F is required to hold the wire in equilibrium against the magnetic force acting on it. The magnitude of the force is given by the *Lorentz force law*

$$F = -B\,\ell\,i \tag{8.1}$$

The direction of the force is determined by the left-hand Fleming's rule. If the conductor moves at a speed $\dot{z}$ through the magnetic field in the z-direction, a voltage v is generated in the conductor. According to *Faraday's law* of magnetic induction the magnitude of the voltage is

$$v = B\,\ell\,\dot{z} \tag{8.2}$$

The polarity of v is given by Fleming's right-hand rule. That is, if conductor moves in the direction of the force F, the polarity of v with respect to i is such that an electrical power is generated.
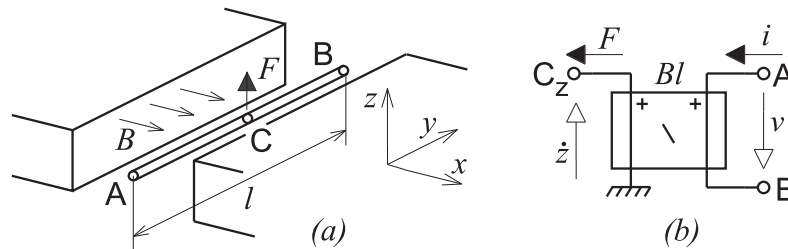
Figure 8.1: (a) Current-carrying conductor moving in a magnetic field, (b) its ideal-transformer model.

Equations (8.1) and (8.2) form together the constitutive relationship of an ideal energy-transfer transformer which can be used for modeling this simple device as illustrated in Fig. 8.1b. The transformer poles A and B represent electrical terminals of the wire, whereas pole C$_z$ represents motion of the wire along the z axis. Coupling ratio of the transformer is obviously

$$n = \frac{\dot{z}}{v} = \frac{1}{B\,\ell} = \frac{1}{B2\pi rN} \tag{8.3}$$

8.2 Coil moving in magnetic field.

As another example of an energy-transfer transducer, we consider a coil which can move in a uniform magnetic field. The voice coil of a loudspeaker and the meter movement of an ammeter are representative applications. Fig. 8.2a indicates a typical geometric configuration for a loudspeaker voice coil. A permanent magnet maintains a uniform radial magnetic field B in the annular gap. Within the gap is the voice coil, which can move longitudally with velocity $\dot{x}$. Flexible lead-in wires introduce a current i

into the moving coil. The external force F acting on the coil is required to hold the coil in equilibrium against the magnetic forces. The voltage across the voice coil is v.

The constitutive relations for the moving coil can be obtained from (8.1) and (8.2) by substituting $\ell = 2\pi\, r\, N$, where r is the coil radius and N is the number of turns of the coil winding. Thus the moving coil can be modeled by the ideal energy-transfer transformer shown in Fig. 8.2b where the transforming ratio

$$n = \frac{v}{\dot{x}} = 2\pi\, N\, B\, i \tag{8.4}$$

In the model shown in Fig. 8.2b we neglect the electrical resistance and self-inductance of the voice-coil, as well as any capacitance. We also neglect the mechanical mass and friction, as well as any restraint from the lead-in wires. These effects can be respected by augmenting the ideal transformer with physical elements representing these effects.
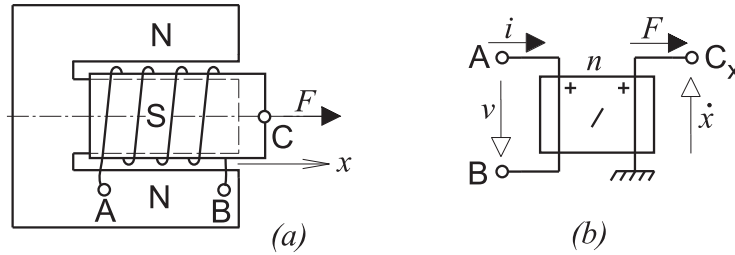
Figure 8.2: Moving-coil transducer.

8.3   Single-phase alternator.

A model of a simple single-phase alternator is easy to construct based on the same principle. A geometric configuration of such a device is shown in Fig. 8.3a. Wires wrapped around a rotor or armature rotating about the z axis are carried through a gap of substantially constant x-directed flux density B. The component of the conductor velocity perpendicular to the flux is

$$\dot{y} = r\, \dot{\varphi}\, \cos\varphi \tag{8.5}$$

where r is the radius of the armature and $\dot{\varphi}$ is its angular velocity. It is this component which must be used in (8.2) for the voltage equation

$$v = B\, \ell\, r\, \dot{\varphi}\, \cos\varphi \tag{8.6}$$

where ℓ is the effective length of all conductors cutting the flux lines with an average density value B.

Wires may be wound many times around the armature, and the total voltage generated is the sum of all the voltages generated by each wrap. Note that voltage induced on one side of the rotor adds to that on the other because although the direction of flux cutting is opposite on two ends of the rotor diameter, the direction of current flow is also opposite on the two ends. The electric circuit can be completed with clip rings as shown.

If current starts to flow through the rotor winding, a force given by (8.1) will act on it giving rise to a torque opposing the rotation. The magnitude of the external torque required to hold the rotor in equilibrium will be

$$\tau = F\, r\, \cos\varphi = -B\, \ell\, r\, i\, \cos\varphi \tag{8.7}$$

This together indicates, that the alternator can be modeled by a pure transformer with the variable ratio

$$n = \frac{\dot{\varphi}}{v} = \frac{1}{B\, \ell\, \sin\varphi} \tag{8.8}$$

as shown in Fig. 8.3b. Pole C_φ represents the rotational motion of the rotor.

Real alternators have more complicated configurations than the one shown schematically in Fig. 8.3a an may have sets of windings to generate three-phase power, but the basic modeling idea based on and energy-transfer transformer still applies.
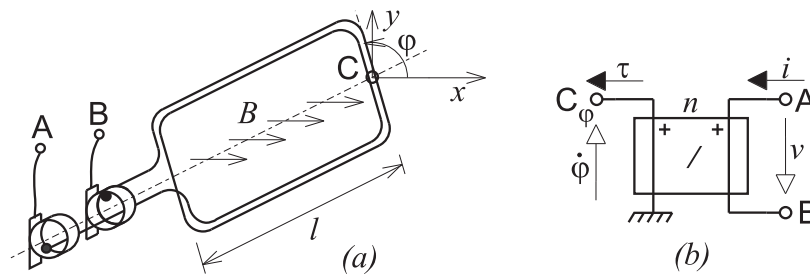
Figure 8.3: Single-phase ac rotational transducer.

8.4 Permanent-magnet dc machine

This machine consist of several windings situated in a magnetic field of constant flux density B much like alternator windings but with a commutator (mechanical with carbon brushes, or electronic brushless) that switches the windings into and out of the external electrical circuit as the armature rotates. As shown schematically in Fig. 8.4a, a coil is connected for only a small fraction of revolution. During the time any coil is connected, the $\cos\varphi$ terms in (8.6) and (8.7) are nearly unity. The equations therefore are approximately

$$v = B\,\ell\,r\,\dot\varphi \quad \text{and} \quad \tau = -B\,\ell\,r\,i \tag{8.9}$$

which can be represented, as in Fig. 8.4b, by a simple ideal-energy transfer transformer with the transforming ratio

$$n = \frac{\dot\varphi}{v} = \frac{1}{B\,\ell\,r} \tag{8.10}$$

There is some ripple in the characteristics for v versus $\dot\varphi$ and i versus φ due to the finite number of coils in a dc machine, but (8.10) are accurate enough for many design purposes.
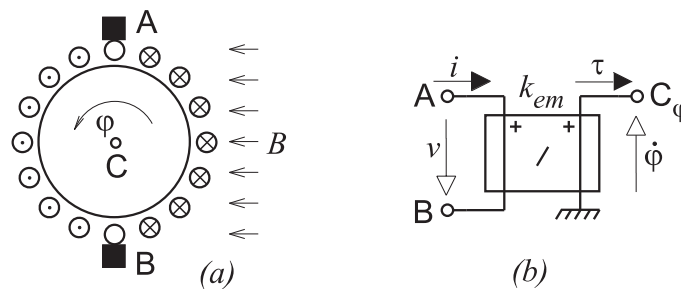
Figure 8.4: Pure model of dc permanent magnet machine.

Equations (8.6) are usually written as

$$v = K_E\,\dot\varphi \quad \text{and} \quad \tau = -K_T\,i \tag{8.11}$$

where K_E is the *back-emf constant* of the dc machine and K_T is its *torque constant*. The designation of the former constant comes from the custom to call the voltage v induced in the dc machine rotor *back electromotive force* (back emf). It is important to note that both constants are exactly the same. Their values are only equal when self-consistent unit system is used. Expressed in the SI units, K_E $\left[\text{V.s.rad}^{-1}\right]$ and K_T $\left[\text{N.m.A}^{-1}\right]$. Thus both the constants can be replaced in (8.7) by a constant K_{EM} called *electromechanical constant*. This constant is determined by the machine dimensions and by the state of its magnetisation.

Fig. 8.5a shows a configuration of a permanent magnet dc machine in which R_a and L_a represents the armature circuit resistance and inductance, respectively. Naturally, we can add these elements also to the basic ideal-transformer model of the machine together with the elements modeling mechanical friction b_r of the rotor bearing and the rotor inertia J as shown in Fig. 8.4b.
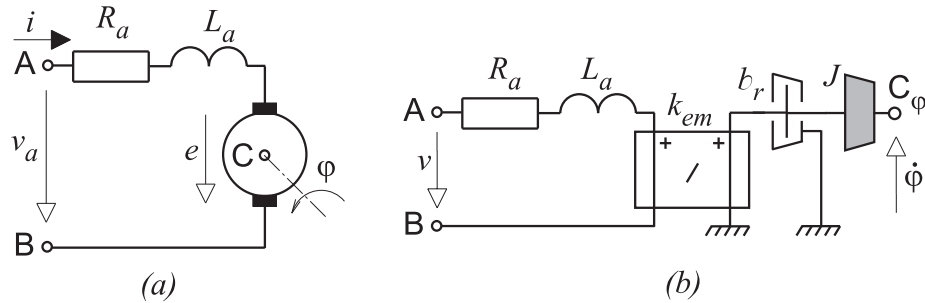
Figure 8.5: Dynamic model of a dc permanent magnet machine.

8.5 Movable-plate condenser

Pure energy-transfer transducers in the form of energy-transfer transformers and gyrators are not sufficient for modeling some real electro-mechanical transducers which not only transfer, but also store energy when either mechanical or electrical work is done on them. The stored energy can be recovered at a later time. Furthermore, the energy removed can be taken out as either mechanical or electrical work without regard to the form in which the energy was originally stored.

The first example of an energy-storing transducer is the movable-plate condenser shown in Fig. 8.6a. The charge on the condenser is q, and the voltage across the plates is v. The displacement of the movable plate is x, and the external force required to hold the movable plate in equilibrium (against the electrical attraction of the fixed plate) is F.
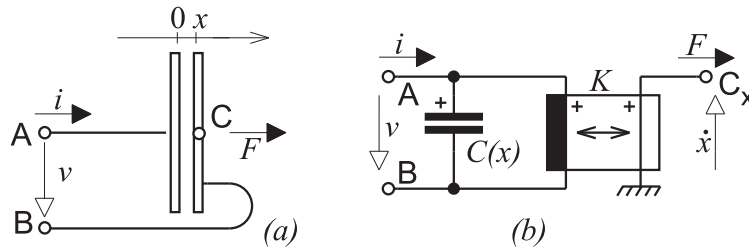
Figure 8.6: (a) Movable-plate condenser, (b) pure electro-mechanical model.

We shall replace the condenser by a pure capacitor assuming that the phenomena like electrical inductance and resistance or mechanical mass and friction could be modeled by additional physical elements.

The constitutive relations for the movable-plate capacitor can be expressed as

$$v = v(q, x) \qquad F = F(q, x) \tag{8.12}$$

In electrically linear case, the first of the relations (8.12) has the form $v = q/C(x)$, where $C(x)$ is the capacitance when the movable plate is in the position x. In general, $C(x)$ is a nonlinear function of x. An important fact is that when $q = 0$, the force F must be zero for any x. If there is no charge, there is no electric field, and hence no attractive force between the plates.

The electrical and mechanical power delivered to the capacitor in time dt represents the increase dW_e in its stored electrical energy, i.e.

$$dW_e = vi\,dt + F\dot{x}\,dt = v\,dq + F\,dx = \frac{\partial W_e}{\partial q}\,dq + \frac{\partial W_e}{\partial x}\,dx \tag{8.13}$$

Because of its conservative nature, the total electrical energy of the capacitor $W_e(x, q)$ is obtained by integrating (8.13) along any path from the datum configuration with $x = 0$ and $q = 0$. If we integrate (8.13) from $(x = 0, q = 0)$ to a configuration (q, x) along the rectangular path following first the x-axis up to the point $(q = 0, x)$, and then the q-axis up to (q, x), the electrical energy is, simply,

$$W_e(q, x) = \int_0^q \frac{q\,dq}{C(x)} = \frac{q^2}{2C(x)} \tag{8.14}$$

as there is no contribution from the segment along the x axis (where the force F is zero for any x).

Once the energy function $W_e(q,x)$ is known, the constitutive relations (8.12) can be recovered by its differentiation:

$$v = \frac{\partial W_e}{\partial q} = \frac{q}{C} \qquad F = \frac{\partial W_e}{\partial x} = -\frac{q^2 C'}{2C^2} \tag{8.15}$$
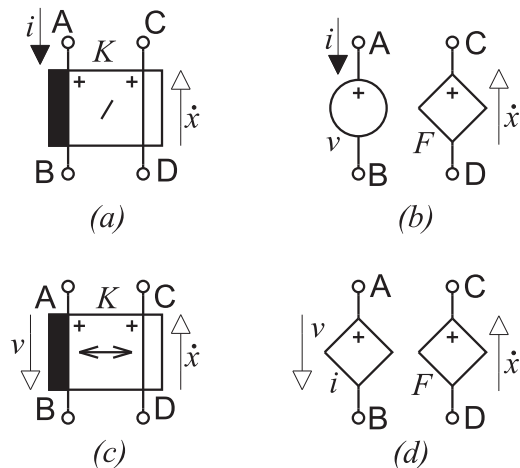
where the derivative $C'(x) = dC(x)/dx$.

(a) (b)

(c) (d)

Figure 8.7: (a) Energy-storing transformer, (b) its source implementation. (c) Energy-storing gyrator, (b) its source implementation.

To compose the corresponding model let us rewrite (8.15) as

$$i = \frac{dq}{dt} = C(x)\,\dot{v} + K(x,v)\,\dot{x} \qquad F = -\frac{1}{2}K(x,v)\,v \tag{8.16}$$

where $K(x,v) = C'(x)\,v$. Than it should be seen that a variable pure capacitor combined with a pure *energy-storing gyrator* can model the electro-mechanical coupling as shown in Fig. 8.6b. Fig. 8.7d shows that the energy-storing gyrator consistscan be formed from a controlled source of current, and of a controlled source of force.

8.6   Movable-core solenoid

Fig. 8.8a shows a solenoid, or movable-core coil – the magnetic counterpart of the movable-plate condenser.
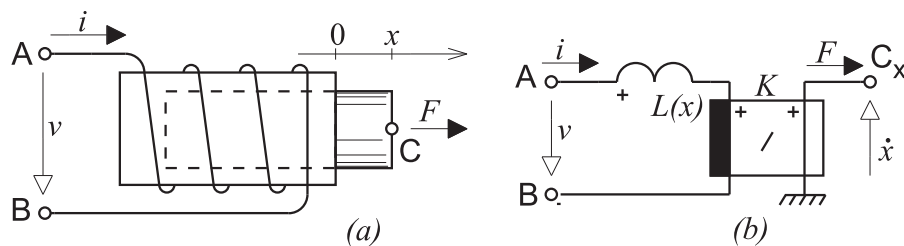
Figure 8.8: (a) Movable-core solenoid, (b) pure electro-mechanical model.

Replacing the coil by a pure inductor, we can express its constitutive relations in the form of equations for its current i and the external force F (required to hold the core in equilibrium against the magnetic attraction) in terms of the inductor flux linkage λ, and the movable core displacement x as

$$i = i(\lambda, x) \qquad F = F(\lambda, x) \tag{8.17}$$

If the relation between current and flux linkage is linear, the first equation becomes $i = \lambda/L(x)$ where $L(x)$ is the inductance of the coil when the core is in the position x. When $\lambda = 0$, there is no magnetic field, and hence no magnetic attraction. The force F is therefore zero for any x when $\lambda = 0$.

Using a procedure analogous to that used in the previous example, the total magnetic energy of the inductor $W_m(\lambda, x)$ can be obtained by integrating the increase dW_m in its stored magnetic energy corresponding to the electrical and mechanical power delivered to the inductor in time dt along a path from the datum configuration $(\lambda = 0, x = 0)$. In this way we find

$$W_m(\lambda, x) = \int_0^\lambda \frac{\lambda \, d\lambda}{L(x)} = \frac{\lambda^2}{2L(x)} \tag{8.18}$$

Again, the constitutive relations (8.17) can be recovered by differenting the energy function $W_m(\lambda, x)$:

$$i = \frac{\partial W_m}{\partial \lambda} = \frac{\lambda}{L} \qquad F = \frac{\partial W_m}{\partial x} = -\frac{\lambda^2 L'}{2L^2} \tag{8.19}$$

where the derivative $L'(x) = dL(x)/dx$.

Taking into consideration (8.19), we can assume that

$$v = \dot{\lambda} = L(x) \frac{di}{dt} + K(x, i) \, \dot{x} \qquad F = -\frac{1}{2} K(x, i) \, i \tag{8.20}$$

where

$$K(x, i) = L'(x) \, i \tag{8.21}$$

Hence, the corresponding pure model can be of the form shown in Fig. 8.8b. It consists of a variable pure inductor combined with an *energy-storing transformer* the implementation of which in terms of controlled sources is shown in Fig. 8.7b.

8.7   Electromagnetic relay

This result is readily applicable to the electromagnetic relay shown in Fig. 8.9a. The relay model given in Fig. 8.9b neglects saturation of the magnetic circuit, which is assumed to be infinitely permeable, and ignores leakage and fringing fluxes. As the relay inductance

$$L(x) = \frac{N^2 \mu_0 A}{x}, \quad \text{the factor} \quad K(x, i) = -\frac{N^2 \mu_0 A}{x^2} \, i$$

where N is the number of winding turns, x is the air-gap width, A is the cross-sectional area of the air-gap, and μ_0 is the air permeability. The electrical resistance of the relay winding, the mass of the movable part, its friction, and the spring effect are represented in the model by physical elements.

Fig. 8.9c shows a relay model in which the magnetic circuit is represented in a more authentic way. Coupling between the electrical and magnetic circuits is modeled there by a gyrator of gyration ratio equal to N. The elements P_f and P_a represent permeances of the ferromagnetic part of the magnetic circuit and of the air-gap, respectively. The magneto-mechanical coupling is modeled by an energy-storing gyrator. The electrical voltage is replaced there by magnetic voltage, the electrical charge by magnetic flux, and the electrical capacitance by permeance. In this case,

$$K(x, w_a) = P'(x) \, w_a = \frac{w_a}{\mu_0 A}$$

where w_a is the magnetic voltage across the air-gap.

The element R_f corresponds to the magnetic circuit losses. Saturation or hysteresis of the ferromagnetic material can be taken into consideration within the element P_f, and also such effects like leakage and fringing could be respected in this model in a straightforward manner by adding the relevant elements to it.
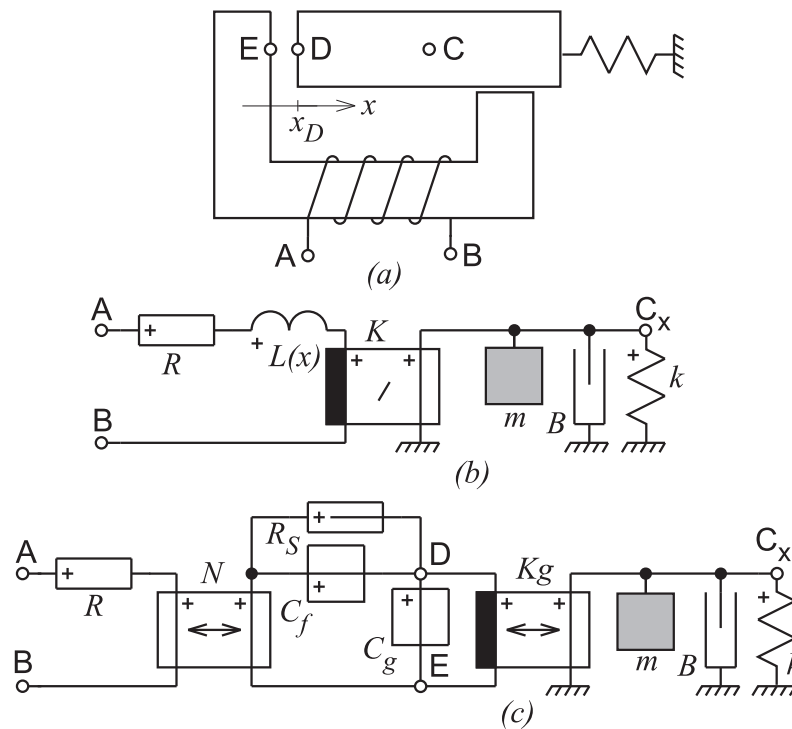
Figure 8.9: (*a*) Electromagnetic relay, (*b*) electro-mechanical and (*c*) electro-magneto-mechanical multi-pole model.

8.8 Synchronous reluctance machine

The proposed ideal energy-storing transducer suits well also to rotational systems. Let us assume, that the rotor and the stator of an elementary singly excited reluctance machine shown in Fig. 8.10*a* are shaped so that the variation of the exciting winding inductance L is sinusoidal with respect to the rotor position θ as shown in Fig. 8.10*b*, that is,

$$L(\theta) = \frac{1}{2}[L_d + L_q + (L_d - L_q)\cos 2\theta] \tag{8.22}$$

where L_d and L_q is the direct-axis and quadrature-axis inductance, i.e. the maximum and minimum value of the inductance $L(\theta)$, respectively.

In accordance with (8.21), the transducer factor K in the reluctance machine model given in Fig. 8.10*c* can be computed as

$$K(\theta, i) = i(t)\frac{dL}{d\theta} = i(t)(L_q - L_d)\sin 2\theta$$

For an excitation

$$i = I_m \sin \omega t$$

the model exhibits the synchronization phenomenon, i.e. a nonzero average torque is developed only at the synchronous speed $\dot{\theta} = \omega_m$ such that at any instant $\theta = \omega_m t - \delta$, where δ is the rotor position at $t = 0$, when the current i is also zero.

The model is augmented with additional physical elements representing the winding resistance, the rotor inertia, and the bearing friction.

8.9 Variable-reluctance stepping motor

As an extension of the reluctance machine model, Fig. 8.11 gives a multipole model of a variable-reluctance multiple-stack three-phase stepping motor which has a wound stator and an unexcited rotor with three separate sets of teeth sections. The three sets of rotor teeth are magnetically independent. In general, for an n-phase motor, the stator teeth are displaced by $1/n$ of a tooth pitch from section to section.
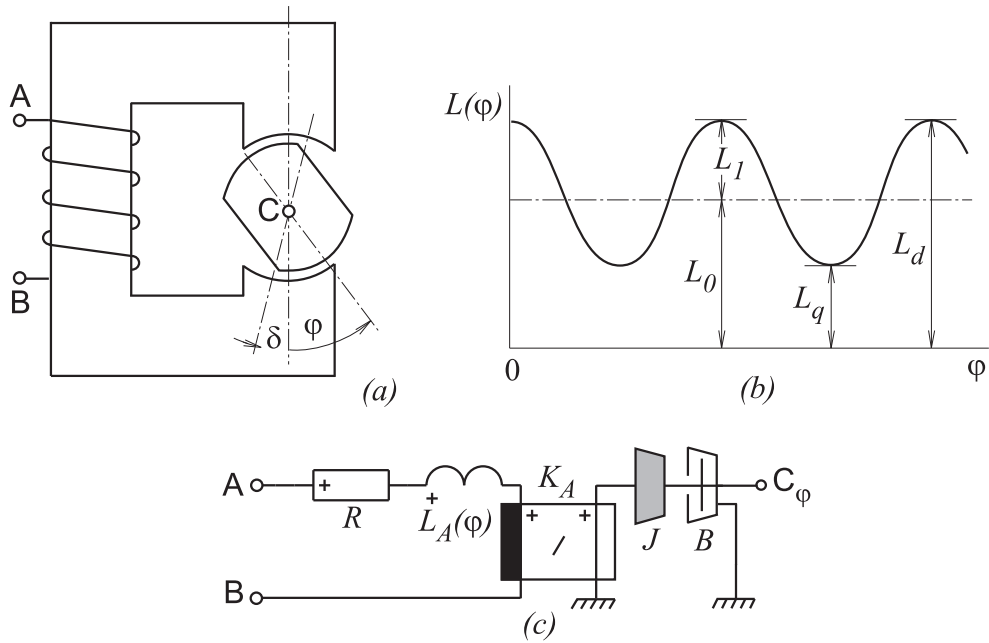
Figure 8.10: Electro-mechanical multipole model of a reluctance machine.

To form a multipole model of the stepping motor, we need again to know the form of its inductance. In practice, the motor inductance L as a function of displacement θ may be again approximated by a cosine wave, that is,

$$L(\theta) = L_1 + L_2 \cos r\theta \tag{8.23}$$

where L_1 and L_2 are constants and r is the number of teeth on each rotor section.

Now, in the case of a three-phase motor with an 10-teeth rotor, $r = 10$, let the equilibrium position be the situation when phase A is energized. Then the inductance for phase A is given by

$$L_A(\theta) = L_1 + L_2 \cos 10\theta \tag{8.24}$$

Substituting (8.24) into (8.21), we get

$$K_A(\theta, i_A) = -i_A(t)\, L_2 \sin 10\theta$$

Phase B has its equilibrium position $120°$ behind the reference point. Therefore, the inductances and the K-factors for phases B and C are then written as follows:

$$L_B(\theta) \quad = \quad L_1 + L_2 \cos(10\theta - 120°)$$
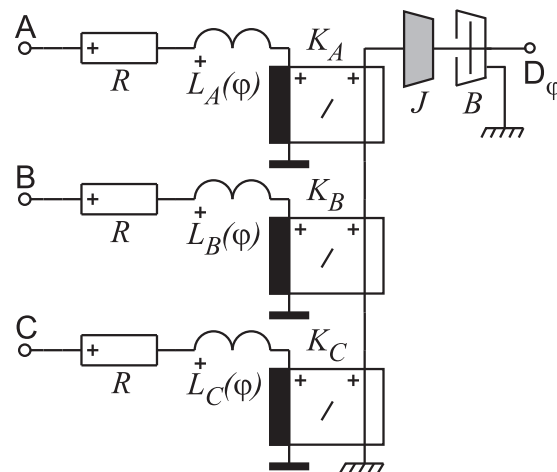
Figure 8.11: Multipole model of a multiple-stack three-phase variable-reluctance stepping motor.

$$\begin{aligned}
L_C(\theta) &= L_1 + L_2\cos(10\theta + 120°) \\
K_B(\theta, i_B) &= -i_B(t)\,L_2\sin(10\theta - 120°) \\
K_C(\theta, i_C) &= -i_C(t)\,L_2\sin(10\theta + 120°)
\end{aligned}$$

The electrical circuits of the three phases are isolated so that each phase can be modeled in a separate way. The total torque developed on the rotor is the algebraic sum of torques of the three phases. Thus

$$\tau = \tau_A + \tau_B + \tau_C \tag{8.25}$$

Module 9

Fluid systems

9.1 Fluid energy interactions

9.1.1 Fluid pressure

Pressure is the quantity which causes (or results from) fluid flow or sustains the weight of a column of fluid. **Fluid pressure** is defined as the normal force exerted on a surface (real or imaginary) in a fluid per unit area. When dealing with fluids contained in pipes or ducts, we shall assume pressure uniform over the cross section areas of the pipes or ducts. Therefore, the total axial force F exerted on the cross section area A is

$$F = p\,A$$

where p is the average bulk pressure over A.

Pressure is measured in the unit called a pascal, $1\text{ Pa} = 1\text{ N/m}^2$. Two other commonly used pressure units are the bar, $1\text{ bar} = 100\text{ kPa}$, and standard atmosphere, $1\text{ atm} = 101.325\text{ kPa}$. The **absolute pressure** is measured relative to absolute vacuum. Most pressure-measuring devices, however, are calibrated to read zero in the atmosphere, and so they indicate the difference between the absolute zero pressure and the local atmospheric pressure. This difference is called the **gauge pressure**. Throughout this text, the pressure p will denote gauge pressure unless it is otherwise specified.

Gauge pressure is considered positive if the fluid is in the state of compression. Since most fluids will not support tension without cavitation (evaporation), we shall be concerned only with positive pressures (cavitation requires a treatment utilizing thermodynamics).
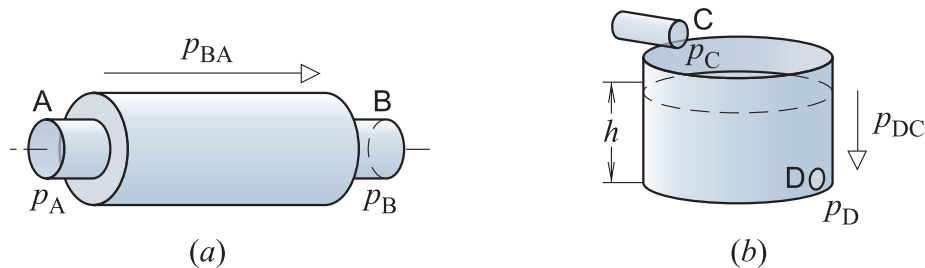
Figure 9.1: Pressure across (a) a flow-through component, (b) an open tank supplied by liquid.

Fig. 9.1a shows a fluid-system component with two inlets. The bulk values of the gauge pressures at the inlets A and B are denoted as p_A and p_B, respectively. The empty-head arrow in Fig. 9.1 indicates the assumed positive polarity of the difference $p_{BA} = -p_{AB}$ between the inlet gauge pressures. The pressure difference

$$p_{BA} = p_B - p_A \tag{9.1}$$

is positive if $p_B > p_A$. Such a pressure difference is called the **pressure drop** across the component.

Another fluid-system component with two inlets is shown in Fig. 9.1b. It is an open tank in the form of a cylinder of the cross sectional area A filled with a liquid coming to the tank via the inlet C. The liquid is leaving the tank through the opening D situated in the tank wall close to its bottom. Recollect that the pressure at any point in a fluid at rest is the same in all directions. If the fluid flow through the

opening D is slow enough and the diameter of the opening is negligible when compared with the hight h of the liquid in the tank above the tank bottom, we can assume that the pressure p_D at the opening D is the same as the pressure acting on the bottom of the tank. Thus,

$$p_D = \frac{m\,g}{A} \qquad (9.2)$$

where m is the mass of the liquid and g is the gravitational acceleration.

The mass m of a fluid enclosed in a volume V equals

$$m = \rho V \qquad (9.3)$$

where ρ is the **mass density** of the fluid defined as the mass of the fluid per unit volume with units kg/m^3.

Therefore,

$$p_D = \frac{V\,\rho\,g}{A} = h\,\rho\,g \qquad (9.4)$$

as the volume of the liquid in the tank is $V = A\,h$.

9.1.2   Mass and volume flow

A liquid or gas usually flows between system components through pipes or ducts. In most practical applications, such a fluid flow can be approximated to be **one-dimensional flow**. That is, the properties can be assumed to vary in the direction of flow only. As a result, the properties such as pressure, density or temperature are assumed to have uniform bulk average values over each cross section. They may change, however, with time.

The one-dimensional **mass-flow rate** $\dot{m}$ of fluid flowing in a pipe or duct is considered as

$$\dot{m} = \frac{dm}{dt} = \rho\,v A$$

where A [m^2] is the cross-sectional area of the pipe or duct normal to the flow direction, ρ is the average mass density over A, and v is the average value of the fluid velocity in the flow direction over A.
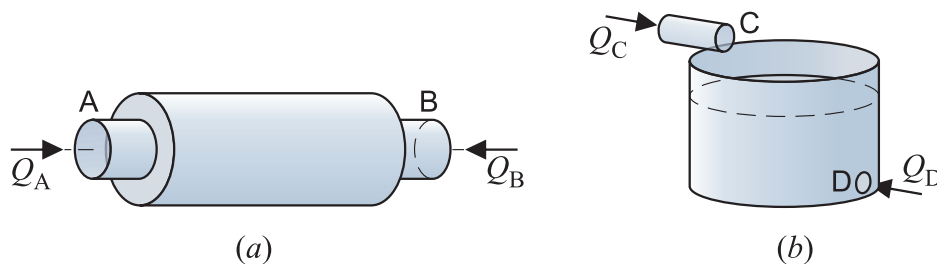
Figure 9.2: Inlet volume flow of two-inlet components: (a) flow-through component, (b) open tank supplied by liquid.

As measuring of volume-flow rate is much easier then measuring mass-flow rate, engineers prefer the former variable when analyzing fluid systems. **Volume-flow rate** Q is the variable which expresses the volume of fluid passing a given area per unit time, so its unit is m^3/s. This quantity, denoted in Fig. 9.2 by full-head arrows, is given as

$$Q(t) = \frac{dV}{dt} = v\,A \qquad (9.5)$$

where V is the fluid volume and v is the bulk velocity of the fluid flow through the area. Note, that the relation between the mass and volume flow rates is

$$\dot{m} = \rho\,Q$$

9.1.3 Fluid work, power and energy

If a quantity of fluid in a pipe or conduct is passing an area A in the direction of p, the amount of work done by the force $F = p\,A$ in moving this fluid through a distance dx is

$$d\mathcal{W} = p\,A\,dx$$

The quantity of volume dV of fluid passing A is

$$dV = A\,dx$$

Therefore

$$p = d\mathcal{W}/dV \qquad (9.6)$$

Thus pressure is the work done in passing a unit volume of fluid across the area on which p acts.

Power, as we know, is the rate of flow of work. Hence from (9.5) and (9.6), the **fluid power**

$$\mathcal{P} = \frac{d\mathcal{W}}{dt} = p\frac{dV}{dt} = pQ$$

The net power delivered to a two-inlet component shown in Fig. 9.1 is

$$\mathcal{P} = p_A Q_A + p_B Q_B$$

If the fluid and the component is such that $Q_A + Q_B = 0$, i.e. if the flow in equals to flow out,

$$\mathcal{P} = p_{AB} Q_A = p_{BA} Q_B$$

The **fluid energy** delivered to a fluid-system component is the time integral of the power.

9.2 Modeling of fluid systems

9.2.1 Fluid multipole diagrams

Modeling of fluid systems is very easy if the system can be represented by multipole models of system components interconnected by ideal links. Fig. 9.3a shows the graphical symbol of a twopole model representing a two-inlet component. The poles A and B corresponding to the component inlets are denoted by short line segments called pins. The pins are associated with volume-fluid flows into the components Q_A and Q_B as well as with the pole pressures p_A and p_B with respect to a reference (note its symbol).
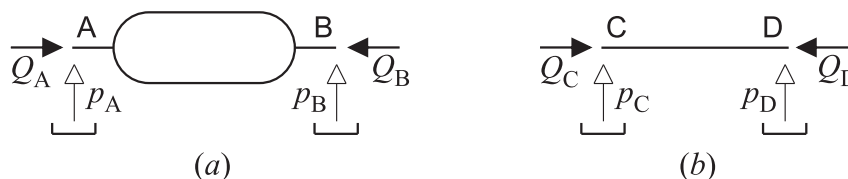
Figure 9.3: (a) Two-pole element. (b) Ideal fluid link.

The line segment shown in Fig. 9.3b represents a segment of an ideal pipe with inlets A and B containing an ideal fluid such that

$$p_A = p_B \quad \text{and} \quad Q_A + Q_B = 0$$

Symbols of fluid-system components with their pins interconnected by ideal fluid links form a multipole diagram of the system. The multipole diagram in Fig. 9.4a shows the way of measuring pressures of a two-inlet component using ideal pressure-measuring instruments. The way of direct measuring of volume-flow rate between elements is shown in Fig. 9.4b.

Note, that pressure is the across-variable in fluid systems. To measure the volume-flow rate between components, we must sever the pipe interconnecting the components at the section of interest and include
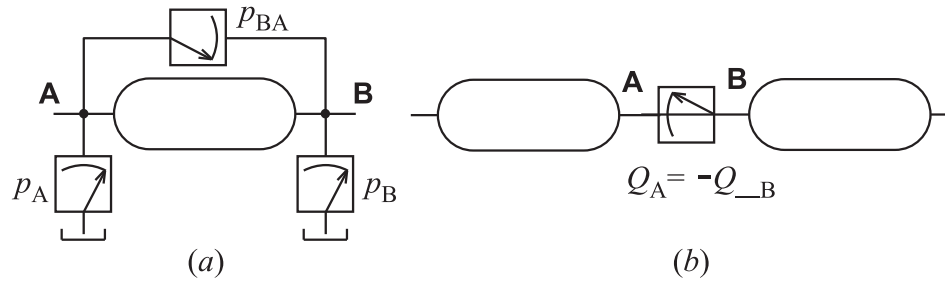
Figure 9.4: (a) Measurement of (a) element pressures and (b) of volume-flow rate between elements.

a flow-rate measuring instrument to renew the connection. It is thus evident that the volume-flow rate is the through-variable.

Relation (9.1) is an example of the geometric constraints which are placed on pressures in a system due to continuity of space. It is the expression of the **postulate of pressure compatibility** – called also the **axiom of pressure composition** – for the two-inlet subsystem.

Mass, like energy, is a conserved property, and it cannot be created or destroyed. Mass m and energy $\mathcal{E}$ can be converted to each other according to the famous formula proposed by Einstein: $\mathcal{E} = m\,c^2$ where $c = 2.998.10^8$ m/s is the speed of light. This equation suggests that the mass of a subsystem may change when its energy changes. However, for all energy interactions encountered in engineering practice, with the exception of nuclear reactions, the change in mass is extremely small and cannot be detected by even the most sensitive devices.

We can thus assume validity of the **principle of conservation of mass** according to which the mass entering a region in space minus the mass leaving it must equal the change of mass stored within the region.
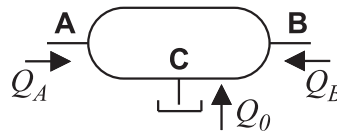
Figure 9.5: Threepole model of a two-inlet component to satisfy the postulate of continuity.

Let us consider the component with two fluid inlets shown in Fig. 9.2. The volume flow rates at the component inlets A and B are denoted as Q_A and Q_B. The assumed positive directions of the fluid flows are indicated by the full-head arrows.

The principle of conservation of mass for the two-inlet component

$$\dot{m}_A + \dot{m}_B + \dot{m} = 0 \tag{9.7}$$

where $\dot{m}_A = \rho\,Q_A$ and $\dot{m}_B = \rho\,Q_B$ is the mass-flow rate into the inlet A and B, respectively. As $m = \rho V$ is the mass of the fluid contained in the component if V is the fluid volume of the component,

$$\dot{m} = \dot{\rho}V + \rho\dot{V} \tag{9.8}$$

where $\dot{\rho} = d\,\rho/dt$ and $\dot{V} = dV/dt$ is the time rate of the mass density and component volume, respectively.

Unlike mass, fluid volume is not a conserved property as (9.8) indicates. Only if $\dot{\rho} = 0$, i.e., if the fluid is incompressible, and if $\dot{V} = 0$, i.e. if the fluid volume in the component is constant, the flow entering the component through one inlet equals the flow leaving the component through the other inlet

$$Q_A + Q_B = 0, \quad \text{or} \quad Q_A = -Q_B \tag{9.9}$$

This is the **postulate of continuity** expressed for the fluid flow into the two-inlet component, which is valid under the above assumptions only. If the fluid cannot be considered as incompressible, or the container volume as constant, we must respect accumulation of fluid mass in the component by adding a third pole C to the two-inlet component model linked to the reference as shown in Fig. 9.5. To satisfy the postulate of continuity, the volume-flow rate of the third pole must be

$$Q_C = -Q_A - Q_B$$

Fig. 9.6b shows three ideal pipe segments passing fluid freely between any two of the inlets A, B and C via the interconnection D. Such an ideal-pipe structure is characterized by the relations

$$p_A = p_B = p_C \qquad Q_A + Q_B + Q_C = 0$$

where the latter statement is the expression of the postulate of continuity for the interconnection C.
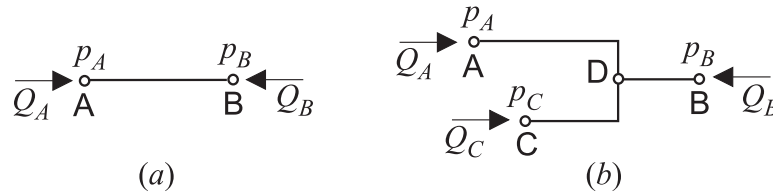

Figure 9.6: (a) Ideal pipe segment. (b) Ideal-pipe interconnection.

9.3 Fluid accumulation

9.3.1 Pure fluid capacitor

We shall define a **pure fluid capacitor** as an idealized physical element in which fluid volume V is a function of pressure p inside the element

$$V = f(p) \tag{9.10}$$

For an **ideal fluid capacitor** the relation (9.10) becomes linear, i.e.,

$$V(t) = C_f \cdot p(t) \tag{9.11}$$

where C_f [m^3.Pa^{-1}] is the **fluid capacitance** of the capacitor.
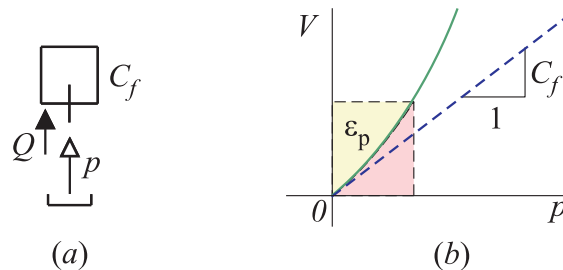
Figure 9.7: (a)Symbol and (b) characteristics of pure fluid capacitor.

The relationship between the volume-flow rate of fluid into the capacitor and the fluid pressure at the capacitor inlet is

$$Q(t) = C_f \cdot \frac{dp}{dt} \tag{9.12}$$

or

$$p(t) = \frac{1}{C_f} \int_{t_0}^{t} Q \, d\tau + p(t_0) \tag{9.13}$$

where $p(t_0)$ is the capacitor pressure at $t = t_0$.

Figure 9.7a gives our symbol for pure fluid capacitors. Only one the pole representing the fluid intake of the capacitor is shown in the symbol. This pole is associated with the pressure p at the intake and with the volume-flow rate $Q(t)$ into the capacitor. The second pole is hidden as it must be always fixed to the pressure reference.

The symbol consists of a square representing the capacitor volume and pole representing the capacitor inlet. The capacitor is associated with two variables, the capacitor pressure p measured with respect to a constant pressure reference, and the capacitor volume-flow rate Q. The assumed positive polarity of p is indicated by the empty-head arrow placed between the symbol for the pressure reference and the

symbol pole. The orientation of the full-head arrow shows that the positive Q is always directed into the capacitor.

In general, a fluid capacitor can be nonlinear and time-variable. Then it is characterized by the relation

$$Q(t) = \frac{dV}{dt} = \frac{\partial V}{\partial p} \cdot \frac{dp}{dt} + \frac{\partial V}{\partial t} \qquad (9.14)$$

Figure 9.7b shows V-p characteristics of a nonlinear and linear fluid capacitors specified by their constitutive relations (9.10) and (9.11).

Power $\mathcal{P}$ supplied to a capacitor is

$$\mathcal{P} = Q\,p \qquad (9.15)$$

providing that the fluid density is constant.

Energy $\mathcal{E}_p$, called **fluid potential energy** and stored in a fluid capacitor by virtue of the pressure, is

$$\mathcal{E}_p = \int_0^t \mathcal{P}\,dt \qquad (9.16)$$

$$dV = C_f dp \qquad (9.17)$$

$$\mathcal{E}_p = \int_0^p C_f\,p\,dp = \frac{C_f\,p^2}{2} = \frac{V^2}{2C_f} \qquad (9.18)$$

Open cylindrical tank

As a first example of a fluid capacitor we shall consider the **open tank** or **reservoir** of a cylindrical shape shown in Fig. 9.8a. Let us assume that the liquid in the tank is incompressible, the tank walls are rigid, and the flow resistance through the opening A at the bottom of the tank is negligible. Then the volume of fluid in the tank is

$$V = A\,h \qquad (9.19)$$

where A is the tank horizontal area and h is the height of the liquid column in the tank.
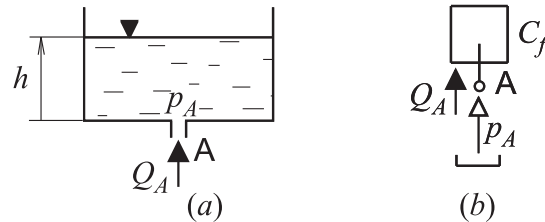
Figure 9.8: (a) Open cylindrical tank, (b) its fluid capacitor model.

The fluid pressure by the liquid level in the open tank is zero as it is the ambient reference pressure. If there are no fluid accelerations in the tank except due to gravity, the fluid pressure by the tank bottom equals to the weight of the liquid per the tank horizontal area, or

$$p = \frac{m\,g}{A} = \rho\,g\,h \qquad (9.20)$$

where $m = \rho\,A\,h$ [kg] is the liquid mass, ρ [kg/m³] is the liquid mass density, and g [m/s²] is the acceleration due to gravity.

Substituting p for h from (9.20) and comparing the result with (9.11) we obtain the open tank capacitance as

$$C_f = \frac{A}{\rho g} \qquad (9.21)$$

Fig. 9.8b shows an ideal fluid capacitor of the fluid capacitance C_f modeling dynamics of the open tank. In Fig. 9.9a, the liquid volume flow Q is supplied into the open tank by a pump. This situation is modelled in Fig. 9.9b where the pump is represented by an independent source of fluid flow. The relationship (9.20) between the height h of the liquid level and the pressure p_A in the tank is expressed in the model using a scaling block.
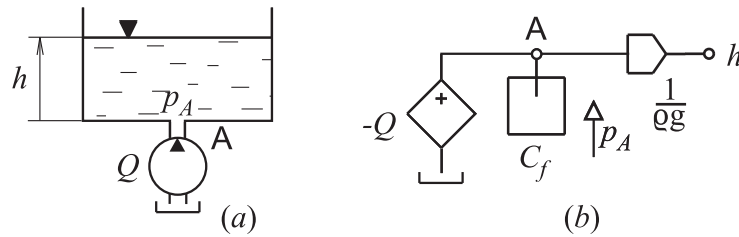
Figure 9.9: (a) Open tank supplied by a pump, (b) model of the fluid system.

Open spherical tank

As an example of a nonlinear fluid capacitor let us consider a spherical tank with a fluid outlet at the bottom and a vent at the top shown in Fig. 9.10a.
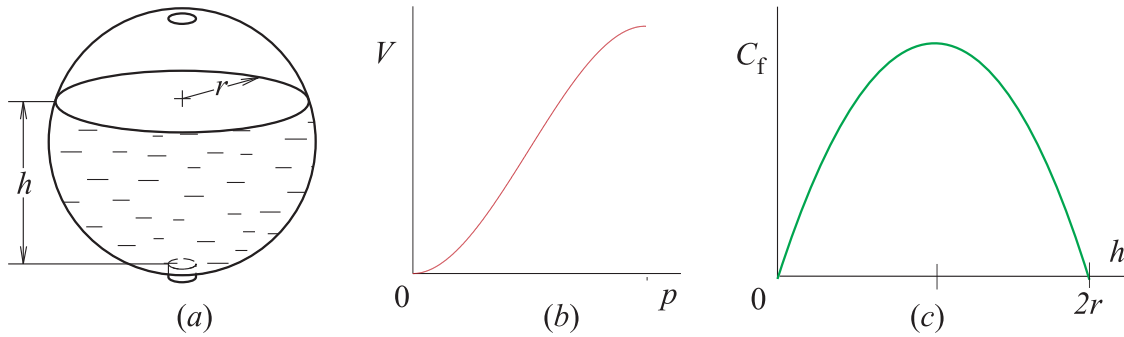
Figure 9.10: (a) Open spherical tank, (b) its V-p characteristic and (c) capacitance vs. liquid-level height.

The volume of liquid in the spherical tank is

$$V(h) = \frac{\pi}{3}h^2(3r - h) \tag{9.22}$$

and

$$\frac{dV}{dh} = \pi(2h\,r - h^2) \tag{9.23}$$

where r is the tank radius and h is the height of the liquid level in the tank.

After expressing the pressure p by the tank outlet in terms of h using (9.20) we arrive at

$$C_f(p) = \frac{\pi}{\rho\,g}\left(2r\,p - \frac{1}{\rho\,g}p^2\right) \tag{9.24}$$

Fig. 9.10b shows the constitutive relationship of the spherical tank, and the relationship $C_f(h)$ is plotted in Fig. 9.10c. Note that

$$V_{max} = \frac{4}{3}\pi, \quad p_{max} = 2\rho g r \quad \text{and} \quad C_{f\,max} = \pi r^2$$

Rigid pressurized tank.

Another example of a component which may behave approximately like an ideal fluid capacitor is a closed **pressurized tank** or chamber with rigid walls completely filled with fluid as shown in Fig. 9.11a. The energy is stored in the tank because of the compressibility of the fluid.

In this case we shall neglect the possible variation of pressure in the tank due to gravity, and consider only the variation in pressure which occurs as a result of the amount of fluid that has been forced into the tank. Fluid inertia and frictional effects will be also neglected.

According to the principle of conservation of mass the time rate of mass entering the chamber through the inlet A must equal the increase of mass in the chamber, or

$$\rho Q_A = \frac{d}{dt}(\rho V_0) = V_0\frac{d\rho}{dt} \tag{9.25}$$
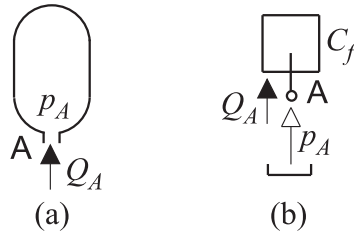
Figure 9.11: (a) Tank containing compressed fluid. (b) Model of the pressurized tank.

where ρ [kg/m^3] is the fluid density and V_0 [m^3] is the constant volume of the tank.

To employ tank pressure p rather than the mass density ρ as a variable, we must utilize the equation of state of the fluid. For most liquids, a reasonably good first-order approximation for their equation of state is

$$d\rho = \frac{\rho}{\beta}dp \tag{9.26}$$

where β [N/m^2] is the **bulk modulus of elasticity** of the liquid.

For most gases including air,

$$d\rho = \frac{\rho}{n\,p}dp \tag{9.27}$$

where p is the absolute fluid pressure and n is a constant whose value is between 1.0 and 1.4, depending on how rapidly the fluid is compressed. If the pressure variations in the gas are small, it may be considered to have a bulk modulus of elasticity $\beta \approx n\,p$.

Substituting (9.26) into (9.25) yields

$$Q_A = \frac{\rho}{\beta}\frac{dp}{dt} \tag{9.28}$$

Comparing this result with (9.14) indicates that the pressurized tank behaves like an ideal fluid capacitor with the capacitance

$$C_f = \frac{V_0}{\beta} \tag{9.29}$$

Under the above assumptions the pressurized chamber given in Fig. 9.11a can be represented graphically as shown in Fig. 9.11b. The capacitor pole representing the accumulator inlet is coalesced with node A of a system model. The capacitor pressure p corresponds to the gauge pressure p_A of the accumulator.

9.3.2   Equivalent bulk modulus

The bulk modulus of a liquid can be substantially lowered by gas or vapor entrained in the liquid in the form of bubbles and/or pockets and by the mechanical compliance of a flexible container. The equation which gives the **equivalent bulk modulus** of liquid-gas mixture in a flexible container is

$$\frac{1}{\beta_e} = \frac{1}{\beta_l} + \frac{1}{\beta_c} + \frac{V_g}{V_t} \cdot \frac{1}{\beta_g} \tag{9.30}$$

where the subscripts g, l, and c refer to the gas, liquid, and container, respectively. It is assumed that the initial total volume of the container $V_t = V_l + V_g$, and that $\beta_l \gg \beta_g$. Thus the effective bulk modulus will be less than any one of the values β_l, β_c, or $V_t/V_g\beta_g$. The bulk modulus of the liquid β_l is obtained from manufactures' data. The isothermal bulk modulus of air is equal to the pressure level p, the adiabatic value used for air is $(C_p/C_v)p = 1.4p$.

Usually, the major source of mechanical compliance is the hydraulic lines connecting valves and pumps to actuators. The bulk modulus for a thick-walled cylindrical container is

$$\frac{1}{\beta_c} = \frac{2}{E} \cdot \frac{(1+\nu)D_0^2 + (1-\nu)D^2}{2\delta(D_0 + D)} \tag{9.31}$$

where D is the inner diameter, D_0 is the outer diameter, δ is the wall thickness ($2\delta = D_0 - D$), E is the modulus of elasticity of the wall material, and ν is the Poisson's ratio for the material. For a thin-walled cylinder such that $D_0 = D$, and because $\nu = 0.25$ for metals, (9.31) approximates to the formula

$$\beta_c = \frac{\delta E}{D} \tag{9.32}$$

generally used for hydraulic tubing.

Estimates of entrapped air in hydraulic systems run as high as 20% when the fluid is at atmospheric pressure. As pressure is increased, much of this air dissolves into the liquid and does not affect the bulk modulus. In any practical case it is difficult to determine the effective bulk modulus other than by direct measurement.

9.3.3 Temperature variations of liquids

The density of a liquid is a function of both pressure and temperature. A function relating density, pressure, and temperature of a fluid is, by definition, the equation of state. The equation of state for a liquid cannot be mathematically derived from physical principles. In contrast, the kinetic theory of gases yields an equation of state. However, because changes in density as a function of pressure and temperature are small for a liquid, the first three terms of a Taylor's series for two variables may be used as an approximation. Therefore,

$$\rho = \rho_0 + \left(\frac{\partial \rho}{\partial p}\right)_\vartheta (p - p_0) + \left(\frac{\partial \rho}{\partial \vartheta}\right)_p (\vartheta - \vartheta_0) \tag{9.33}$$

where ρ, p, and ϑ are the mass density, pressure, and temperature, respectively, of the liquid about initial values of ρ_0, p_0, and ϑ_0. A more convenient form of (9.33) is

$$\rho = \rho_0 \left[1 + \frac{1}{\beta}(p - p_0) - \alpha(\vartheta - \vartheta_0)\right] \tag{9.34}$$

where

$$\beta \equiv \rho_0 \left(\frac{\partial p}{\partial \rho}\right)_\vartheta \quad \text{and} \quad \alpha \equiv -\frac{1}{\rho_0}\left(\frac{\partial \rho}{\partial \vartheta}\right)_p$$

Equation (9.34) is the linearized equation of state for a liquid. The mass density increases as pressure is increased and decreases with temperature increase. Because mass density is mass divided by volume, equivalent expressions for β and α are

$$\beta = -V_0 \left(\frac{\partial p}{\partial \rho}\right)_\vartheta \quad \text{and} \quad \alpha = \frac{1}{V_0}\left(\frac{\partial \rho}{\partial \vartheta}\right)_p$$

where V is the total volume and V_0 is the initial total volume of the liquid.

The quantity β is the change in pressure divided by the fractional change in volume at a constant temperature and is called the **isothermal bulk modulus** or simply **bulk modulus** of the liquid. It is the most important fluid property in determining the dynamic performance of hydraulic systems related to the 'stiffness' of the liquid. Note that it is always a positive quantity. The reciprocal of β is often termed the **compressibility** of the liquid.

An **adiabatic bulk modulus**, β_a may also be defined. It can be shown that the adiabatic bulk modulus is related to the isothermal bulk modulus by

$$\beta_a = \frac{C_p}{C_v}\beta \tag{9.35}$$

where C_p/C_v is the ratio of specific heats. Because this ratio is only slightly in excess of unity for a liquid, the distinction between adiabatic and isothermal moduli is insignificant.

The quantity α is the fractional change in volume due to a change in temperature and is called the **cubical expansion coefficient** of the fluid.

9.4 Fluid flow restrictions

9.4.1 Pure fluid resistor

We shall now define a **pure fluid conductor** as a physical element characterized by the function

$$Q = f(p) \tag{9.36}$$

where $Q = 0$ when $p = 0$, and the signs of Q and p are the same.

For an **ideal fluid conductor**,

$$Q = G_f p \tag{9.37}$$

where Q is the volume-flow rate of the conductor, p is the pressure drop across the conductor, and G_f [m^{3}Pa^{-1}s^{-1}] is the *fluid conductance*. The reciprocal value $R_f = 1/G_f$ is the *fluid resistance* characterizes the physical elements called fluid resistors.

It is important to note that (9.36) and (9.37) hold only when the rate of change of flow through the conductor is small enough to avoid fluid inertia effects.

We see that fluid resistance dissipates fluid power. For incompressible fluids. the dissipated power $\mathcal{P}$ is

$$\mathcal{P} = p\,Q = R_f Q^2 = p^2 / Rf$$
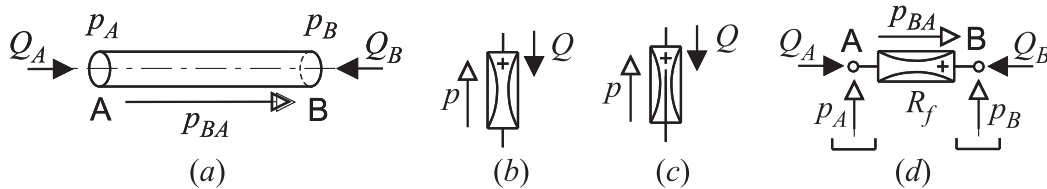
Figure 9.12: (*a*) Pipe segment. (*b*) Pure fluid resistor and (*c*) conductor. (*d*) Pipe model.

Fig. 9.12*b* gives our graphical symbol for pure fluid resistors. The pure conductor is associated with two variables: the conductor pressure drop p and the conductor fluid flow Q. Polarities of these two variables are always related to the polarity of the symbol indicated by the $+$ sign as shown in Fig. 9.12*b*. This means that the pressure at the $+$ pole is assumed larger than that at the second pole. The conductor flow is considered positive if it is oriented from the $+$ pole towards the conductor.

The symbol of the pure fluid conductor is utilized in Fig. 9.12*c* to model the pipe segment shown in fig Fig. 9.12*a*. The nodes A and B represent energy interactions at the corresponding inlets of the real pipe segment. The gauge pressures p_A and p_B at the pipe inlets are denoted by empty-head arrows placed between the symbols for the reference pressure and the related nodes. Respecting the conductor orientation, the pressure drop p_{BA} corresponds to the conductor pressure p, and the flow Q_B corresponds to the conductor flow Q. As the postulate of continuity applies to the pure conductor $Q_A + Q_B = 0$, or $Q_A = -Q_B$.

Laminar flow through pipes

Fluid flows are generally dominated either by viscosity or inertia of the fluid. The dimensionless ratio of inertia force to viscous force is called **Reynolds number** defined by

$$Re = \frac{\rho\,v\,d}{\nu} \tag{9.38}$$

where ρ is the fluid mass density, v is the average velocity of the flow, and ν [N.s.m^{-2}] is the fluid kinematic viscosity.

Flow dominated by viscosity forces is referred to as **laminar** or **viscous flow**. Laminar flow is characterized by an orderly, smooth, parallel line motion of the fluid. Inertia dominated flow is generally *turbulent* and characterized by irregular, erratic, eddy like paths of the fluid particles.

Reynolds number inside a pipe of circular cross section with diameter d is given by

$$Re = \frac{4\rho\,Q}{\pi \nu d} \tag{9.39}$$

where Q is the volume-flow rate, and μ is the absolute viscosity of the liquid. Transition from laminar to turbulent flow has been experimentally observed to occur in the range $2000 < R < 4000$. Below $R = 2000$ the flow is always laminar.

For example, the laminar incompressible flow of a liquid through a long capillary tube shown in Fig. 9.12*a* can be approximated by the **Hagen-Poiseuille law** according to which the fluid conductance of the capillary is

$$R_f = \frac{128\nu\ell}{\pi\rho d^4} \tag{9.40}$$

where ν is the absolute viscosity of the fluid, ℓ is the length and d is the inside diameter of the capillary.

The ideal fluid resistor is applicable if the tube is long enough in relation to its diameter ($\ell \gg 100d$) so that the effects of nonuniform flow near the tube entrance are negligible. At the same time, the rate of change of volume flow must be small enough that inertia effects are negligible.

Also the effect of an incompressible flow through a porous plug can be approximated by an ideal fluid conductor. In this case the constitutive relation (9.37) is expressed by the **D'Arcy's law**. The corresponding linear resistance R_f is usually determined for a given porous medium and working fluid experimentally.

Example
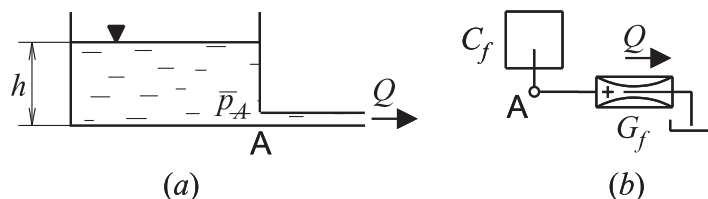
Figure 9.13: (*a*) Discharging water tank. (*b*) Reservoir model.

Fig. 9.13*a* shows a water tank which discharges to the atmosphere through a porous plug. Recollect that such a fluid restrictor produces a pressure drop linearly proportional to the flow through it. A dynamic model of the tank is shown in Fig. 9.13*b*. Node A represents the interconnection of the plug with the tank. Note that the direction of the volume-flow rate Q is in agreement with the direction with the flow of the conductor but opposite to that of the capacitor.

Turbulent flow through pipes

When the flow rate through a tube becomes large so that the Reynolds number than 4000, the flow through a tube is very likely to be turbulent, and the following approximate relation exists:

$$p = a_t Q \, |Q|^{3/4}$$

where the bars indicate the absolute value and a_t is a constant whose value depends on the volume-flow rate at which transition to turbulent flow occurs, the dimensions of the pipe (diameter and length), the properties of the fluid (density ρ and viscosity μ), and the roughness of the inner walls of the pipe.

For a smooth pipe

$$a_t = \frac{0.3164}{4^{0.25}} \frac{8\ell\rho^{0.75}\nu^{0.25}}{\pi^{0.75}d^{4.75}} \tag{9.41}$$

Turbulent flow in closed conduits of non-circular cross section may be approximately computed from (9.41) if the diameter is considered to be the hydraulic diameter defined by

$$d_h = \frac{4A}{S} \tag{9.42}$$

where A is the flow section area and S is the flow section perimeter. The concept of hydraulic diameter cannot be used for laminar flows because such flows are highly dependent on passage geometry. It is often simplest to employ an experimental measurement to determine a_t for a given specific pipe.

Flow through narrow orifices

An orifice is a sudden restriction of short length in a flow passage and may have a fixed or variable area. Orifices are a basic means for the control of fluid power.

Let us assume a rectangular orifice of width h and of length b (perpendicular to the plane of the figure). Assuming turbulent flow, the flow Q through the orifice can be found as

$$Q = hbC_d\sqrt{\frac{2p}{\rho}} \tag{9.43}$$

where p is the pressure drop across the orifice, ρ is the specific mass of the liquid, and C_d is a constant **discharge coefficient**. Experience shows that the theoretical value $C_d = \pi/(\pi+2) = 0.611$ can be used for all sharp-edged orifices, regardless of the particular geometry, if the flow is turbulent and $A_0 \ll A_1$.

The turbulent character of the flow is ensured only at large enough Reynolds numbers. At smaller values of Re the flow becomes laminar and the discharge coefficient varies with Re and depends on the geometry of the orifice edges. It is common in practice, however, to use the turbulent flow equation (9.43) regardless of the Reynolds number unless flows through very small openings are studied.

9.5   Fluid inertia

The physical element called *pure fluid inductor* or *pure fluid inertor* models the inertia effects encountered in accelerating a fluid in a pipe or passage. An *ideal fluid inductor* is defined by the linear relation

$$r(t) = L_f \cdot Q(t) \tag{9.44}$$

or

$$p(t) = L_f \frac{d}{dt} Q(t) \tag{9.45}$$

where $r(t)$ is the inductor pressure momentum, $p(t)$ is the inductor pressure, $Q(t)$ is the inductor volume flow, and the constant parameter L_f [Pa.s^{2}m^{-3}] is the *fluid inductance* of the fluid inductor, also termed *fluid inertance*.
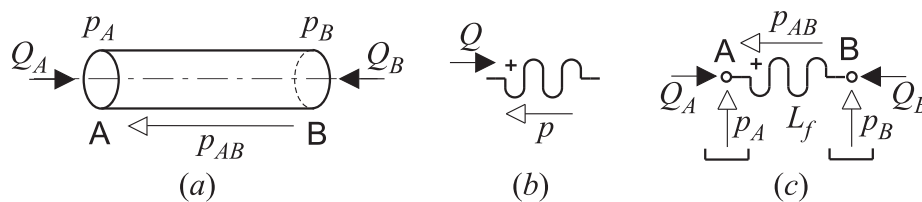
Figure 9.14: (a) Pipe segment. (b) Pure fluid inductor. (c) Pipe model.

To visualize the concept of fluid inductance, let us consider the unsteady frictionless flow of an incompressible fluid in a nonaccelerating pipe segment of length ℓ. If the pipe has constant area cross-section A and the velocity v of the fluid is uniform across any cross section of the pipe, we can say that every fluid particle has the same velocity v and hence the same acceleration dv/dt. Then the force F necessary to produce an acceleration dv/dt of the fluid mass in the pipe is

$$F(t) = A p_{AB}(t) = A\ell\rho \frac{dv}{dt}$$

where $p_{AB}(t)$ is the pressure drop across the pipe segment. As ρ [kg.m^{-3}] denotes the mass density of the fluid, $\rho A\ell$ is the mass of all the fluid in the pipe segment. The volume flow $Q_A(t) = Av(t)$, so that the *fluid inductance* of the flow in the pipe is

$$L_f = \rho \frac{\ell}{A} \tag{9.46}$$

This relation holds only when the pipe is not being accelerated. If the pipe itself has an acceleration, additional pressure difference effect between the inlets of the pipe segment will have to be taken into account.

Fig. 9.14b gives our graphical symbol for the pure fluid inductor (or resistor). The pure inductor is associated with two variables: the inductor pressure drop p and the conductor fluid flow Q. Polarities of these two variables are always related to the polarity of the symbol indicated by the $+$ sign as indicated in Fig. 9.14b. This means that the pressure at the $+$ pole is assumed larger than that at the second pole. The inductor flow is considered positive if it is oriented from the $+$ pole towards the inductor.

The symbol of the pure fluid inductor is utilized in Fig. 9.14c to model the pipe segment shown in fig Fig. 9.14a. The nodes A and B represent energy interactions at the corresponding inlets of the real pipe segment. The gauge pressures p_A and p_B at the pipe inlets are denoted by empty-head arrows placed between the symbols for the reference pressure and the related nodes. Respecting the conductor orientation, the pressure drop p_{AB} corresponds to the conductor pressure p, and the flow Q_A corresponds to the conductor flow Q. As the postulate of continuity applies to the pure inductor $Q_A + Q_B = 0$, or $Q_A = -Q_B$.

In actual fluid piping, significant friction effects are often present along with the inertance effects, and the inertance effect tends to predominate only when the rate of change of flow rate (fluid acceleration) is relatively large. Since flow resistance in a pipe decreases more rapidly with increasing pipe area A than does inertance, it is easier for inertance effects to overshadow resistance effects in pipes of large sizes. However, when the rate of change of flow rate is large enough, significant inertance effects are sometimes observed even in fine capillary tubes.
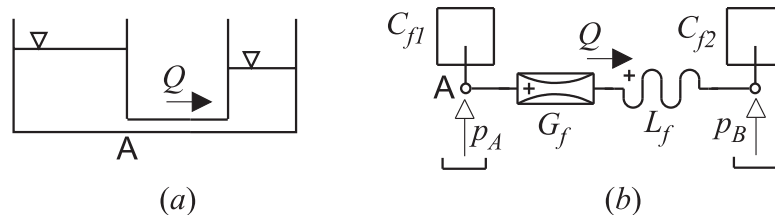
Figure 9.15: (*a*) Two-tank system. (*b*) Dynamic model.

A fluid-flow system consisting of two interconnected tanks is shown in Fig. 9.15*a*. The corresponding model respecting fluid-flow inertia is in Fig. 9.15*b*.

9.6 Fluid transducers

9.6.1 Fluid-mechanical-fluid transformer

Fig. 9.16*a* shows the principle of a fluid transformer. The device consists of two chambers filled with fluid separated by a common piston. The cross-sectional areas A_a and A_b on each side of the piston are different. As the forces acting on both sides of the piston must be balanced

$$p_A A_A = p_B A_B$$

where p_A and p_B are presures exerted on the piston by the fluid in each of the chambers. To obtain a constitutive relation characterizing the pure model of the device shown in Fig. 9.16*b* we must consider this expression together with the energy-transfer relation taking on the form

$$p_A Q_A + p_B Q_B = 0$$

where Q_A and Q_B are the fluid volume flows into the chambers through the inlets A and B. Thus the constitutive relation is

$$\left[\begin{array}{c} p_A(t) \\ Q_B(t) \end{array} \right] = \left[\begin{array}{cc} 0 & n \\ -n & 0 \end{array} \right] \cdot \left[\begin{array}{c} Q_A(t) \\ p_B(t) \end{array} \right]$$

where the coupling ratio

$$n = \frac{p_A}{p_B} = -\frac{Q_B}{Q_A} = -\frac{A_b}{A_a}$$

To respect such effects like fluid compressibility and inductance, piston friction and mass, fluid leakage, etc., the energy-transfer transformer should be combined with the corresponding physical elements.
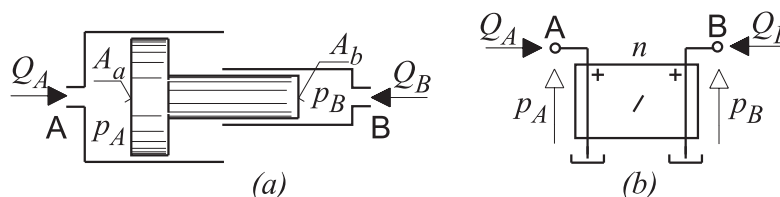
Figure 9.16: Fluid transformer.

9.6.2   Mechanical-fluid-mechanical transformer

Fig. 9.17a shows another fluid-based transformer, This time, however, the transformer is arranged to convert rectilinear motions. It consists of a cylinder with two pistons the cross-sectional areas A_a and A_b of which are different. The space between the pistons is filled with fluid exerting on both pistons the same pressure p which is balanced by the external forces F_A and F_B acting in the pistons, i.e.,

$$p = F_A/A_a = -F_B/A_b$$

Combining this expression with the energy-transfer relation in the form

$$\dot{x}_A F_A + \dot{x}_B F_B = 0$$

we obtain the constitutive relation of the rectilinear-motion transformer pure model shown in Fig. 9.17b

$$\left[\begin{array}{c} \dot{x}_A(t) \\ F_B(t) \end{array} \right] = \left[\begin{array}{cc} 0 & n \\ -n & 0 \end{array} \right] \cdot \left[\begin{array}{c} F_A(t) \\ \dot{x}_b(t) \end{array} \right]$$

where

$$n = \frac{\dot{x}_A}{\dot{x}_B} = -\frac{F_B}{F_A} = \frac{A_b}{A_a}$$
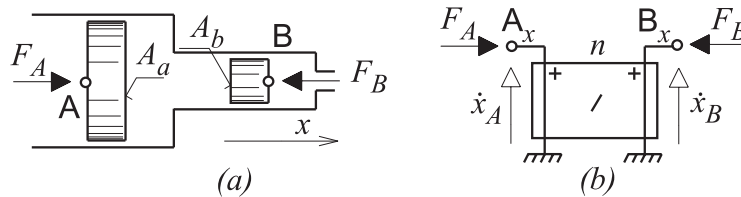
Figure 9.17: Fluid-based rectilinear-motion transformer.

9.6.3   Fluid-mechanical transducers

Table 9.1 shows pure models of some typical fluid-mechanical transducers utilizing energy-transfer gyrators.
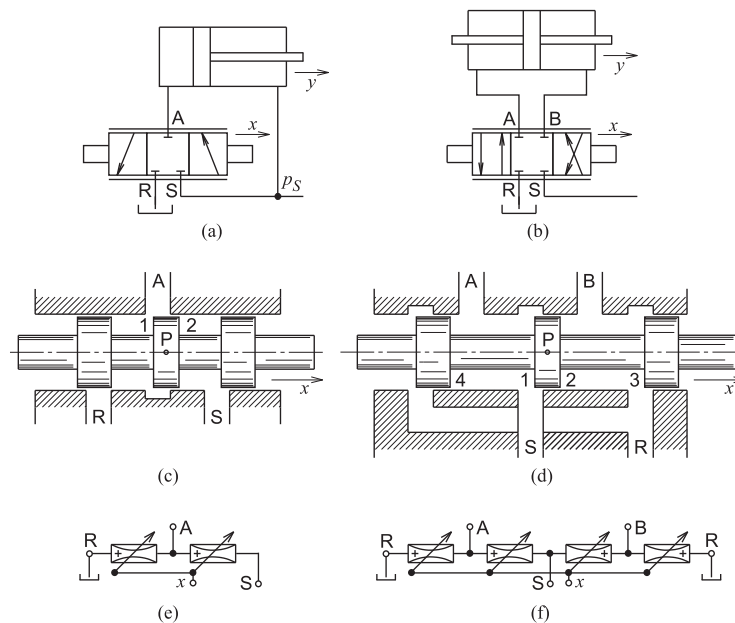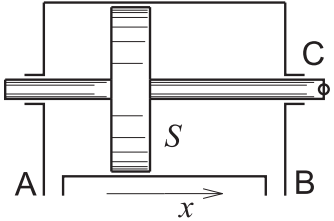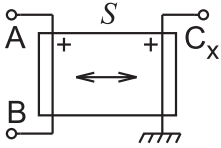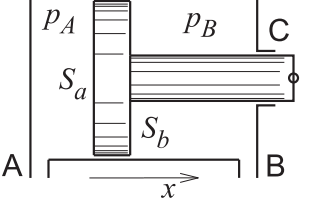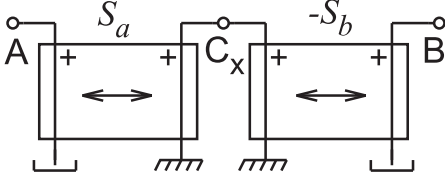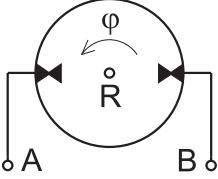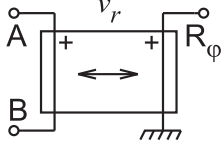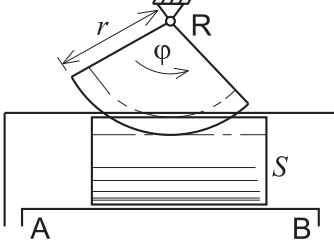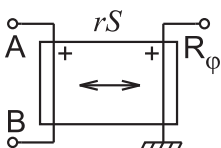
Figure 9.18: Three-land-three-way spool valves with cylinder load (S ... supply, R ... return).

Table 9.1: Pure models of fluid-mechanical transducers

Transducer	Pure model
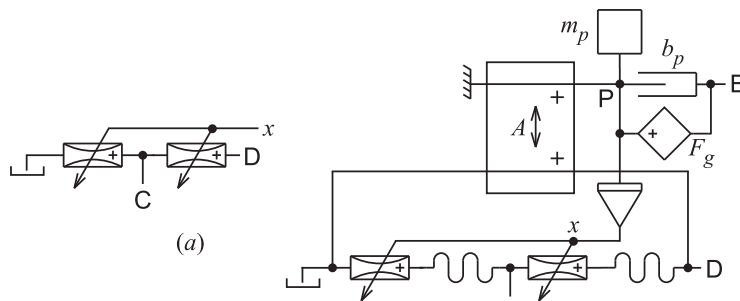
Figure 9.19: Spool valve model.
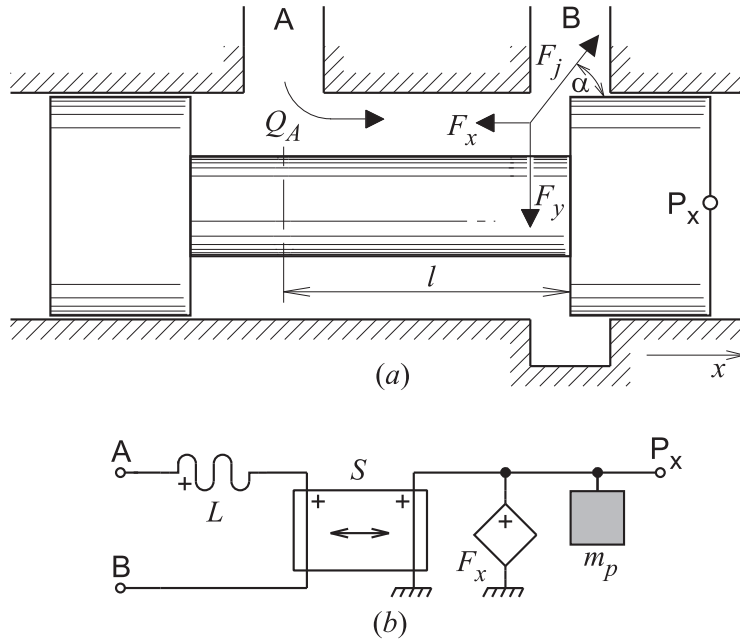
Figure 9.20: Flow forces acting on spool valves.
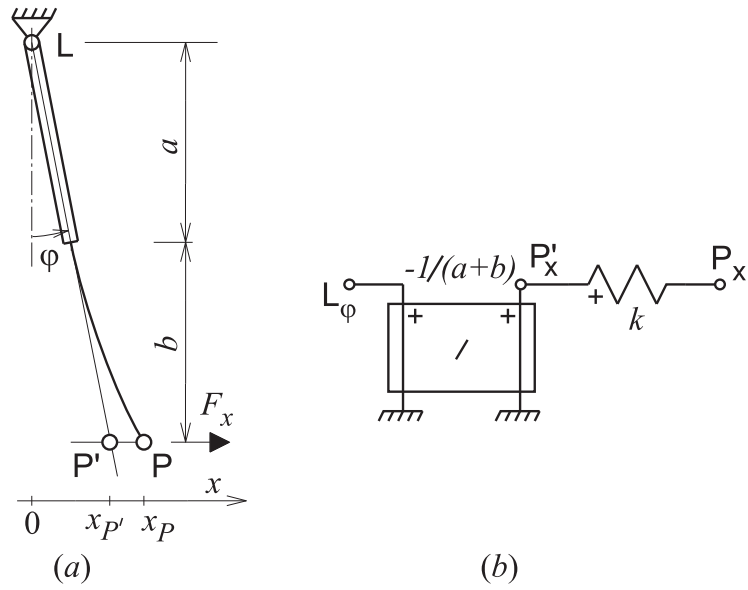
Figure 9.21: Flapper valve.
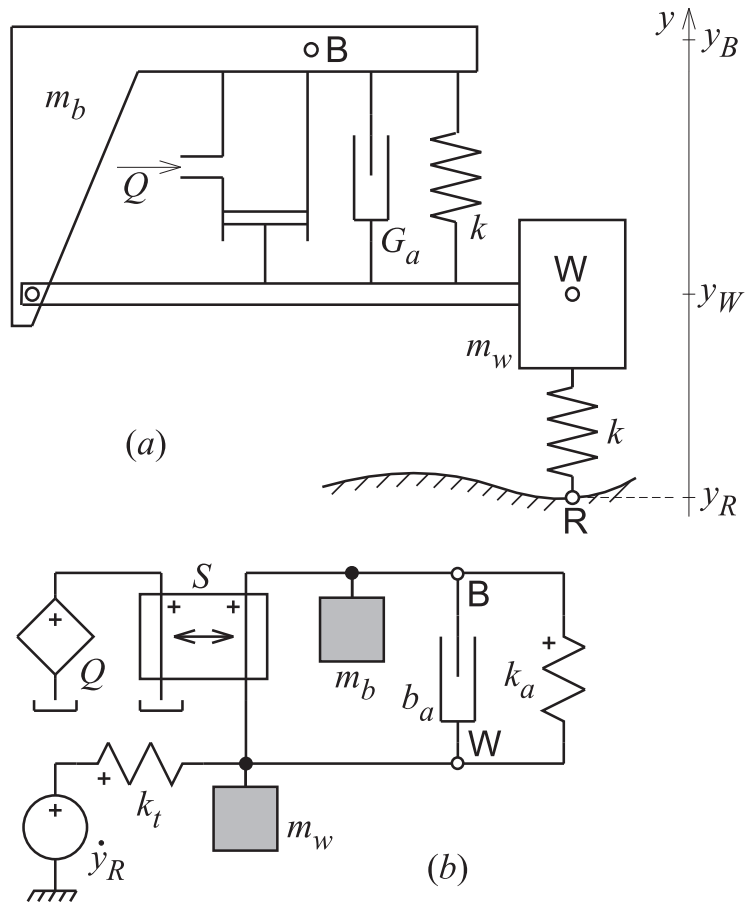
Figure 9.22: Fluid-damped car suspension.

Module 10

Thermal systems

10.1 Thermal interactions

10.1.1 Temperature

Temperature is the quantity related to the mean kinetic energy of molecules in a substance. When the temperature of a substance varies, its various physical characteristics change. For example, as the temperature of a metal increases, its dimensions and electrical resistance usually also increases, and its color may change.

Such changes may be used in thermometers to establish a quantitative measure of temperature. For instance, in a mercury-bulb thermometer, the scale of temperature is associated with the length of the mercury column. The change in length of the column which occurs when the thermometer is immersed first in ice water and then in boiling water is divided into equal increments called degrees. In the Celsius or centigrade system [°C] the interval is divided into 100 one-degree increments, and the ice-water temperature is defined as 0°C.

The absolute scale of temperature is independent of physical characteristics of substances. The second law of thermodynamics shows that negative absolute temperatures are impossible. When the absolute temperature is measured in degrees centigrade the scale is called the Kelvin scale and the units are kelvins [K]. The freezing point of water 0°C is expressed as 273.2 K. We shall use the symbol ϑ to represent temperature measured by any of the above scales. Thus the interrelation between the Kelvin and Celsius scales can be expressed as

$$\vartheta \, [\text{K}] = \vartheta \, [°\text{C}] + 273.15$$

Consideration of the methods by which temperature could be measured reveals that temperature is an across-variable (it can be measured without breaking into the system).

10.1.2 Heat flow

If two bodies having different temperatures are brought into contact, their temperatures will approach each other in such a way that one temperature will increase and the other will decrease. The quantity that has been transferred from one body to the other to produce the observed temperature changes is called **heat**. If the body temperature is decreased by the transfer, the heat flow is considered to be out of the body. Since temperature is a measure of the mean energy of the molecules of the body, heat is a form of energy.

Heat can be measured in calories [cal]. One calorie is the amount of heat required to raise the temperature of 1 gram of water by 1 °C. Since heat is a form of energy, it may also be expressed in joules by means of the equivalence of mechanical work and heat determined by the first law of thermodynamics. Thus 1 cal is equivalent to 4.1868 J.

We shall use the symbol $\mathcal{H}$ for quantity of heat. The flow rate of heat $\dot{\mathcal{H}}$ is obtained by differentiating $\mathcal{H}$

$$\dot{\mathcal{H}} = \frac{d\mathcal{H}}{dt} \tag{10.1}$$

In the systems we have studied previously, power has been given by the product of the through- and across variables at any energy interaction in the system. In thermal systems this situation does not prevail, since heat flow – the through-variable – is itself the thermal power.

10.1.3   Thermal power and energy

Thermal power is thus

$$\mathcal{P} = \dot{\mathcal{H}} \tag{10.2}$$

Thermal power is measured in watts [W].

The thermal energy $\mathcal{E}$ transferred through a surface (real or imaginary) in a body is the time integral of the heat flow

$$\mathcal{E} = \int_0^t \dot{\mathcal{H}}\, d\tau$$

10.2   Composition of thermal interactions

10.2.1   Composition of temperatures

The temperature drop between two points A and B in a system equals the difference between temperatures of these points, i.e.

$$\vartheta_{AB} = \vartheta_A - \vartheta_B \tag{10.3}$$

This is the zeroth law of thermodynamics generalized for transient states of thermal systems. The zeroth law states that if two bodies are in thermal equilibrium with a third body, they are also in thermal equilibrium with each other. Bodies in contact are said to have reached thermal equilibrium if the heat transfer between them stops.

10.2.2   Composition of heat flows

The first law of thermodynamics tells us that for any subsystem defined by a closed imaginary surface, the total heat into the subsystem must equal the energy transferred out of the subsystem in other forms (such as mechanical work, electrical energy, or fluid energy) plus the increase of energy stored in the system.

10.3   Accumulation of heat

10.3.1   Pure thermal capacitors

The ability of a body to store internal energy by virtue of a temperature rise when it receives a flow of heat can be modelled by a pure thermal capacitor. Let us consider heat flow taking place into a body having uniform (but not necessarily constant) temperature ϑ relative to a constant reference temperature.

By definition, a **pure thermal capacitor** modeling the thermal-energy-storage phenomenon has a heat content $\mathcal{H}$ which is a function of the body temperature ϑ

$$\mathcal{H} = f(\vartheta) \tag{10.4}$$

In an **ideal thermal capacitor**, $\mathcal{H}$ and ϑ are proportional:

$$\mathcal{H} = C_t \vartheta \tag{10.5}$$

where C_t is the thermal capacitance in J/K.

The thermal capacitance C_t of a body is determined as

$$C_t = c_p m \tag{10.6}$$

where m [kg] is the body mass, c_p [J/kg] is the **specific heat** of the body material.

The symbol for a pure thermal capacitor is shown in Fig. 10.1a . As for a fluid capacitor and inertor, one pole of the thermal capacitor must be always associated with a reference temperature which is zero or constant. As no heat occurs through the reference "connection" the reference is not shown in the symbol.

For a body to be modelled by an ideal thermal capacitor, all thermal resistance effects (discussed below) should be negligible within it (usually in comparison with external resistances) so that the temperature will be uniform throughout the mass which comprises the capacitor. A mass of metal or a well-stirred tank of fluid often behave very nearly like ideal thermal capacitors.
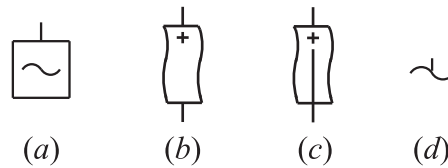
Figure 10.1: Symbol of pure thermal (*a*) capacitor, (*b*) resistor and (*c*) conductor. (*d*) Symbol of thermal reference.

10.3.2 Energy of thermal capacitors

The energy $\mathcal{E}$ stored in a thermal capacitor in the absence of work effects is simply equal to the heat transferred into it. Here again, the energy does not enter the picture in the same way as in the case of elements in the other energy domains, because the stored energy is a function of only the first power of the across-variable ϑ as

$$\mathcal{E} = \mathcal{H} = f(\vartheta) \tag{10.7}$$

10.4 Heat transfer

10.4.1 Pure thermal resistors

Heat can be transferred in three different ways: conduction, convection, and radiation. All modes of heat transfer require the existence of a temperature difference, and all modes of heat transfer are from the high temperature medium to a lower temperature one.

By analogy with the other pure resistors, we will define a **pure thermal resistor** by the equation

$$\vartheta = f(\dot{\mathcal{H}}) \tag{10.8}$$

An **ideal thermal resistor** has the defining equation

$$\vartheta = R_t \dot{\mathcal{H}} \tag{10.9}$$

where R_t [K/W] is the thermal resistance.

An **ideal thermal conductor** is defined as

$$\dot{\mathcal{H}} = G_t \vartheta \tag{10.10}$$

where G_t [W/K] is the thermal conductance.

All materials offer some resistance to heat flow, which is evidenced by the temperature drops in the direction of heat flow through material. When the material offers a large degree of resistance to heat flow, it is called a thermal insulator. A material through which heat flows relatively freely is called a thermal conductor. (At very low temperatures near the absolute zero certain materials exhibit "superconductivity", in which case heat may flow practically at zero temperature difference.)

10.4.2 Thermal conduction

The flow of heat through a solid material, such as the sheet illustrated in Fig. 10.2, occurs by conduction, that is, by the transfer of thermal kinetic energy from atom to atom of the material. This type of heat flow is described quantitatively by **Fourier's law**

$$\dot{\mathcal{H}} = \frac{\sigma_c A}{\ell} \vartheta_{AB} \tag{10.11}$$

where A is the area normal to the heat flow direction, ℓ is the length in the flow direction, and ϑ_{AB} is the temperature drop across the sheet. The thermal conductivity σ_c, expressed in W.m^{-1}.K^{-1}, is a specific property of a material defined by (10.11).

Equation (10.11) relates the through-variable $\dot{\mathcal{H}}$ to the across-variable ϑ by a simple constant factor. Comparison of (10.11) and (10.9) shows that the thermal resistance of conduction is

$$R_t = \frac{\ell}{\sigma_c A} \tag{10.12}$$
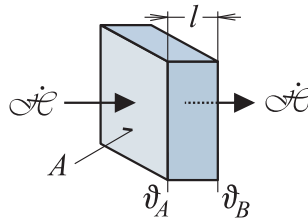
Figure 10.2: Heat flow through a conducting material.

A given material may be considered as a pure or ideal thermal resistance only if the amount of heat stored in it is negligible or does not change appreciably during operation. Fig. 10.1*b* shows the symbol for pure thermal resistances.

When two sheets of solid material are placed together with imperfect contact (which is typical), the total resistance of the combination is greater than the sum of the individual resistances of each of the sheets because of the small air space (or vacuum or oxide film in some cases) which exists at the interface. Although the thickness of the air space is very small, this extra resistance can be appreciable, because still air is a relatively poor conductor of heat.

10.4.3   Thermal convection

When the material through which heat is transferred is a fluid (liquid or gas), one may compute its resistance in much the same way as for a solid, but only so long as the fluid is not in motion. When fluid motion occurs (natural convection, forced flow, etc.), the heat-transfer picture becomes very complex. This heat-transfer mechanism is called **convection**, and is illustrated in Fig. 10.3. Motion, especially if it is turbulent, reduces the resistance to heat flow through a fluid so much, that the major thermal resistance exists in a very thin layer near the wall – described in terms of a film – where fluid motion is small.
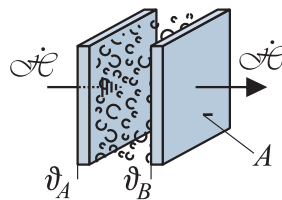
Figure 10.3: Convective heat transfere.

The notion of an over-all coefficient of heat transfer for a given physical arrangement of components in a thermal system is frequently employed, and it is defined as

$$c_h = \frac{\dot{\mathcal{H}}}{A\vartheta} \tag{10.13}$$

where c_h is the coefficient of heat transfer [kg.cal/^{o}C.s.m^2], A is the cross-sectional area, and ϑ is the over-all temperature drop.

A determination of the heat-transfer coefficient for a given thermal situation is usually very complex and nearly always involves experimental measurements. The coefficient c_h is not constant for a given geometry, but may often be assumed constant over limited ranges.

Equation (10.13) describes an ideal thermal resistance R_t whose value is

$$R_t = \frac{1}{c_h A} \tag{10.14}$$

10.4.4   Thermal radiation

In addition to thermal conduction and convection, heat may be transferred to or from a body by **thermal radiation**. Radiation is described quantitatively by the **Stefan-Boltzmann law**,

$$\dot{\mathcal{H}} = c_r(\vartheta_A^4 - \vartheta_B^4) \tag{10.15}$$

where c_r is a constant which depends on the shape, area, and surface characteristics of the body which is emanating or receiving radiation, and on the wavelength of the radiation. The temperatures ϑ_A and ϑ_B must be the absolute temperatures in K of the surfaces emitting and receiving radiation, respectively.

Fig. 10.4, illustrates schematically radiative heat transfer. Here it is assumed that the radiant energy emitted by surface A is absorbed by surface B.
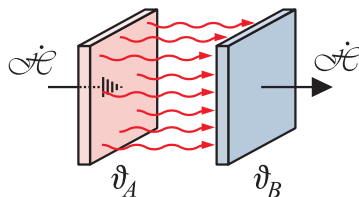
Figure 10.4: Convective heat transfere.

The constant c_r in (10.15), measured in W/K^4 is very small, so that heat transfer by radiation is usually insignificant unless large temperatures are involved. As an example, for radiation from a spherical black body to a black environment which completely surrounds it, the value of c_r is given by σA_o, where σ is the *Stefan-Boltzmann constant*, $\sigma = 1.37 \times 10^{-5}$ [W.m^{-2}K^{-4}] and A_o is the area of the radiating sphere in m^2.

The expression (10.15) for heat transfer is nonlinear and does not represent a pure thermal resistance as we have defined it, because $\dot{\mathcal{H}}$ does not depend on temperature difference. If the temperatures ϑ_A and ϑ_B change by only small amounts from mean values ϑ_{A0} and ϑ_{B0}, (10.15) may be linearized.

Let $\dot{\mathcal{H}}_0$ be the heat flow when $\vartheta_A = \vartheta_{A0}$ and $\vartheta_B = \vartheta_{B0}$, let ϑ_B be constant and $\Delta\vartheta_A$ be a small change (compared with ϑ_{A0} and ϑ_{B0}) of temperature ϑ_A. Then $\Delta\dot{\mathcal{H}}$ is the change in heat flow

$$\begin{aligned} \Delta\dot{\mathcal{H}} &= 4c_r\vartheta_{A0}^3\Delta\vartheta_A = \Delta\vartheta_A/R_{eq} \\ \dot{\mathcal{H}}_0 &= c_r(\vartheta_{A0}^4 - \vartheta_{B0}^4) \end{aligned} \tag{10.16}$$

and R_{eq} is the equivalent linear resistance when $\dot{\mathcal{H}} = \dot{\mathcal{H}}_0$.

When a thermal-resistance effect occurs due to combined radiative and convective heat transfer, it is often true that the over-all resistance is nearly linear and can be represented over the range of interest by an ideal thermal resistance.

A thermal resistance, unlike mechanical, electrical, and fluid resistances, dissipates no energy since the net heat flow is always zero. It also stores no energy since no work is done during the heat-flow process in a thermal resistance (first law of thermodynamics). There is, however, an increase of the property called entropy associated with the flow of heat through a thermal resistance (second law of thermodynamics), and hence a loss or dissipation of the available part of the energy supplied to it at temperature ϑ_A. If the heat flow $\dot{\mathcal{H}}$ were put into a reversible heat engine (a thermal-to-mechanical transducer) an amount of mechanical power equal to $\dot{\mathcal{H}}(\vartheta_A - \vartheta_B)/\vartheta_A$ could have been taken from the engine.

10.5 Thermal inductors and transformers

By analogy to electrical or fluid domain, there should be a pure thermal inductor as the second energy-storage element. While the thermal capacitor stores energy by virtue of its temperature, the thermal inductor should store energy by virtue of a heat flow through it. There is, however, no known thermal phenomenon at ordinary temperatures which acts in this way. Thus there is no thermal element which could be called a thermal inductor.

Pure transformer is a device which provides changes in the magnitudes of the through- and across-variables while maintaining instantaneous power balance. Such a device is clearly impossible in thermal systems because the through-variable itself is power (heat flow). Instantaneous power balance requires that $\dot{\mathcal{H}}_{in} = \dot{\mathcal{H}}_{out}$, and therefore no transformation of $\dot{\mathcal{H}}$ can occur.

10.6 Thermoelectric transducers

There are several kinds of thermal-to-electrical transducers. The most common of these is the thermo-couple, in which a voltage difference is generated between two dissimilar metals when a temperature

difference is applied. This effect has been used for temperature measurement and for the generation of small amounts of electric power. When energy flows from the electrical system to the thermal system, refrigeration or cooling can be obtained. Small thermoelectric refrigerators have been made for the cooling of electric components and for use as automatically controlled constant-temperature references.

Module 11

Unified approach to modeling

11.1   Dynamic behavior of systems

Dynamic behavior of a dynamic system is governed by the flow of energy and matter between the system and its surroundings as well as between subsystems of the system. Within the subsystems, energy and matter may be stored and later released, or changed from one form to another. Therefore, before starting any investigation of a system behavior we should clearly separate the system from its surroundings. Then we should decide in which way to decompose the system into its disjoint subsystems.

Table 11.1 gives examples of configurations of very simple systems from different physical domains. (We could easily extend our scope also to magnetic or thermal systems, but there is no equivalent of the inductor or spring in these domains.) Each of the systems consists from four different parts. The electrical system is formed by an RLC circuit supplied from an electronic source of electrical current. In the fluid system, a pump driven by an electrical motor forces a constant flow of water from a reservoir into an open tank. Water is returned back to the reservoir through a long pipe with a restriction at its end. The rectilinear translational mechanical system is powered by a weight suspended on a cable via a pulley. The cable is pulling a body connected to a hydraulic damper by a helical spring. The pulley is of negligible moment of inertia and bearing friction. The rotational mechanical system consists from a flywheel linked to a ventilator propeller by a long torsionally flexible shaft. The flywheel is driven by a combustion engine.

Evaluation of dynamic behavior of real systems in practice – either by measurements, or by simulation – is very often simplified by the following *approximating assumptions*:

1. the energy interactions between subsystems take place just in a limited number of *interaction sites* formed by adjacent *energy entries* into the subsystems

2. the energy flow through each energy entry can be expressed by a product of two complementary quantities called *power variables*

3. the total energy flow into a subsystem equals to the sum of the energy flows through all its energy entries

The energy interactions in our examples are assumed to take place at the sites denoted by M, N and and 0. In the case of the electrical system, these sites are made by interconnections of the energy entries formed by electrical terminals of the system parts. In the fluid system, the energy entries are formed by pipe inlets of the parts. The spring and the damper in the translational system interact via common cross-sections of their links. We can assume that the cable, the spring and the body interact via a cross-section of the body. We could easily identify similar interaction sites and energy entries of parts in the rotational system

11.1.1   Power variables

Table 11.2 shows pairs of physical quantities that can be chosen as power variables in the simple systems under discussion. The quantities in each power-variable pair complement each other in such a way that one of them is a *through variable* whereas the other one is an *across variable*. The table gives also the

Table 11.1: Examples of simple dynamic systems and their multipole models.

Configurations of real systems	Multipole diagrams

Part	Real parts	Physical elements
1	electrical energy supply	source of electrical current
2	electrical condenser	electrical capacitor
3	coil of wire	electrical inductor
4	electrical resistor	electrical conductor

Part	Real parts	Physical elements
1	water pump driven by motor	source of volume flow-rate
2	open water tank	fluid capacitor
3	long pipe	fluid inductor
4	water-flow restriction	fluid conductor

Part	Real parts	Physical elements
1	weight suspended on cable via pully	source of force
2	mass of moving body	inertor
3	helical spring	pure spring
4	oil-filled damper	pure damper

Part	Real parts	Physical elements
1	combustion engine	source of torque
2	flywheel	rotational inertor
3	long flexible shaft	torsional spring
4	ventilator propeller	rotational damper

Table 11.2: Pairs of through- and across-variables

Physical domain	Power variables		Energy variables	
	through i	across v	through $\int i\,dt$	across $\int v\,dt$
electrical	Electrical current $[A]$	electrical voltage $[V]$	electrical charge $[C]$	flux linkage $[V.s]$
magnetic	magnetic flow rate $[Wb/s]$	magnetic voltage $[A]$	magnetic flow $[Wb]$	
thermal	entropy flow $[W/K]$	temperature $[K]$	entropy $[J/K]$	
fluid or acoustic	volume flow $[m^3/s]$	pressure $[N/m^2]$	volume $[m^3]$	pressure momentum $[N.s/m^2]$
translatory	force $[N]$	velocity $[m/s]$	momentum $[N.s]$	displacement $[m]$
rotary	torque $[N.m]$	angular velocity $[rad/s]$	angular momentum $[N.m.s]$	angular displacement $[rad]$

related pairs of *energy variables*, i.e. the through and across variables integrated with respect to time. The vacancies in Table 11.2 correspond to quantities which have no physical meaning.

Note that the through and across variables differ by the way in which they are directly measured. Through variables are measured between interacting adjacent energy entries by instruments included between the entries after the entries were disconnected. Across variables are measured between distant entries by instruments applied to the entries without any disconnections (across variables between adjacent entries are zero). This is illustrated by Fig. 11.6 showing a two-entry part connected to a system.

An important role is played by across variables measured with respect to an *absolute across-variable reference*. In each of the examples given in Table 11.1, such a reference is denoted by 0. The absolute reference of voltages in electrical systems – electrical ground – is embodied in the example by the system chassis. In the fluid system, the free atmospheric pressure was chosen as the pressure reference. In both the mechanical systems, the system frame fixed to the Earth surface is considered as the absolute reference for velocities.

The third approximating assumption mentioned above can be expressed for a subsystem with n entries as

$$P(t) = \sum_{j=1}^{n} i_j(t) \cdot v_j(t) \tag{11.1}$$

where P is the total power consumed in the subsystem, i_j is the through variable of the j-th entry, and v_j is the across variable of this entry with respect to the absolute reference, $j = 1, 2, \ldots, n$. We thus
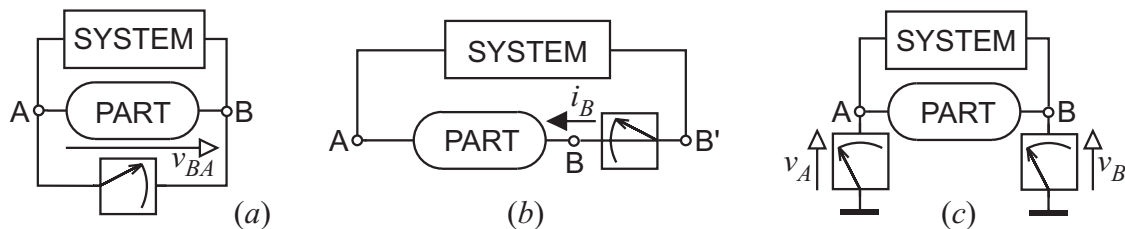
Figure 11.1: Measuring of (*a*) an across variable between distant energy entries, (*b*) a through variable between adjacent entries, (*c*) across variables of entries with respect to a reference.

assume that the power consumed (dissipated or accumulated) in a subsystem is positive whereas the power retrieved from the subsystem is negative.

11.1.2   Orientation of variables

The value of a variable is either positive or negative depending on the orientation of the variable with respect to its polarity or direction reference. To denote the assumed positive orientation of variables engineers usually use arrows. If the actual orientation of a variable is opposite to the direction of the arrow, the value of the variable is taken as negative. Let us agree that the variable orientation is governed by the following conventions.

Arrow Orientation Conventions

- Orientation of across variables in a system is indicated by arrows with empty arrowheads. These arrows are always directed from the point of the assumed smaller value to the point of the assumed larger value of the related across variable with respect to its absolute reference.

- Orientation of through variables is indicated by arrows with full arrowheads. The full-head arrow direction is in agreement with the assumed positive direction of the motion of the associated medium.

Thus the empty-head arrow points in the direction of the assumed increasing value of the across variable. The full-head arrows point in the direction of the assumed positive motion of a flow of positively charged particles in the electrical domain, magnetic flux in the magnetic domain, heat flow in the thermal domain, and flow of mass particles in the fluid or acoustic domain. In the mechanical domain, a full-head arrow indicates the direction of the motion the related force or torque tends to cause.

11.1.3   Modeling with physical elements

Multipoles model energy interactions between subsystems or between subsystems and the system surroundings under the approximating assumptions mentioned above. Each energy entry into a subsystem is represented in its multipole model by a pole associated with a pair of the power variables. In the multipole model of a subsystem, each of the multipole *poles* stands for an energy entry into the subsystem. It is associated with the pair of power variables related to the entry. Multipoles are represented graphically by symbols with poles denoted by *pins*, i.e. by short line segments sticking out of the symbol outlines.
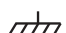
The multipole model of a complete system is portrayed by the *multipole diagram* consisting of graphical symbols of the individual multipole models. The sites of energy interaction between adjacent energy entries in a real system are represented in the related multipole model by its *nodes*. Pins denoting the entries interacting at a site are interconnected with the node representing the site by line segments called *ideal links*.

The drawings of systems shown in the left column of Table 11.1 can be readily converted into multipole diagrams shown in the right column of the table. Each of the two-entry parts is represented there by a symbol of an idealized *physical element*. Each of such elements models just one specific energy phenomenon like energy generation, accumulation, or dissipation. For simplicity, only the dominant dynamic effect of each part is respected in the diagrams in Table 11.1. More realistic models could be set up for each part by combining several such elements.

Nodes M, N and 0 in the diagrams shown in Table 11.1 are related to the sites of energy interaction in the real systems denoted by the respective characters. *Reference nodes* representing the absolute across-variable references 0 are denoted in the multipole diagrams by graphical symbols shown in Table 11.3.

The links can be viewed as interconnections capable of transferring energy in both directions without any dissipation, accumulation or delay. Depending on the related physical domain, the links can be viewed either as idealized electricity-conducting wires or as fluid-conducting pipes, idealized shafts or other mechanical links, etc. This does not mean, however, that real interconnections should be always modelled in such an idealized way; they can be considered as independent subsystems with any of their non-ideal features respected. This is the case of the long pipe segment in the fluid-system example, and of the long torsionally flexible shaft in the rotational-system example in Table 11.1.

Table 11.3: Absolute across-variable references

Physical domain	Reference across variable	Symbol
electrical	voltage of the electrical ground	
magnetic	magnetic voltage at a reference point	
thermal	zero-point on a temperature scale	
fluid or acoustic	free-atmosphere pressure (usually)	
mechanical	reference-frame (angular) velocity	

11.2 Dissipative and accumulative elements

11.2.1 Symbols of dissipative and accumulative elements

Table 11.4 gives graphical symbols for physical elements modeling dissipation and accumulation of energy in multipole diagrams. The entries for thermal and magnetic inductors are empty in the table as no corresponding physical phenomena are known. The notion of a resistor is not common in the mechanical domain. Besides the element symbols specific for different physical domains, Table 11.4 gives also generic symbols applicable to elements in any of the domains.

   The physical elements are very useful approximations of dynamic effects associated with real subsystems. The elements are called *pure models* as each of them represents just one specific dynamic effect. Depending on their physical domain, the elements model energy effects associated with the one-dimensional motion of electrical or magnetic charges, fluids (liquids or gases), particles or bodies. The thermal-domain elements are concerned about reversible heat-transfer effects.

   Pure capacitors model accumulation of energy by the virtue of an across variable in the non-mechanical domains. Inertors do the same in the mechanical domain, they model accumulation of inertial energy associated with either rectilinear or rotational motion of a mass. Pure inductors and springs model accumulation of energy by the virtue of a through variable. The energy accumulated in these elements can be retrieved back at any time. With the exception of the thermal-domain elements, pure conductors, resistors and dampers model dissipation of energy, i.e. the conversion of energy into heat. This energy cannot be retrieved and returned back into the systems. Pure thermal conductors and resistors model the increase of system entropy due to the flow of heat.

11.2.2 Constitutive relations of physical elements

As shown in Fig. 11.2, each of the physical elements is associated with a pair of **power variables** i_e and v_e. Whereas i_e is the element-through variable 'flowing' through the element, v_e is the element-across variable between the element poles. These two variables complement each other in the sense that their product

$$P_e(t) = i_e(t) \cdot v_e(t) \tag{11.2}$$

expresses the power consumed (dissipated or accumulated) in the element. Thus, if the power is retrieved from an element, its value is negative.
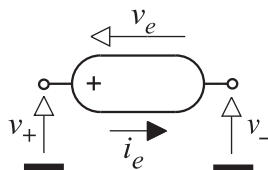
Figure 11.2: Variables associated with a generic physical element.

   Each of the physical elements is characterized by a specific **constitutive relation** between the **element variables**. Constitutive relations for the dissipative and accumulative elements are given in

Table 11.4: Physical elements dissipating or accumulating energy.
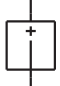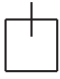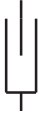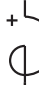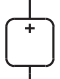
Type	G	R	C	L
	Conductor/Damper	Resistor	Capacitor/Inertor	Inductor/Spring
Non-mechanical	Conductor	Resistor	Capacitor	Inductor
electrical				
magnetic				
thermal				
fluid or acoustic				
Mechanical	Damper		Inertor	Spring
translational				
rotational				
generic				

Table 11.5. The letter p denotes the **element parameter** p in these relations. Table 11.5 gives also physical dimensions of the parameter p in different physical domains and their units. The fact that the constitutive relation of the dissipative and accumulative elements are in the form of algebraic of ordinary differential equations indicates that the elements belong to lumped-parameter models.

In the case of **ideal elements**, the parameter p is constant. The elements given in Table 11.4 need not be ideal, however. DYNAST allows also for **nonlinear** and time-variable elements as well as for elements the parameters of which are are controlled by variables or parameters of some other elements, blocks or equations.

In general, the parameter p of a controlled nonlinear and time-variable element can be given by an expression of the form

$$p = f(z_1, z_2, \ldots, \dot{z}_1, \dot{z}_2, \ldots, t) \tag{11.3}$$

where $z_1, z_2, \ldots$ are elementcontrolling variables or parameters, $\dot{z}_1, \dot{z}_2, \ldots$ are their time derivatives, and t denotes time.

Despite the fact that all the physical elements are two-pole models, **one-pin symbols** are given in Table 11.4 for thermal, fluid or acoustic capacitors as well as for the translational and rotational inertors. According to physical laws governing accumulation of energy by these elements, their element-across variable v_e must be always considered with respect to the related reference. In other words, one pole of

Table 11.5: Parameters of dissipative and accumulative physical elements.

Element	Conductor or damper	Resistor	Capacitor or inertor	Inductor or spring
Constitutive relation	$i_e = p\, v_e$	$v_e = p\, i_e$	$i_e = p\, \frac{d}{dt} v_e$	$v_e = p\, \frac{d}{dt} i_e$
electrical	conductance $[S]$	resistance $[\Omega]$	capacitance $[F]$	inductance $[H]$
magnetic	conductance $[\Omega]$	resistance $[S]$	permeance $[H]$	
thermal	entropic conductance $[W/K^2]$	entropic resistance $[K^2/W]$	entropic capacitance) $[J/K]$	
fluid or acoustic	conductance $[m^3/(Pa.s)]$	resistance $[Pa.s/m^3]$	capacitance $[m^3/Pa]$	inertance $[Pa.s^2/m^3]$
mechanical translatory	damping $[N.s/m]$		mass $[kg]$	compliance $[m/N]$
mechanical rotary	torsional damping $[N.m.s/rad]$		moment of intertia $[m^2kg/rad]$	torsional compliance $[rad/(N.m)]$

these elements must be always coalesced with a reference node. Only one pin needs to be shown in the graphical symbols of these elements to simplify the multipole diagrams.

11.3   Sources of energy

11.3.1   Independent sources of energy

Besides the energy storing and dissipating elements we need still another type of physical elements to be able to set up multipole models of dynamic systems – pure sources of energy. Two limiting cases are considered in which either an across variable or a through variable is specified independently of the amount of energy drawn from or delivered into the source – a source of across variable and a source of through variable. Our symbols for such sources are given in Table 11.6. We shall use the generic sources in all non-mechanical domains. The last row in Table 11.6 shows that the parameter p in the constitutive relations of sources equals directly to the source nominal variable, either i_e or v_e.

In general, pure sources are either independent or controlled by various variables or parameters. The independent sources can be ideal or time-variable. An **ideal independent across-variable source** $v_e(t)$ is defined by the constituency relation

$$v_e(t) = V \tag{11.4}$$

and, similarly, an **ideal independent source of through variable** $i_e(t)$ is described as

$$i_e(t) = I \tag{11.5}$$

where V and I are known constant parameters.

The independent sources are usually used to model external energy reservoirs large enough relative to the amount of energy they supply to the system or absorb from it without undergoing any change either in across or through variable. Fig. 11.3*a* shows a system and its surroundings modelled by twopoles. If the surroundings is capable of delivering energy into the system with negligible variations of the through variable $i(t)$ involved in the interaction, the surroundings can be modelled by an across-variable source as shown in Fig. 11.3*b*. If, on the other hand, the surroundings delivers energy without noticeable fluctuations of the across variable $v(t)$, the model configuration with a through-variable source of Fig. 11.3*c* can be utilized.

Examples of real sources that approximate independent sources:

- A low-resistance electrical battery supplying a low-consumption electronic device is very often considered as an independent source of constant voltage. Energy supply in the form of electrical mains is usually modelled as an ideal source of sinusoidal voltage.

Table 11.6: Independent sources of energy.

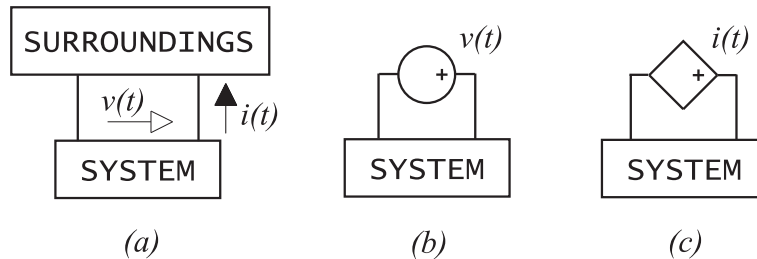| Type	J	E
Generic	through-variable source	across-variable source
Mechanical		
translational	source of force	source of velocity
rotational	source of torque	source of angular velocity
Constitutive relation	$p = i_e$	$p = v_e$

Figure 11.3: (a) Interaction between a system and its surroundings modelled by (b) across-variable source, or (c) through-variable source.

- An independent source of magnetic voltage can be used to model generation of magnetic field in a permanent magnet.

- In the analysis of the heat dissipation from a system in a room, the air in the room can be treated as an independent source of temperature if the heat transfer from the system to the room air is not large enough to have a noticeable effect on the room air temperature.

- Most of the hydraulic pumps are usually modelled as independent sources of volume flow.

- A large accumulator supplying fluid to a small fluid-power system may be replaced by an independent source of pressure.

- A sufficiently powerful motor driving a light mechanism represents from the point of view of the mechanism an independent source of angular velocity.

- When modeling motion of a body close to the earth surface, the effect of the earth gravitational field on the body can be respected by an independent source of gravitational force $F_g = g \cdot m$, where g is the gravitational constant and m is the mass of the body.

It is assumed in each of the examples given in Table. 11.1 that the system under our investigation consists of parts 2, 3 and 4 while the part 1 is considered there as the system surroundings. For this reason, each of the parts 1 is modelled by an independent source of through variable. If modeling of a real source or the system surroundings by an independent source alone is inadequate, the independent source is combined with other physical elements.

11.3.2 Ideal connections, indicators and sensors

Also zero-valued independent sources deserve our attention. An independent source of zero across variable is equivalent to an **ideal closed connection**, or simply, an **ideal connection**. This is a two-pole element the across variable v_e of which is identically zero irrespective of its through variable i_e, i.e., its constituency relation is $v_e = 0$. Similarly, a two-pole element makes an **ideal open connection** if its through variable i is identically zero irrespective of its across variable v, i.e., its description is $i = 0$. Obviously, such an element is equivalent to an independent source of zero through variable. We shall find not only the ideal closed connections, but also the open connections, very useful when modeling a changing system structure. Fig.11.4 shows characteristics of these elements the v-i and i-v planes.
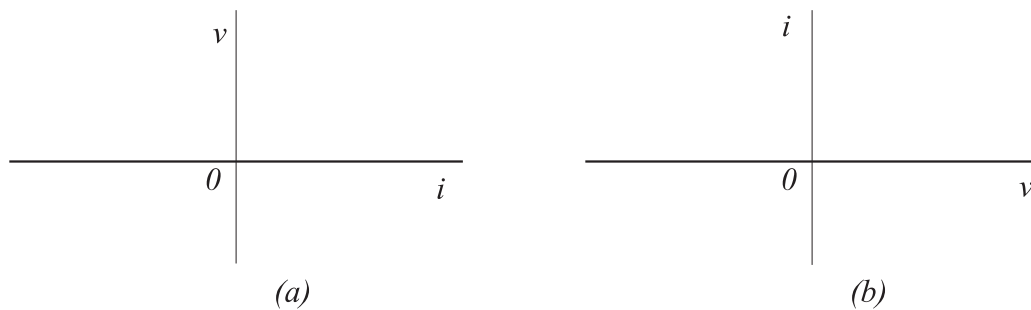
Figure 11.4: Characteristic of ideal (a) closed and (b) open connection.

Note also, that the zero-valued independent sources can be used to imitate measuring instruments and sensors of power variables. An **ideal through-variable indicator** models ideal through-variable measuring or sensing devices. It behaves like an ideal connection the through-variable of which corresponds directly to the indicated quantity. Similarly, an **ideal across-variable indicator** acts as an ideal open connection and indicates its own across variable. Therefore, the ideal through-variable indicator is equivalent to an independent source of zero across variable, whereas the ideal across-variable indicator is equivalent to an independent source of zero through variable.

Figure 11.5: Graphical symbols for an ideal (a) across-variable and (b) through-variable indicator.

In cases when we shall need to stress the presence of ideal measuring instruments in a system model, we shall use the graphical symbols shown in Fig. 11.5. Each of the symbols for the ideal indicators represents a two-pole with its +pole at the top.

Fig. 11.6 shows configurations in which ideal indicators are used to 'pick-up' power variables of a generic physical element in a system. The instrument orientation with respect to the element orientation was chosen in such a way that the variable polarities are in mutual agreement.
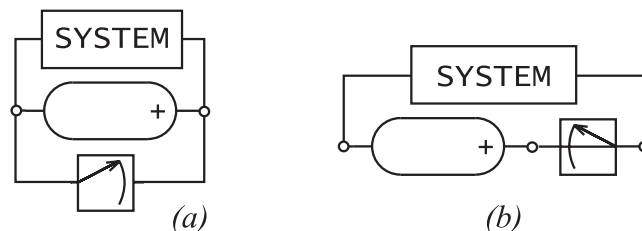

Figure 11.6: Configurations for indicating (a) element-across variable and (b) element-through variable.

11.3.3   Controlled sources

Many physical devices controlling a flow of energy or transforming one form of energy into another form may often be adequately modelled by means of controlled sources. The element-across variable v_e or element-through variable i_e of these two-pole physical elements is a function of some other variables in the system model. In ideal controlled sources, this function is proportionality. Table 11.7 lists four types of **ideal controlled sources**, controlled either by an across variable v_c or by a through variable i_c. No energy input is required to control the sources. The symbol given in Table 11.6 will be used throughout this text both for independent and controlled sources.

Table 11.7: Ideal controlled sources.

Source of	Controlled by	Relation	Parameter p
across variable	across variable	$v_e = p \cdot v_c$	across-variable transfer ratio
across variable	through variable	$v_e = p \cdot i_c$	transresistance
through variable	through variable	$i_e = p \cdot i_c$	through-variable transfer ratio
through variable	across variable	$i_e = p \cdot v_c$	transconductance

In general, the controlled sources of through variables are characterized by the constitutive relation

$$i_e = f(z_1, z_2, \ldots, \dot{z}_1, \dot{z}_2, \ldots, t)$$

The counterparts, controlled sources of across variables are characterized by the relation

$$v_e = f(z_1, z_2, \ldots, \dot{z}_1, \dot{z}_2, \ldots, t)$$

11.4   Orientation of physical elements

11.4.1   Element Polarity Convention

To simplify the polarity determination of variables associated with physical elements as much as possible, we can assume that the variable orientation is fixed to each element symbol once for ever. For the element-polarity reference, we are associating one of the poles of each element with the $+$ sign, and the other pole with the $-$ sign. The $-$ sign is not shown in the element symbols given in Table 11.4, however, in order to simplify the notation. In the case of the elements with an asymmetric symbol even the $+$ sign is omitted for the same reason. We will always assumed that the pin of asymmetric symbols shown in Table 11.4 in the upper position is associated with the $+$ sign.

   To interrelate orientation of physical elements and their variables, let us adopt the following conventions:

- The element-across variable v_e is the across variable of the element $+$pole with respect to its $-$pole (or to the absolute reference if the second pin is not shown in the element symbol).

- The positive orientation of the element-through variable i_e is always directed from the $+$pole towards the $-$pole.

   Fig. 11.2 shows that according to our conventions the empty-head arrow for v_e is always directed from the $-$pole towards the $+$pole of the element, whereas the full-head arrow for i_e is always directed in the opposite way. The empty-head arrow for the pole variable v_+ and v_- is always directed away from the absolute reference towards of the $+$pole and $-$pole, respectively. Note, however, that once we have interrelated the variable orientation with the element polarity, we do not need to use the arrows at all.

11.4.2   Orientation of non-mechanical elements

Fig. 11.7*a* shows a real subsystem with two energy entries of non-mechanical nature, Fig. 11.7*b* gives a generic symbol for a physical element modeling such a subsystem. The orientation of the element was chosen in such a way that its $+$pole represents the entry A and its $-$pole the entry B of the subsystem. Then, in conformity with the *Element Polarity Convention*, the element-across variable v_e corresponds

to the across variable v_{BA} of the entry B with respect to the entry A as indicated in Fig. 11.7a. Similarly, the orientation of the element polarity with respect to the entries A and B determines orientation of the element-through variable i_e. It corresponds in this case to the through variable entering the subsystem at the entry A and leaving it at the entry B.

If we had chosen the opposite orientation of the element with respect to the subsystem entries, also the orientation of the variables i_e and v_e would be opposite. Note that the presumption (11.2) is satisfied regardless of the chosen element orientation with respect to the entries.
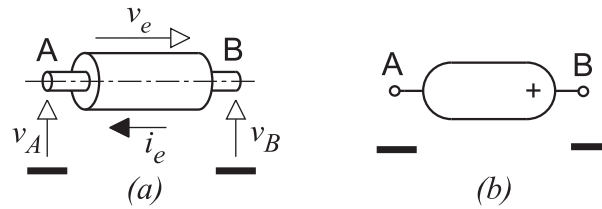
Figure 11.7: (a) Subsystem with two energy entries of non-mechanical nature, (b) its generic-element model.

11.4.3 Orientation of mechanical elements

Fig. 11.8 shows a two-entry subsystem in a translational motion along the axis x and its model in the form of a generic physical element. The energy entries A and B of the subsystem Fig. 11.8a are represented by the element poles A_x and B_x of the element in Fig. 11.8b. Once the direction of the x-axis has been chosen from A towards B, it is advantageous to choose the orientation of the element as shown in Fig. 11.8b to simplify the variable orientation. Then, in conformity with the *Element Polarity Convention*, the element-across variable v_e represents the velocity $\dot{x}_{BA}$ of the entry A with respect to the entry B. Note that in this case v_e is positive if the subsystem is elongating and negative if it is shortening.

To satisfy the presumption (11.2), we must assume that the element-through variable i_e represents the subsystem internal force counterbalancing an external force stretching the subsystem. Thus, a positive i_e indicates that the subsystem is in tension, whereas a negative i_e indicates a compression of the subsystem. Had we chosen the opposite orientation of the element with respect to the direction of the related coordinate, also the orientation of the two variables v_e and i_e would change.
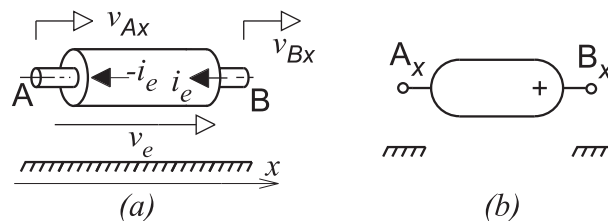

Figure 11.8: (a) Subsystem with two energy entries in translational motion, (b) its generic-element model.

Fig. 11.9 shows the similar situation for a subsystem with entries in rotational motion. In summary, the mutual orientation of variables associated with a mechanical subsystem and its elemental model must be related to the mutual orientation of the subsystem coordinate axes and the element polarity. Whenever possible, we shall always prefer the mutual subsystem-element orientation shown in Fig. 11.8b and Fig. 11.9b.

11.4.4 Orientation of sources of energy

The Element-Polarity Convention applies also to sources. The source of force in Fig. 11.10b models the translational actuator shown in Fig. 11.10a providing a pair of forces acting between the attachment points A and B. The forces F and $-F$ making up the pair have a common line of action but are in opposite directions. If F is positive, the forces pull on the points A and B, and if F is negative the forces push on the points. Fig.11.10b and c show sources of force of different polarities with respect to the mutual orientation of the modelled actuator and the x axis. Note that the sign of the force is related to the source polarity.
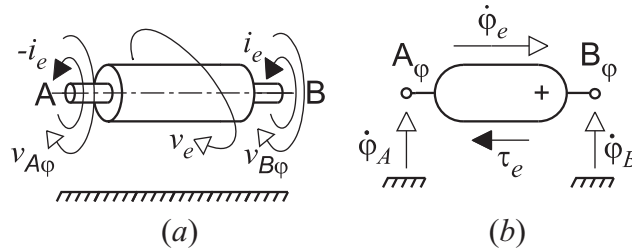
Figure 11.9: (*a*) Subsystem with two entries in rotational motion, (*b*) its generic physical-element model.
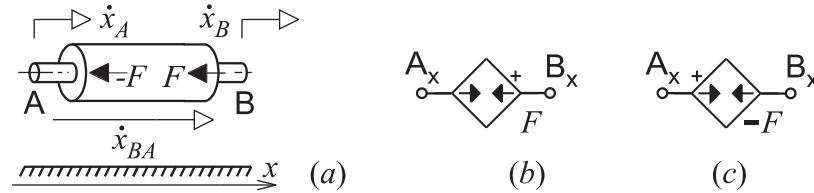

Figure 11.10: (*a*) Force actuator, (*b*) and (*c*) corresponding sources of force.

Source of velocity imposes a relative motion of a specified velocity between two points it represents. Fig. 11.11*a* shows point A that is in a rectilinear motion along the x-axis of a given absolute velocity $\dot{x}_A(t)$. In Fig. 11.11*b* the x motion of the point A is represented by node A_x, the actuator giving the velocity $\dot{x}_A(t)$ to the point A an ideal source of velocity modeling motion of a point A along the x-axis with known absolute velocity $\dot{x}_A(t)$.

The source of velocity shown in Fig. 11.11*b* models imposing a relative motion of point B with respect to point A with known relative velocity $\dot{x}_{BA}(t)$ along the x-axis as shown in Fig. 11.11*a*.
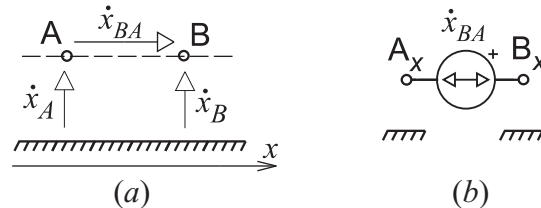
Figure 11.11: (*a*) Moving points, (*b*) source of velocity modeling an imposed motion of the points.

11.5   Configurations of physical elements

11.5.1   Setting up a physical-element model

- Sketch the geometric configuration of your system

- Define the system and its surroundings and denote by identifiers the sites of energy interaction between them

- Decompose the system into subsystems and denote the sites of energy interaction between the subsystems

- Associate all the sites of mechanical-energy interaction with a suitable coordinate system

- Start sketching the multipole model of your system by placement of nodes representing the individual sites of energy interaction

- Add reference nodes using the symbols given in Table 11.3

- Choose a suitable physical-element model for each subsystem and place it between the nodes corresponding to the subsystem interaction sites

- Orient the polarity of each mechanical element in conformity with the chosen coordinate system

- Repeat the previous two steps for the surroundings

- You may add ideal indicators for the across and through variables you are interested in

Though the symbols were chosen to remind real subsystems you should never forget about the difference between a real subsystem and its model. As a matter of fact, no real subsystems behave exactly like the physical elements. The elements are, however, very useful first-order approximations of dynamic effects taking place in real subsystems. If modeling of a subsystem by a single element appears to be inadequate, a more realistic subsystem model can be constructed using several physical elements as standardized building bricks.

11.5.2 Forbidden source configurations

The independent sources discussed so far can be used in a very flexible way, yet not without any restrictions. Fig. 11.12a shows a system model with three independent across-variable sources forming a close loop. According to Postulate of Compatibility the element-across variables of the sources must satisfy the equation

$$v_1(t) - v_2(t) - v_3(t) = 0 \tag{11.6}$$

for any t. Otherwise the variable would be inconsistent. If, however, (11.6) is satisfied, any one of the three across-variable sources can be omitted without any impact on the system-model dynamics. Therefore, if (11.6) is not satisfied, the equations characterizing the system configuration in Fig. 11.12a have no solution. If (11.6) is satisfied, the equations are singular unless the superfluous source is removed from the system model.
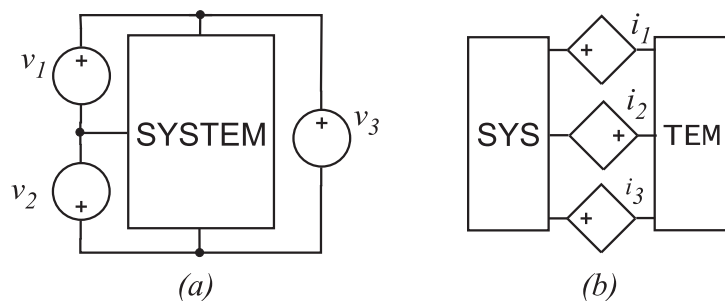

Figure 11.12: Forbidden (a) loops of across-variable sources and (b) cut-sets of through-variable sources.

The three through-variable sources in Fig. 11.12b form a cut-set, or – in other words – if the three sources are removed from the system model, the model gets separated into two isolated parts. At the same time, according to Postulate of Continuity the element-through variables of the sources must for any t satisfy the equation

$$i_1(t) - i_2(t) + i_3(t) = 0 \tag{11.7}$$

Then again, if (11.7) is satisfied any one of the sources can be omitted in the configuration without affecting the system-model behavior. Also in this case, unless the superfluous source is removed from the system model, the equations characterizing the system are either having no solution or they are singular.

This observation, that can be easily proven in a general way, results in the following conclusion: Loops of across-variable sources and cut-sets of through-variable sources are forbidden in the system-model configurations.

Fig. 11.13 and Fig. 11.14 give examples of permitted and forbidden source configurations. Explain the reason why the configurations in Fig. 11.14 are forbidden and try to submit them to DYNAST to see what kind error messages DYNAST will give you.
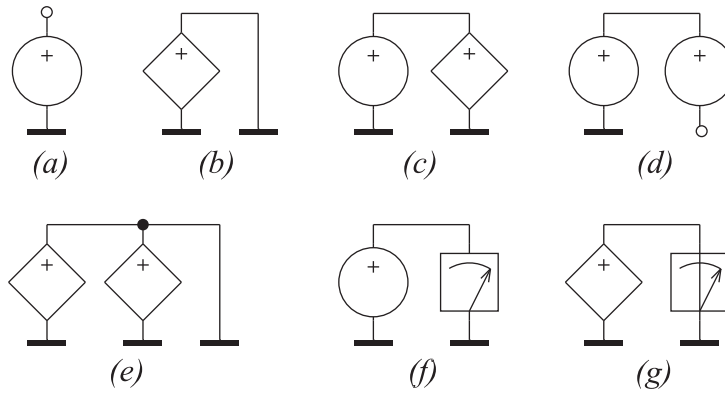
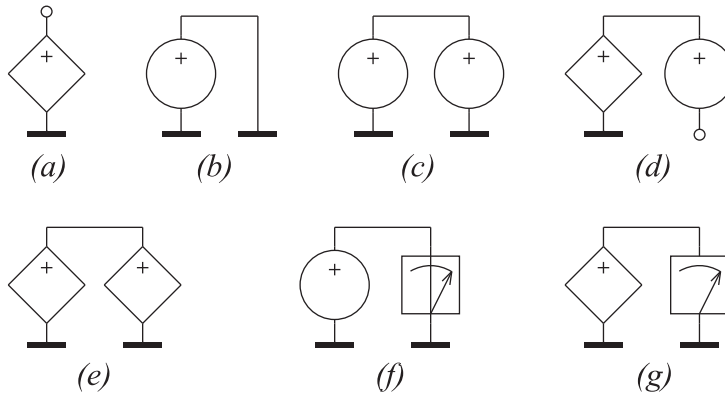Figure 11.13: Examples of permitted configurations.

Figure 11.14: Examples of forbidden configurations.

11.6   Energy transducers

11.6.1   Energy-transfer transducers

In general, transducers are devices converting energy from one form to another. For example, motors and other actuators convert electrical, fluid or some other energy into the mechanical one, sensors usually convert different forms of energy into the electrical form, etc.

In this section we are going to introduce *pure transducers* which are multipoles modeling energy conversion without any energy loss. They allow not only for very easy and unified way of modeling various real transducers converting energy between different energy domains, but they are also convenient for modeling various couplings within the individual energy domains. Combined with two-pole physical elements, pure transducers make fundamental 'bricks' in our kit from which realistic models of very diverse dynamic systems can be set up in an extremely easy way.

Pure transducers are subdivided into transducers which can store energy and those which only transfer energy. An *energy-transfer transducer* is a multipole for which the instantaneous power out always equals the instantaneous power in without dissipating or accumulating any energy. The pure energy-transfer transducers are either pure energy-transfer transformers or pure energy-transfer gyrators.
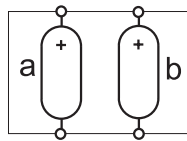

Figure 11.15: Generic pure transducer.

Let us consider the four-pole shown in Fig. 11.15 which consists of two generic two-pole elements which are mutually controlled by each other's element variables. Assuming that the coupling is pure, i.e.

that the total power lost or accumulated in the coupling is zero, the across and through variables $v_a(t)$ and $i_a(t)$ of the element a together with the analogous variables $v_b(t)$ and $i_b(t)$ of the element b must justify the *energy-transfer relation*

$$i_a(t) \cdot v_a(t) + i_b(t) \cdot v_b(t) = 0 \tag{11.8}$$

With regards to signs of the variables, we have respected here the Element-Variable Polarity Convention.

11.6.2 Energy-transfer transformers

Let us assume, that the coupling between variables of the generic elements a and b in Fig. 11.15 can be characterized by the *describing relation*

$$f\big(q_a(t), q_b(t)\big) = 0 \tag{11.9}$$

where $f(.)$ is a time-independent function and $q_a(t), q_b(t)$ are time-integrated element-through variables of the elements a and b, respectively (in mechanics such couplings are called holonomous scleronomous). The variables come possibly but not necessarily from different energy domains.

If the function $f(.)$ is differentiable, we can apply the chain rule to differentiate (11.9) with respect to time to obtain

$$\frac{\partial f}{\partial q_a} \cdot \frac{dq_a}{dt} + \frac{\partial f}{\partial q_b} \cdot \frac{dq_b}{dt} = 0 \tag{11.10}$$

Taking into consideration that $dq_a/dt = i_a(t)$ and $dq_b/dt = i_b(t)$, (11.10) can be rewritten as

$$n_a \cdot i_a(t) + n_b \cdot i_b(t) = 0 \tag{11.11}$$

where $n_a = \partial f/\partial q_a$ and $n_b = \partial f/\partial q_b$.

By combining (11.11) with (11.8) we are arriving at the constitutive relationship of the pure energy-transfer transformer which is usually written in the explicit matrix form

$$\begin{bmatrix} v_a(t) \\ i_b(t) \end{bmatrix} = \begin{bmatrix} 0 & n \\ -n & 0 \end{bmatrix} \cdot \begin{bmatrix} i_a(t) \\ v_b(t) \end{bmatrix} \tag{11.12}$$

where

$$n = \frac{n_a}{n_b} \quad [-] \tag{11.13}$$

is the dimensionless *coupling ratio* of the energy-transfer transformer.

To arrive at the same pure energy converting model, Instead from (11.9) we could have started the derivation of the energy-transfer transformer constitutive relation from the describing relation

$$g\big(\lambda_a(t), \lambda_b(t)\big) = 0 \tag{11.14}$$

specifying a coupling between the time-integrated element-across variables $\lambda_a(t), \lambda_b(t)$ of the elements a and b. Following a similar procedure, in this case we would arrive at the constitutive realtion

$$\begin{bmatrix} i_a(t) \\ v_b(t) \end{bmatrix} = \begin{bmatrix} 0 & m \\ -m & 0 \end{bmatrix} \cdot \begin{bmatrix} v_a(t) \\ i_b(t) \end{bmatrix} \tag{11.15}$$

where

$$m = -\frac{n_b}{n_a} = -\frac{1}{n} \tag{11.16}$$

Obviously, m is a negative reciprocal of the coupling ratio n defined by (11.13).

Fig. 11.16 presents examples of pure energy-transfer transformer implementations in which the generic elements a and b are replaced by controlled sources. The source combinations shown in Fig. 11.16*a* and *b* correspond directly to (11.12) and (11.15). The source combinations given in Fig. 11.16*c* and *d* must be considered simultaneously with (11.11) and 11.8). Thanks to the implicit form of the equations, the latter transformer models are more flexible from the point of view of their interconnection with other multipoles in a system models.

Graphical symbols which we shall use for pure energy-transfer transformers are indicated in Fig. 11.17. In the case of the symbol with the slash sign shown in Fig. 11.17*a* the parameter k equals to the coupling ratio (11.13), i.e., $k = n_a/n_b$, whereas in the case of the symbol with the backslash sign shown in
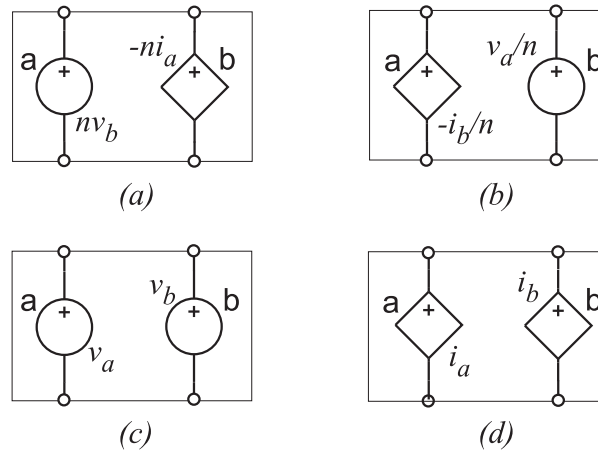
(a)   *(b)*

(c)   *(d)*

Figure 11.16: Implementation of energy-transfer transformers in terms of controlled sources.

(a)   *(b)*

Figure 11.17: Graphical symbol for energy-transfer transformers with (a) $k = n_a/n_b$ and (b) $k = n_b/n_a$.

Fig. 11.17b the parameter k is defined by the reciprocal expression, i.e., $k = n_b/n_a$. We are assuming, that the index a is always associated with the left-hand pair of poles of the symbol, whereas the index b always belongs to the right-hand pole-pair. For this reason, the symbol must be always situated horizontally in a multipole diagram.

An *ideal energy-transfer transformer* is the pure transformer the coupling ratio of which is a constant. We shall encounter numerous examples, however, in which the ratios are functions of some system variables or parameters.

11.6.3   Load conversions with transformers

(a)   *(b)*
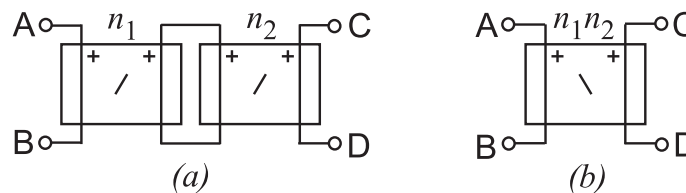
Figure 11.18: (a) Cascade interconnection of energy-transfer transformers, (b) one-transformer equivalent.

Fig. 11.18a shows a 'cascade' interconnection of energy-transfer transformers of coupling ratios n_1 and n_2. A simple analysis of the total transformation of across and through variables in the interconnection indicates that the cascade can be replaced by only one transformer with the coupling ratio $n_1 n_2$ shown in Fig. 11.18b.

Fig. 11.19 indicates the way in which series or parallel combinations of physical elements connected to a pole-pair of an energy-transfer transformer are 'seen through' the transformer, or referred to at the other transformer pole-pair. Z resp. Y is an impedance resp. admittance of the generic element, E resp. J is an independent source of an across resp. through variable. This is the principle behind utilizing various transducers and couplings to convert the amount of an actuator load at the price of changed related across and through variables.
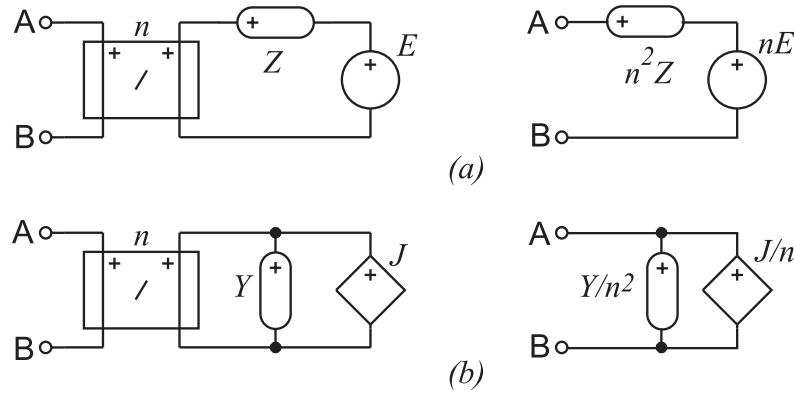
(a)

(b)

Figure 11.19: Load 'seen through' an energy-transfer transformer.

11.6.4   Energy-transfer gyrators

To model electro-magnetic, fluid-mechanical or acoustic-mechanical transducers, for instance, we need still another kind of a pure converter – the energy-transfer gyrator. The corresponding constitutive relation can be derived in a similar way that we used for the energy-transfer transformer. Let us assume this time, that the coupling between variables of the generic elements a and b in Fig. 11.15 can be characterized by the *describing relation*

$$f\big(\lambda_a(t), q_b(t)\big) = 0 \tag{11.17}$$

where $f(.)$ is a time-independent function and $\lambda_a(t)$ is a time-integrated element-across variable of the element a whereas $q_a(t)$ is a time-integrated element-through variable of the element b. The variables come possibly but not necessarily from different energy domains.

   If the function $f(.)$ is differentiable, we can apply the chain rule to differentiate (11.17) with respect to time to obtain

$$\frac{\partial f}{\partial \lambda_a} \cdot \frac{\lambda_a}{dt} + \frac{\partial f}{\partial q_b} \cdot \frac{q_b}{dt} = 0 \tag{11.18}$$

Taking into consideration that $d\lambda_a/dt = v_a(t)$ and $dq_b/dt = i_b(t)$, (11.18) can be rewritten as

$$n_a \cdot v_a(t) + n_b \cdot i_b(t) = 0 \tag{11.19}$$

where $n_a = \partial f/\partial \lambda_a$ and $n_b = \partial f/\partial q_b$.

   By combining (11.19) with (11.8) we are arriving at the constitutive relationship of the pure energy-transfer transformer

$$\left[\begin{array}{c} i_a(t) \\ i_b(t) \end{array} \right] = \left[\begin{array}{cc} 0 & S \\ -S & 0 \end{array} \right] \cdot \left[\begin{array}{c} v_a(t) \\ v_b(t) \end{array} \right] \tag{11.20}$$

where

$$S = \frac{n_a}{n_b} \tag{11.21}$$

is the *gyrating ratio* of the energy-transfer gyrator. Note that S is a transconductance and its physical dimension is energy-domain dependent.

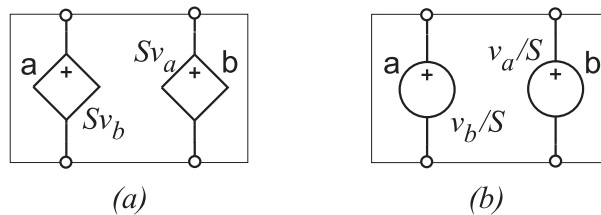*(a)*   *(b)*

Figure 11.20: Implementation of energy-transfer gyrators in terms of controlled sources.

   Fig. 11.20 presents examples of pure energy-transfer transformer implementations in which the generic elements a and b are replaced by controlled sources. The source combination shown in Fig. 11.20*a* corresponds directly to (11.20), Fig. 11.20*b* corresponds to the inversion of (11.20).
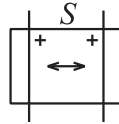
Figure 11.21: Graphical symbols for energy-transfer gyrators.

Graphical symbols which we shall use for pure energy-transfer transformers are indicated in Fig. 11.21.

An *ideal energy-transfer gyrator* is a pure gyrator the gyrating ratio of which is a constant. We shall encounter numerous examples, however, in which the ratios are functions of some system variables or parameters.
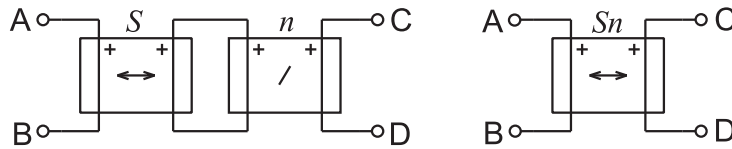
11.6.5   Load conversions with gyrators

Figure 11.22: (*a*) Cascade interconnection of an energy-transfer gyrator and transformer, (*b*) gyrator equivalent.

Fig. 11.22a shows a 'cascade' interconnection of an energy-transfer gyrator of gyrating ratio S and an energy-transfer transformer of coupling ratio n. A simple analysis of the total transfer of across and through variables through the interconnection indicates that the cascade can be replaced by only one gyrator with the gyrating ratio Sn shown in Fig. 11.22b.

Fig. 11.23 indicates the way in which series or parallel combinations of physical elements connected to a pole-pair of an energy-transfer gyrator are 'seen through' the gyrator, or referred to at the other gyrator pole-pair. Note that gyrators convert inductors or springs into capacitors or inertors and capacitors or inertors into inductors or springs. This principle can be utilized both in system analysis as well as in system construction.
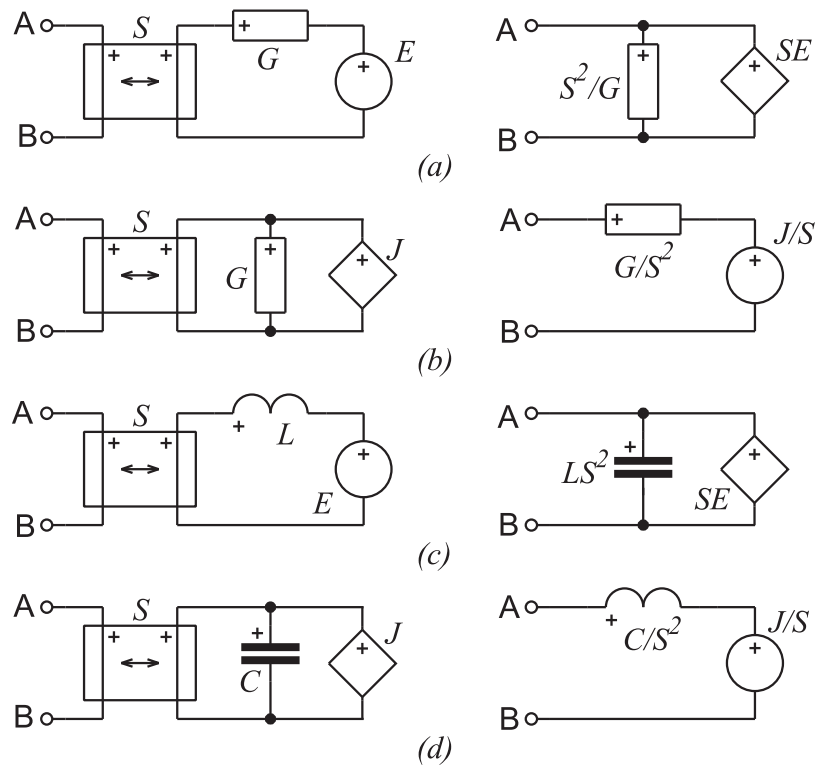
Figure 11.23: Loads 'seen through' an energy-transfer gyrator.

Module 12

Formulation of system equations

12.1 Full set of equations

Values or waveforms of variables in a system multipole model can be obtained by solving a set of equations characterizing the model. To formulate such equations, we must take into our consideration the following three types of relations.

(a) Constitutive relations characterizing each of the individual multipoles in the model.

(b) Postulate of continuity reflecting the physical laws governing the balance of energy and mass at the individual sites of interaction in the system. The laws are given for different physical domains in Table **??**. According to this postulate the sum of all the elemental through variables i_k at a node

$$\sum_k i_k = 0 \tag{12.1}$$

assuming that $i_k > 0$ if i_k leaves the node, and $i_k < 0$ if i_k enters the node.

(c) Postulate of compatibility resulting from the laws respecting the geometric connectedness of real systems given in Table **??**. According to this postulate the sum of all the elemental across variables v_k along a closed oriented loop in the diagram

$$\sum_k v_k = 0 \tag{12.2}$$

where $v_k > 0$ if the v_k direction is in agreement with the loop orientation, and $v_k < 0$ if the v_k direction is opposite to the orientation of the loop.

To demonstrate the principles of such equation formulation, let us start with the examples presented in Table 11.1 already.

(a) Constitutive relations of physical elements involved in the examples are given in Table 12.1 in three different forms where J, C, L and G are parameters of the elements, i_k is the through variable, v_k is the across variable of the k-th element in each of the diagrams. Let us choose the implicit form:

Table 12.1: Constitutive relations of the elements in Table **??**.

Part	Physical elements	Implicit relations	Relations for i	Relations for v
1	through-variable source	$i_1 - J = 0$	$i_1 = J$	—
2	capacitor or invertor	$i_2 - C\frac{dv_2}{dt} = 0$	$i_2 = C\frac{d}{dt}v_2$	$v_2 = \frac{1}{C}\int i_2 dt$
3	inductor or spring	$v_3 - L\frac{di_3}{dt} = 0$	$i_3 = \frac{1}{L}\int v_3 dt$	$v_3 = C\frac{d}{dt}i_3$
4	conductor or damper	$i_4 - Gv_4 = 0$	$i_4 = G\,v_4$	$v_4 = \frac{1}{G}i_4$

$$
\begin{aligned}
i_1 - J &= 0 \\
i_2 - C\tfrac{d}{dt}v_2 &= 0 \\
v_3 - L\tfrac{d}{dt}i_3 &= 0 \\
i_4 - G\cdot v_4 &= 0
\end{aligned}
\tag{12.3}
$$

(b) Fig. 12.1 shows the graph of the multipole diagrams in Table 11.1. The graph nodes are identical with the nodes of the diagrams. Each of the diagram elements is represented in the graph just by a line segment. In Fig. 12.1(a) the line segments are associated with arrows indicating orientation of the elemental through variables (fixed to the orientation of the individual elements). According to the postulate of continuity (12.1) for the elemental through variables at nodes M and N

$$\begin{aligned}
\text{node M:} \quad & i_1 + i_2 - i_3 & = & \quad 0 \\
\text{node N:} \quad & i_3 + i_4 & = & \quad 0
\end{aligned} \qquad (12.4)$$

(c) Fig. 12.1(b) shows two independent loops in the graph. The loop a is made up by elements 1 and 2, and the loop of elements 2, 3 and 4. Arrows indicate the chosen orientation of the loops with respect to the orientation of the elemental across variables. According to the postulate of compatibility (12.2), the elemental across variables along the loops a and b

$$\begin{aligned}
\text{loop a:} \quad & v_1 - v_2 & = & \quad 0 \\
\text{loop b:} \quad & v_2 + v_3 - v_4 & = & \quad 0
\end{aligned} \qquad (12.5)$$
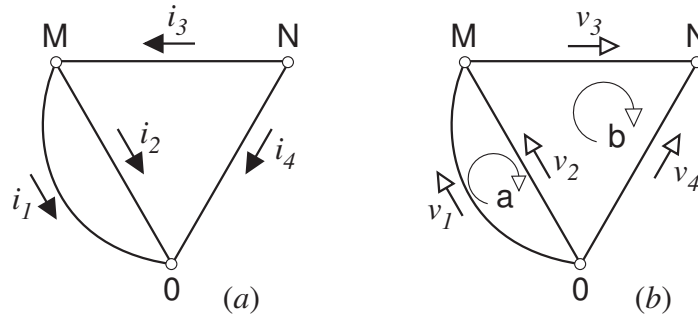
Figure 12.1: Graph of the multipole diagrams in Table 11.1 with arrows indicating orientation of elemental variables and chosen loops.

The four constitutive relations (12.3) together with the two continuity relations (12.4) and two compatibility relations (12.5) form eight equations for eight unknown variables. In this case, the number of equations can be reduced by one after substituting $i_1 = J$ to (12.4).

In general, for a model composed from m physical elements, the described procedure, called also the **tableau formulation**, results in $2m$ differential equations to be solved to obtain $2m$ unknown system variables.

12.2   Reduced equations

12.2.1   Nodal formulation

For practical reasons, engineers tend to decrease the number of equations to be solved simultaneously. Nodal formulation is one of the procedures resulting in such reduced equations.

A systematic method of carrying out the nodal formulation for a model of n non-reference nodes (i.e. nodes that were not chosen as reference nodes) is following:

Step 1. For each of the n non-reference nodes write the continuity equation (12.1).

Step 2. Express all the elemental through variables in the continuity equations in terms of the elemental across variables using the constitutive relations of the individual elements.

Step 3. Write the elemental across variables in terms of the **nodal across variables**, i.e. the across variables of the non-reference nodes relative to the reference node.

Step 4. Solve the resulting n equations for the n nodal across variables.

Step 5. Find the elemental across variables in the model as a difference of two of the nodal across variables.

Step 6. Express the through variables of the elements using their constitutive relations.

Examples

These steps can be illustrated again with the system models shown in Table 11.1.

Step 1. This step results in equations stated already in (12.4).

Step 2. Substituting the explicit constitutive relations for the elemental through variables from Table 12.1 into (12.4) gives

$$
\begin{aligned}
J + C\tfrac{d}{dt}v_2 - \tfrac{1}{L}\int v_3 dt - i_3(0) &= 0 \\
\tfrac{1}{L}\int v_3 dt + i_3(0) + Gv_4 &= 0
\end{aligned}
\tag{12.6}
$$

Step 3. The elemental across variables expressed in terms of the nodal across variables v_M and v_N are

$$
\begin{aligned}
v_1 = v_2 &= v_M \\
v_3 &= v_N - v_M \\
v_4 &= v_N
\end{aligned}
\tag{12.7}
$$

After substituting (12.7) into (12.6) we obtain

$$
\begin{aligned}
C\tfrac{d}{dt}v_M - \tfrac{1}{L}\int(v_N - v_M)dt &= i_3(0) - J \\
\tfrac{1}{L}\int(v_N - v_M)dt + Gv_N &= -i_3(0)
\end{aligned}
\tag{12.8}
$$

where the known variables were shifted to the right-hand sides of the equations.

Step 4. Using the nodal formulation, we have arrived at only two equations (12.8) to be solved simultaneously for the two unknown nodal across variables v_M and v_N.

Step 5. The elemental across variables are expressed in terms of the nodal across variables as in (12.7).

Step 6. The elemental through variables can be evaluated using the explicit constitutive relations given in Table 12.1.

Note, however, that the nodal formulation cannot be applied directly to models with physical elements like sources of across variable, for example, as the explicit constitutive relation for their through variables necessary in *Step* 2 of the formulation does not exist. Also, the integro-differential form of the equations (12.8) does not suit to common computer computational routines for simultaneous solving of the equations.

12.2.2 Loop formulation

An alternative formulation method for formulating equations well known from electrical-engineering textbooks is the loop formulation (or mesh formulation for planar models). The number of equations resulting from this formulation is ℓ for a model with ℓ independent loops. A systematic method of carrying out the loop formulation is the following.

Step 1. For each of the ℓ loops write the compatibility equation (12.2).

Step 2. Express all the elemental across variables in the compatibility equations in terms of the elemental through variables using the constitutive relations of the individual elements.

Step 3. Write the elemental through variables in terms of the **loop through variables**.

Step 4. Solve the resulting ℓ equations for the ℓ loop through variables.

Step 5. Find the elemental through variables in the model as a difference of two of the loop through variables.

Step 6. Express the across variables of the elements using their constitutive relations.

Example

To illustrate these steps let us apply them to the system models shown in Table 11.1 in which the source of through variable was replaced by the source of across variable characterized by the constitutive relation

$$v_1 = E \tag{12.9}$$

Step 1. The the compatibility equations for this example are already in (12.5).

Step 2. Substituting the explicit constitutive relations for the elemental through variables from Table 12.1 into (12.4) gives

$$
\begin{aligned}
E - \tfrac{1}{C} \int i_2 dt - v_2(0) &= 0 \\
\tfrac{1}{C} \int i_2 dt + v_2(0) + L \tfrac{d}{dt} i_3 + \tfrac{1}{G} i_4 &= 0
\end{aligned}
\tag{12.10}
$$

Step 3. The elemental through variables expressed in terms of the loop through variables i_a and i_b are

$$
\begin{aligned}
i_1 &= -i_a \\
i_2 &= i_a - i_b \\
i_3 &= -i_b \\
i_4 &= i_b
\end{aligned}
\tag{12.11}
$$

After substituting (12.11) into (12.10) we obtain

$$
\begin{aligned}
-\tfrac{1}{C} \int (i_a - i_b) dt &= -E + v_2(0) \\
\tfrac{1}{C} \int (i_a - i_b) dt - L \tfrac{d}{dt} i_b + \tfrac{1}{G} i_b &= -v_2(0)
\end{aligned}
\tag{12.12}
$$

where the known variables were shifted to the right-hand sides of the equations.

Step 4. Using the loop formulation, we have arrived at only two equations (12.12) to be solved simultaneously for the two unknown nodal across variables i_a and i_b. (By adding the second equation to the first one the number of equations to be solved is reduced only to one in this special case.)

Step 5. The elemental through variables are expressed in terms of the loop through variables as in (12.11).

Step 6. The elemental across variables can be evaluated using the explicit constitutive relations given in Table 12.1 and (12.9).

Note, however, that the loop formulation cannot be applied directly to models with sources of through variable as the constitutive relation explicitly expressing their through variables necessary in *Step* 2 of the formulation does not exist. Also, the integro-differential form of the equations (12.8) does not suit to common computer computational routines for simultaneous solving of the equations.

12.3   Extended nodal formulation

12.3.1   Principles of the method

To overcome its limitations, the nodal formulation can be extended in such a way that the formulated equations include not only the nodal across variables, but also the through variables of some of the physical elements in the model. A moderate increase in the number of the resulting equations to be solved simultaneously is outweighed by the applicability of the extended nodal method to models consisting of any physical elements.

Let us first demonstrate that the equations for the system models in Table 12.1 resulting from the extended nodal formulation can be expressed directly in the first-order algebro-differential form. This form suits much better to computer computational routines than the integro-differential form of the equations (12.8) derived using the plain nodal formulation.

The undesirable integration operation in (12.8) originated from substituting the constitutive relation of the L element for its through variable i_3 into (12.4) in *Step* 2 of the nodal formulation. We can avoid this by leaving i_3 in (12.4) without any change, and by adding the implicit constitutive relation of the L element from Table 12.1 as a third equation. Then,

$$
\begin{aligned}
J + C\tfrac{d}{dt}v_2 - i_3 &= 0 \\
i_3 + Gv_4 &= 0 \\
v_3 - L\tfrac{d}{dt}i_3 &= 0
\end{aligned}
\tag{12.13}
$$

When writing the elemental across variables in terms of the nodal across variables (12.7) we obtain the three first-order algebro-differential equations for three unknown variables v_M, v_N and i_3

$$
\begin{aligned}
C\tfrac{d}{dt}v_M - i_3 &= -J \\
i_3 + Gv_N &= 0 \\
v_N - v_M - L\tfrac{d}{dt}i_3 &= 0
\end{aligned}
\tag{12.14}
$$

These equations can be expressed in the matrix form

$$
\begin{bmatrix} Cs & 0 & -1 \\ 0 & G & 1 \\ -1 & 1 & -Ls \end{bmatrix} \cdot \begin{bmatrix} v_M \\ v_N \\ i_3 \end{bmatrix} = \begin{bmatrix} -J \\ 0 \\ 0 \end{bmatrix}
\tag{12.15}
$$

where the symbol $\frac{d}{dt}$ is replaced by the operator s assuming that the product $s\,x$ should be interpreted as $\frac{d}{dt}x$.

The left-hand-side square and right-hand-side column matrices of (12.15) can be arranged in the tabular form convenient for manual formulation of equations

	v_M	v_N	i_3		
M	Cs		-1		$-J$
N		G	1		
L	-1	1	$-Ls$		

$$\tag{12.16}$$

The empty entries in the tables stand for zeros.

In a similar manner, the nodal formulation can be extended towards sources of across variables or any other physical elements. In the next paragraphs, you will learn how to form the extended nodal equations very easily following a straightforward pattern.

12.3.2   Stamp submatrices of uncontrolled elements

The 'stamp submatrices' in Table 12.2 allow formulating the extended nodal equations as simply as imprinting stamps. The submatrix entries should be added to the entries of the equation matrices in a tabular form similar to that in the example (12.16). The element symbols in the table are mostly in their generic multi-physical-domain form.

The Table 12.2 gives submatrices for formulation of the equations with elemental through variables for all the physical elements listed in the table. It gives also submatrices for nodal equation formulation without the elemental through variable for those elements for which such submatrices exist.

The initial conditions at the time instant $t = 0+$ shown in the right-hand-side submatrices of some of the elements apply to the case when the resulting equations are considered as Laplace transforms of algebro-differential equations. If this is the case, s represents the Laplace-transform operator.

The pattern of the extended nodal formulation exploiting the stamp submatrices is easily identified.

Step 1. Inspect the system model and count the non-reference nodes as well as the elements the through variables of which should be introduced as additional variables in the formulated equations. These will be

- sources of across variables

- inductors and springs

- sources of through variables, conductors, dampers, capacitors, and inertors if their through variable is used to control an element in the model, or if it is requested as the output variable.

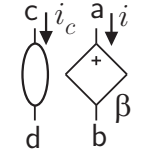Table 12.2: Stamp submatrices of uncontrolled physical elements
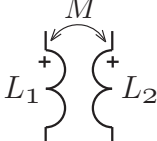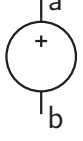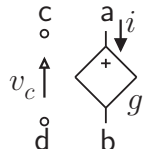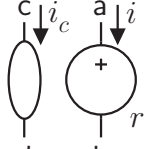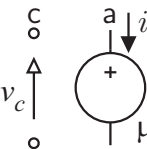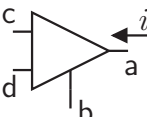
Physical element		Without through variable	With through variable
Conductor or damper		v_a $\quad$ v_b a $\boxed{G \mid -G}$ b $\boxed{-G \mid G}$	v_a v_b i a: i column = 1 b: i column = -1 bottom row: $G \mid -G \mid -1$
Resistor		v_a $\quad$ v_b a $\boxed{1/R \mid -1/R}$ b $\boxed{-1/R \mid 1/R}$	v_a v_b i a: i column = 1 b: i column = -1 bottom row: $1 \mid -1 \mid -R$
Capacitor or inertor		v_a $\quad$ v_b a $\boxed{Cs \mid -Cs}$ $\boxed{Cv(0)}$ b $\boxed{-Cs \mid Cs}$ $\boxed{-Cv(0)}$	v_a v_b i a: i column = 1 b: i column = -1 bottom row: $Cs \mid -Cs \mid -1$ $\boxed{Cv(0)}$
Inductor or spring			v_a v_b i a: i column = 1 b: i column = -1 bottom row: $1 \mid -1 \mid -Ls$ $\boxed{-Li(0)}$
Mutual inductance			i_1 $\quad$ i_2 L_1: i_2 column = $-Ms$, $\boxed{\begin{array}{c}-L_1 i_1(0) \\ -M i_2(0)\end{array}}$ L_2: i_1 column = $-Ms$, $\boxed{\begin{array}{c}-L_2 i_2(0) \\ -M i_2(0)\end{array}}$
Source of through variable		v_a $\quad$ v_b a: $\boxed{-J}$ b: $\boxed{J}$	i a $\boxed{1}$ b $\boxed{-1}$ bottom row: 1 $\boxed{J}$
Source of across variable			v_a v_b i a: i column = 1 b: i column = -1 bottom row: $1 \mid -1 \mid$ $\boxed{E}$

Table 12.3: Stamp submatrices of controlled elements

Physical element		Without through variable	With through variable
Source of through variable controlled by across variable	(symbol: c, a, v_c, i, g, d, b)	v_c, v_d: a: g, $-g$ b: $-g$, g	v_c, v_d, i: a: _, _, 1 b: _, _, -1 _: g, $-g$, -1
Source of through variable controlled by through variable	(symbol: c i_c, a i, β, d, b)	i_c: a: β b: $-\beta$	i_c, i: a: _, 1 b: _, -1 _: β, -1
Source of across variable controlled by through variable	(symbol: c i_c, a i, r, d, b)		v_a, v_b, i_c, i: a: _, _, _, 1 b: _, _, _, -1 _: 1, -1, $-r$, _
Source of across variable controlled by across variable	(symbol: c, a i, v_c, μ, d, b)		v_a, v_b, v_c, v_d, i: a: _, _, _, _, 1 b: _, _, _, _, -1 _: 1, -1, $-\mu$, μ, _
Ideal operational amplifier	(symbol: c, i, d, a, b)		v_a, v_b, i: a: _, _, 1 b: _, _, -1 _: 1, -1, _

Step 2. If the number of he counted elements is m and the number of the non-reference nodes is n, draw tables for the $(m+n)$-dimensional square and column matrices. Denote the first n columns of the square table by the identifiers of the nodal across variables, and the remaining m columns by identifiers of the computed through variables. At the same time, denote the first n rows of both tables by the identifiers of the system model nodes and the remaining m rows by identifiers of the elements related to the computed through variables.

Step 3. For each of the elements in the system model associate its poles a and b shown in Table 12.2 with the nodes of the system model. Add then the entries of the element submatrices to the related entries of the resulting matrices. Ignore the entries related to the reference node.

For example, to form matrices (12.16) for the system models in Table 11.1, the poles of the involved elements should be associated with the model nodes in the following way:

$$
\begin{aligned}
\text{element J:} &\quad \mathsf{a} \leftrightarrow \mathsf{M}, \quad \mathsf{b} \leftrightarrow 0 \\
\text{element C:} &\quad \mathsf{a} \leftrightarrow \mathsf{M}, \quad \mathsf{b} \leftrightarrow 0 \\
\text{element L:} &\quad \mathsf{a} \leftrightarrow \mathsf{N}, \quad \mathsf{b} \leftrightarrow \mathsf{M} \\
\text{element G:} &\quad \mathsf{a} \leftrightarrow \mathsf{N}, \quad \mathsf{b} \rightarrow 0
\end{aligned}
\tag{12.17}
$$

Try now to form matrices (12.16) using the stamp submatrices of the elements.

12.3.3 Stamp matrices of controlled physical elements

The stamp-matrix approach can be easily applied also the models with controlled elements. If an element is controlled by a through variable, this controlling through variable should be introduced as the additional variable in the formulated equations.
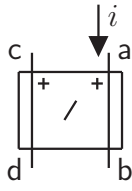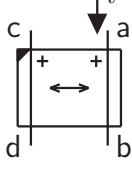
Table 12.4: Stamp submatrices of ideal transducers

Transducer		Without through variable	With through variable
Ideal transformer	(diagram)		$\begin{array}{c c c c c c} & v_a & v_b & v_c & v_d & i \\ a & & & & & 1 \\ b & & & & & -1 \\ c & & & & & -n \\ d & & & & & n \\ & 1 & -1 & -n & n & \end{array}$
Ideal gyrator	(diagram)	$\begin{array}{c c c c c} & v_a & v_b & v_c & v_d \\ a & & & g & -g \\ b & & & -g & g \\ c & g & -g & & \\ d & -g & g & & \end{array}$	$\begin{array}{c c c c c c} & v_a & v_b & v_c & v_d & i \\ a & & & & & 1 \\ b & & & & & -1 \\ c & g & -g & & & \\ d & -g & g & & & \\ & & & g & -g & -1 \end{array}$

　　Table 12.3 gives stamp matrices of controlled sources. The controlling through variables are denoted as i_C, while i_C stands for the controlling across variables between system model nodes c and d.

12.3.4　Stamp matrices of transducers

Table 12.4 demonstrates that the extended nodal method can be easily applied also to systems containing such four-pole elements like an ideal transformer, an ideal gyrator, or an ideal operational amplifier.

12.3.5　Stamp matrices of blocks

The above given procedure for equation formulation can be applied also to system models represented by block diagrams as well as by multipoles combined with blocks. Table 12.5 gives the stamp matrices for basic blocks.

12.4　Block diagrams

12.4.1　Construction of block diagrams

Though block diagrams might look similar to multipole diagrams at the first sight, their principle is very different. We shall demonstrate the procedure required for the block-diagram construction using again the system examples given in Table 11.1.

Step 1: Formulation of a set of equations.
Any of the school-book pencil-and-paper procedures yielding consistent equations characterizing the system model can be used for this purpose.
　　Let us utilize for our demonstration the implicit equations (12.3), (12.4) and (12.5) formulated in the previous section.

Step 2: Decreasing the order of the differential equations.
Any n-th order differential equation can be converted to n first-order equations by substitution for the higher-order derivatives.
　　There are no higher-order equations among those considered in our demonstration, however.

Step 3: Conversion of equations into explicit form.
Such a conversion should result in a set of equations each of which expresses explicitly one of the unknown variables.
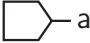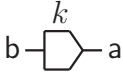
Table 12.5: Stamp submatrices of basic blocks
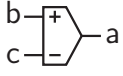
Block	Stamp submatrix
signal source	v_a : a | 1 | □
scalor (k)	v_a v_b : a | 1 | $-k$ | □
comparator	v_a v_b v_c : a | 1 | -1 | 1 | □
integrator	v_a v_b : a | s | -1 | $v_a(0)$
differentiator	v_a v_b : a | 1 | $-s$ | $-v_b(0)$

transfer block: $\dfrac{v_a}{v_b} = \dfrac{b_3 s^3 + b_2 s^2 + b_1 s + b_0}{s^3 + a_2 s^2 + a_1 s + a_0}$

	v_A	v_B	x_1	x_2	x_3	
a	1		$-b_0$	$-b_1$	$-b_2 - sb_3$	$-b_3 x_3(0)$
		1	$-a_0$	$-a_1$	$-a_2 - s$	$-x_3(0)$
			s	-1		$x_1(0)$
				s	$-a$	$x_2(0)$

Table 12.1 shows the constitutive relations of the physical elements from our example in two different explicit forms (except the through-variable source for which only one explicit form exists). So, we are supposed to choose one of the explicit expressions for each of the elements and, at the same time, to rearrange the relations (12.4) and (12.5) into the explicit form in such a way that there is just one relation for each variable. Therefore, we are faced with the so called *causality problem*.

For computational reasons numerical integration is preferred to numerical differentiation in block-diagram oriented packages. Let us just form the first three explicit relations as

$$
\begin{aligned}
i_1 &= J \\
v_2 &= 1/C \int i_2 \, dt + v_2(t_0) \\
i_3 &= 1/L \int v_3 \, dt + i_3(t_0)
\end{aligned}
\tag{12.18}
$$

Once we made this choice, it can be proven that the rest of the explicit relation must be formed in the following way:

$$
\begin{aligned}
v_4 &= 1/G \cdot i_4 \\
i_2 &= -i_1 + i_3 \\
i_4 &= i_3 \\
v_1 &= v_2 \\
v_3 &= -v_2 + v_4
\end{aligned}
\tag{12.19}
$$

For example, if we had chosen the relation $i_4 = G\,v_4$ for the fourth element, we would not be able to solve the problem. For some system configurations, even some of the integral relations must be replaced by differential ones to solve the causality problem.

Step 5: Setting up the block diagram.
The resulting block diagram is shown in Fig. 12.2 using the DYNAST graphical notation. Each of the blocks in the diagram represents just one of the explicit relations from (12.18) and (12.19) (no blocks are needed for the trivial relations for i_4 and v_1).
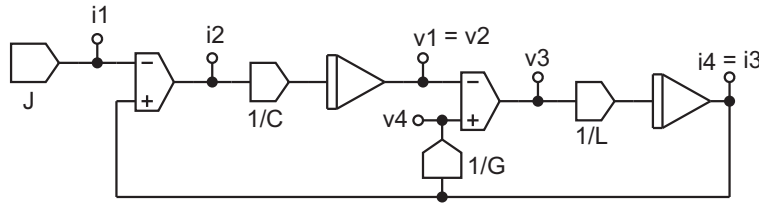
Figure 12.2: Block diagram representing the systems in Table 11.1.

12.4.2   Block diagrams vs. multipoles

Let us summarize the experience learnt from this simple example:

- If we want to represent energy interactions of a real subsystem by a block, for most of the subsystems we must have at our disposal two different blocks at least, each of them representing the same constitutive relation, but expressing explicitly different variables. In the case of the multipole approach, only one model is sufficient for each subsystem, and this model is reusable in any consistent system configuration.

- In the block-diagram model of a complete system, in addition to the blocks representing the individual subsystems, there must be also blocks respecting the postulates of continuity and compatibility. The latter blocks are not reusable as they suit just to one specific system configuration. For the multipole models the postulate-respecting relations can be formed automatically and no additional blocks are needed.

- To choose which block should model a particular subsystem, and to form blocks respecting the postulates, we have to solve the causality problem. In the multipole approach such a problem is not encountered at all.

The manual procedure for setting up a block diagram for the physical-level model of a real-life system, usually nonlinear, is much more involved than could be shown in this example, of course. However, there is also a big difference between DYNAST and the common block-diagram oriented packages in the way of solving equations.

Once a block diagram is submitted to DYNAST, a set of implicit algebro-differential equations is formed, and these are solved simultaneously as it is the case of the equations for multipole models. The common block-diagram oriented programs usually do not solve any equations in reality. They would not treat the relations (12.18) and (12.19) as equations, but as assignments.

The variables are processed successively by one block only at a time at discrete time steps. The process starts from blocks with no input like the block specifying $i_1(t_1) \Leftarrow J(t_1)$ in Fig. 12.2. But this is not so simple in the case of feedback loops in the block diagram. For example, the summing block for the output variable $i_2(t_1) \Leftarrow -i_1(t_1) + i_3(t_0)$ cannot specify the correct value of this variable at the end of the first time step, but only after a number of time steps and iterations. This problem is even more difficult if there is no integrator delaying the variable propagation in the feedback loop by one step. Solving such *algebraic loop problems* requires special techniques.

In many cases, the blocks in a block diagram must be rearranged before the simulation starts as their order is critical to the validity of the computed results. There are, however, system models characterized by systems of differential equations the order of which is time-variable. Solving such an *change-of-order* problem requires reconfiguration of the block diagram not only prior, but also during the simulation.

As all the equations are solved simultaneously in DYNAST, there are no algebraic-loop problem. As, in addition, the equations are solved in DYNAST directly in their natural implicit algebro-differential form, there is no change-of-order problem. Not only this, the related computational procedures for such equations are in principle more efficient and robust then those implemented in the common block-diagram packages. Obviously, developing software for automated construction of physical-level system models as a pre-processor for a common block-diagram oriented package is not the optimal way of coping with the problem.

12.5 Lagrange's equations of multipoles

Multipole models of subsystems can be characterized by constitutive relations formed using different approaches. Lagrange's equations of second kind combined with undetermined multipliers can be exploited to form the constitutive relations using the following procedure.

Step 1. Identify the subsystem energy entries and mass centers of the bodies within the subsystem.

Step 2. Determine the degree of freedom i of the subsystem bodies.

Step 3. Choose $n \geq i$ coordinates s_j, $j = 1, 2, \ldots, n$, to characterize motions of the entries and of the body mass centers.

Step 4. Form $r = n - i$ relations between the coordinates implied by the geometric constraints

$$f_k(s_j, t) = 0, \qquad k = 1, 2, \ldots r \tag{12.20}$$

Step 5. Differentiate (12.20) to obtain $n - i$ relations for the subsystem geometric compatibility

$$\frac{d}{dt} f_k(s_j, t) = 0, \qquad k = 1, 2, \ldots r \tag{12.21}$$

Step 6. Consider the 'free' diagram, i.e., consider the disconnected from a system. Show all the external forces the system exerts on the to hold it in equilibrium.

Step 7. Formulate n Lagrange's equations in the form

$$\frac{d}{dt} \frac{\partial \mathcal{K}}{\partial \dot{s}_j} = \frac{\partial \mathcal{K}}{\partial s_j} + Q_j - \frac{\partial \mathcal{P}}{\partial s_j} - \frac{\partial \mathcal{D}}{\partial \dot{s}_j} - \sum_{k=1}^{r} \lambda_k \frac{\partial f_k}{\partial s_j} \qquad j = 1, 2, \ldots, n \tag{12.22}$$

where $\mathcal{K}$, $\mathcal{P}$, and $\mathcal{D}$ is the kinetic, potential, and dissipative energy of the. Q_j is a generalized external force associated with the generalized coordinate s_j, whereas λ_k is the Lagrange's multiplier representing the generalized reaction force associated with the coordinate s_k.

Step 8. By excluding the r multipliers λ_k from (12.22) obtain $n - r$ equations for quasi-static balance of inertial, potential and dissipative forces.

Example: Body with two revolute joints
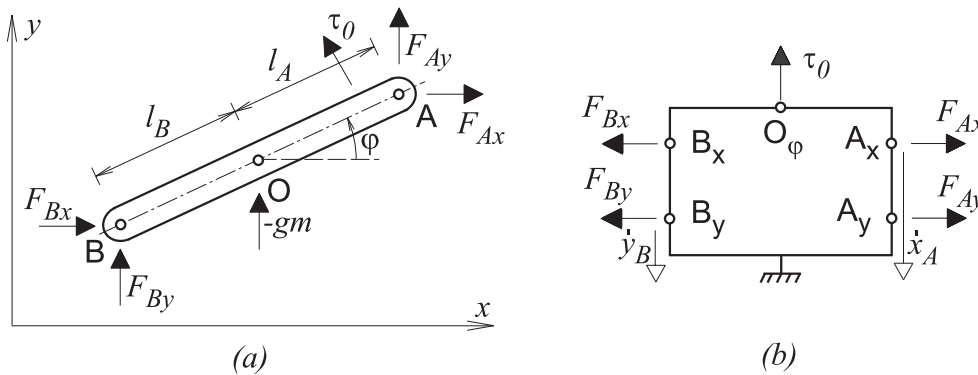
Figure 12.3: (*a*) Body with two revolute joints, (*b*) its multipole model.

The subsystem shown in Fig. 12.3*a* is a body constrained to a planar motion with two revolute joints denoted by A and B. O denotes the mass center of the body. Each of the joints is represented by two poles in the multipole model of the body given in Fig. 12.3*b*. Poles A_x and B_x represent translational motions of the joints along the x-axis whereas the poles A_y and B_y along the y-axis. Pole O_φ corresponds to the rotational motion of the body about the mass center O.

The body shown in Fig. 12.3a is of $i = 3$ degrees of freedom. Let us consider $n = 7$ coordinates: $x_A, y_A, x_B, y_B, x_O, y_O$, and φ. Then the $r = n - i = 4$ geometric constraints can be expressed as:

$$\begin{aligned}
f_1 &= x_O - x_B - l_B \cos \varphi &= 0 \qquad & f_2 = y_O - y_B - l_B \sin \varphi &= 0 \\
f_3 &= x_A - x_O - l_A \cos \varphi &= 0 \qquad & f_4 = y_A - y_O - l_A \sin \varphi &= 0
\end{aligned}$$

By differentiating the constrains we obtain the first part of the constitutive relations:

$$\begin{aligned}
\dot{x}_O - \dot{x}_B + l_B \dot{\varphi} \sin \varphi &= 0 \qquad & \dot{y}_O - \dot{y}_B - l_B \dot{\varphi} \cos \varphi &= 0 \\
\dot{x}_A - \dot{x}_O + l_A \dot{\varphi} \sin \varphi &= 0 \qquad & \dot{y}_A - \dot{y}_O - l_A \dot{\varphi} \cos \varphi &= 0
\end{aligned} \qquad (12.23)$$

The body kinetic and potential energies are

$$K = \frac{1}{2} m \dot{x}_O^2 + \frac{1}{2} m \dot{y}_O^2 + \frac{1}{2} J_O \dot{\varphi}^2 \qquad\qquad P = mg y_O$$

where J_O is the moment of inertia of the body with respect to its center of mass.
  Substitution into (12.22) yields for the individual coordinates:

$$\begin{aligned}
x_A : &\qquad 0 &=&\quad F_{Ax} - \lambda_3 \qquad & y_A : &\qquad 0 &=&\quad F_{Ay} - \lambda_4 \\
x_B : &\qquad 0 &=&\quad F_{Bx} + \lambda_1 \qquad & y_B : &\qquad 0 &=&\quad F_{By} + \lambda_2 \\
x_O : &\qquad \tfrac{d}{dt} m \dot{x}_O &=&\quad -\lambda_1 + \lambda_3 \qquad & y_O : &\qquad \tfrac{d}{dt} m \dot{y}_O &=&\quad -mg - \lambda_2 + \lambda_4 \\
\varphi : &\qquad \tfrac{d}{dt} J_O \dot{\varphi} &=&\quad \multicolumn{5}{l}{\tau_O - \lambda_1 l_B \sin \varphi - \lambda_3 l_A \sin \varphi + \lambda_2 l_B \cos \varphi + \lambda_4 l_A \cos \varphi}
\end{aligned}$$

Finally, after excluding the multipliers, we are arriving at the equations for the force dynamic equilibrium forming the second part of the constitutive relations for the multipole model of the body with two revolute joints

$$\begin{aligned}
m \ddot{x}_O &= F_{Ax} + F_{Bx} \\
m \ddot{y}_O &= F_{Ay} + F_{By} - mg \\
J_O \ddot{\varphi} &= \tau_O + F_{Bx} l_B \sin \varphi - F_{By} l_B \cos \varphi - F_{Ax} l_A \sin \varphi + F_{Ay} l_A \cos \varphi
\end{aligned} \qquad (12.24)$$

Example: Flexible crank-and-slide mechanism
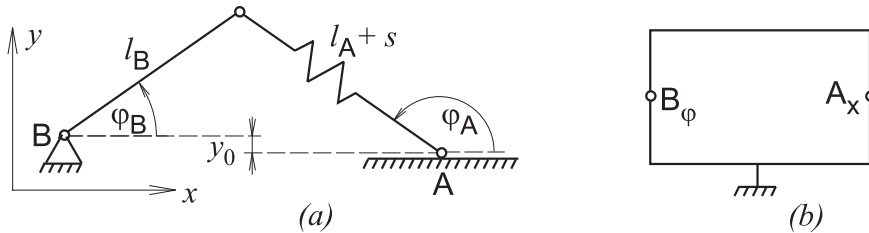
Figure 12.4: (a) Slider-crank mechanism with a flexible connecting rod, (b) its multipole model.

Fig. 12.4a shows a slider-crank mechanism which is considered as massless, but its connecting rod is assumed to be flexible with dissipative losses. In the corresponding multipole model given in Fig. 12.4b, the rotational motion of the crank is represented by the pole B_φ whereas the translational motion of the slider represents the pole A_x.
  The mechanism shown in Fig. 12.4a is of $i = 2$ degrees of freedom. Let us consider $n = 4$ coordinates: $x_A, \varphi_A, \varphi_B$ and s. Then the $r = n - i = 2$ geometric constraints can be expressed as:

$$\begin{aligned}
f_1 &= x_A - l_B \cos \varphi_B + (l_A + s) \cos \varphi_A &= 0 \\
f_2 &= y_0 + l_B \sin \varphi_B - (l_A + s) \sin \varphi_A &= 0
\end{aligned}$$

By differentiating the constrains with respect to time we obtain:

$$\begin{aligned}
\dot{x}_A + l_B \dot{\varphi}_B \sin \varphi_B + \dot{s} \cos \varphi_A - (l_A + s) \dot{\varphi}_A \sin \varphi_A &= 0 \\
l_B \dot{\varphi}_B \cos \varphi_B - \dot{s} \sin \varphi_A - (l_A + s) \dot{\varphi}_A \cos \varphi_A &= 0
\end{aligned} \qquad (12.25)$$

The potential and dissipative energies are in this case

$$P = \frac{1}{2} k s^2 \qquad D = \frac{1}{2} b \dot{s}^2$$

where k and b is the stiffness and damping factor of the connecting rod, respectively.

Substitution into (12.22) yields for the individual coordinates:

$$
\begin{array}{rcl}
x_A: & 0 & = & F_{Ax} + \lambda_1 \\
\varphi_B: & 0 & = & \tau_B + \lambda_1 l_B \sin \varphi_B + \lambda_2 l_B \cos \varphi_B \\
\varphi_A: & 0 & = & -ks - b\dot{s} + \lambda_1 \cos \varphi_A - \lambda_2 \sin \varphi_A \\
s: & 0 & = & -\lambda_1 (l_A + s) \sin \varphi_A - \lambda_2 (l_A + s) \cos \varphi_A
\end{array}
$$

Finally, after excluding the multipliers, we can complete the constitutive relations by the equations

$$
\begin{array}{rcl}
\tau_B - F_{Ax} l_B (\sin \varphi_B + \tan \varphi_A \cos \varphi_B) & = & 0 \\
-ks - b\dot{s} - F_{Ax} (\cos \varphi_A - \tan \varphi_A \sin \varphi_A) & = & 0
\end{array}
$$

Module 13

Formulation of transfer functions

13.1 Formulation of system-response transforms

Let us consider a linear time-invariant dynamic system described in the Laplace transform domain by a set of n algebraic equations. Such equations, resulting e.g. from the extended nodal formulation, are of the general form

$$\mathbf{A}(s) \cdot \mathbf{X}(s) = \mathbf{B}(s) \cdot \mathbf{U}(s) + \mathbf{C}(0+) \tag{13.1}$$

where $\mathbf{A}(s)$ is a given n-dimensional square matrix, $\mathbf{X}(s)$ is the n-dimensional column vector of the system variables to be determined, $\mathbf{B}(s)$ is the given $n \times p$ matrix, $\mathbf{U}(s)$ is the p-dimensional column vector which represents the system excitation by independent sources, and $\mathbf{C}(0+)$ is the given n-dimensional column vector representing the system initial conditions related to the energy accumulated in the system.

Obviously, the Laplace transform $\mathbf{X}(s)$ of the unknown vector $\mathbf{x}(t)$ can be written immediately in terms of the inverse matrix $\mathbf{A}^{-1}(s)$ as

$$\mathbf{X}(s) = \mathbf{A}^{-1}(s) \left[\mathbf{B}(s) \cdot \mathbf{U}(s) + \mathbf{C}(0+) \right] \tag{13.2}$$

After the inverse Laplace transformation is applied to (13.2), the vector of system responses $\mathbf{x}(t)$ can be expressed as the sum of two response components

$$\mathbf{x}(t) = \mathbf{x}_{in}(t) + \mathbf{x}_0(t)$$

where

$$\mathbf{x}_{in}(t) = \mathcal{L}^{-1}\{\mathbf{A}^{-1}(s) \cdot \mathbf{B}(s) \cdot \mathbf{U}(s)\}$$

is the response of the system with zero initial conditions to an independent excitation, and

$$\mathbf{x}_0(t) = \mathcal{L}^{-1}\{\mathbf{A}^{-1}(s) \cdot \mathbf{C}(0+)\}$$

is the response of the system with zero excitation from independent sources to system initial conditions.

Thus, the complete solution of (13.1) involves no more than the determination of the inverse of a given matrix and the inverse Laplace transformation. Nevertheless, to calculate the inverse of a matrix, say, anything more than a 3×3 matrix, is not a simple job without the help of a computer.

However, if we are required to find only one or two of the unknowns in (13.1), we need not compute the inverse of the matrix $\mathbf{A}$. Using the *Cramer's rule*, the i-th component of $\mathbf{X}(s)$ in (13.1) can be expressed as

$$X_i(s) = \frac{\Delta_i(s)}{\Delta(s)} \tag{13.3}$$

assuming that the determinant $\Delta(s)$ of the matrix $\mathbf{A}(s)$ is nonzero. $\Delta_i(s)$ is obtained form $\Delta(s)$ by replacing the i-th column of $\Delta(s)$ by the right-hand-side of (13.1).

13.2 Determinant evaluation

Determinant Δ of a 1×1 matrix $\mathbf{A} = [a]$ is defined as $\Delta = a$. Determinant of a 2×2 matrix

$$\mathbf{A} = \left[\begin{array}{cc} a_{11} & a_{12} \\ a_{21} & a_{22} \end{array} \right]$$

is

$$\Delta = \begin{vmatrix} a_{11} & a_{12} \\ a_{21} & a_{22} \end{vmatrix} = a_{11} \ a_{12} - a_{21} \ a_{22}$$

Determinants of larger matrices can be computed by means of the *Laplace expansion.* In general, expansion of the determinant Δ of an n-dimensional square matrix $\mathbf{A}$ along its k-th row, resp. along its l-th column, yields

$$\Delta = \sum_{l=1}^{n} a_{kl}(-1)^{k+l}\Delta_{kl}, \qquad \text{resp.} \qquad \Delta = \sum_{k=1}^{n} a_{kl}(-1)^{k+l}\Delta_{kl} \tag{13.4}$$

where a_{kl} is the element in the k-th row and l-th column of the determinant, and Δ_{kl} is the $(n-1)$-st order determinant obtained from the determinant Δ by deleting the k-th row and l-th column of Δ.

For example, the determinant Δ of the order $n = 3$ associated with the 3×3 matrix

$$\mathbf{A} = \begin{bmatrix} a_{11} & a_{12} & a_{13} \\ a_{21} & a_{22} & a_{23} \\ a_{31} & a_{32} & a_{33} \end{bmatrix}$$

expanded along its first row

$$\Delta = a_{11} \begin{vmatrix} a_{22} & a_{23} \\ a_{32} & a_{33} \end{vmatrix} - a_{12} \begin{vmatrix} a_{21} & a_{23} \\ a_{31} & a_{33} \end{vmatrix} + a_{13} \begin{vmatrix} a_{21} & a_{22} \\ a_{31} & a_{32} \end{vmatrix}$$

You may wish to show that expanding along another row or column gives the same result. This method is valid for any n. Determinant evaluation using the Laplace expansion, however, is not suitable for the analysis of large systems as it requires $(n-1)n!$ multiplications. While for $n = 3$ the number of multiplications is 12, for $n = 4$ it becomes 72 already.

Fortunately, the system matrices are usually rather sparse so that the formulas (13.4) give us the chance to take advantage of this matrix property. In general: the larger is the analyzed system, the higher is the percentage of zero-value elements in its matrix $\mathbf{A}$. By starting the determinant expansion from the row or column with the least number of nonzero elements we can reduce the amount of computations considerably.

13.3   Formulation of system transfer functions

In many design situations, rather than system responses, we need to compute a system transfer function (or a matrix of such functions). Let us thus assume, that a **system transfer function** $H_{ij}(s)$ of a system described by (13.1) is defined as

$$H_{ij}(s) = \frac{X_i(s)}{U_j(s)} \tag{13.5}$$

where the dependent variable $X_i(s)$, which is the i-th element of the vector $\mathbf{X}(s)$, is taken as the **system output**, and the independent excitation variable $U_j(s)$, being the j-th component of the vector $\mathbf{U}(s)$, is considered as the **system input**. (According to the transfer function definition $\mathbf{C}(0+) = \mathbf{0}$.)

Utilizing the Cramer's rule (13.3), we can express the transfer function (13.5) as

$$H_{ij} = \frac{\Delta_{i \leftarrow j}(s)}{\Delta(s)} \tag{13.6}$$

where $\Delta_{i \leftarrow j}(s)$ is the determinant of the matrix $\mathbf{A}(s)$ the i-th column of which has been replaced by the j-th column of the v $\mathbf{B}(s)$.

13.4   Solved examples

Mechanical translation system.   Consider the spring-mass-dashpot system shown in Fig. 13.1. Let us obtain the transfer function of the system

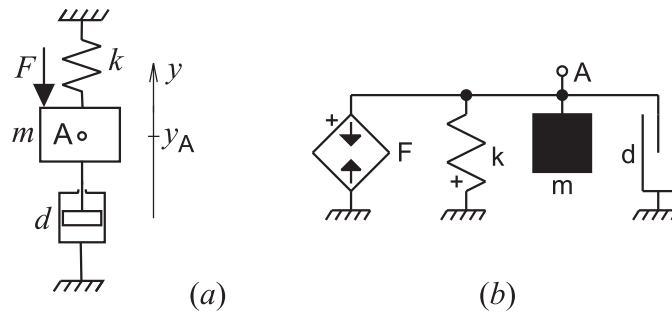$$H(s) = \frac{y(s)}{F(s)} \tag{13.7}$$

Figure 13.1: Mechanical translational system.

by assuming that the force $F(t)$ is the input and the displacement $y(t)$ of the mass is the output.

The multipole model of the system is given in Fig. 13.1a. The node A represents the vertical motion of the mass. The polarity of the input-force source has to comply with the chosen orientation of the velocity $\dot{y}(t)$. In this simple case only one equation is needed to describe the dynamics of the given system. This is the equation in Fig. 13.1b are

	$\dot{y}$	F
A	$b + sm + k/s$	1

The transfer-function $H(s)$ can then be readily expressed as

$$H(s) = \frac{1/s}{b + sm + k/s} = \frac{1}{s^2 m + sb + k} \tag{13.8}$$

Mechanical rotational system. Consider the system shown in Fig. 13.2a. The system consists of a load inertia and a viscous-friction damper driven by a rotational motor by means of a flexible shaft. The motor is modelled as it is seen from the load.

System parameters:

τ_m = motor torque applied to the system

b_m = motor damping (corresponding to the slope of its loading characteristics)

k = shaft torsional stiffness
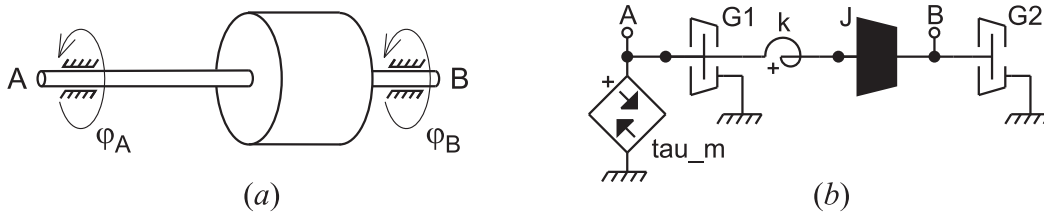
Figure 13.2: Mechanical rotational system.

J_l = moment of inertia of the load

b_l = load viscous-friction

ω_l = load angular velocity

Let us obtain the transfer function of the system

$$H(s) = \frac{\omega_l(s)}{\tau_m(s)} \tag{13.9}$$

The multipole diagram model of system is given in Fig. 13.2b. The nodes A and B represent the rotational motions of the motor and the load, respectively. The equations describing the dynamics of the system are

	ω_m	ω_l	τ_m
A	$b_m + k/s$	$-k/s$	1
B	$-k/s$	$b_l + sJ + k/s$	

The transfer-function $H(s)$ can then be expressed as

$$H(s) = \frac{\Delta_{21}}{\Delta} \tag{13.10}$$

where

$$\Delta = \begin{vmatrix} b_m + k/s & -k/s \\ -k/s & b_l + sJ + k/s \end{vmatrix} \qquad \Delta_{21} = -|-k/s| \tag{13.11}$$

Thus

$$H(s) = \frac{k}{s^2 J b_m + s(kJ + b_m b_l) + k(b_m + b_l)} \tag{13.12}$$

L-R-C circuit. Consider the electrical circuit shown in Fig. 13.3a. The circuit consists of an inductor L, a resistor R, and capacitor C.

Figure 13.3: L-R-C circuit

If e_i is assumed to be the input and v_0 the output, then the transfer function of the system is assumed to be

$$H(s) = \frac{v_0(s)}{e_i(s)} \tag{13.13}$$

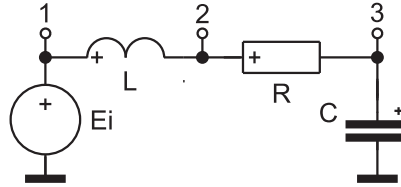The multipole diagram of the system is given in Fig. 13.3b. It differs from the actual circuit diagram by the voltage source representing the input excitation e_i.

When formulating equations describing the system, we shall first take into consideration all the three nodes shown in the diagram:

	v_1	v_2	v_3	i	e_i
1	$\dfrac{1}{sL}$	$\dfrac{-1}{sL}$		1	
2	$\dfrac{-1}{sL}$	$G + \dfrac{1}{sL}$	$-G$		
3		$-G$	$G + sC$		
e_i	1				1

$$\Delta(s) = \begin{vmatrix} \dfrac{1}{sL} & \dfrac{-1}{sL} & 0 & 1 \\ \dfrac{-1}{sL} & G + \dfrac{1}{sL} & -G & 0 \\ 0 & -G & G + sC & 0 \\ 1 & 0 & 0 & 0 \end{vmatrix} = G\left(\dfrac{1}{sL} + sC\right) + C/L$$

$$\Delta_{31}(s) = (-1)^{3+1} \begin{vmatrix} \dfrac{1}{sL} & \dfrac{-1}{sL} & 1 \\ \dfrac{-1}{sL} & G + \dfrac{1}{sL} & 0 \\ 0 & -G & 0 \end{vmatrix} = \dfrac{G}{sL}$$

The transfer function $H(s)$ can then be expressed as

$$H(s) = \frac{1}{LCs^2 + RCs + 1} \tag{13.14}$$

In this case we can considerably simplify the problem by formulating just two equations, one for the node 3 and the second one for the series combination of the elements $e_i - L - R$. Then we shall obtain

	v_3	i	e_i
3	sC	1	
$e_i - L - R$	1	$-sL - R$	1

In this case

$$\begin{aligned} \Delta(s) &= \begin{vmatrix} sC & 1 \\ 1 & -sL - R \end{vmatrix} &= -(R + sL)sC - 1 \\ \Delta_{11}(s) &= (-1)^{1+1}|-1| &= -1 \end{aligned} \tag{13.15}$$

The resulting transfer-function $H(s)$ is identical to (13.14).

Seismograph. Fig. 13.4a shows a schema of seismograph. A seismograph indicates the displacement of its case relative to the inertial reference. It consists of a mass m fixed to the seismograph case by a spring of stiffness k, b is a linear damping between the mass and the case.
  Let us define:
  x_i = displacement of the seismograph case relative to the inertial reference (the absolute frame)
  x_0 = displacement of the mass m within the seismograph relative to its case
  $y = x_0 - x_i$ = displacement of the mass m relative to the case.
  Note that y is the variable we can actually measure. Since gravity produces a steady spring deflection, we measure the displacement x_0 of mass m from its static equilibrium position.
  Considering x_i as input an y as output, the transfer function is

$$F(s) = \frac{Y(s)}{X_i(s)} = \frac{V_0(s) - V_i(s)}{V_i(s)} \tag{13.16}$$
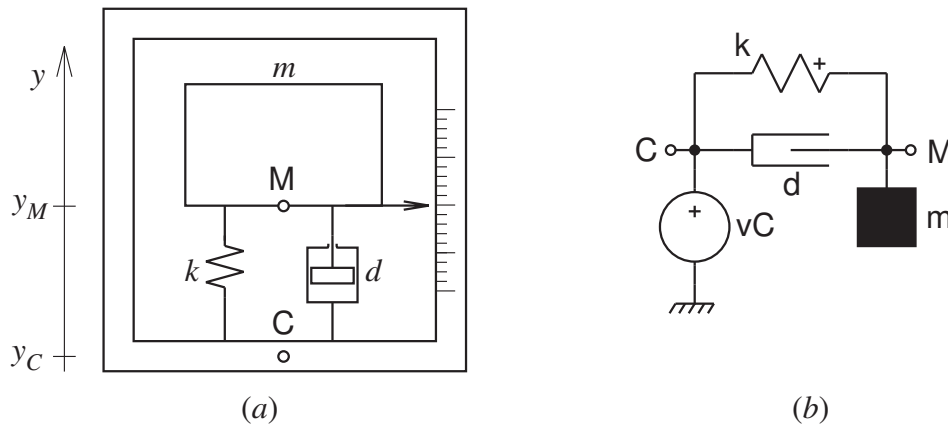
Figure 13.4: Seismograph

The multipole model of the seismograph is given in Fig. 13.4b. It is advantageous to take there as a reference node the node C corresponding to the case instead of the node F corresponding to the actual inertial reference. The transfer function can than be expressed as

$$F(s) = \frac{v_{MC}(s)}{v_{FC}(s)} \tag{13.17}$$

Exploiting the fact that the velocity between nodes F and C is constrained by the input velocity source v_i, we can write the matrix-form equations for the multipole diagram in the following way

	v_{MC}	v_{FC}	v_i
M	$b + sm + k/s$	$-sm$	
F	0	1	-1

The determinants are in this case

$$\Delta(s) = b + ms + k/s \qquad \Delta_{11}(s) = -sm \tag{13.18}$$

From this

$$F(s) = -\frac{sm}{b + sm + k/s} = -\frac{s^2}{s^2 + sb/m + k/m} \tag{13.19}$$

Note that

$$\lim_{\omega \to 0} F(j\omega) = 0 \quad and \quad \lim_{\omega \to \infty} F(j\omega) = -1 \tag{13.20}$$

Thus for low frequency inputs x_i the mass m follows the case up and down. However, if the input variable has a sufficiently high frequency, then the mass m remains almost fixed with respect to the inertial reference and the motion of the case indicates the relative motion between the case and the mass. For this reason the undamped natural frequency $\omega_0 = \sqrt{k/m}$ is made small in seismographs.

Liquid-level system.   Consider the system of two interacting tanks shown in Fig. 13.5a.
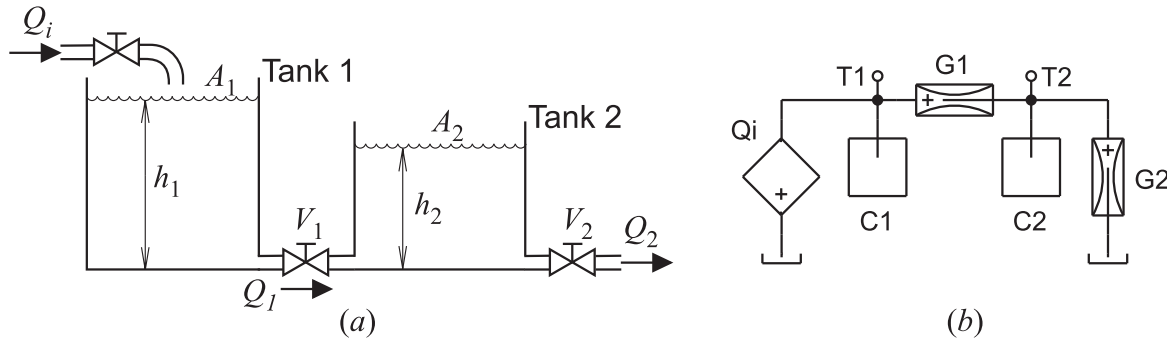

Figure 13.5: Interacting tanks.

The fluid capacitance of the tanks is

$$C_1 = \frac{A_1}{\rho g} \quad and \quad C_2 = \frac{A_2}{\rho g} \tag{13.21}$$

where A_1, A_2 [m²] are horizontal areas of the tanks, ρ [kg.m⁻³] is the mass density of the liquid, and g [m.s⁻²] is the acceleration due to gravity. The volume fluid flow into the first tank through the control valve is Q_i. The tanks are interconnected by a short pipe with a valve representing a restriction of fluid R_1. The fluid resistance of the second tank outlet is R_2.

The task is to compute the transfer function between the intake flow Q_i and the outlet flow Q_2 which can be expressed as

$$F(s) = \frac{Q_2}{Q_i} = \frac{p_2}{R_2 Q_i} \tag{13.22}$$

where p_2 is the liquid pressure at the bottom of the second tank.

Based on the assumption that the system is either linear (for the laminar flow in the restriction) or linearized (for the turbulent flow), it can be modelled by the multipole diagram given in Fig. 13.5 (the fluid conductances $G_1 = 1/R_1$, $G_2 = 1/R_2$).

The port diagram equations are then

	p_1	p_2	Q_i
1	$G_1 + sC_1$	$-G_1$	1
2	$-G_1$	$G_1 + G_2 + sC_2$	0

The relevant determinants are

$$\Delta(s) = G_1 G_2 + s[C_1(G_1 + G_2) + C_2 G_1] + s^2 C_1 C_2 \qquad \Delta_{21}(p) = G_1 \tag{13.23}$$

From there

$$F(s) = G_2 \frac{\Delta_{21}}{\Delta} = \frac{1}{R_1 C_1 R_2 C_2 s^2 + (R_1 C_1 + R_2 C_2 + R_2 C_1) + 1} \tag{13.24}$$
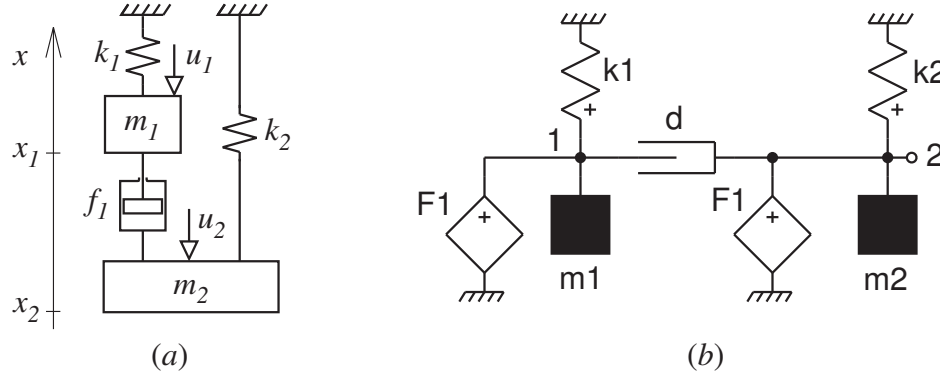

Figure 13.6: Multivariable mechanical system.

Multivariable mechanical system.   Consider the system shown in Fig. 13.6a. We assume that the system, which is initially at rest, has two inputs $F_1(t)$ and $F_2(t)$ and two outputs $x_1(t)$ and $x_2(t)$. In this problem we would like to demonstrate formulation of a multivariable system transfer-function description

$$\begin{bmatrix} x_1(s) \\ x_2(s) \end{bmatrix} = \mathbf{H}(s) \cdot \begin{bmatrix} F_1(s) \\ F_2(s) \end{bmatrix} \tag{13.25}$$

where the transfer-function matrix

$$\mathbf{H}(s) = \begin{bmatrix} H_{11}(s) & H_{12}(s) \\ H_{21}(p) & H_{22}(s) \end{bmatrix} \tag{13.26}$$

The equations describing the multipole diagram model of the system given in Fig. 13.6b are

	$\dot{x}_1$	$\dot{x}_2$	F_1	F_2
1	$b_1 + sm_1 + k_1/s$	$-b_1$	-1	
2	$-b_1$	$b_1 + sm_2 + k_2/s$		-1

The transfer-function matrix $\mathbf{H}(s)$ can then be expressed as

$$\mathbf{H}(s) = \frac{1/s}{\det \mathbf{A}(s)} \cdot \begin{bmatrix} \det \mathbf{A}_{11}(s) & \det \mathbf{A}_{12}(s) \\ \det \mathbf{A}_{21}(s) & \det \mathbf{A}_{22}(s) \end{bmatrix} \tag{13.27}$$

where

$$\det \mathbf{A} = \Delta(s) = (b_1 + sm_1 + k_1/s)(b_1 + sm_2 + k_2/s) - b_1^2 \tag{13.28}$$

and

$$\begin{aligned}
\det \mathbf{A}_{11}(s) &= -(-1)^{1+1}\Delta_{11}(s) &=& \quad |b_1 + sm_2 + k_2/s| &=& \quad -b_1 - sm_2 - k_2/s \\
\det \mathbf{A}_{12}(s) &= -(-1)^{1+2}\Delta_{12}(s) &=& \quad -|-b_1| &=& \quad b_1 \\
\det \mathbf{A}_{21}(s) &= -(-1)^{2+1}\Delta_{21}(s) &=& \quad -|-b_1| &=& \quad b_1 \\
\det \mathbf{A}_{22}(s) &= -(-1)^{2+2}\Delta_{22}(s) &=& \quad -|b_1 + sm_1 + k_1/s| &=& \quad -b_1 - sm_1 - k_1/s
\end{aligned} \tag{13.29}$$

Clearly, the time responses $x_1(t)$ and $x_2(t)$ are given by

$$\begin{aligned}
x_1(t) &= \mathcal{L}^{-1}\left[H_{11}(s) \cdot F_1(s) + H_{12}(s) \cdot F_2(s)\right] \\
x_2(t) &= \mathcal{L}^{-1}\left[H_{21}(s) \cdot F_1(s) + H_{22}(s) \cdot F_2(s)\right]
\end{aligned}$$

assuming zero initial conditions.

Show, that the equivalent of inertia and friction of the gear train referred to shaft 1 are given by

$$
\begin{aligned}
J_{1eq} &= J_1 + n_{21}^2 J_2 + n_{21}^2 n_{43}^2 J_3 \\
b_{1eq} &= b_1 + n_{21}^2 b_2 + n_{21}^2 n_{43}^2 b_3
\end{aligned}
$$

Similarly, the equivalent moment of inertia and friction of the gear train referred to the load shaft are

$$
\begin{aligned}
J_{3eq} &= J_3 + 1/n_{21}^2 \cdot J_2 + 1/n_{21}^2 \cdot 1/n_{43}^2 \cdot J_1 \\
b_{3eq} &= b_3 + 1/n_{21}^2 \cdot b_2 + 1/n_{21}^2 \cdot 1/n_{43}^2 \cdot b_1
\end{aligned}
$$

The relation between J_{1eq} and J_{3eq} is thus

$$
J_{1eq} = n_{21}^2 n_{43}^2 J_{1eq} \tag{13.30}
$$

and that between b_{1eq} and b_{3eq} is

$$
b_{1eq} = n_{21}^2 n_{43}^2 b_{1eq} \tag{13.31}
$$

Note, that if $n_{21} \ll 1$ and $n_{43} \ll 1$ for a speed-reducing gear train, then the effect of J_2, J_3, b_2 and b_3 referred to shaft 1 is negligible.

Rotary-to-linear motion conversion.   In motion control problems, it is often necessary to convert rotational motion into a translational one. For instance, a load may be controlled to move along a straight line through a rotary motor and screw assembly, such as that shown in Fig. 13.7a.

Figure 13.7b shows a similar situation in which a rack and pinion is used as the mechanical linkage. Another common system in motion control is the control of a mass through a pulley by a rotary prime mover, such as that shown in Fig. 13.7c.
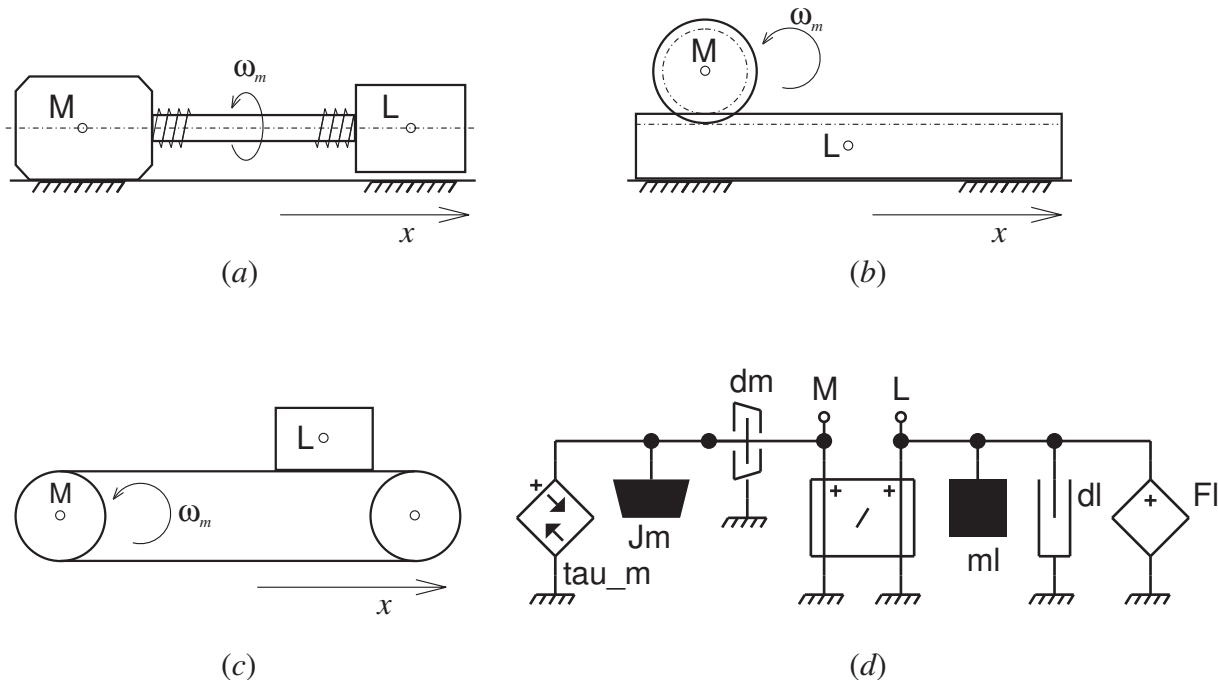

Figure 13.7: Rotary-to-linear motion conversion.

The system shown in Figs. 13.7a, 13.7b and 13.7c are all represented by a simple port diagram in Fig. 13.7d. Elements τ_m, J_m and b_m are modeling the drive motor there, and the elements F_ℓ, m_ℓ and b_ℓ model the mechanical load of the systems. The ideal transformer models the actual motion conversion.

In case of the system shown in Fig. 13.7a, the transformer ratio n corresponds to the lead of the screw, which is defined as the linear distance which the load travels per revolution of the screw. In the other two systems $n = r$ where r is the radius of either the pinion or of the pulley.

The equations describing the dynamics of the systems are following:

	ω_M	v_L	F	τ_m	F_ℓ
M	$b + sJ_m$		$-n$	1	
L		$b_\ell + sm_\ell$	1		1
transformer	n	-1			

The determinant of the system matrix is

$$\Delta = b_m + sJ_m + n^2(b_\ell + sm_\ell) \tag{13.32}$$

Using this, we can easily derive the following transfer functions

$$\frac{v_L}{\tau_m} = \frac{n}{b_m + sJ_m + n^2(b_\ell + sm_\ell)}$$

$$\frac{\omega_M}{\tau_m} = \frac{1}{b_m + sJ_m + n^2(b_\ell + sm_\ell)}$$

$$\frac{F}{\tau_m} = \frac{-n(b_\ell + sm_\ell)}{b_m + sJ_m + n^2(b_\ell + sm_\ell)}$$

$$\frac{v_\ell}{F_\ell} = \frac{-n^2}{b_m + sJ_m + n^2(b_\ell + sm_\ell)}$$

From the second transfer function we can conclude that the equivalent torque τ_e, inertia J_e and damping b_e of the load that the motor sees is

$$\tau_e = nF_\ell, \qquad J_e = n^2m_\ell, \qquad \text{and} \qquad b_e = n^2b_\ell$$

Thus any of the three rotary-to-linear conversion systems can be represented from the point of view of loading the drive motor just by the elements τ_e, J_e and b_e as shown in Fig. 13.7e.

Note also, that the third transfer function becomes

$$\frac{F}{\tau_m} = -\frac{1}{n}$$

for $b_m = J_m = 0$ as could be expected.

From the last transfer function it is obvious, that the load sees the motor as shown in Fig. 13.7f where the elements F_e, m_e and b_e are

$$F_e = \tau_m/n, \qquad m_e = J_m/n^2, \qquad \text{and} \qquad b_e = b_m/n^2$$

Rotary-to-rotary motion conversion. Consider the system shown in Fig. 13.8a. In this system, a load is driven by a motor through the gear train. Assuming that the stiffness of the shafts of the gear train is infinite (there is neither backslash nor elastic deformation) and that the number of teeth on each gear is proportional to the radius of the gear, obtain the equivalent moment of inertia and equivalent friction referred to the motor shaft and referred to the load shaft.

In Fig. 13.8a, the numbers of teeth on gears 1, 2, 3 and 4 are N_1, N_2, N_3 and N_4, respectively. The angular displacements of shafts are $\varphi_1, \varphi_2, \varphi_3$ and φ_4, respectively. Thus, $\varphi_2/\varphi_1 = -N_1/N_2 = -n_{21}$ and $\varphi_4/\varphi_3 = -N_4/N_3 = -n_{43}$. The moment of inertia and viscous friction of each gear train component are denoted by $J_1\,b_1, J_2\,b_2, J_3\,b_3$, and $J_4\,b_4$, respectively. $J_1\,b_1$ include the moment of inertia and friction of the motor, $J_4\,b_4$ include the moment of inertia and friction of the load.

The multipole model of the gear train system is given in Fig. 13.8b. The equations describing the multipole diagram model of the system given in Fig. 13.8 are

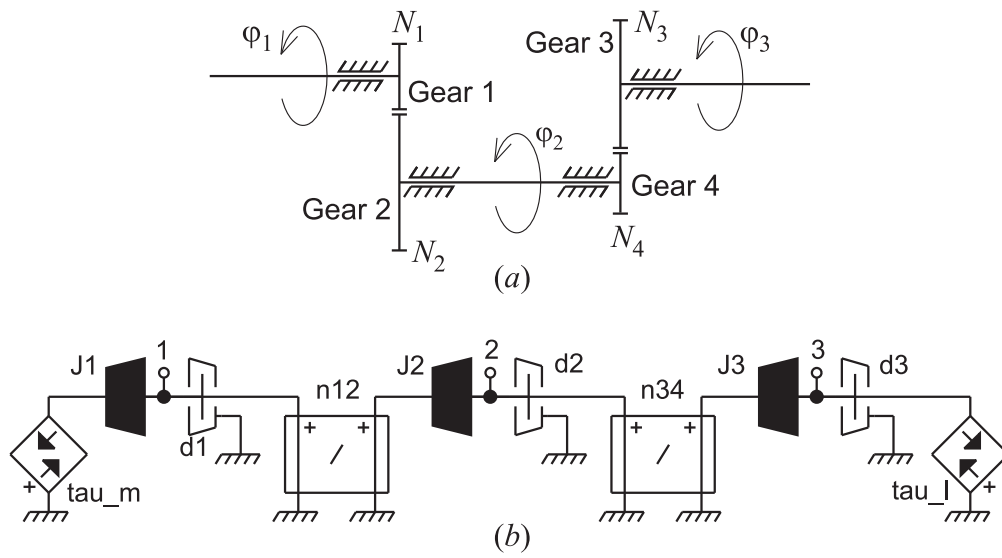|	$\dot\varphi_1$	$\dot\varphi_2$	$\dot\varphi_3$	τ_2	τ_4	τ_m	τ_l
1	$b_1 + sJ_1$			n_{21}		1	
2		$b_2 + sJ_2$		1	n_{43}		
3			$b_3 + sJ_3$		1		1
T12	$-n_{21}$	1					
T34		$-n_{43}$	1				

Figure 13.8: Gear train system.